

**GEOCHEMISTRY OF BIOTITE AND CHILLED MARGINS IN THE VOISEY'S
BAY TROCTOLITE**

by

© Jennifer Glasgow

A Thesis submitted to the

School of Graduate Studies

in partial fulfillment of the requirements for the degree of

Master of Science

Earth Sciences

Memorial University of Newfoundland

May 2014

St. John's

Newfoundland and Labrador

ABSTRACT

The Voisey's Bay troctolite is one of the oldest members of the Nain Plutonic Suite (NPS), and hosts the Voisey's Bay Ni-Cu-Co deposits. This study involves detailed mineralogy, geochemistry and oxygen isotope chemistry of the Voisey's Bay Complex (VBC) chamber, feeder and marginal rocks to determine: (1) the geochemical-isotopic fingerprint of biotite in troctolite, and (2) the composition of chilled margins on troctolite as indicators of parental magma composition and of the role of contaminants within the VBI. There are variations in the Ni and F contents of biotite in chamber versus feeder rocks as determined via electron microprobe analysis. Oxygen isotope analyses of biotite separates indicate that $\delta^{18}\text{O}$ ratios of biotite in the Western Deeps and Mushaua intrusions are enriched relative to the mantle water value of 5.7 ‰, whereas ratios of biotite in the Eastern Deeps, Discovery Hill and Ovoid are depleted. Gabbronorite chilled margins are present in three settings within the VBI, and formed when hot magma quenched against country rock. Several chilled margins show evidence of country rock contamination, however, three chilled margin samples represent uncontaminated mafic magma parental to the VBI. The geochemical variations seen in biotite and chilled margins can be explained by a multiple-stage emplacement history that included at least two distinct mega-pulses of magma.

ACKNOWLEDGEMENTS

This study was made possible through the generous financial and technical support of Vale Newfoundland and Labrador. First and foremost I would like to thank the Vale Exploration staff at Voisey's Bay and in St. John's. In particular, Dawn Evans-Lamswood and Brad King for their help leading up to my 2011 field season and for continued support over the life of the project. My fellow geologists Kimberley Morrissey, Danny Mulrooney and Sheldon Pittman were excellent technical advisors and fantastic colleagues. I'm especially thankful for the chance to work with my cross-shift Krista Reddy. Appreciation is also due to the technical staff at Voisey's Bay who assisted me with sample collection, who cut my core for me and who took me out in to the field for breaks from the repetitiveness of sampling drill core.

My supervisor Derek Wilton is gratefully acknowledged for his academic guidance over the course of the project. Derek developed this project and provided great direction as it unfolded and moved in various directions. I am very thankful he supported me in my decision to join Vale for two years while continuing to pursue my degree. I received invaluable technical assistance from Michael Shaffer at Memorial University and Peter Jones at Carleton University and would like to thank Peter Lightfoot for his focused suggestions and advice to my many questions. I owe special thanks to Matthew Spencer, Mike Piller and Matt Minnett for their hard work preparing my samples. I would also like to thank Steven Green, who assisted me with my fieldwork during the 2011 summer field season.

Finally, my family is thanked for their continued encouragement and support over the years. Only now do I fully appreciate their kind warning regarding the commitment involved in working full time while pursuing a degree. So thank you mum, dad, Claire, and granny. Thanks especially to Robert Foley for his patience and confidence in my ability to complete my program. I am grateful to have found someone to help me make Newfoundland my home over these past few years.

Table of Contents

ABSTRACT	ii
ACKNOWLEDGEMENTS	iii
Table of Contents	v
List of Tables	viii
List of Figures	ix
List of Appendices	xii
1. Chapter 1 - Introduction and Overview	1
1.1. Discovery of the Voisey's Bay deposit.....	1
1.2. Purpose of this study	2
1.3. Regional Geology	2
1.3.1. Magmatic components of the Nain Plutonic Suite	4
1.3.2. Geology of the mining block and the Voisey's Bay Ni-Cu-Co deposits	7
1.4. Current understanding of the VBC	8
1.5. Thesis goals and rationale	12
1.6. Methodology	14
1.6.1. Field Component.....	14
1.6.2. Petrography	14
1.6.3. Mineral liberation analysis.....	14
1.6.4. Whole rock analysis	15
1.6.5. Electron microprobe analysis.....	16
1.6.6. Oxygen isotopes.....	18
1.7. Structure of the thesis.....	18
1.7.1. Chapter 2 summary – Major, trace and oxygen isotope geochemistry of biotite in troctolite from the Voisey's Bay Ni-Cu-Co deposit and Mushuau Intrusion, Labrador	19
1.7.2. Chapter 3 summary – A petrographical and lithogeochemical evaluation of chilled marginal rocks from the Voisey's Bay Intrusion, Labrador	19
1.8. Co-authorship statement	20
Bibliography	22
2. Chapter 2 – Major, trace and oxygen isotope geochemistry of biotite in troctolite from the Voisey's Bay Ni-Cu-Co deposit and Mushuau Intrusion, Labrador	26

ABSTRACT	26
2.1. Property Geology	27
2.1.1. Regional Geology	27
2.1.2. Voisey's Bay and Mushau intrusions	28
2.2. Petrography and mineralogy	33
2.2.1. Voisey's Bay Intrusion	34
2.2.2. Mushau Intrusion	44
2.3. Biotite chemistry	44
2.3.1. Biotite major element chemistry	45
2.3.2. Biotite trace element chemistry	54
2.3.3. Oxygen isotope chemistry.....	59
2.4. Discussion and conclusions	66
Bibliography	78
3. Chapter 3 – A petrographical and lithogeochemical evaluation of chilled marginal rocks from the Voisey's Bay Intrusion, Labrador	82
ABSTRACT	82
3.1. Introduction.....	83
3.2. Sampling	87
3.3. Description of chilled marginal rocks.....	87
3.4. Two generations of chilled margins.....	91
3.5. Occurrence of chilled margins	92
3.6. Major and trace element whole rock lithogeochemistry	98
3.6.1. Major element chemistry of chilled margins	98
3.6.2. Trace element chemistry of chilled margins	100
3.7. Rare earth element lithogeochemistry of chilled margins	102
3.8. Discussion and significance	107
Bibliography	110
4. Chapter 4 - Summary	114
Bibliography	121
Appendix A	
Appendix B	
Appendix C	
Appendix D	

Appendix E

List of Tables

Table 2-1. Mineralogical composition of samples.....	38
Table 2-2. Sample list.	46
Table 2-3. Summary of biotite chemistry data.....	55
Table 2-4. Sample list.	63
Table 2-5. Mean composition of biotite samples.....	70
Table 3-1. Summary of chilled margin samples.	88
Table 3-2. Modal mineralogies of the lithological units.....	94
Table B-1. Master sample list.	Appendix B

List of Figures

Fig. 1-1. Structural provinces and major tectonic features of Labrador	4
Fig. 1-2. Geologic map of the NPS.....	6
Fig. 1-3. Datamine screen capture of the Voisey's Bay Intrusion.	9
Fig. 2-1. Geologic map of the Voisey's Bay region.	28
Fig. 2-2. Simplified geologic map of coastal Labrador.	30
Fig. 2-3. North and west-facing cross sections of the VBI.	31
Fig. 2-4. Geological relationship between the Ovoid and Eastern Deep.....	32
Fig. 2-5. Troctolite photomicrographs.	36
Fig. 2-6. Diorite photomicrographs.....	40
Fig. 2-7. Olivine norite photomicrographs.	41
Fig. 2-8. Gabbronorite photomicrographs.	43
Fig. 2-9. Ternary diagram showing origin of VBI biotite.....	48
Fig. 2-10. Voisey's Bay and Mushau biotite composition.....	50
Fig. 2-11. Biotite major element chemistry.	53
Fig. 2-12. X-Y plots of biotite major and trace element chemistry.	58
Fig. 2-13. $\delta^{18}\text{O}$ SMOW (‰) versus δD SMOW (‰).	59
Fig. 2-14. $\partial^{18}\text{O}$ ratios of biotite separates.	61
Fig. 2-15. Plot of Mg# (Mg/Mg+Fe) versus $\delta^{18}\text{O}$ for biotite.....	62
Fig. 2-16. $\partial^{18}\text{O}$ ratios of biotite in norite from the Western Deep.....	65
Fig. 2-17. $\partial^{18}\text{O}$ ratios of biotite in troctolite from the Eastern Deep.....	66
Fig. 3-1. Simplified geologic map of coastal Labrador.	84

Fig. 3-2. Plan map and north-facing section through VBI.....	85
Fig. 3-3. Gabbronorite in drill core.....	89
Fig. 3-4. Photomicrographs gabbronorite	92
Fig. 3-5. West-facing schematic through the Reid Brook dyke.....	96
Fig. 3-6. West-facing schematic through the Eastern Deeps chamber.	97
Fig. 3-7. Bi-variant major element plots for marginal rocks.	99
Fig. 3-8. Basalt discrimination plots after Pearce and Norry (1979).	101
Fig. 3-9. Basalt discrimination plot after Floyd and Winchester (1975).	101
Fig. 3-10. Bivariant plots showing Ce vs. Yb for chilled margins.	103
Fig. 3-11. Chondrite-normalized REE plot.....	105
Fig. 3-13. Plot of La/Sm vs. Th/Nb in chilled margins.....	106
Fig. 4-1. TiO ₂ -K ₂ O-P ₂ O ₅ discrimination diagram.	117
Fig. 4-2. Composition of biotite in chilled margins.....	118
Fig. A-1. QAPF Classification of igneous rocks.....	Appendix A
Fig. A-2. Classification of mafic-ultramafic rocks.....	Appendix A
Fig. A-3. Samples plotted on Streckeisen's 1974 classification diagram.....	Appendix A
Fig. A-4. Diorite samples on Streckeisen's 1976 classification scheme.....	Appendix A
Fig. A-5. Photomicrographs of troctolite from the VBI.....	Appendix A
Fig. A-6. Photomicrographs of troctolite from the Mushaua intrusion.....	Appendix A
Fig. A-7. Photomicrographs of diorite from the VBI.....	Appendix A
Fig. A-8. Photomicrographs of norite from the VBI.....	Appendix A
Fig. A-9. Photomicrographs of olivine gabbro from the VBI.....	Appendix A

Fig. A-10. Photomicrographs of gabbronorite from the VBI.....Appendix A

Fig. B-1. Plan map showing locations of borehole samples.....Appendix B

Fig. B-2. MLA legend (mineral key).....Appendix B

List of Appendices

- Appendix A Streckeisen's classification of igneous rocks and photomicrographs
- Appendix B Master sample list and MLA grain boundary maps
- Appendix C EMPA images of individual biotite grains probed
- Appendix D Whole rock lithogeochemical data
- Appendix E Biotite composition tables

1. Chapter 1 - Introduction and Overview

1.1. Discovery of the Voisey's Bay deposit

The Voisey's Bay deposits were discovered in 1993 during a grass roots diamond exploration program funded by Diamond Fields Resources. Two prospectors, Chris Verbinski and Al Chislett, discovered gossanous outcroppings on what is now referred to as Discovery Hill while surveying northern Labrador for diamond indicator minerals. The initial samples from Discovery Hill yielded promising assay results, and were followed up in 1994 and 1995 with an exploration drilling and geophysical surveying program which included four diamond drill holes and a HLEM ground survey (Evans-Lamswood et al., 2000). The geophysical program identified extensive and continuous conductivity at depth and significant massive sulphide was intersected in all four original drill holes (Diamond Fields Resources data, 1995 in Evans-Lamswood, 2000). The favourable results of early exploration activities prompted further exploration projects and lead to the discovery of the 110m thick massive sulphide body now known as the Ovoid and the extension of the Discovery Hill mineralization for approximately 800m along strike (Evans-Lamswood et al., 2000). Following the discovery and exploration rush associated with the Voisey's Bay deposit, subsequent work has focused on developing a genetic model for this type of mineral deposit.

1.2. Purpose of this study

This study focuses on the petrography, geochemistry and stable isotope compositions of biotite and chilled marginal rocks from the Voisey's Bay and Mushau mafic intrusives. The aim of the study is two-fold. Firstly, a geochemical and isotopic analysis of biotite in the Voisey's Bay and Mushau troctolites, diorites, norites, and gabbros is completed. Secondly, a petrographical, mineralogical and geochemical evaluation of chilled margins on weakly mineralized mafic rocks in the Voisey's Bay Intrusion (VBI) is presented.

Chapter one provides a focused overview of the study area and outlines the framework for the following chapters of the thesis. Firstly, an overview of the regional geology and magmatic history of the Nain Plutonic Suite (NPS) will be presented followed by an introduction to the geology of the main mining block and Voisey's Bay Ni-Cu-Co deposits. The second component of the regional geology section is a discussion of the current understanding of the Voisey's Bay Intrusion and its emplacement history. Next, the main objectives of the thesis project are presented. Finally, the methodology employed during this project is briefly introduced and the first chapter concludes with a synopsis of the main chapters of the thesis.

1.3. Regional Geology

The geological history of Labrador spans more than 3.5 Ga and is widely varied in terms of magmatic and tectonic formation processes. Intrusive igneous troctolitic and gabbroic bodies are important components of the regional geologic framework of

Labrador. The Voisey's Bay deposits are hosted within the troctolitic component of the Nain Plutonic Suite (NPS), which occurs at the suture zone between the Nain and Churchill provinces. As such, a brief introduction to the magmatic evolution of the NPS in the context of its geological setting is given below.

Labrador encompasses five major lithotectonic provinces that in turn record a crustal history spanning 3.85 to 0.6 Ga (Wardle, 1995). The oldest rocks belong to the Archean Nain and Superior provinces, which are bounded by the Early Proterozoic Churchill and Makkovik provinces. The Proterozoic Churchill Province separates the Archean Nain Province in the east from the Archean Superior Province in the west. The central part of the Churchill Province consists of a terrane of reworked Archean gneiss, which is welded to the adjacent Superior and Nain cratons by the New Quebec and Torngat orogens respectively (Wardle, 1995). The Makkovik Province is a metasedimentary sequence developed on the southeast flank of the Nain Province (Gower et al., 1982; Ryan, 1984). The Grenville Province, which includes components of the Early Proterozoic Labrador Orogen (Wardle, 1995), truncates the Churchill and Makkovik provinces in the south (Fig. 1-1).

The suture between the Proterozoic metasedimentary Tasiuyak garnet paragneiss of the Churchill Province in the west and the Archean amphibolite to granulatite facies orthogneiss belonging to the Nain Province in the east (Wardle, 1995) focused the intrusion of the 1.34-1.29 Ga, 20 000 km² NPS (Ryan, 1995). The Voisey's Bay main block includes portions of both the suture and the NPS (Fig. 1-2).

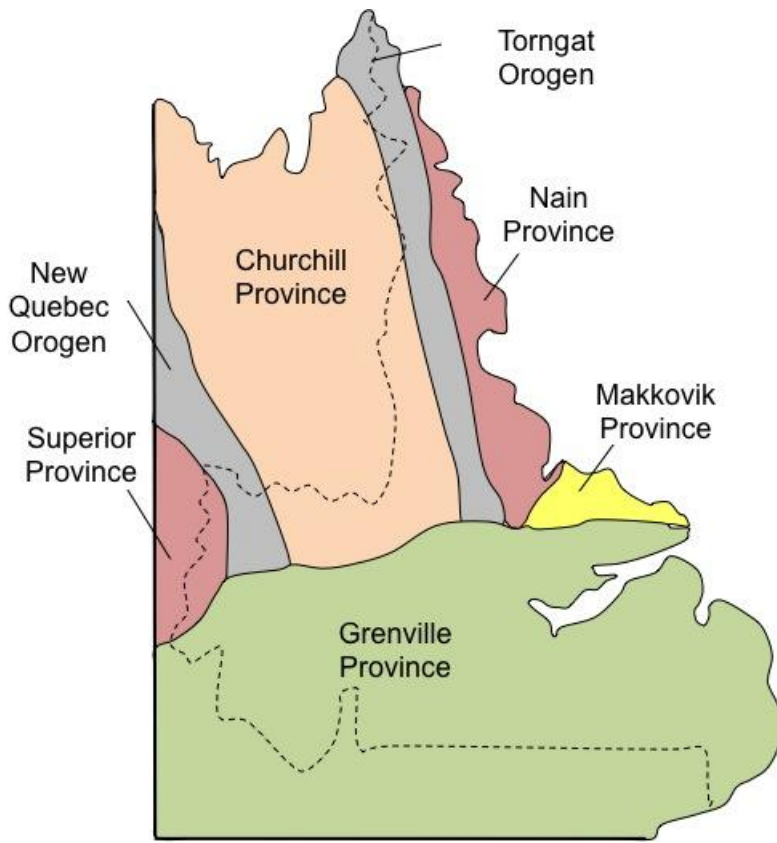


Fig. 1-1. Structural provinces and major tectonic features of Labrador. The border between Labrador and Quebec is shown by the dashed line (simplified from Wardle et al., 1997).

1.3.1. Magmatic components of the Nain Plutonic Suite

The multiphase NPS comprises coalesced anorthosite, troctolite, diorite, and granite plutons. The anorthositic plutons of the NPS are numerous and consist of plagioclase cumulates with interstitial orthopyroxene (Ryan, 1997) and as such include intrusions of leuconorite. Representative anorthosite plutons belonging to the NPS include the Bird Lake massif, the Mount Lister intrusion, the Pearly Gates intrusion, and the Tunungayaluk Island intrusion (Wardle, 1995). Yu and Morse (in Ryan, 1997) proposed that the Bird Lake massif crystallized *ca.* 1328 Ma and Hamilton (in Berg et al., 1994) suggested the Mount Lister intrusion was emplaced *ca.* 1331 Ma.

The granitic plutons of the NPS range from fayalite- and pyroxene-bearing quartz monzonite to hornblende biotite granite and have mineralogical and chemical similarities to the rapakivi batholiths of Finland (Emslie and Stirling, 1993). The granites were derived from high-temperature, water-poor magmas that coexisted with the ferrodioritic and troctolitic liquids parental to the NPS (Ryan, 1995). The granites intrude in to the anorthositic and mafic rocks of the NPS. Some examples of the granitic intrusions include the 1322 Ma Makhavinekh Lake pluton (Ryan, 1991), the 1319 Ma Umiakovik Lake batholith, which is located along the western margin of the NPS (Emslie and Russell, 1988; Emslie and Loveridge, 1992) and the younger, poorly constrained Voisey's Bay granite.

The Voisey's Bay Complex (VBC) is made up of several smaller intrusions of troctolite-olivine gabbro including the Voisey's Bay Intrusion (VBI), the Ashley Intrusion and the Floodplain Intrusion. The Voisey's Bay troctolite-olivine gabbro is the main host to nickel-copper-cobalt sulphide mineralization at the Voisey's Bay deposit in northern Labrador and includes plutons in which olivine is a significant mineralogical component.

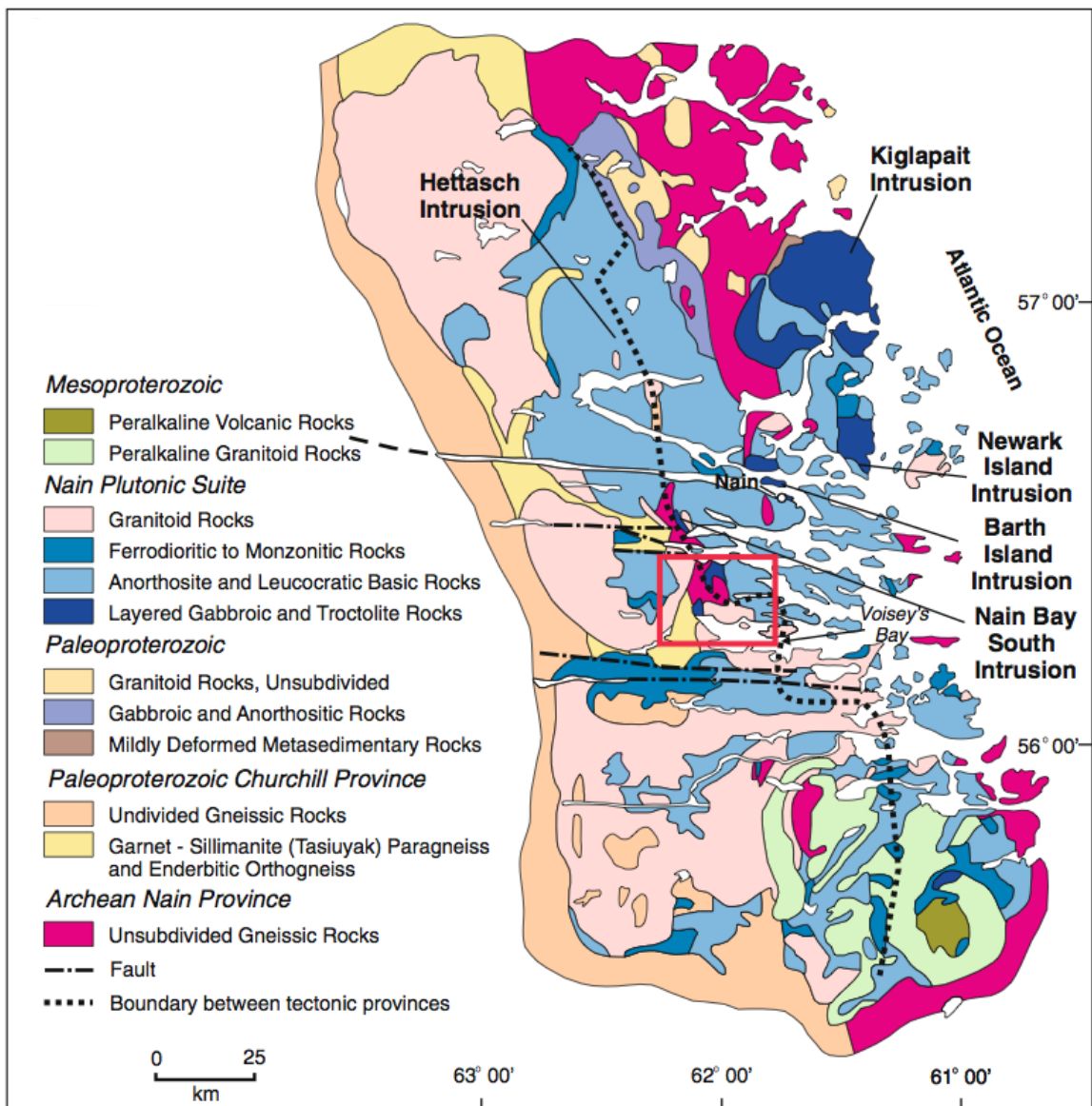


Fig. 1-2. Geologic map of the NPS showing the location of the Voisey's Bay intrusion (red square). Other troctolitic intrusions belonging to the NPS are labeled and include the Hettasch Intrusion, the Kiglapait Intrusion, the Newark Island Intrusion, the Barth Island Intrusion, and the Nain Bay South Intrusion. From Ryan, 2000 in Lightfoot et al., 2012.

The Voisey's Bay troctolite is one of the lesser voluminous troctolitic members of the NPS, and other members include the Hettasch intrusion, the 1305 Ma Newark Island and Kiglapait intrusions (Simmons et al., 1986; Morse, 1969 in Ryan, 1995), the Barth Island

Intrusion, and the 1312 Ma Jonathon Island Intrusion at the eastern margin of the NPS (Berg and Briegel, 1983). Apart from the VBI, the Kiglapait intrusion is one of the better-studied composites in the area. The Voisey's Bay troctolite is a chamber and dyke complex hosted within orthogneiss and paragneiss country rock. The troctolitic plutons display weak layering and different generations of chilled marginal rocks, indicative of a system fed by multiple pulses of magma. While the Voisey's Bay intrusion straddles the 1.85 Ga suture separating the Archean Nain and Proterozoic Churchill provinces, there is another troctolitic intrusion to the north, which occurs entirely within the Nain province; the Mushauau intrusion. The Mushauau intrusion consists of a layered unit comprising a stellate-textured, coarse-grained leucotroctolite margin, an olivine-rich melatrotroctolite centre, and a cumulate olivine gabbro core (Li et al., 2000). The Mushauau intrusion has been dated at 1313 Ma, which is 20 million years younger than its southern cousin, the Voisey's Bay intrusion. While the Voisey's Bay intrusion is host to the >124 million ton Ni-Cu-Co sulphide deposit (reserves + resources) (Li et al., 2000), significant mineralization has not yet been discovered in the Mushauau intrusion.

1.3.2. Geology of the main mining block and the Voisey's Bay Ni-Cu-Co deposits

The existence of the Voisey's Bay magmatic Ni-Cu-Co deposit is linked to its occurrence within a plumbing system, which has served to focus numerous pulses of magma (Naldrett and Li, 2007). Troctolite is present in two large magma chambers, which are connected and fed by diorite-norite feeder dykes. As such, the portions of the VBI associated with the sulphide deposits are divided into two domains: the magma

chambers and the feeder dykes. The first magma chamber is referred to as the Eastern Deep and it is the more shallowly emplaced troctolite body located on the eastern half of the main mining block at Voisey's Bay. The second magma chamber is referred to as the Western Deep and is a deep magma chamber located on the west half of the main block. The second domain is the feeder dyke, which encompasses several zones within the VBI. The dyke extends north of the Eastern Deep, acting as a feeder to the base of the chamber, and extends west through the Ovoid, Discovery Hill and Western Deep (often referred to as Reid Brook) zones (Evans-Lamswood et al., 2000). A schematic showing the different domains of the VBC can be seen in Figure 1-3. Both the chamber and feeder domains plunge gently to the east and significant mineralization occurs in both domains. The mineralization occurs at the base of the upper Eastern Deep chamber and in the conduit connecting it to the Western Deep chamber. The chamber and dyke complex has been episodically intruded by the younger members of the NPS including the Voisey's Bay and Makhavinekh granites.

1.4. Current understanding of the VBC

Ryan (2000) postulates NPS magmatism as being preceded by the trapping of sulphur-bearing paragneiss within the 1.85 Ga continental collisional suture between the Nain and Churchill provinces. From 1.34 to 1.29 Ga, this paragneiss influenced (contaminated) the passage of magmas ascending from depth, contributing to contamination and the subsequent precipitation of metalliferous phases. The resulting magma chamber and its sulphides were gradually exposed between the Mesozoic and

Holocene by faulting and uplift associated with the opening of the Labrador Sea (Ryan, 2000).

At the deposit scale, the Western Deep and Eastern Deep chambers formed when magma swelled up and out of the magmatic plumbing system (Naldrett and Li, 2007). Following the formation of these chambers, continued flow of magma through the conduit system allowed for the accumulation of sulphides in hydrodynamically favourable zones.

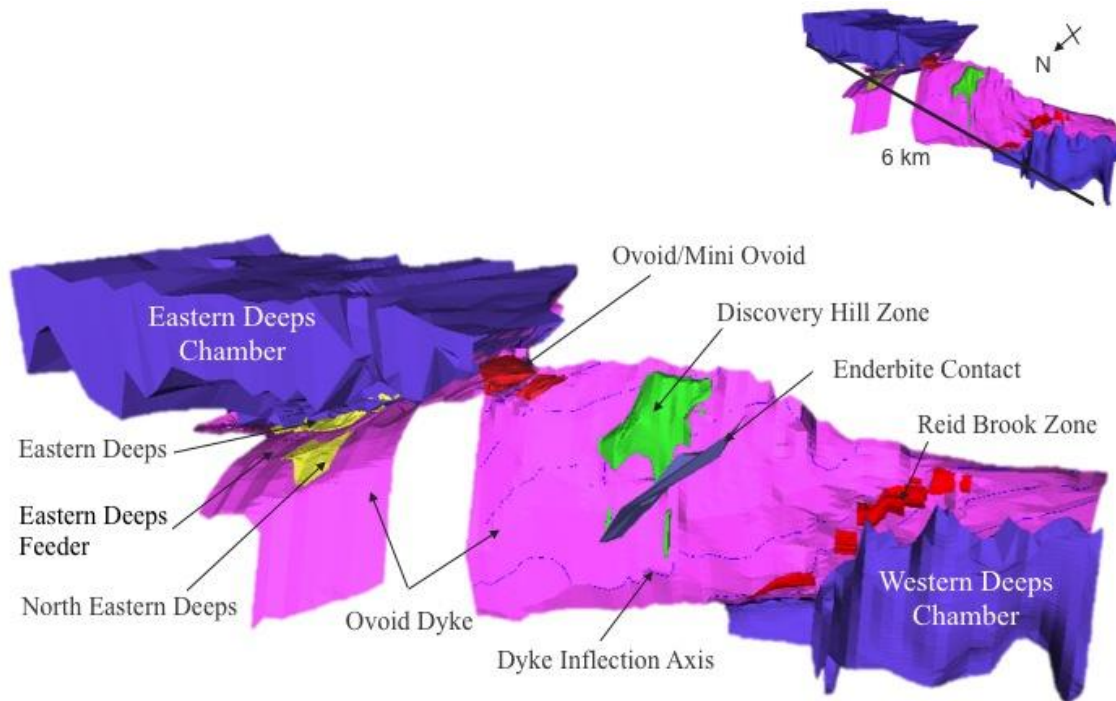


Fig. 1-3. Datamine screen capture of the Voisey's Bay Intrusion. Troctolite magma chambers are shown in deep purple, the feeder dyke is shown in pink, massive sulphide deposits are shown in red, and semi-massive sulphide accumulations are shown in yellow. The Discovery Hill zone is highlighted in green and the contact between enderbitic orthogneiss underlying the central part of the intrusion and the Tasiuyak paragneiss that hosts the western half of the intrusion is shown in grey (Vale, 2013).

In particular, the floors of the magma chambers and the feeders connecting them to their mantle source are ideal reservoirs for sulphide magma concentration (Ryan, 2000) and

this floor-hugging aspect of sulphide liquids may be critical for the exploration of deposits of this nature. Naldrett et al. (1996) interpreted the three sulphide depositional environments at Voisey's Bay as being representative of different erosional levels through a single mineralized intrusion. The deepest erosional level is located to the west and exposes the feeder sheet at surface. The base of the intrusion is exposed between the east and west subchambers and the eastern portion of the deposit is overlain by 600 to 900m of troctolite. Following initial emplacement, the parent magma was forced out of the lower chamber along with some of the segregated sulphide liquid (Naldrett and Li, 2007). The new magma forcing the parent out then continued through the system, disrupting early cumulates. This magma also picked up sulphides and transported them into the lower part of the upper (Eastern Deeps) chamber.

The Voisey's Bay intrusion is unique within the NPS and a variety of factors contributed to its high degree of mineralization. Specifically, the Voisey's Bay Intrusion is the oldest of the mafic intrusives in the NPS and predates almost all granitoid magmatism in the suite (Amelin et al., 2000). Of all the intrusions within the NPS, the VBI has the most mantle-like and least contaminated initial isotopic composition (Amelin et al., 2000). The emplacement of the Voisey's Bay intrusion and subsequent Ni-Cu-Co deposit follows a two-stage model. Firstly, the parental source underwent mantle melting and magma evolution preceding emplacement and is followed by contamination in the near surface magma chambers (Amelin et al., 2000). Amelin et al. (2000) proposed that the primary melt of the VBI was produced by melting of either hydrated continental lithospheric mantle or by melting within a plume head.

The sulphide saturation observed at Voisey's Bay likely occurred late in the crystallization history of the troctolitic magmas, following the depletion of Ni concentrations *via* olivine fractionation (Scoates and Mitchell, 2000). Initial sulphide-saturation may have resulted from the assimilation of sulphur-bearing Tasiuyak paragneiss and contributed to subsequent segregation of sulphide liquids from the magma. Naldrett et al. (2007) established that early troctolite injections at Voisey's Bay experienced significant chalcophile depletion, whereas later influxes of magma experienced less depletion and were thus able to upgrade the early sulphides in chalcophile metals.

At Voisey's Bay, host troctolitic rocks display high Re/Os ratios, attributable to high Re values associated with ore-forming environments overprinted onto radiogenic Os signatures obtained from magma interaction with Nain-Churchill crustal materials (Lambert et al., 2000). Trace element Pb and Nd isotope geochemistry of the Voisey's Bay troctolites indicate that their parental magmas have interacted with crustal rocks, likely at a depth similar to the level of intrusion (Naldrett and Li, 2007). Both S and O isotopes suggest interaction with local Tasiuyak gneisses, and the radiogenic nature of Os and recorded troctolite concentrations support this interpretation (Naldrett and Li, 2007).

The Voisey's Bay and Mushauau intrusions differ in age, parental magma composition, degree and nature of crustal contamination, internal structure, and scale of known mineralization (Li et al., 2000). The primary magma of the Voisey's Bay intrusion was derived from an enriched continental mantle or contaminated by crustal material during ascent through lower-middle crust. On the other hand, the parental magmas to the

Mushuau intrusion (as well as most of the other mafic magmas from the NPS) were probably extensively contaminated with hot restites left over from intracrustal melting and/or granitoid melts (Amelin et al., 2000). These magmas would have reached early sulphide-saturation and lost much of their chalcophile metal content. Geochemical signatures presented by Amelin et al. (2000) for the Mushuau intrusion are distinct from Voisey's Bay and more typical of the other members of the NPS.

In summary, formation of these large igneous province-related magmatic Ni-Cu-Co deposits requires a high-MgO parental magma that has not previously undergone substantial olivine crystallization, an external source of sulphur to promote sulphide-saturation, and large volumes of magma in staging chambers or magma mixing in conduits during ascent (Scoates and Mitchell, 2000). According to Li et al. (2000) the Voisey's Bay intrusion exists because of a combination of several key factors: the ascent of unfractionated basaltic magma into shallow crustal environments, the subsequent reaction of this magma with a sulphur-bearing paragneiss, a continued flow of magma after the development of immiscible sulphide liquids, and fresh, Ni- and Cu-rich magma re-using the conduit system and upgrading pre-existing sulphides.

1.5. Thesis goals and rationale

The purpose of this research is to address some of the fundamental questions relating to the origin of the magmas parental to the Voisey's Bay troctolites. The work will be approached from two different angles. Firstly, a geochemical and isotopic analysis of biotite from the Voisey's Bay troctolite-diorite-norite and biotite from the Mushuau troctolite will be completed. Secondly, a detailed petrographical, mineralogical and

lithogeochemical analysis of chilled margins on VBI troctolite intrusions will be carried out.

Biotite is a hydroxyl-bearing phase accounting for up to 10% modal mineralogy within the Voisey's Bay and Mushuau troctolites, making it apparent that the magma parental to these intrusions is not in fact "dry" and must contain water to have contributed to the biotite crystal chemical structure. It is important to note that biotite is closely associated with sulphide minerals in the aforementioned troctolites and as such the mica can be linked to ore formation. The major element chemistry of biotite from the VBI and Mushuau intrusion will allow for the distinction of mineral chemistry within and across the intrusions. Trace element compositions of biotite, specifically Ni, will be important as an indicator of ore forming processes as they relate to the evolution of the magmatic system. Oxygen isotope analyses can also be used to trace magma evolution and to potentially identify the influence of system contaminants.

This project will also investigate indicators of parental magma composition, specifically chilled margins on troctolitic intrusions in the VBC. The goal of this portion of the study is to use the chemistry of the chilled margins to provide information on the parental magma composition at the time of sulphide segregation and crystallization.

The overall goal of this research is to assess whether a geochemical-isotopic fingerprint can be determined for the ore-forming magma associated with the Voisey's Bay and Mushuau intrusions. If possible, this information could have a great impact on further exploration for large igneous province-related magmatic mineral deposits.

1.6. Methodology

1.6.1. Field Component

The aim of the field component was to re-log historical drill core, with particular attention given to identifying variations in biotite content between the mafic intrusives belonging to the VBI and to map out the distribution of chilled marginal rocks in drill core. The fieldwork was carried out between May and August 2011. Intervals from 41 drill holes were logged and 146 drill core samples were collected for geochemical and isotopic analysis. A plan map showing borehole locations can be found in Appendix B.

1.6.2. Petrography

Petrography was completed on 146 polished thin sections (PTS) that were made at Vancouver Petrographics (Vanpetro). A Nikon LV100POL polarizing microscope with transmitted and reflected light capabilities was used for all thin section observations and photomicrographs of individual PTS were taken using a digital camera attachment and associated software for image capture. Photomicrographs of individual PTS constitute Appendix A.

1.6.3. Mineral liberation analysis

Mineral liberation analysis (MLA) was carried out on 49 carbon-coated PTS samples. The scanning electron microscope (SEM)-based MLA grain boundary mapping was completed at the Micro Analytical Facilities (MAF-IIC) laboratories in the Bruneau Centre at Memorial University of Newfoundland. The instrument used was an FEI MLA

650F SEM. The SEM operating conditions were 25kv accelerating potential with a beam current of 10 nano-amperes (nA). This instrument is equipped with dual Bruker Xflash 5030 SDD X-ray detection and MLA automation and image processing software. The electron backscatter diffraction (EBSD) system includes the Mineralogical Society of America minerals database for verifying mineral identification and determining crystal lattice orientations. Grain X-ray maps produced during the analyses allowed for the quantification of mineral phases present in the various lithologies (by both weight and area), in particular the percent biotite in rocks from various parts of the Voisey's Bay Intrusion. MLA mineral maps and the master sample list constitute Appendix B.

1.6.4. Whole rock analysis

Whole rock lithogeochemistry was carried out at the Eastern Analytical laboratory facilities in Vancouver, BC. Initial sample preparation was done at the Eastern Analytical facilities in Springdale, NL. Major oxides were analyzed using Inductively Coupled Plasma – Atomic Emission Spectroscopy (ICP-AES). For this method each sample is decomposed using a lithium metaborate/lithium tetraborate ($\text{LiBO}_2/\text{Li}_2\text{B}_4\text{O}_7$) fusion. The 0.200 g prepared sample is added to the lithium metaborate/lithium tetraborate flux (1.8 g), mixed well and fused in a furnace at 1025°C. The resulting melt is then cooled and dissolved in an acid mixture containing nitric, hydrochloric and hydrofluoric acids. This solution is then analyzed by ICP-AES. Results are corrected for inter-element interferences and calculated from the ICP analyte concentrations and loss on ignition (LOI) values. LOI is determined via gravimetric methods. A prepared sample (1.0 g) is placed in an oven at 1000°C for one hour, cooled and then weighed. The percent loss on

ignition is calculated from the difference in weight. Samples were also analyzed for trace elements and rare earth elements and were prepared in the same manner as described above for the major oxides but the prepared samples are analyzed using Inductively Coupled Plasma – Mass Spectroscopy (ICP-MS). Total carbon and sulphur are analyzed using a Leco analyzer and infrared spectroscopy. While a stream of oxygen passes through a prepared sample (0.05 to 0.6 g), it is heated in a furnace to approximately 1350°C. Sulphur dioxide and carbon dioxide released from the sample are measured by an infrared detection system, giving the total sulphur and total carbon result. For the base metals, each prepared sample (0.25 g) is digested with perchloric, nitric, hydrofluoric, and hydrochloric acids. The residue is topped up with dilute hydrochloric acid and the resulting solution is analyzed via ICP-AES. Again, the results are corrected for spectral interelement interferences. The following elements were determined using the Aqua Regia Digestion method: As, Bi, Hg, Sb, Se, and Te. A prepared (0.50 g) sample is digested with aqua regia for 45 minutes. After cooling, the resulting solution is diluted to 12.5 mL with de-ionized water, mixed and analyzed by ICP – MS. Original whole rock lithogeochemical data constitute Appendix E.

1.6.5. Electron microprobe analysis

A large portion of data collected for this research was by electron microprobe analysis. Thirty-six PTS samples were selected based on the results from MLA for analysis via electron microprobe. Quantitative major and trace element data were determined via an automated four-spectrometer Camebax MBX electron probe using wavelength dispersive X-ray (WDX) analytical techniques at Carleton University.

Operating conditions were 20kv accelerating potential with a beam current of 20 nano-amperes (nA) for silicates and oxides. Minerals were analyzed using a rastered electron beam 5-10 microns in size. Peak counting times for analyzed elements were generally 15-40 seconds, or 40,000 accumulated counts. Ni, however, was counted for 80 seconds, as Ni is significant in understanding the evolution of the rocks from this deposit.

Background positions were chosen carefully to avoid interferences from adjacent peaks. Background measurements were made at 50% peak counting time on each side of the analyzed peak. Raw X-ray data were converted to elemental weight % by the Cameca PAP matrix correction program. A suite of well characterized natural and synthetic minerals and compounds were used as calibration standards. Elements analyzed include the following and the standards for each are noted in parentheses: Si (olivine), Al (synthetic spinel), Mg (olivine), Na (albite), K (USNM microcline), Ca (wollastonite), Ti (synthetic MnTiO₃), V (synthetic YVO₄), Cr (synthetic Cr₂O₃), Mn (synthetic MnTiO₃), Fe (synthetic fayalite), Ni (synthetic NiO), Ba (barite), Cl (tugtupite), and F (synthetic lithium fluoride). Analyses are accurate to 1-2 % relative for major elements (>10 wt %) and 3-10 % relative for minor elements (<10 wt% >0.5wt %). As detection limit is approached (<0.1 wt %), relative errors approach 100 %.

Digital BSE images were collected by an Electron Optic Services digital imaging system. Images were collected at 512 x 512 pixel resolution with a Lamont 4 element solid state BSE detector and BSE Quad Summing Amplifier. Images were interfaced to a 4Pi Analysis Inc. digital imaging and EDX X-ray system and Power Macintosh computer

running NIH image and NIST desktop spectrum analyzer programs. Digital backscatter electron images constitute Appendix C. Biotite chemistry is summarized in Appendix E.

1.6.6. Oxygen isotopes

Thirty-three samples were processed for oxygen isotope ratios. Drill core samples were milled by mortar and pestle and sieved to a -40+60 mesh (0.422-0.251 mm) size fraction. Oxygen isotopic analyses were carried out on the grain separates at the Laboratory for Stable Isotope Science at the University of Western Ontario and are reported in delta notation relative to the Vienna Standard Mean Ocean Water (VSMOW) standard. Dried biotite samples were heated and pumped into Ni-reaction vessels under a vacuum at 300°C two hours prior to reaction with ClF₅. The samples were then reacted at 580°C for eight hours. Oxygen was extracted from the silicates using the method of Clayton and Mayeda (1963), as modified to use ClF₃ and converted quantitatively to CO₂ over red-hot graphite. Samples were analyzed using either an Optima or Prism dual inlet mass spectrometer.

1.7. Structure of the thesis

This thesis has been prepared in manuscript format and is divided in to four chapters. Chapter 1 is the introductory chapter and defines the exploration history of the study area, the regional geologic setting, the goals and rationale behind the project, and briefly outlines the methodologies used. Chapters 2 and 3 present the research as a series of papers that have been prepared for publication. As chapters 2 and 3 have been prepared as stand-alone manuscripts there is some repetition with regards to regional geology,

sampling procedures and references. Chapter 4 is a brief summary of the conclusions drawn from each research paper and links the two research components of the project. The following section is a brief outline of chapters 2 and 3.

1.7.1. Chapter 2 summary – Major, trace and oxygen isotope geochemistry of biotite in troctolite from the Voisey’s Bay Ni-Cu-Co deposit and Mushau Intrusion, Labrador

This paper investigates the composition of biotite in the mafic intrusive rocks of the VBI and Mushau intrusion. The paper characterizes and classifies the mineral-poor mafic lithologies of the chamber and dyke complex that make up the VBC, according to the IUGS classification scheme, and investigates variations in biotite chemistry across the deposits. The data are used to theorize an emplacement model for the barren and ore-bearing rocks in the VBC and to highlight differences in mineral chemistry between the Western Deeps, Eastern Deeps and Mushau intrusions.

1.7.2. Chapter 3 summary – A petrographical and lithogeochemical evaluation of chilled marginal rocks from the Voisey’s Bay Intrusion, Labrador

This paper evaluates the petrography and geochemistry of chilled marginal rocks from the VBI as a means to constrain the composition of the magma parental to the ore-bearing system. The paper defines the occurrences of marginal rocks and identifies three distinct geochemical signatures amongst the chilled margins. This paper addresses some of the fundamental questions about the Voisey’s Bay deposits: firstly, whether the Eastern

Deeps and Western Deeps zones were fed by the same magma, and; secondly, considers the relative timing of multiple pulses of magma to the system and how this episodic magmatism relates to the emplacement of ore bodies.

1.8. Co-authorship statement

Derek Wilton identified this thesis project in conjunction with Vale brownfield exploration staff. Derek Wilton wrote the research proposal originally submitted to Vale and Jennifer Glasgow and Derek Wilton together wrote the thesis proposal submitted to Memorial University of Newfoundland in partial fulfillment of the requirements for the degree of Master of Science.

Jennifer Glasgow carried out all fieldwork including sample selection, drill core logging and sampling, under the technical guidance of Vale exploration staff. Brad King, senior mineral technician with Vale, assisted with the identification and selection of drill holes to be sampled. Department of Earth Sciences staff carried out sample preparation. Jennifer Glasgow completed all petrographic analysis and carried out all mineral liberation analysis and electron microprobe analysis work under the supervision of laboratory coordinators. Michael Shaffer operates the SEM-MLA and Memorial University of Newfoundland and Peter Jones operates and maintains the microprobe facility at Carleton University. Kimberly Law performed oxygen isotope analyses at the University of Western Ontario Laboratory for Stable Isotope Science. Whole rock lithogeochemical analyses were performed at the Eastern Analytical laboratory facility in Springdale, NL.

Jennifer Glasgow analyzed and interpreted all data obtained for this project. Derek Wilton provided technical advice and assisted with data interpretation. Jennifer Glasgow prepared the final manuscript, which was reviewed thoroughly by Derek Wilton.

Bibliography

- Amelin, Y. V., Li, C., Valeyev, O., & Naldrett, A. J. (2000). Nd-Pb-Sr isotope systematics of crustal assimilation in the Voisey's Bay and Mushauau intrusions, Labrador, Canada. *Economic Geology and the Bulletin of the Society of Economic Geologists*, 95 (4), 815-830. Retrieved from
<http://search.ebscohost.com/login.aspx?direct=true&AuthType=ip,url,uid&db=geh&AN=2000-054365&site=ehost-live&scope=site>; <http://www.segweb.org/journal.htm>
- Berg, J. H., & Briegel, J. S. (1983). Geology of the Jonathon Intrusion and associated rocks. *Contribution - Geology Department, University of Massachusetts*, 40, 42-50. Retrieved from
<http://search.ebscohost.com/login.aspx?direct=true&AuthType=ip,url,uid&db=geh&AN=1988-072807&site=ehost-live&scope=site>
- Clayton, R. N., & Mayeda, T. K. (1963). The use of bromine pentafluoride in the extraction of oxygen from oxides and silicates for isotopic analysis. *Geochimica Et Cosmochimica Acta*, 27(1), 43-52. Retrieved from
<http://search.ebscohost.com/login.aspx?direct=true&AuthType=ip,url,uid&db=geh&AN=1963-014328&site=ehost-live&scope=site>;
<http://www.sciencedirect.com/science/journal/00167037>
- Emslie, R. F., & Loveridge, W. D. (1992). Fluorite-bearing early and middle Proterozoic granites, Okak Bay area, Labrador; geochronology, geochemistry and petrogenesis. *Lithos*, 28(2), 87-109. Retrieved from
<http://search.ebscohost.com/login.aspx?direct=true&AuthType=ip,url,uid&db=geh&AN=1993-036065&site=ehost-live&scope=site>;
<http://www.sciencedirect.com/science/journal/00244937>
- Emslie, R. F., & Russell, W. J. (1988). Umiakovik Lake batholith and other felsic intrusions, Okak Bay area, labrador. *Paper - Geological Survey of Canada*, 88-1C, 27-32. Retrieved from
<http://search.ebscohost.com/login.aspx?direct=true&AuthType=ip,url,uid&db=geh&AN=1988-027710&site=ehost-live&scope=site>
- Emslie, R. F., & Stirling, J. A. R. (1993). Rapakivi and related granitoids of the Nain Plutonic Suite; geochemistry, mineral assemblages and fluid equilibria. *Canadian Mineralogist*, 31, Part 4, 821-847. Retrieved from
<http://search.ebscohost.com/login.aspx?direct=true&AuthType=ip,url,uid&db=geh&AN=1998-023167&site=ehost-live&scope=site>
- Evans-Lamswood, D., Butt, D. P., Jackson, R. S., Lee, D. V., Muggridge, M. G., Wheeler, R. I., et al. (2000). Physical controls associated with the distribution of

sulfides in the Voisey's Bay Ni-Cu-Co deposit, Labrador. *Economic Geology and the Bulletin of the Society of Economic Geologists*, 95(4), 749-769. Retrieved from <http://search.ebscohost.com/login.aspx?direct=true&AuthType=ip,url,uid&db=geh&AN=2000-054362&site=ehost-live&scope=site>; <http://www.segweb.org/journal.htm>

Gower, C. F., Flanagan, M. J., Kerr, A., & Bailey, D. G. (1982). Geology of the Kaipokok Bay-Big River area, central mineral belt, Labrador. *Report - Province of Newfoundland.Dept.of Mines and Energy.Mineral Development Division* 82-7 Retrieved from <http://search.ebscohost.com/login.aspx?direct=true&AuthType=ip,url,uid&db=geh&AN=1983-023740&site=ehost-live&scope=site>

Lambert, D. D., Frick, L. R., Foster, J. G., Li, C., & Naldrett, A. J. (2000). Re-Os isotope systematics of the Voisey's Bay Ni-Cu-Co magmatic sulfide system, Labrador, Canada; II, implications for parental magma chemistry, ore genesis, and metal redistribution. *Economic Geology and the Bulletin of the Society of Economic Geologists*, 95(4; 4), 867-888. Retrieved from <http://search.ebscohost.com/login.aspx?direct=true&AuthType=ip,url,uid&db=geh&AN=2000-054368&site=ehost-live&scope=site>; <http://www.segweb.org/journal.htm>

Li, C., Lightfoot, P. C., Amelin, Y. V., & Naldrett, A. J. (2000). Contrasting petrological and geochemical relationships in the Voisey's Bay and Mushauau intrusions, Labrador, Canada; implications for ore genesis. *Economic Geology and the Bulletin of the Society of Economic Geologists*, 95(4; 4), 771-799. Retrieved from <http://search.ebscohost.com/login.aspx?direct=true&AuthType=ip,url,uid&db=geh&AN=2000-054363&site=ehost-live&scope=site>; <http://www.segweb.org/journal.htm>

Lightfoot, P. C., Keays, R. R., Evans-Lamswood, D., & Wheeler, R. (2012). S saturation history of Nain Plutonic Suite mafic intrusions; origin of the Voisey's Bay Ni-Cu-Co sulfide deposit, Labrador, Canada. *Mineralium Deposita*, 47(1-2), 23-50.

Morse, S. A. (1969). The Kiglapait layered intrusion, Labrador. *Memoir - Geological Society of America*, 112 Retrieved from <http://search.ebscohost.com/login.aspx?direct=true&AuthType=ip,url,uid&db=geh&AN=1970-027350&site=ehost-live&scope=site>

Naldrett, A. J., Keats, H., Sparkes, K., & Moore, R. (1996). Geology of the Voisey's Bay Ni-Cu-Co deposit, Labrador, Canada. *Exploration and Mining Geology*, 5, 169.

Naldrett, A. J., & Li, C. (2007). *The Voisey's Bay deposit, Labrador, Canada. special publication no. 5* Geological Association of Canada, Mineral Deposits Division.

Ryan, B. (1991). Makhavinekh lake pluton, Labrador, Canada; geological setting, subdivisions, mode of emplacement, and a comparison with Finnish rapakivi

granites. *Precambrian Research*, 51(1-4; 1-4), 193-225. Retrieved from
<http://search.ebscohost.com/login.aspx?direct=true&AuthType=ip,url,uid&db=geh&AN=1993-000835&site=ehost-live&scope=site;>
<http://www.sciencedirect.com/science/journal/03019268>

Ryan, B. (1997). The Mesoproterozoic Nain Plutonic Suite in eastern Canada, and the setting of the Voisey's Bay Ni-Cu-Co sulphide deposit. *Geoscience Canada*, 24(4; 4), 173-188. Retrieved from
<http://search.ebscohost.com/login.aspx?direct=true&AuthType=ip,url,uid&db=geh&AN=1998-022986&site=ehost-live&scope=site;>
<http://www.gac.ca/JOURNALS/geocan.html>

Ryan, B. (2000). The Nain-Churchill boundary and the Nain Plutonic Suite; a regional perspective on the geologic setting of the Voisey's Bay Ni-Cu-Co deposit. *Economic Geology and the Bulletin of the Society of Economic Geologists*, 95(4; 4), 703-724. Retrieved from
<http://search.ebscohost.com/login.aspx?direct=true&AuthType=ip,url,uid&db=geh&AN=2000-054360&site=ehost-live&scope=site;> <http://www.segweb.org/journal.htm>

Scoates, J. S., & Mitchell, J. N. (2000). The evolution of troctolitic and high al basaltic magmas in Proterozoic anorthosite plutonic suites and implications for the Voisey's Bay massive Ni-Cu sulfide deposit. *Economic Geology and the Bulletin of the Society of Economic Geologists*, 95(4; 4), 677-701. Retrieved from
<http://search.ebscohost.com/login.aspx?direct=true&AuthType=ip,url,uid&db=geh&AN=2000-054359&site=ehost-live&scope=site;> <http://www.segweb.org/journal.htm>

Simmons, K. R., Wiebe, R. A., Snyder, G. A., & Simmons, E. C. (1986). U-Pb zircon age for the Newark Island layered intrusion, Nain anorthosite complex. [Abstract]. *Geological Society of America*, 18 751.

Streckeisen, A. (1974). Classification and nomenclature of plutonic rocks recommendations of the IUGS subcommission on the systematics of igneous rocks. *Geologische Rundschau*, 63(2), 773-786.

Vale Newfoundland and Labrador. (2013). *Nineteenth year assessment report on geological, geophysical and geochemical exploration on claims in the Voisey's Bay area, northern Labrador*. St. John's: Department of Natural Resources, Government of Newfoundland and Labrador.

Wardle, R. J. (1995). In Wilton D. H. C., et al (Eds.), *The geology and mineral deposits of Labrador: A guide for the exploration geologist*. Centre for Earth Resources Research, Memorial University of Newfoundland, St. John's: Geological Survey, Department of Natural Resources, Government of Newfoundland and Labrador.

- Wardle, R. J., Gower, C. F., Ryan, B., Nunn, G. A. G., James, D. T., & Kerr, A. (1997). *Geological map of Labrador; 1: 1 million scale.* (Geological Survey, Map 97-07 ed.) Government of Newfoundland and Labrador, Department of Mines and Energy.
- Yu, Y., & Morse, S. A. (1993). $^{40}\text{Ar}/^{39}\text{Ar}$ chronology of the Nain anorthosites, Canada. *Canadian Journal of Earth Sciences = Revue Canadienne Des Sciences De La Terre*, 30 (6), 1166-1178. Retrieved from <http://search.ebscohost.com/login.aspx?direct=true&AuthType=ip,url,uid&db=geh&AN=1993-046004&site=ehost-live&scope=site>

2. Chapter 2 – Major, trace and oxygen isotope geochemistry of biotite in troctolite from the Voisey’s Bay Ni-Cu-Co deposit and Mushuau Intrusion, Labrador

ABSTRACT

The Voisey’s Bay troctolite and associated mafic intrusives, collectively the so-called Voisey’s Bay Intrusion (VBI), are the main host rocks for the nickel-copper-cobalt sulphide mineralization at the Voisey’s Bay deposit in northern Labrador. The mafic rocks occur in three environments, *viz.*; a) as the dominant phase in large layered magmatic chambers, b) as younger feeder dykes above and below the chambers and c) as chilled margins to both chamber and feeder troctolites. Biotite, a hydroxyl-bearing phase, accounts for up to ten modal percent of the mafic rocks. The igneous mica is the product of crystallization from a residual silicate melt and its spatial association with disseminated sulphides, suggesting a link to a high temperature event associated with the formation of the Voisey’s Bay ore. Scanning electron microscopy and mineral liberation analyses (SEM-MLA) were used to map mineralogical associations of biotite with other mineral phases and to define the overall biotite modal concentrations in samples collected for this study. Biotite is coarser-grained and modally more abundant in feeder rocks, where it preferentially rims blebby and disseminated sulphide and oxide phases. Electron probe (EMPA) microanalyses determined major and trace element data for biotite from different host rocks. There are distinct spatial variations in F and Ni contents of biotite between the chamber rocks. The highest nickel concentrations are in biotite from the Eastern Deeps chamber. Stable isotope analyses ($\delta^{18}\text{O}$) of biotite separates defined variations between the different deposits of the Voisey’s Bay Intrusion (VBI). $\delta^{18}\text{O}$ ratios of biotite in the

Western Deeps chamber and Mushuau intrusion are enriched relative to the meteoric water value (5.7‰), whereas $\delta^{18}\text{O}$ ratios of biotite in the Eastern Deeps, Discovery Hill and Ovoid are depleted relative to this value.

2.1. Property Geology

To date, an investigation of the chemistry of biotite from the Voisey's Bay and Mushuau troctolites has not been carried out. Trace element compositions of biotite from the two intrusions (specifically Ni) are important because of their ability to monitor ore forming processes as they relate to the evolution of magmatic systems. Stable element isotope analyses of biotites are used to evaluate differences in the water contained within the crystalline structure of the silicate melt across the Voisey's Bay deposit.

2.1.1. Regional Geology

The Voisey's Bay and Mushuau intrusions are early magmatic components of the 1.34 to 1.29 Ga Nain Plutonic Suite (NPS), located in the central part of the suite (Fig. 2-1). The NPS is comprised of anorogenic granite, anorthosite, diorite, layered troctolite, norite, and gabbro. Igneous members of the suite intruded through and along the east-dipping, 1.85 Ga collisional suture between the Archean Nain and Paleoproterozoic Churchill Provinces (see Figure 2-2 after Ryan, 1995). The Voisey's Bay intrusion essentially straddles this suture, whereas the Mushuau intrusion mainly occurs within the Nain Province.

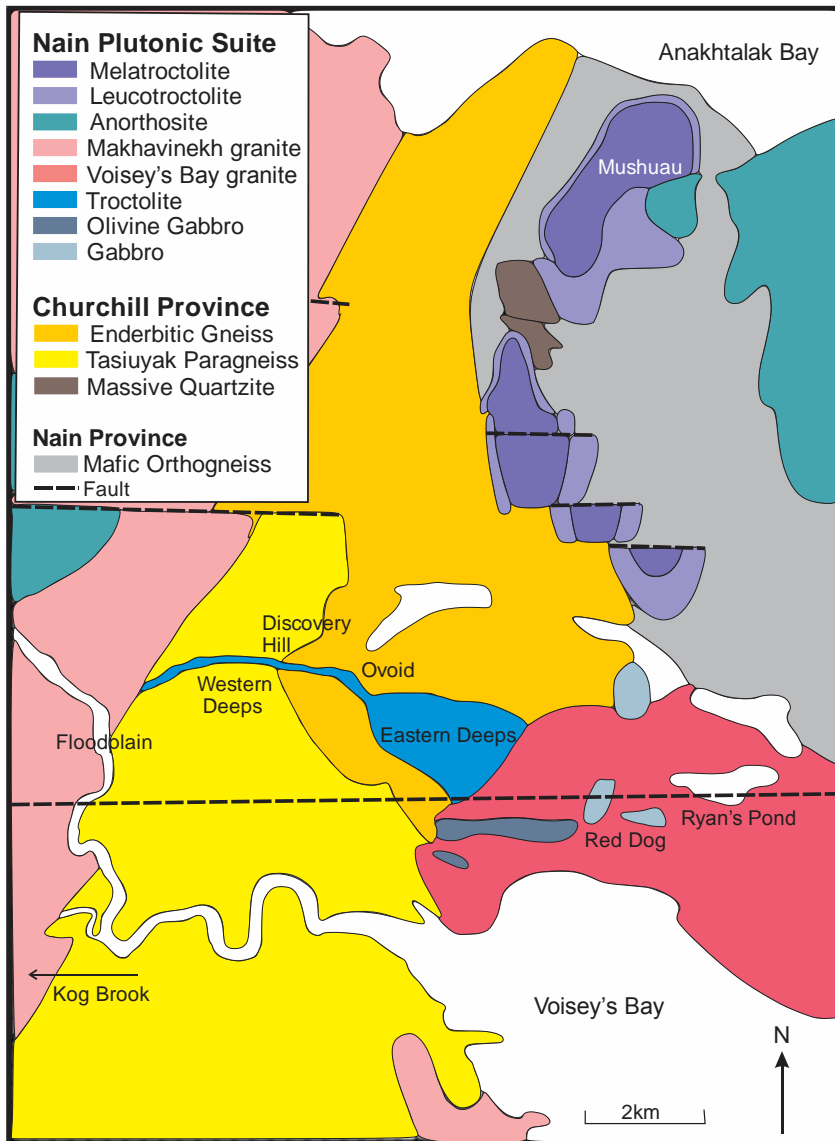


Fig. 2-1. Geologic map of the Voisey's Bay region – modified after Ryan et al. (2000). The Voisey's Bay mineral deposits are hosted within the blue troctolitic rocks of the VBI. The VBC occurs at the suture between the Archean Nain Province in the east (grey) and the Paleoproterozoic Churchill Province in the west (yellow).

2.1.2. Voisey's Bay and Mushauau intrusions

The Voisey's Bay deposit (Fig. 2-3) consists of several different components, including: (1) an upper troctolite chamber (the Eastern Deeps), which is discretely layered with barren, fragment-poor troctolite in the upper half and fragment-bearing troctolite at

depth (below 600m); (2) a lower chamber termed the Western Deep zone; (3) a steeply north-dipping feeder dyke system that connects the two chambers and which is being mined at surface in the Ovoid and Mini Ovoid zones where it widens; the feeder is exposed at surface in the Discovery Hill zone (Evans-Lamswood et al., 2000; Li et al., 2000). The Ashley, Floodplain and Kog Brook intrusions consist of thick sequences of olivine gabbro and lesser norite, which are both crosscut by rapakivi granite and contain older blocks (xenoliths) of Tasiuyak paragneiss. The Ashley and Kog Brook intrusions are located west of the Western Deep deposits and the Floodplain intrusion is located south of the Western Deep. The Kog Brook intrusion is overlain by a thick cover of overburden and is locally highly fractured with clayey gouge filling fractures. The Kog Brook rocks are locally crosscut by amygdaloidal mafic dykes.

Disseminated and massive sulphides in the Eastern Deep chamber occur in fragment-bearing troctolite and troctolite breccia at the base of a barren or weakly mineralized troctolite chamber (Evans-Lamswood et al., 2000). Massive sulphide mineralization occurs within the chamber along the feeder entry line and within the feeder itself near the point of entry into the chamber. The feeder into the Eastern Deep consists mainly of basal breccia, so-called leopard-textured troctolite and massive sulphide with chilled gabbroic margins along the gneissic hanging-wall (Evans-Lamswood et al., 2000). Leopard-textured troctolite contains disseminated and blebby sulphides with black clinopyroxene and olivine oikocrysts that yield a spotted texture to the troctolite.

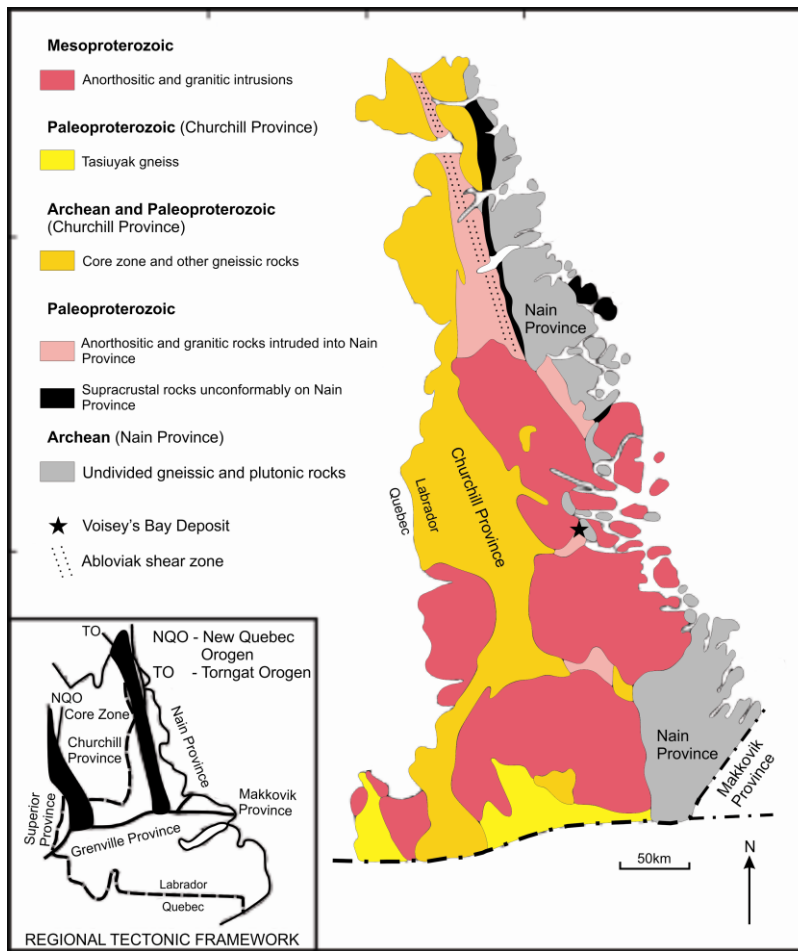


Fig. 2-2. Simplified geological map of coastal Labrador – modified after Ryan (1995). The regional tectonic framework is shown in the bottom left corner and the location of the Voisey's Bay mine site is shown by the black star. The VBC occurs at the suture between the Nain and Churchill Provinces.

The Ovoid massive sulphide deposit is a 110 m thick body underlain by variably mineralized troctolite and a basal breccia sequence all of which is hosted within enderbitic gneiss, the garnet-poor orthogneiss component of the Proterozoic Churchill Province (Naldrett et al., 2000). The Ovoid deposit pinches out to the east and the dyke feeding the system from the north flattens slightly along the north wall contact of the Eastern Deeps chamber (Fig. 2-4). In the Discovery Hill zone, disseminated and local semi-massive sulphides occur in the north-dipping troctolite feeder.

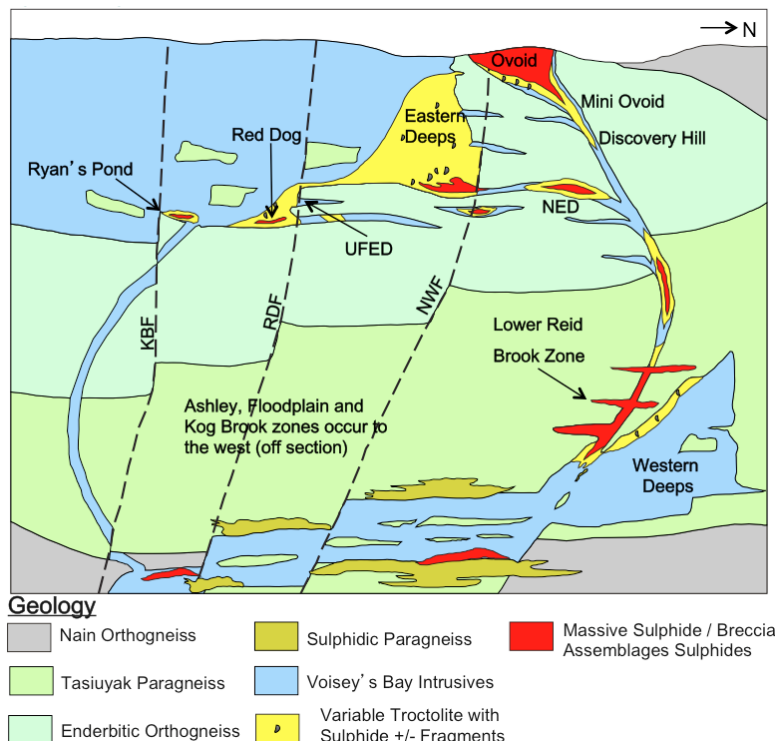
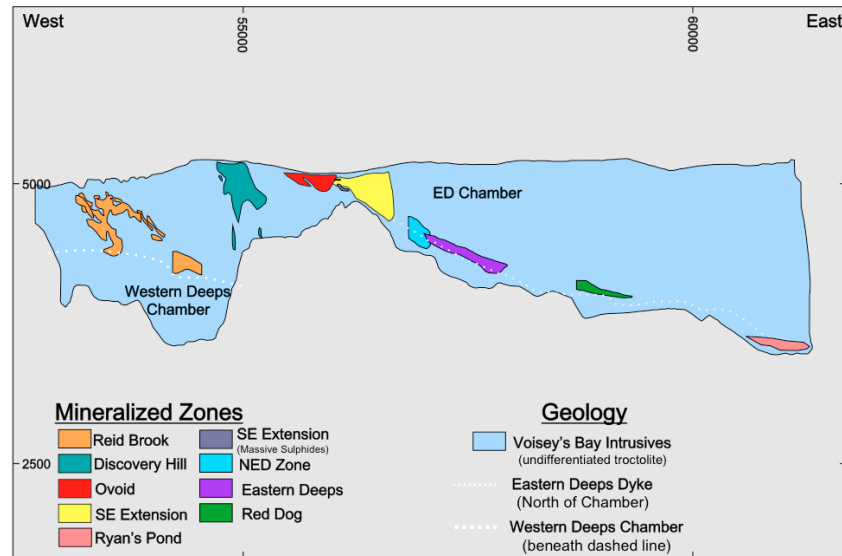


Fig. 2-3. North- (top) and west-facing (bottom) cross sections of the Voisey's Bay Intrusions (VBI). Mineralized zones are displayed with various colours on the north-facing section and the Voisey's Bay Intrusives are shown in pale blue. The Eastern Deeps dyke, which feeds the Eastern Deeps chamber from the north and intersects the base of the Eastern Deeps chamber, is shown by a white dotted line. The approximate top of the Western Deeps chamber is shown by the white dashed line at the base of the Reid Brook mineralized zone. The west-facing cross section highlights the occurrence of the massive sulphide deposits, the disseminated sulphide zones and the troctolitic-gabbroic intrusions within the paragneiss and orthogneiss country rock (Vale, 2013).

The margins of the feeder are fine grained, sulphide-poor, chilled gabbronorite, which grade into diorite. The centre of the feeder dyke is composed of weakly to moderately mineralized (10-35% sulphide minerals) fragment-bearing norite and olivine norite. Where the feeder widens toward surface, norite grades into leopard-textured diorite that contains oikocrysts of pyroxene and hornblende and massive sulphide veins. Fragments of Tasiuyak gneiss country-rock occur in zones subparallel to the walls of the conduit and these zones are referred to as feeder breccia (Li et al., 2000).

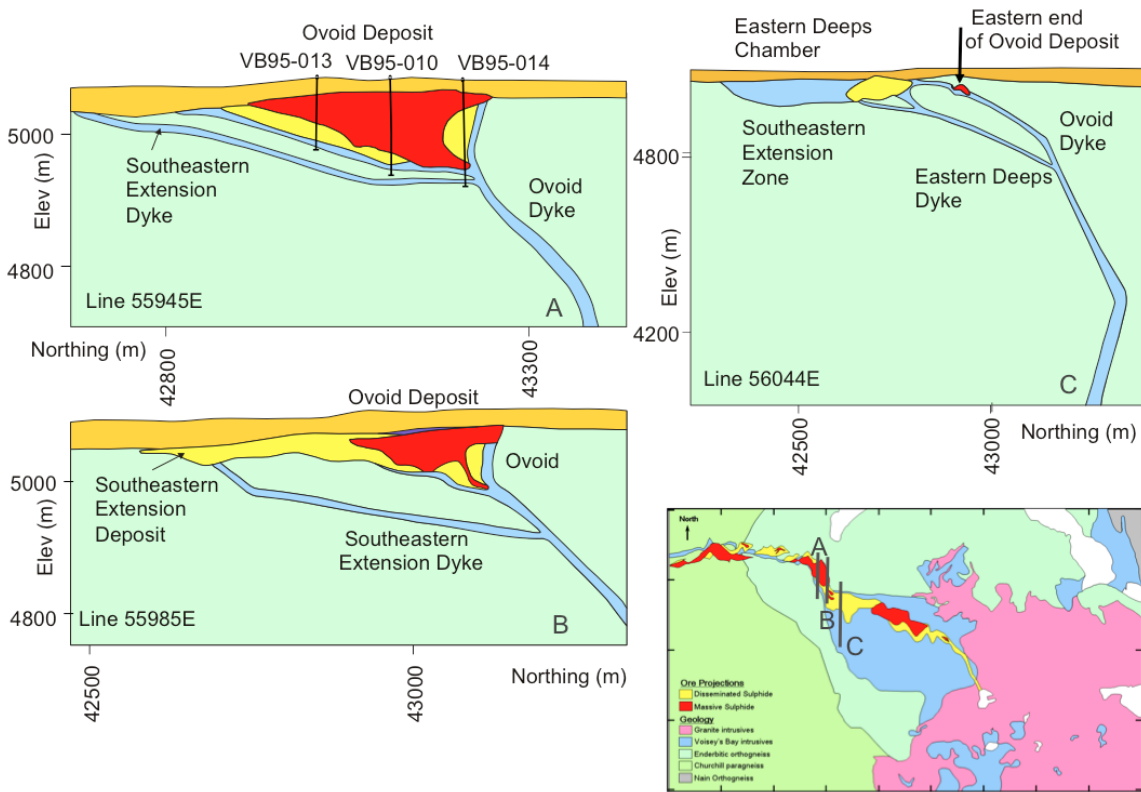


Fig. 2-4. Geological relationship between the Ovoid and Eastern Deeps deposits. The Ovoid and Mini Ovoid massive sulphide deposits (A) are currently being mined at surface and are contained within a swell of the gabbro feeder dyke. The Ovoid pinches out in the east (B) where the feeder dyke dips steeply to the south and feeds in to the Eastern Deeps chamber (C). Breccia and disseminated sulphide sequences occur along this feeder entry line at the western extent of the Eastern Deeps chamber (Vale, 2013).

Sulphide mineralization in the Western Deep zone occurs in the feeder dyke as leopard-textured troctolite and breccias and as massive sulphide lenses that fill fractures and planes of weaknesses in the S-fabric of the Churchill Province paragneiss, which hosts the dyke. In the dyke, the leopard-textured mineralization grades downwards into weakly mineralized norite and breccias (mentioned above) (Li et al., 2000).

The Mushau intrusion is a basin-shaped troctolitic body hosted by Nain Province orthogneiss. It has been dated at *ca.* 1.313 Ga, approximately 20 million years younger than the 1.33 Ga Voisey's Bay intrusion (Li et al., 2000). The Mushau (Fig. 2-2) has a central melatrotroctolite core, which passes outward to a coarse-grained, purple-grey leucotrotroctolite margin. Both varieties of troctolite are massive and homogeneous except for local gneissic fragments and blotchy sulphides (Li et al., 2000).

Sulphide mineralization in the Ashley, Floodplain and Kog Brook zones consists of trace fine-grained disseminations in olivine gabbro. Massive sulphide deposits similar to those observed in the Western Deep have not yet been discovered in these zones.

2.2. Petrography and mineralogy

The modal mineralogies of the Voisey's Bay and Mushau lithologies sampled for this study and their relative spatial locations are briefly described below and summarized in Table 2-1. A plan map showing the location of individual drill holes sampled can be found in Appendix B. The nomenclature used in this study varies slightly from the original rock names given to the mafic lithologies of the NPS (as logged by Vale geologists). The new rock names herein are based on the exact MLA identification of

minerals (and their modal percentages in individual samples) using the IUGS classification scheme (Streckeisen, 1976; Streckeisen, 1974; Le Bas and Streckeisen, 1991). Additional photomicrographs of individual thin sections and Streckeisen's classification diagrams constitute Appendix A.

2.2.1. Voisey's Bay Intrusion

Troctolite, as observed across the main deposit area in the samples from this study, occurs in the Eastern Deeps, Western Deeps and Mushau chambers, but is absent from the VBI feeder dykes. The troctolitic rocks sampled for this study can be broken down into four distinct varieties: 1) troctolite without fragments, 2) troctolite containing up to 5 modal percent fragments (gneissic and/or ultramafic), 3) leopard-textured troctolite, and 4) the melatrotroctolite core and leucotroctolite margin of the Mushau intrusion (discussed in the following section).

VBI troctolite is inequigranular, consisting of cumulus plagioclase (47.32-65.88 wt %) and olivine (9.07-38.26 wt %) with interstitial biotite (2.01-5.82 wt %), hornblende (1.29-13.12 wt %), ilmenite (0.60-8.90 wt %), and sulphide minerals (pyrrhotite, pentlandite and chalcopyrite) (0.08-7.86 wt %). Fragment-poor troctolite is present in the upper portion of the Eastern Deeps chamber and at various depths within the Western Deeps chamber. Troctolite containing fragments was only sampled from the Eastern Deeps and only in the lower half of the chamber. Fragment-bearing troctolite is compositionally the same as other troctolites of the VBI except that it includes up to five modal percent gneiss or mafic-ultramafic fragments. The gneiss inclusions have typically reacted with the troctolitic magma and are partially converted to a variable aluminous

assemblage consisting predominantly of hercynite and plagioclase (Li and Naldrett, 2000). Sulphide minerals in the fragment-bearing troctolite are rounded, blebby and medium to coarse grained, whereas sulphides in fragment-less troctolite are fine-grained and disseminated.

Troctolite (Fig. 2-5) in the Voisey's Bay and Mushuau intrusions (all varieties) is medium- to coarse-grained; plagioclase grains are >3mm long and usually 0.5-1 mm wide and olivine grains are 1-2 mm long and approximately 0.5 mm wide. Interstitial minerals (biotite and minor hornblende) are finer grained, <0.5 mm long/wide. Troctolite from the Eastern Deep and Mushuau is slightly coarser grained than troctolite in the Western Deep. Plagioclase grains are euhedral and the crystals are well developed, whereas olivine crystals are subhedral as some crystal faces abut against the lath-like plagioclase grains. Interstitial minerals are anhedral to subhedral and locally show one or two well-developed crystal faces.

Leopard-textured troctolite (logged and sampled as LEOP) occurs in the lower Eastern Deep chamber as late material injected from the conduit. LEOP contains disseminated and blebby sulphides (41.25 wt %) with clinopyroxene (6.02 wt %) and olivine (3.15 wt %) oikocrysts that give the rock a spotted appearance. Interstitial biotite (4.07 wt %) in these troctolites is medium-grained (average 1 mm long) and also forms rims around the sulphide minerals.

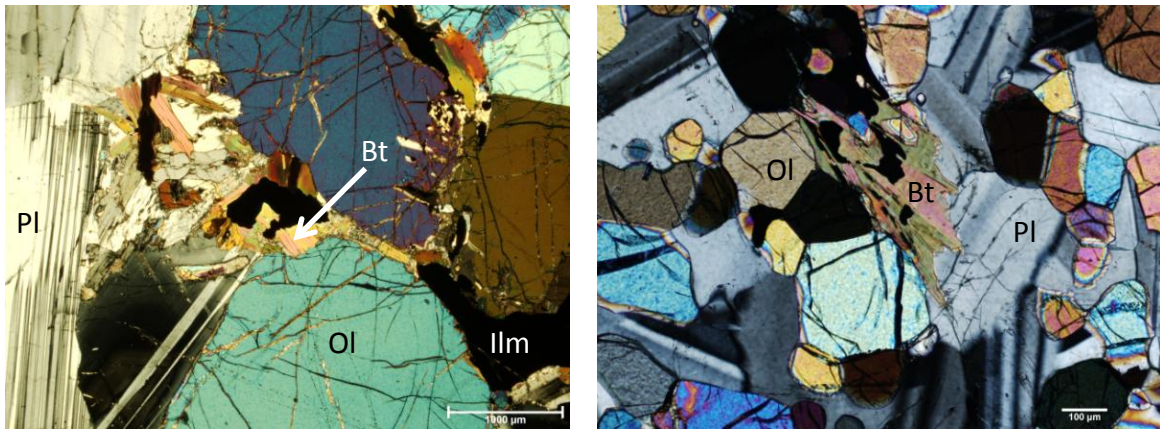


Fig. 2-5. Coarse-grained troctolite (JG-11-047) from the Western Deep chamber (left) and fine-grained melatroctolite (JG-11-134) from the Mushuau intrusion (right). In the troctolite sample coarse-grained olivines are visible near the centre of the photomicrograph. Subhedral, elongate plagioclase laths are visible on the left-hand side of the photomicrograph and the interstitial ilmenite grain near the centre of the photo is rimmed by fine-grained biotite. Fine, subrounded, anhedral grains of cumulus olivine and plagioclase occupy the field of view of the melatroctolite sample from the Mushuau intrusion. The opaque grains are trace, fine disseminations of ilmenite. Pl = plagioclase, Ol = olivine, Bt = biotite, Ilm = ilmenite.

In addition to the troctolitic rocks in the VBI, four other rock types were sampled from chamber and feeder/dyke environments; diorite, norite, olivine norite, and olivine gabbro. Diorite occurs exclusively in feeder rocks of the VBI. Diorite is present in the feeder to the base of the Eastern Deep chamber (Fig. 2-6), the North Eastern Deep feeder, the Ovoid and Discovery Hill zones, and the South East Extension between the Ovoid and Eastern Deep. One diorite sample (JG-11-021) was collected from the Eastern Deep chamber and may represent a failed feeder environment. Diorite is absent from the Western Deep. Diorite contains cumulus plagioclase (41.97-57.05 wt %) with interstitial hornblende (7.52-25.83 wt %), biotite (3.95-14.82 wt %) and lesser interstitial pyroxene. Diorite does not contain significant olivine, however, two samples contain minor amounts of olivine (JG-11-084 and JG-11-089 with 5.20% and 5.71% olivine, respectively). Diorite from the Eastern Deep basal feeder is medium-grained with plagioclase laths

approximately 1.5 mm long. Interstitial hydrous minerals (hornblende, biotite) and pyroxene are fine grained and typically <0.2 mm long/wide. Diorite in the South East Extension is also medium grained. Diorite in the NED feeder is fine grained and plagioclase is partially saussuritized and cloudy. Diorite from Discovery Hill and near the Ovoid massive sulphide deposit is fine grained and pervasively weakly altered. Typically, diorite in the Eastern Deeps feeder contains more plagioclase and biotite than the other varieties of diorite. Sulphide minerals are present in trace quantities in this rock type, typically as fine to medium-grained disseminations. Compared to the troctolitic rocks described above, diorite in the VBI contains significantly more “other” mineral phases. The presence of “other” minerals could be attributed to one of several things, including: the presence of fragments (gneissic, mafic-ultramafic, etc.) within the diorite, compositional variation across the intrusion, weak alteration, and the influence of or proximity to mineralized zones.

Table 2-1. Mineralogical composition (weight %) of the lithological units sampled in the Voisey's Bay and Mushuaau intrusions, as determined by MLA mapping. Locations are WD = Western Deep, (N)ED = (North) Eastern Deep, MU = Mushuaau, DH = Discovery Hill, SE = south east extension, OV = Ovoid, AF = Ashley/Floodplain, RP = Ryan's Pond, KB = Kog Brook.

Lithology	Sample	Mineralogy determined by MLA (weight percent)							Location	Depth	
		Plag	Olv	Opx	Cpx	Hbl	Biot	Sulph	Oxide		
Troctolite (no fragments)	JG11-001	60.2	23.1	2.6	1.9	6.6	2.0	0.1	0.9	2.6	ED
	JG11-003	62.7	17.6	3.7	1.7	9.1	2.0	0.1	0.6	2.5	ED
	JG11-012	61.7	13.7	4.0	4.6	3.9	4.2	1.8	2.6	3.6	ED
	JG11-035	60.7	20.3	6.2	1.8	1.3	3.6	0.2	2.7	3.2	WD
	JG11-042	65.9	19.7	3.6	2.2	1.5	3.3	0.1	1.4	2.3	WD
	JG11-044	57.3	12.6	7.9	3.6	2.0	4.3	0.2	6.6	5.6	WD
	JG11-047	47.3	38.3	2.1	2.2	0.7	3.7	0.2	3.8	1.7	WD
Troctolite (trace-5% fragments)	JG11-006	55.5	9.7	3.3	1.9	7.7	2.5	7.9	8.9	2.7	ED
JG11-016	57.1	9.1	5.0	1.0	11.0	5.8	4.3	4.1	2.7	2.7	ED
JG11-024	59.2	14.2	5.2	2.2	13.1	2.5	0.2	0.9	2.5	ED	Chamber
Leopard troctolite	JG11-017	20.1	3.2	4.6	1.4	13.3	4.1	41.3	8.4	3.7	ED
Mela- troctolite	JG11-134	48.3	43.8	0.1	3.3	2.0	0.2	0.1	1.1	1.2	MU
Leuco- troctolite	JG11-137	84.3	2.3	3.2	3.0	1.3	2.0	0.1	1.8	2.1	MU
Diorite	JG11-021	55.1	0.0	11.4	1.0	11.3	12.3	0.2	1.0	7.7	ED
	JG11-072	57.1	0.0	9.7	0.1	9.1	13.0	0.1	6.0	4.9	ED
	JG11-075	42.7	0.0	6.9	0.0	17.7	12.7	0.3	8.4	11.3	ED
	JG11-076	52.9	0.0	3.3	5.2	9.6	11.2	1.9	9.1	6.8	ED
	JG11-084	50.4	5.2	4.2	4.8	7.5	9.4	0.4	11.7	6.4	NED
	JG11-086	44.2	0.0	0.1	2.2	18.1	4.0	14.4	0.2	16.8	Feeder
	JG11-037	42.0	0.0	1.4	0.9	13.2	9.0	1.7	5.8	26.1	DH
	JG11-088	49.9	0.5	7.0	1.8	17.1	6.9	2.3	2.5	9.1	SE
											Feeder
											30m

	JG11-089	42.4	5.7	7.5	1.0	17.8	8.8	3.03	4.9	8.7	SE	Feeder	120m
Norite	JG11-090	45.9	0.0	0.9	2.1	7.8	14.8	0.03	4.1	24.3	SE	Feeder	135m
	JG11-124	44.7	0.1	5.5	0.1	25.8	9.0	0.07	7.9	6.3	OV	Feeder	235m
	JG11-040	62.1	0.1	12.6	1.5	2.3	7.7	0.31	2.0	11.5	WD	Chamber	300m
	JG11-093	51.8	2.3	9.7	1.6	10.8	10.9	0.93	3.0	9.0	DH	Feeder	10m
	JG11-097	34.7	1.0	16.2	0.2	22.2	8.7	1.46	6.1	9.5	DH	Feeder	210m
	JG11-059	55.6	4.2	8.0	1.9	11.9	11.3	0.20	3.7	3.3	AF	Chamber	450m
Olivine norite	JG11-032	61.0	8.2	9.2	0.1	8.9	8.2	0.12	2.1	2.4	WD	Chamber	600m
	JG11-033B	56.1	10.3	15.2	1.9	3.4	5.3	0.57	3.2	4.0	WD	Chamber	700m
	JG11-091	49.1	7.0	7.4	1.4	16.0	6.7	0.35	6.7	5.4	OV	Feeder	230m
	JG11-078	53.8	9.9	8.7	0.1	4.5	5.6	2.95	0.9	13.7	WD	Feeder	240m
	JG11-080	51.6	15.4	5.2	3.5	17.2	2.6	0.16	1.9	2.6	WD	Feeder	300m
Olivine gabbro	JG11-061	39.0	9.9	8.5	6.6	1.2	3.3	0.21	2.7	28.5	AF	Chamber	600m
	JG11-068	33.8	37.0	2.4	12.4	2.6	2.2	0.11	5.8	3.6	AF	Chamber	400m
	JG11-069	45.6	5.7	7.3	12.1	1.8	3.7	18.01	2.3	3.3	AF	Chamber	500m
Gabbro-norite	JG11-100	49.0	0.1	19.5	17.9	2.7	3.6	0.14	1.5	5.7	ED	Chill	435m
	JG11-101	52.1	0.1	13.6	19.8	1.9	2.2	0.13	4.5	5.7	ED	Chill	520m
	JG11-102	48.4	0.0	3.6	8.8	23.0	1.4	0.14	11.3	3.4	ED	Chill	535m
	JG11-104	48.8	0.0	18.4	20.6	2.4	5.3	0.25	1.6	2.7	ED	Chill	800m
	JG11-105	41.7	0.0	13.5	11.5	27.5	2.1	0.25	0.2	3.3	ED	Chill	600m
	JG11-130	49.1	0.0	23.0*	12.2*	1.1	2.0	0.06	4.5	8.1	RP	Chill	250m
	JG11-106	52.3	0.0	0.7	6.4	5.6	18.5	0.02	2.4	14.2	OV	Chill	35m
	JG11-114	34.6	0.1	3.3	31.9	7.5	1.2	2.86	10.6	7.9	WD	Chill	120m
	JG11-125	39.1	0.1	0.2	14.6	14.8	1.7	0.08	3.1	26.5	KB	Chill	170m
	JG11-127	45.8	1.3	2.7	8.3	6.9	4.4	0.32	12.0	18.4	KB	Chill	375m

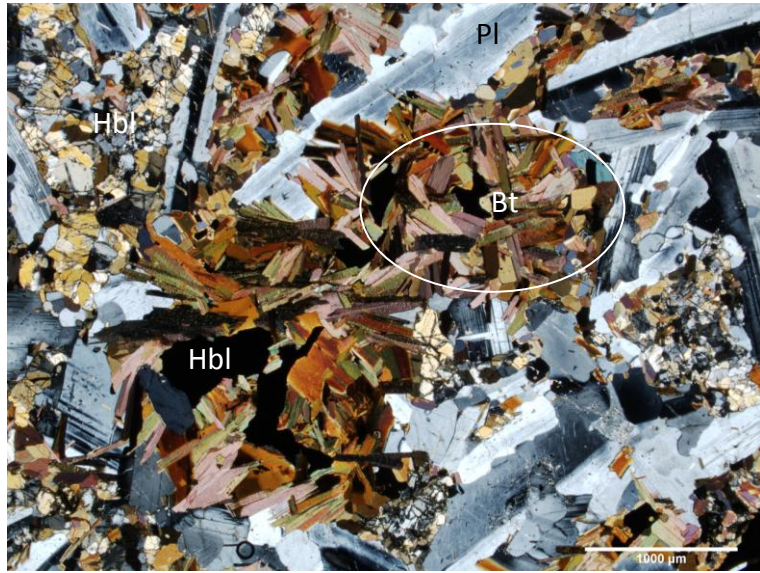


Fig. 2-6. Diorite from the Eastern Deeps feeder (JG-11-076). Subhedral, unaltered cumulus plagioclase framework with large clusters of hydrous interstitial mineral phases including biotite and hornblende. Trace fine ilmenite disseminations. Hbl = hornblende, Bt = biotite, Pl = plagioclase.

Norite occurs in the Western Deeps, Ashley and Floodplain chambers and within the Discovery Hill feeder dyke. Norite contains cumulus plagioclase (34.73-62.05 wt %) with interstitial orthopyroxene (8.02-16.16 wt %), hornblende (10.77-22.15 wt %) and biotite (7.68-11.29 wt %). The Western Deeps chamber sample (JG-11-040), however, contains much less hornblende and is fine-grained, unlike the other norite samples. Individual plagioclase grains are rounded to subrounded (not elongate laths as in the other norite samples) and approximately ≤ 1.5 mm across. Interstitial grains are smaller than the plagioclase framework. Norite from Discovery Hill dyke and Ashley and Floodplain intrusions contain coarse plagioclase grains that are elongate, have sharp grain boundaries and are typically > 1.5 mm long. Interstitial mineral phases are fine to medium-grained. Plagioclase is weakly to moderately altered (possibly saussuritized) and almost sieve-like in appearance in norite from Discovery Hill unlike norite in the chamber environments,

which appears unaltered. Sulphide minerals are present in norite in minor amounts (2.01-6.08 wt %) as fine disseminations.

Olivine norite (Fig. 2-7) is almost identical to norite observed in the VBI except that it contains >7.02 wt % olivine. Olivine norite is present in the Western Deeps chamber (at greater depths than norite) and feeder dyke as well as in the mafic intrusives proximal to the Ovoid massive sulphide deposit.

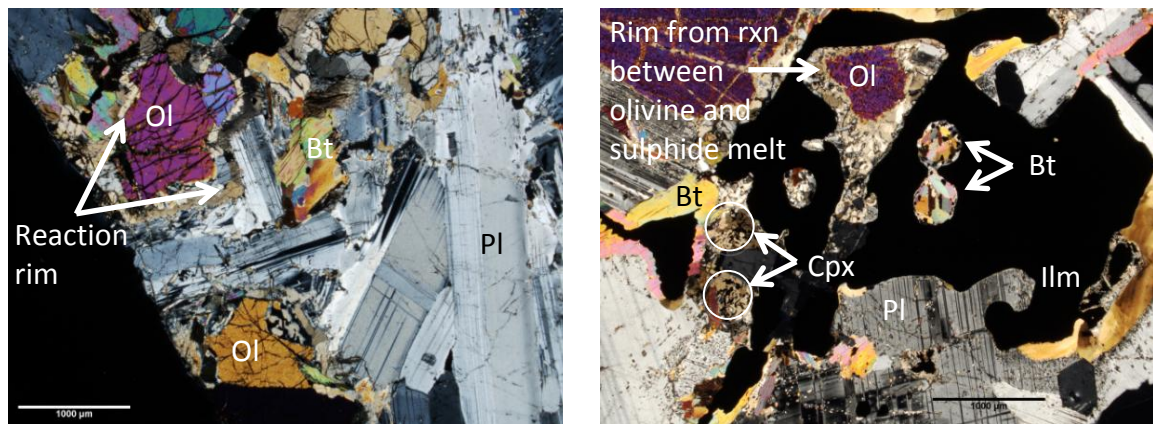


Fig. 2-7. Olivine norite (JG-11-080) from the Western Deeps chamber (left) and olivine gabbro (JG-11-068) from the Ashley intrusion (right). The olivine norite (left) is coarse grained and euhedral plagioclase laths can be seen in the lower right corner with interstitial hornblende and minor biotite. The coarse olivine grain toward upper left corner is mantled with a pyroxene reaction rim. In the olivine gabbro (right) plagioclase grains enclose large bleb of ilmenite. Olivine oikocryst enclosed within ilmenite has a pyroxene mantle, likely a reaction rim from interaction with melt. Two small blebs of biotite are visible near the centre of the photo and are probably either rims around very fine disseminated sulphide grains or results from incomplete late stage reactions between magmatic liquid and partially crystallized minerals. Ol = olivine, Bt = biotite, Pl = plagioclase, Cpx = clinopyroxene, Ilm = ilmenite.

The final cumulate mafic lithology sampled from the VBI is olivine gabbro (Fig. 2-7), which is only present in the Ashley and Floodplain chambers. This cumulate rock type is coarse-grained (plagioclase grains >2.0 mm long) and homogeneous. Olivine gabbro contains euhedral cumulus plagioclase (33.83-45.61 wt %) and olivine (5.66-36.97 wt %) with interstitial orthopyroxene (2.37-8.52 wt %), clinopyroxene (6.63-12.44

wt %), and trace amounts of magnetite, ilmenite and biotite. Sample JG-11-061 contains some fragmental material and appears to be weakly altered when viewed under petrographic microscope. Some olivine grains in these samples display reaction coronas and are mantled by pyroxene and hornblende, which are interpreted to be due to magmatic reactions between the olivine and melt (Nesse, 2004.) Sulphide minerals are present in olivine gabbro as fine disseminations or as medium-grained (0.6-1.0 mm across) blebs.

The final rock type observed and sampled in this study is gabbronorite, which occurs as chilled margins throughout the VBI. Chilled margins occur in three locations in the VBI: 1) at the contact between diorite-norite feeder dykes and gneissic country rocks, including chills at the base of the Ovoid deposit, 2) chilled margins associated with the injection of leopard troctolite, troctolite breccia and semi-massive sulphide in to the Eastern Deep and Discovery Hill zones, and 3) associated with a later pulse of mafic magma to the Western Deep and Kog Brook zones. Chilled margins are discussed in detail in Chapter 3.

The composition of the chilled marginal rocks varies slightly across the intrusion but generally these rocks contain plagioclase (34.64-52.28 wt %), orthopyroxene (0.15-23.03 wt %), clinopyroxene (6.41-31.90 wt %), and variable amounts of hornblende, biotite and oxide minerals (ilmenite and magnetite). Chilled margins sampled for this study, in general, contain only trace (<3.00 wt %) sulphides and it should be noted that pentlandite accounts for \leq 0.01 wt % of the sulphide minerals in the chills. The only

chilled margin that contained >2.00 wt % sulphides is in direct contact with massive sulphide and may have remobilized some of these minerals from this contact.



Fig. 2-8. Chilled gabbro from the Eastern Deeps (JG-11-101). This chill displays overall inequigranular texture with ragged, slightly elongate plagioclase laths and very fine pyroxene grains. The weak alignment of individual grains is possibly due to flow banding.

Chilled margins are dark-grey to black and moderately magnetic in drill core. In these rocks, randomly oriented, ragged plagioclase laths form a discontinuous framework enclosing anhedral pyroxene oikocrysts and interstitial hornblende, biotite, and magnetite (individual minerals are only visible in thin section). The chilled margins are aphanitic; the largest grains visible under petrographic microscope are the plagioclase laths, which are typically 50-150 μm long. The interstitial minerals are extremely fine-grained (<50 μm) and not easily identifiable petrographically (Fig. 2-8). The chilled margin sample from Ryan's Pond is coarser grained than the other chills but individual mineral grains are still <1.0 mm long (plagioclase) and interstitial minerals are <0.10 mm across.

2.2.2. Mushuau Intrusion

Cumulate melatroctolite (Fig. 2-5) forms the central core and main part of this layered intrusion. It consists of fine-grained plagioclase (48.27 wt %) and olivine (43.80 wt %) with very fine-grained interstitial clinopyroxene (3.28 wt %). Melatroctolite lacks notable biotite (<1.00 wt %). Plagioclase grains have slightly rounded grain boundaries and are not as elongate as in the leucotroctolite component of this intrusion. Biotite crystallized as singular, fine (100 μm), interstitial grains, which locally formed incomplete rims on magnetite and ilmenite grains. Sulphide minerals are present only as trace amounts in melatroctolite although small semi-massive sulphide veins have been intersected in the melatroctolite member of the Mushuau intrusion at depth.

Leucotroctolite forms a margin around the melatroctolite core of the Mushuau intrusion. It is composed of medium to coarse-grained, purple, plagioclase laths (84.28 wt %) with interstitial olivine (2.28 wt %) and accessory biotite (1.95 wt %). Plagioclase laths are typically >2 mm long, whereas biotite and olivine grains approach 1mm lengths, giving rise to a coarse-grained rock. The plagioclase crystals define massive cumulate textures and are locally oriented subparallel to one another, forming short chains or rafts. Interstitial biotite is typically associated with ilmenite and minor magnetite. Sulphide minerals are present in the leucotroctolite in trace amounts as fine disseminations.

2.3. Biotite chemistry

One hundred and fourty-six (whole rock) samples were collected for this study of biotite in the mafic rocks of the Voisey's Bay and Mushuau intrusions. Detailed

mineralogical maps highlighting the relationship of biotite to other minerals were derived for forty-nine of these 146 samples using Mineral Liberation Analysis (MLA) techniques. The master sample list and grain boundary maps obtained from MLA constitute Appendix B. The 49 samples were selected based on observations made during petrographic analysis. The mineralogical grain boundary maps were used to identify biotite grains suitable for electron microprobe analysis (EPMA) and biotite grains from 37 samples were actually analyzed; samples selected for electron microprobe analysis are summarized in Table 2-2 and mean compositions of biotite samples from this study are summarized in Table 2-5 at the end of this chapter. The range, mean and median compositions of biotite from the troctolitic and gabbroic rocks constitute Appendix E.

2.3.1. Biotite major element chemistry

Biotite from both the Voisey's Bay and Mushau intrusions is unzoned, and along with intergrowths with other silicate rock-forming minerals, shares grain boundaries with oxide and sulphide minerals. Both cores and rims of biotite grains were analyzed via electron microprobe (where possible) and no variations in composition were identified. As an interstitial magmatic mineral, its presence suggests that the parental magmas to these lithologies were not dry, but contained sufficient hydroxyl to allow biotite crystallization.

Since the main focus of this study was to define biotite composition, and then to infer the isotopic signatures of water in the parental magmas of the Voisey's Bay Intrusion, it first had to be demonstrated that the biotite grains analyzed were of primary igneous origin. Figure 2-9 compares the compositions of the analyzed biotites with

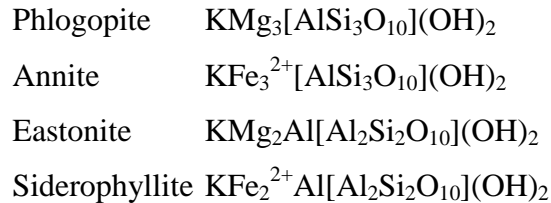
petrogenetic fields derived by Fleet (2003) from Deer et al. (1962) (data for biotite and Mg-rich phlogopite) and Miyano & Miyano (1982) (data for trioctahedral micas with $[^{44}\text{Fe}^{3+}]$). All Voisey's Bay and Mushuau biotite grains plot in the igneous field with greater than 60 mol % FeO, MnO and MgO (summed) and no more than 40 mol % CaO, Na₂O, K₂O (summed) or 40% Al₂O₃. The majority of biotite from the Voisey's Bay and Mushuau troctolites is of the Mg-rich phlogopite variety (yellow field on Fig. 2-9) with only a few samples plotting outside this field (though still within the igneous biotite field). The samples that plot outside the phlogopite field are from chilled marginal rocks. None of the biotite plots within the metamorphic biotite field.

Table 2-2. Sample list including sample locations, sample number, geologic setting of sample, lithology of host rock, number of biotites probed (per PTS), and whether oxygen isotope analyses were completed. The two chilled margin samples which were analyzed for O-isotope ratios are JG-11-116 and JG-11-130. JG-11-116 was not probed and so is not listed in this table. JG-11-130 was probed so is listed in this table. Oxygen isotope ratios for all samples analyzed are summarized in Table 2-4 and plotted on Fig. 2-11.

Location	Zone	Sample	Setting	Lithology	#Biotites probed	O-isotope analysis
Eastern Deeps	<i>Eastern Deeps</i>	JG-11-001	Chamber	Troctolite	25	Yes
		JG-11-003	Chamber	Troctolite	10	Yes
		JG-11-006	Chamber	Troctolite	10	Yes
		JG-11-012	Chamber	Troctolite	7	Yes
		JG-11-016	Chamber	Troctolite	16	No
		JG-11-017	Chamber	Leopard troc	11	No
		JG-11-021	Chamber	Diorite	15	No
		JG-11-024	Chamber	Troctolite	18	Yes
		JG-11-072	Feeder	Diorite	27	Yes
		JG-11-075	Feeder	Diorite	14	Yes
		JG-11-100	Chill	Gabbronorite	7	No
		JG-11-102	Chill	Gabbronorite	4	No
	<i>N. Eastern Deeps</i>	JG-11-084	Feeder	Diorite	15	Yes
	<i>Ryan's Pond</i>	JG-11-130	Chill	Gabbronorite	6	Yes
Western Deeps	<i>Discovery Hill</i>	JG-11-037	Feeder	Diorite	21	No
		JG-11-093	Feeder	Norite	10	Yes
		JG-11-091	Feeder	Olivine norite	9	Yes
		JG-11-106	Chill	Gabbronorite	10	No
	<i>Western Deeps</i>	JG-11-032	Chamber	Olivine norite	17	Yes
		JG-11-033	Chamber	Olivine norite	13	Yes
		JG-11-035	Chamber	Troctolite	9	Yes
		JG-11-040	Chamber	Norite	16	No

Location	Zone	Sample	Setting	Lithology	#Biotites probed	O-isotope analysis
		JG-11-042	Chamber	Troctolite	10	No
		JG-11-044	Chamber	Troctolite	11	No
		JG-11-047	Chamber	Troctolite	12	Yes
		JG-11-078	Feeder	Olivine norite	12	No
		JG-11-080	Feeder	Olivine norite	12	Yes
		JG-11-089	Feeder	Diorite	10	Yes
		JG-11-114	Chill	Gabbronorite	6	No
	Kog Brook	JG-11-127	Chill	Gabbronorite	8	No
Ashley Floodplain		JG-11-059	Chamber	Norite	19	No
		JG-11-061	Chamber	Olivine gabbro	19	No
		JG-11-068	Chamber	Olivine gabbro	20	No
		JG-11-069	Chamber	Olivine gabbro	15	No
Mushauu		JG-11-134	Chamber	Melatroctolite	14	No
		JG-11-137	Chamber	Leucotroctolite	9	Yes

Biotite compositions are defined by phlogopite-annite-eastonite-siderophyllite end members (Fig. 2-6) (Fleet, 2003). Chemical formulae for the biotite series are:



Biotite forms an almost complete isomorphous series between phlogopite and annite with partial solid solutions of eastonite, siderophyllite, tetra-ferriphlogopite, and tetra-ferriannite end members (Fleet, 2003). Phlogopite is more typical of ultramafic igneous rocks, whereas annite is typical of magnesium-poor igneous and metamorphic rocks (Fleet, 2003). Siderophyllite typically occurs in felsic pegmatitic rocks and forms a partial solid solution series with eastonite. Eastonite, as described by Winchell (1925), represents a hypothetical dialuminum magnesium mica and lacks true natural representatives (Geological Survey Professional Paper, 1959).

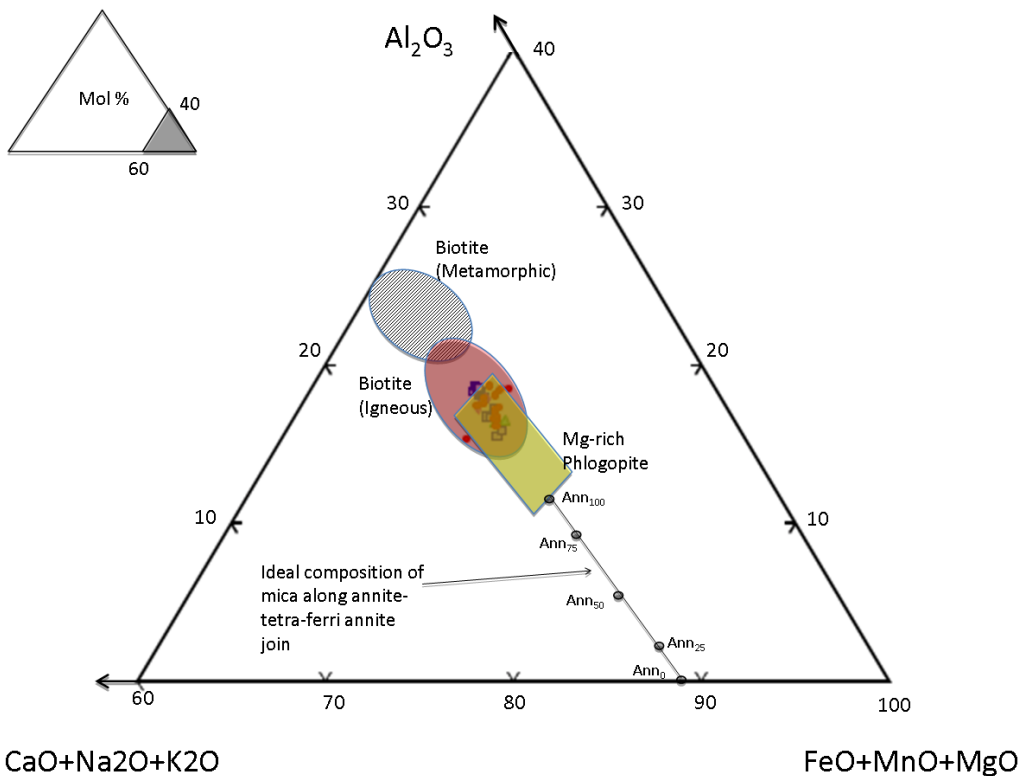
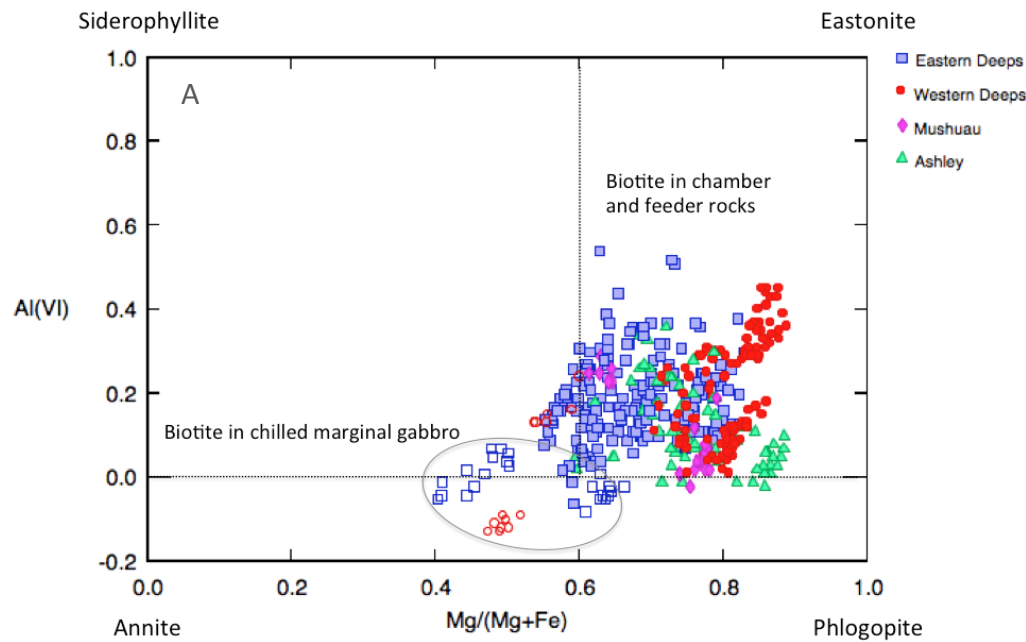


Fig. 2-9. Ternary diagram showing the origin of Voisey's Bay and Mushuau biotite. All biotite probed falls within the red igneous biotite field and most occurs in the overlap with the yellow Mg-rich phlogopite field. Biotite samples which plot outside the Mg-rich phlogopite field are from chilled marginal rocks. Secondary biotite (alteration biotite) would have fallen outside the stability fields for igneous or metamorphic biotite and would have plotted with $\text{CaO}+\text{Na}_2\text{O}+\text{K}_2\text{O} > 40$ mol % and $\text{Al}_2\text{O}_3 > 40$ mol % (modified after Miyano and Miyano, 1982; in Fleet, 2003).

Furthermore, the name eastonite had been previously given by Hamilton (1899) to vermiculite occurring in the same locality as an alteration product of biotite and by Livi and Veblen (1987) to describe a serpentine-phlogopite intergrowth. As such, it is recommended that the name “eastonite” be discarded as referring to natural trioctahedral mica and retained only as a hypothetical end-member (Geological Survey Professional Paper, 1959). For this reason, eastonite will not be considered an appropriate biotite end-member for this study. For the most part, biotite from the Voisey's Bay and Mushuau

mafic intrusives (troctolite, diorite, norite) is phlogopitic, as illustrated by Figure's 2-10A and 2-10B. Biotite in troctolite and norite from the Eastern Deepes and Western Deepes plots in several distinct clusters along the ideal biotite plane (Fig.'s 2-10 and 2-11), especially when grouped based on host environment (i.e. chamber, feeder, or chilled margin) (Fig. 2-10B). The most magnesian biotite is from olivine gabbro associated with the Ashley and Floodplain intrusions. Ferrous biotite occurs in the chilled margin rocks. There are two distinct chemical species of biotite in feeder rocks; one from the Western Deepes (higher Mg number) and the other from the Eastern Deepes (lower Mg number) respectively (Fig. 2-10A & 2-10B).



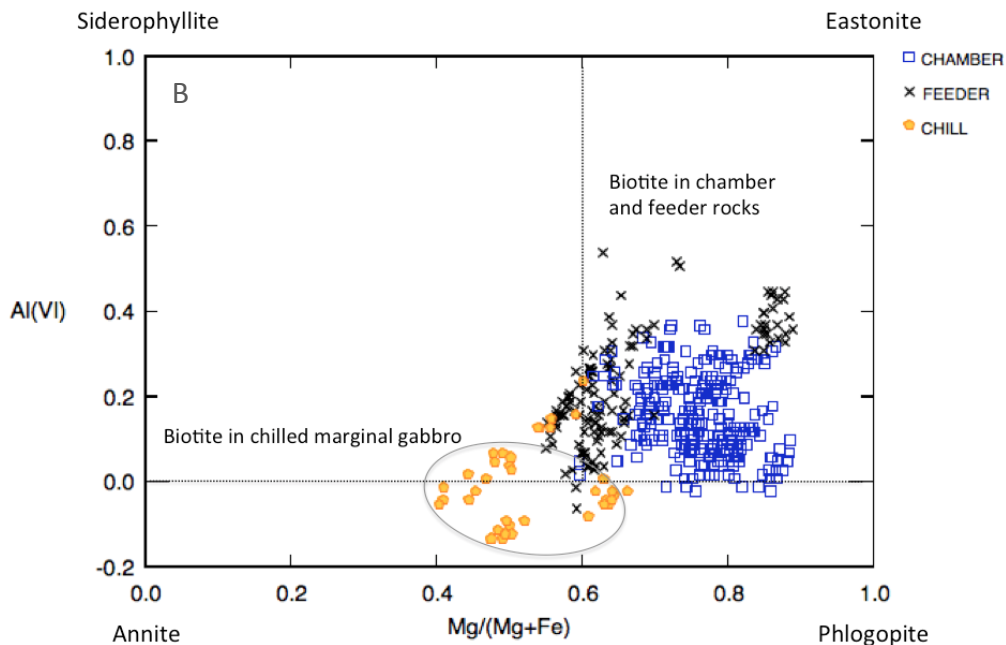


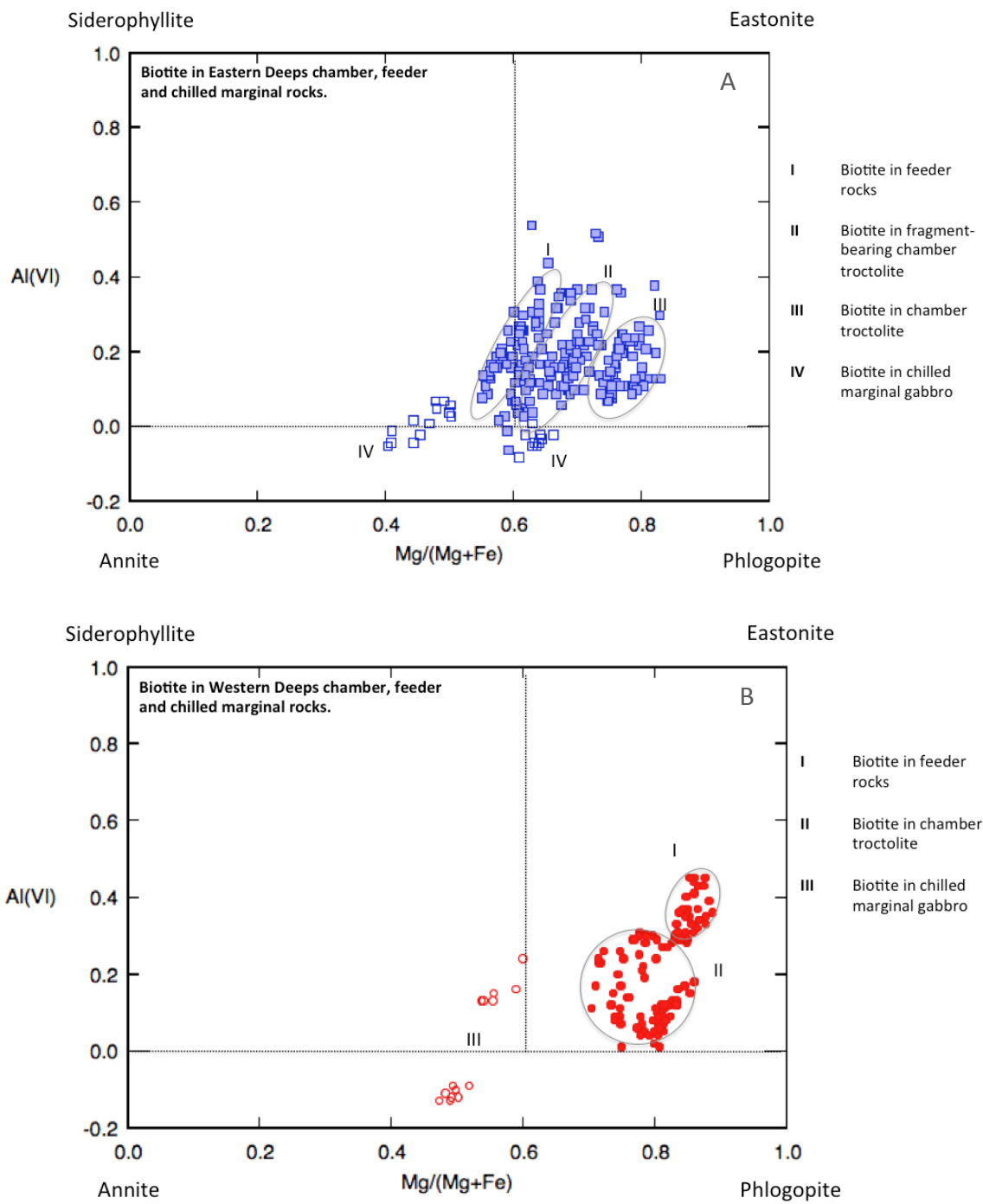
Fig. 2-10. Voisey's Bay and Mushauau biotite composition. A. Biotite chemistry plot based on location. Open symbols represent biotite from chilled margins (open red circles are biotite in chilled margins from the Western Deep and open blue squares represent biotite in chilled margins from the Eastern Deep). B. Biotite chemistry plot based on crystallization setting. Biotite forms a complete isomorphous series with annite and phlogopite end members and a partial solid solution with siderophyllite and eastonite end members. Biotite from chamber and feeder rocks plots toward the phlogopite end member. Biotite from chilled marginal rocks plots near the midpoint between annite and phlogopite end members and contains more modal Fe than biotite from chamber and feeder rocks (modified after Guidotti, 1984).

Biotite from chamber and chilled margin environments are clustered in larger groups when looked at in terms of the VBI (Fig. 2-10B) but can be broken out into smaller groups when examined from each individual deposit. There are four clusters of biotite in troctolite sampled from the Eastern Deep and three clusters of biotite in the Western Deep (Fig. 2-11A & 2-11B). The Eastern Deep biotite clusters in: 1) biotite in feeder diorite and norite, 2) biotite in fragment-bearing chamber troctolite, 3) biotite in fragment-less chamber troctolite, and 4) biotite in chilled marginal gabbronorite (Fig. 2-11A). Biotite from chamber rocks (fragment-bearing and fragment-poor) has higher Mg/Mg+Fe values (>0.6) than biotite in feeder rocks and contains Al in octahedral

coordination. Biotite in Eastern Deep feeder diorite and norite is slightly less magnesian than biotite in chamber troctolite. Biotite in chilled margins has even lower Mg/Mg+Fe values and contains Al in tetrahedral versus octahedral coordination.

Biotite from Western Deep troctolite can likewise be subdivided into three groups: 1) biotite in feeder and upper chamber olivine norite, 2) biotite in chamber troctolite, and 3) biotite in chilled margin gabbronorite (Fig. 2-11B). Biotite in troctolite and olivine norite within the Western Deep chamber and feeder has Mg/Mg+Fe values between 0.6 and 0.85 and contains Al in octahedral coordination. Biotite in chilled marginal gabbro from the Western Deep has lower Mg/Mg+Fe values (<0.6) and contains Al in tetrahedral coordination.

Biotite in Mushau troctolite (Fig. 2-11C) plots in two clusters: 1) biotite in the leucotroctolite sample and 2) biotite in the melatrotroctolite sample. Biotite in the more olivine-rich melatrotroctolite is more Mg-rich. Biotite in the plagioclase-rich has Mg/Mg+Fe between 0.6-0.8.



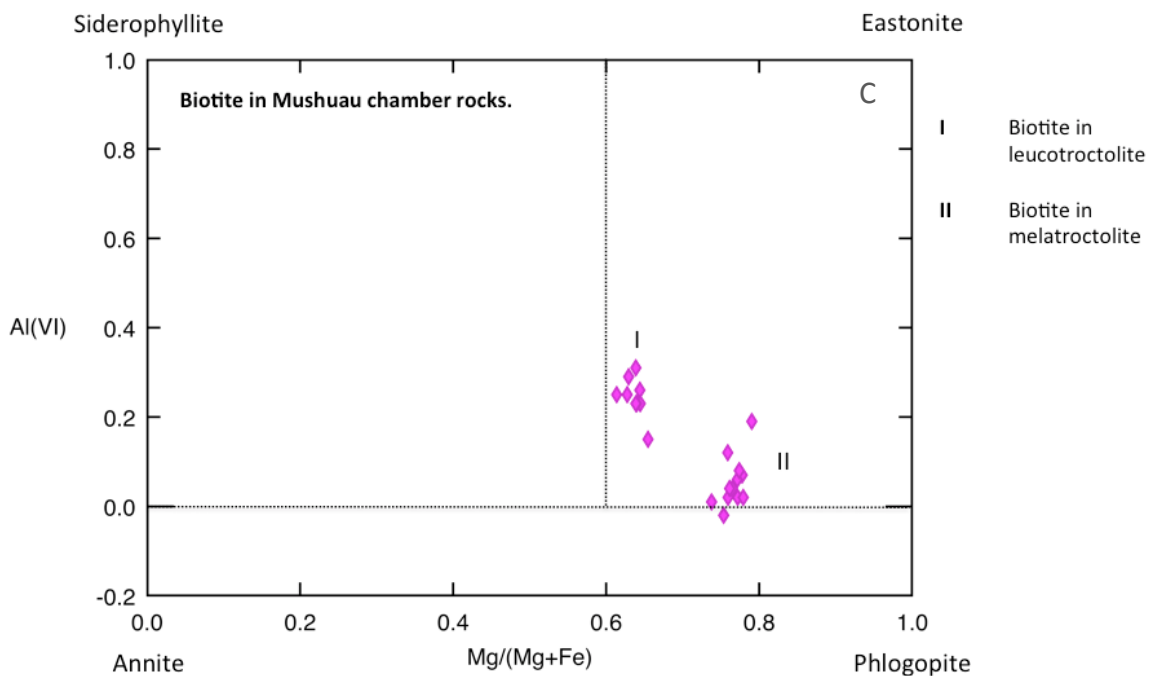


Fig. 2-11. Biotite major element chemistry. A. Eastern Deeps biotite. Biotite in chamber troctolite has a greater Mg/(Mg+Fe) ratio than biotite from feeder gabbro. B. Western Deeps biotite. Biotite in chilled marginal rocks is geochemicall distinct from biotite in chamber and feeder rocks C. Mushuau biotite sampled from leucotroctolite and melatrotroctolite (modified after Guidotti, 1984). Biotite clusters show different chemical varieties of mica based on where the rock hosting the mica is located within the intrusion.

Aluminum can occur in both tetrahedral and octahedral coordination. In high temperature minerals (e.g. feldspar), aluminum is typically in tetrahedral coordination. On the other hand, aluminum typically occurs in octahedral coordination in lower temperature minerals (e.g. kaolinite) (Liese, 1963). According to Buerger (1948), aluminum may have both four- and six-fold coordination in intermediate temperature minerals, such as biotite. As such, the amount of aluminum in tetrahedral coordination is likely a function of temperature of formation and therefore an increase in tetrahedrally coordinated aluminum suggests a higher temperature of formation (Liese, 1963). Biotite in chamber and feeder rocks has significantly more Al in octahedral coordination

compared to biotite in chilled margins. The abundance of biotite in tetrahedral coordination in chilled margins suggests this biotite crystallized at a higher temperature, which is to be expected. Chills formed when a hot magma, which retained significant heat from the parental magma, quenched and crystallized quickly. Normal plutonic rocks in chamber and feeder environments would have lost more heat due to slower cooling and would contain minerals with Al in octahedral coordination.

2.3.2. Biotite trace element chemistry

The covariance of magnesium number ($Mg/Mg+Fe$) vs. F (wt %) and Ni (ppm) vs. F (wt %) in biotite from the Voisey's Bay and Mushau troctolites is shown on Figure 2-12. Maximum and minimum values are summarized in Table 2-3. Although numerous other elements were analyzed, trends and groupings were not noted and so are not discussed here. Where the biotite samples have been discriminated based on host deposit (Fig. 2-12A & 2-12C), several trends are visible on binary plots of magnesium number ($Mg/Mg+Fe$) vs. F (wt %) and Ni (ppm) vs. F (wt %). Roughly half of the biotite in norite and olivine gabbro from the Ashley and Floodplain deposits exhibit elevated F, in the range of 2.50-3.47 (wt %) and is among the most magnesian mica found in Voisey's Bay mafic intrusive rocks. The remaining biotite in the Ashley and Floodplain intrusions has F concentrations similar to biotite in the other deposits. Biotite in troctolite from the Eastern Deeps chamber and in diorite and norite from the Eastern Deeps feeder has the lowest F contents with typical values between 0-0.47 (wt %). There is almost no variation in the F contents of biotite from Eastern Deeps rocks and it is likely not an important volatile phase in the Eastern Deeps (including the feeder rocks of the Ovoid and Discovery Hill).

Biotite in chilled rocks from the Eastern Deep, however, contains fluorine values ranging from 0.700 and 1.75 (wt %). Biotite from the Western Deep plots in three distinct geochemical groups with respect to F and magnesium number. Firstly, low magnesium number and low F biotite from chilled margins typically contains 0-0.88 F (wt %). Secondly low F biotite from Western Deep feeder and chamber rocks contains 0.09-1.09 F (wt %). Rocks from this group contain less plagioclase than the rocks containing more F-rich biotite. The most F-rich biotite in the Western Deep is found in the chamber troctolite and norite and contains 0.670-2.02 F (wt %) and magnesium number values great than 0.800. These rocks contain greater than 60.0 wt % plagioclase.

Table 2-3. Summary of biotite chemistry data plotted on Figure 2-12. This table highlights maximum and minimum values in each deposit and host environment.

Deposit	Environment	F (wt%)		Mg/Mg+Fe (Mg#)		Ni (ppm)	
		Min	Max	Min	Max	Min	Max
Ashley/Floodplain	Chamber	0.91	3.47	0.59	0.88	0.00	460.00
Eastern Deep	Chamber	0.04	0.47	0.67	0.83	329.95	1669.94
	Feeder	0.12	0.32	0.55	0.65	30.02	829.94
	Chill	0.19	1.75	0.40	0.66	40.00	409.94
Mushauu	Chamber	0.51	0.84	0.61	0.79	340.01	610.00
Western Deep	Chamber	0.67	2.02	0.70	0.85	100.03	919.99
	Feeder	0.09	1.09	0.58	0.89	30.02	849.98
	Chill	0.18	0.88	0.44	0.60	70.01	1049.96

Fluorine substitutes for OH in mica. The presence of F depends on the temperature and chemistry of the parent phase and on the metallic ions available in the system (Munoz, 1974). Ramberg (1952) defined a relationship between F, Mg and Fe in silicate mineral lattices in which F/OH ratios are larger in more Mg-rich members (so-called Fe-F avoidance), suggesting that Mg-F bonds are stronger than Fe-F bonds.

There is a slightly positive trend between the magnesium number and F content of biotite in Voisey's Bay mafic intrusives (Fig. 2-12C), with the more magnesian samples containing more F, thus, satisfying the Fe-F avoidance principle. Biotite in feeder and chamber rocks associated with the Eastern Deep contains low concentrations of fluorine with some values below the detection limit of the analytical procedure used (Fig. 2-12A & 2-12C). It is apparent from Figure 2-12 that fluorine is a significant component of biotite in the western half of the VBI but it is present only in minimal amounts (near detection limit) in biotite in the eastern half of the intrusion. This could be a characteristic of the parental magma, a late magmatic fluid-rock interaction in the east versus the west of the VBI, anion exchange *via* late hydrothermal activity, or related to temperature of emplacement. It is possible that different processes were acting in the Western Deep, Kog Brook, Ashley, and Floodplain intrusions than in the Eastern Deep, Ovoid, Discovery Hill, and Mushauau intrusions. It is not possible to determine, from the F-content of biotite alone, which process may have controlled the mineral chemistry.

In addition to the variations in major element geochemistry discussed above, biotite from the Voisey's Bay intrusion also exhibits a wide range in Ni (ppm) values (Fig. 2-12B and 2-12D). Biotite in Eastern Deep chamber troctolite displays some of the highest Ni concentrations, up to 1670 ppm. Biotite from this deposit also demonstrates the greatest range of Ni concentrations. Interestingly, biotite from the fragment-bearing troctolite in the Eastern Deep is distinguished by its high nickel content but is not distinguishable based on Mg/Mg+Fe values. This suggests that Ni is available to crystallizing biotite in fragment-bearing magma but not in the other magmas, irrespective of Mg/Mg+Fe. The

fragments must therefore affect the chemistry of the magma so drastically that olivine cannot crystallize, thus Ni stays in the magma and can be incorporated into minerals such as biotite.

Biotite in Eastern Deep feeder diorite and norite contains between 30-830 ppm Ni. The lowest Eastern Deep Ni values occur in biotite from chilled marginal gabbro where values typically range between 40-410 ppm Ni. Biotite in chamber troctolite from the Ashley/Floodplain and Mushaua intrusions contains 0-460 and 340-610. ppm Ni respectively. Biotite within Western Deep chamber troctolite and norite contains between 100-920 ppm Ni. Biotite within feeder rocks in the Western Deep contains similar Ni contents to biotite from the feeders in the Eastern Deep with values ranging from 30-850 ppm Ni. Unlike biotite within chilled marginal gabbros in the Eastern Deep, biotite within chills in the Western Deep contains significant nickel with typical values ranging between 0-1050 ppm Ni. In summary, the highest overall Ni content is observed in biotite within troctolite in the Eastern Deep chamber and in biotite from chilled marginal gabbros in Western Deep.

Biotite with higher Mg/(Mg+Fe) ratio could have crystallized from an early magma pulse, which was followed by a more evolved pulse of magma containing fragments of country rock and eventually sulphide liquid. The highest nickel values are seen in biotite with moderate Mg# suggesting an increase in the Ni content is associated with a secondary pulse of more evolved magma.

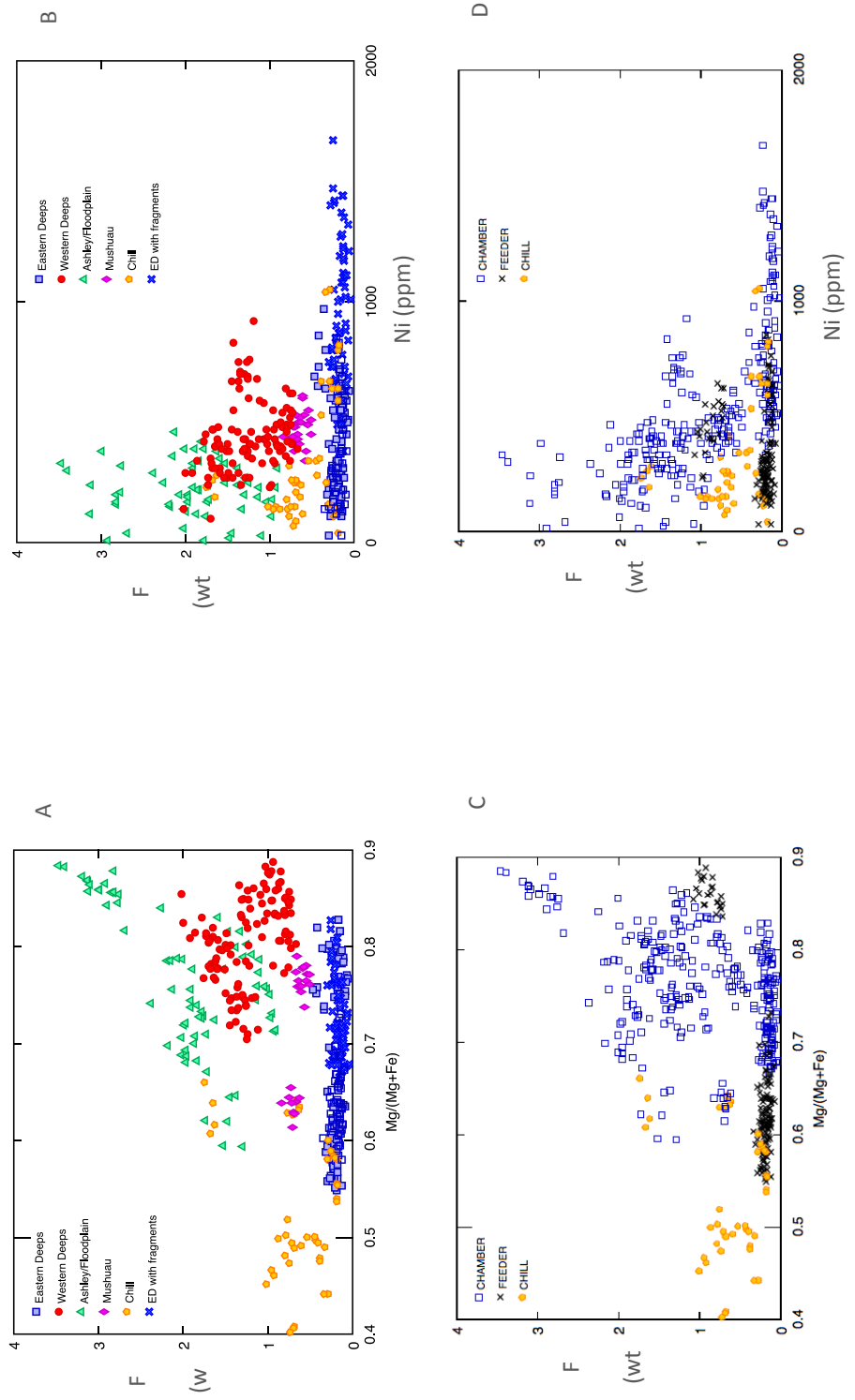


Fig. 2-12. X-Y plots of biotite major and trace element chemistry. Figures A & B plot biotite chemistry based on host deposit. A. Biotite plot of Mg # vs F (wt %). B. Biotite chemistry plot of Ni (ppm) vs F (wt %). Figures C & D plot the same biotite chemistry data based on host environment. C. Biotite chemistry plot of Mg # vs F (wt %). D. Biotite chemistry plot of Ni (ppm) vs F (wt %).

2.3.3. Oxygen isotope chemistry

Oxygen isotope ratios were determined for biotite separates as a means of discriminating mineral deposit environments in the Voisey's Bay intrusion and as a tool for tracking the evolution of the ore-forming magma. Thirty-three biotite separates were analyzed for O isotope ratios and the resultant data are summarized in Table 2-4.

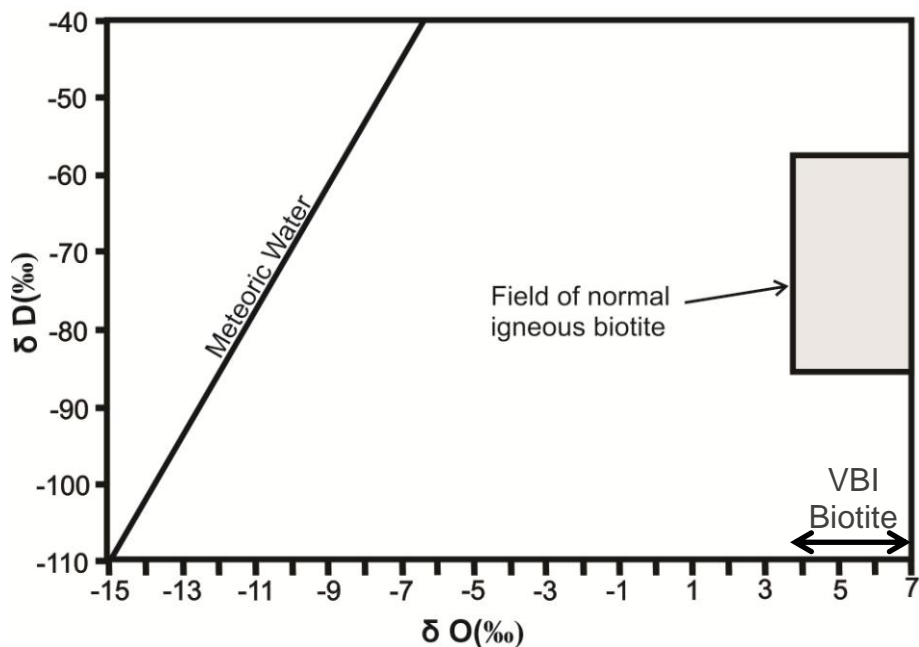


Fig. 2-13. $\delta^{18}\text{O}$ SMOW (‰) plotted versus δD SMOW (‰) showing the meteoric water line, the field of normal igneous biotite and the range of $\delta^{18}\text{O}$ ratios of biotite in troctolite within the Voisey's Bay Intrusion (modified after Taylor and Forester, 1979). Biotite from the study was not analyzed for δD ratios. As such, the arrow in the lower left corner of the figure indicates the range of $\delta^{18}\text{O}$ ratios determined in this study. These $\delta^{18}\text{O}$ ratios are not associated with any δD ratios.

All biotite from the VBI plots within the field of normal igneous biotite (Fig. 2-13): sample JG-11-038 is biotite from paragneiss. Oxygen isotope ratios from biotite separates are plotted on Figure 2-14 and compared with the mantle water isotopic value (summarized in Table 2-4). Biotite from the eastern and central portion of the VBI

contain have $\delta^{18}\text{O}$ ratios depleted relative to the mantle water value of 5.7‰. Biotite in troctolite from the western part of the VBI and the Mushuau intrusion have $\delta^{18}\text{O}$ ratios enriched relative to mantle water. There is a progressive decrease in biotite $\delta^{18}\text{O}$ ratios moving from west to east across the VBI.

Biotite in chilled margins has depleted $\delta^{18}\text{O}$ ratios compared to their plutonic counterparts. This is likely due to the chamber and feeder rocks having cooled more slowly at lower crystallization temperatures. This longer cooling history would have promoted prolonged oxygen isotope exchange compared to the rapid cooling history of the chilled margins (Taylor, 1968). Chills would have formed when their parental magma quenched, effectively stopping oxygen isotope exchange and preserving a more depleted signature. This observation also suggests that the Western Deep intrusion may have undergone a lengthy emplacement and cooling history relative to the Eastern Deep, Discovery Hill and Ovoid zones, effectively allowing for prolonged isotopic exchange and enriched $\delta^{18}\text{O}$ ratios.

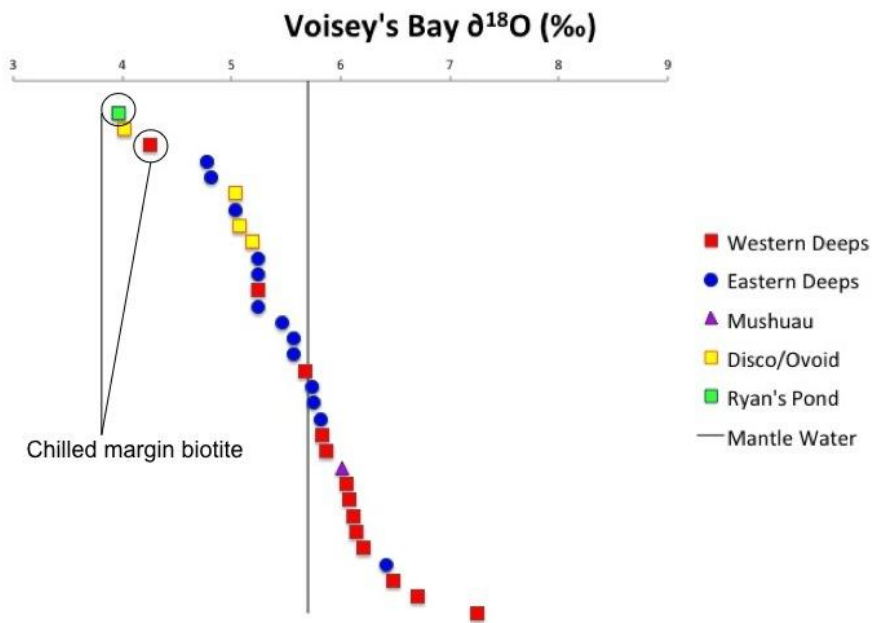


Fig. 2-14. $\delta^{18}\text{O}$ ratios of biotite separates relative to the mantle water $\delta^{18}\text{O}$ ratio of 5.7‰. The samples were sorted based on $\delta^{18}\text{O}$ ratio (highest to lowest) (y-axis) to allow for geographic discrimination. The x-axis is the $\delta^{18}\text{O}$ ratio of individual biotite samples. Nine of the thirteen samples from the Eastern Deeps have $\delta^{18}\text{O}$ ratios $< 5.7\text{\textperthousand}$. All biotite samples from Discovery Hill and the Ovoid have $\delta^{18}\text{O}$ ratios $< 5.7\text{\textperthousand}$. Ten of the thirteen samples from the Western Deeps have $\delta^{18}\text{O}$ ratios $> 5.7\text{\textperthousand}$. Both chilled margin biotite samples have $\delta^{18}\text{O}$ ratios $< 5.7\text{\textperthousand}$.

Biotite in these rocks is likely the product of the crystallization of a residual silicate melt and is strongly associated with ore and oxide minerals. As such, the mica can be linked to a relatively high temperature ($\sim 1000^\circ\text{C}$) event associated with ore formation and magma crystallization. Under these conditions any water in the system was likely contained within the silicate melt structure rather than as a free fluid and oxygen isotopes would be used to track magma evolution versus as a tool to distinguish the source of water within the parental magma (Lightfoot, personal communication, 2012). Figure 2-15 shows the Mg# plotted against $\delta^{18}\text{O}$ ratios of biotite separates from across the deposit and can be compared to the data plotted on Figures 2-10 and 2-11.

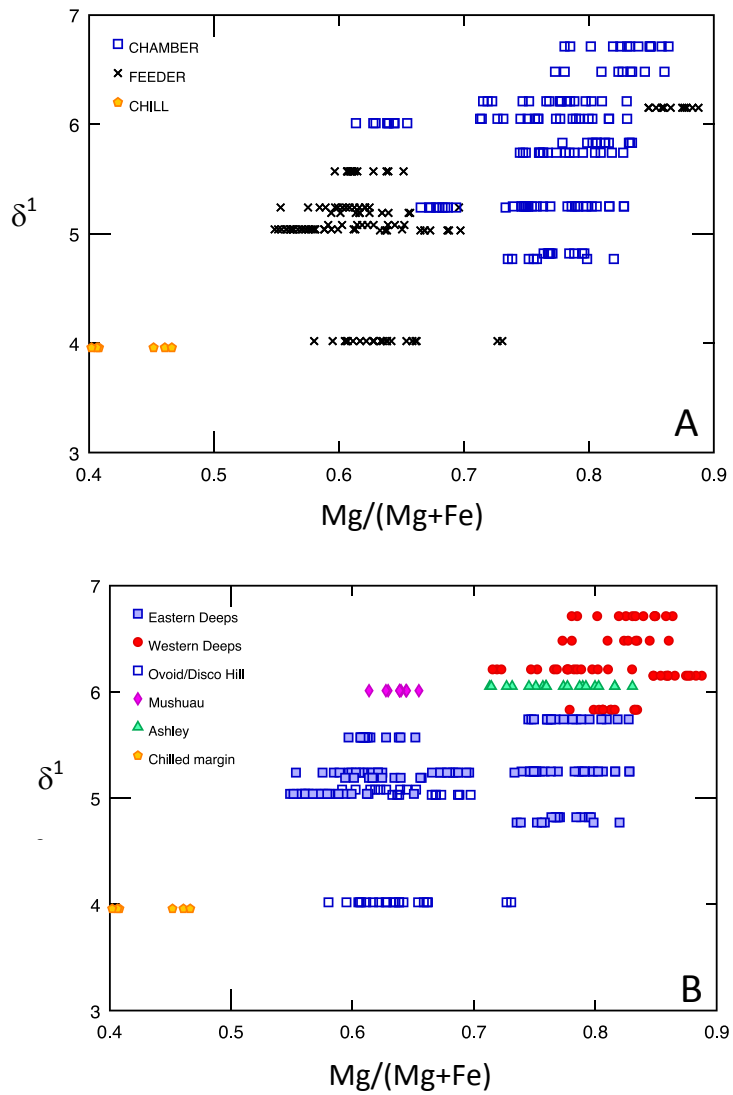


Fig. 2-15. Plot of Mg# ($\text{Mg}/(\text{Mg}+\text{Fe})$) versus $\delta^{18}\text{O}$ for biotite. A. Plot based on host rock emplacement (i.e. chamber, feeder, chill). B. Plot based on host rock deposit. Biotite from the different feeder environments (Eastern Deep versus Western Deep) are geochemically distinct whereas biotite from the different chamber environments are more geochemically similar. Biotite from chilled margins has the lowest $\text{Mg}/(\text{Mg}+\text{Fe})$ and $\delta^{18}\text{O}$ ratios.

Table 2-4. Sample list including sample location, number, host setting, lithology of host rock, and biotite $\delta^{18}\text{O}$ ratios. Not all samples from Table 2-2 are listed in this table. Only samples which were analyzed for $\delta^{18}\text{O}$ ratios are listed in this table.

Location	Zone	Sample	Setting	Lithology	Biotite $\delta^{18}\text{O}$
Eastern Deeps	<i>Eastern Deeps</i>	JG-11-001	Chamber	Troctolite	5.25
		JG-11-003	Chamber	Troctolite	4.82
		JG-11-004	Chamber	Troctolite	5.57
		JG-11-005	Chamber	Troctolite	6.42
		JG-11-006	Chamber	Troctolite	5.24
		JG-11-012	Chamber	Troctolite	4.77
		JG-11-024	Chamber	Troctolite	5.74
		JG-11-072	Feeder	Diorite	5.04
		JG-11-075	Feeder	Diorite	5.57
		JG-11-077	Feeder	Diorite	5.82
		JG-11-123	Chamber	Troctolite	5.46
		JG-11-129	Chamber	Troctolite	5.75
	<i>N. Eastern Deeps</i>	JG-11-084	Feeder	Diorite	5.24
	<i>Ryan's Pond</i>	JG-11-130	Chilled margin	Gabbronorite	3.96
Western Deeps	<i>Western Deeps</i>	JG-11-091	Feeder	Olivine norite	5.08
		JG-11-037	Feeder	Diorite	4.02
		JG-11-093	Feeder	Norite	5.03
		JG-11-029	Chamber	Troctolite breccia	7.25
		JG-11-030	Chamber	Olivine norite	5.25
		JG-11-031	Chamber	Olivine norite	6.08
		JG-11-032	Chamber	Olivine norite	6.21
		JG-11-033	Chamber	Olivine norite	6.71
		JG-11-034	Chamber	Troctolite	6.12
		JG-11-035	Chamber	Troctolite	6.48
		JG-11-036	Chamber	Troctolite	5.87
		JG-11-038	Country Rock	Paragneiss	8.45
	<i>Ashley/Floodplain</i>	JG-11-047	Chamber	Troctolite	5.83
		JG-11-080	Feeder	Olivine norite	6.15
Mushuau	<i>Mushuau</i>	JG-11-089	Feeder	Diorite	5.19
		JG-11-116	Chilled margin	Gabbronorite	4.25
		JG-11-061	Chamber	Olivine gabbro	6.05
		JG-11-070	Chamber	Olivine gabbro	5.67
		JG-11-137	Chamber	Leucotroctolite	6.01

As with the plot of Mg# versus Al (IV) (for biotite), there are two distinct groups of biotite from feeder rocks and biotite from chamber rocks is intermediate between the two feeder end members. There is a decrease in biotite $\delta^{18}\text{O}$ ratio with decreasing Mg# (Fig. 2-15A and 2-15B). Biotite from the Western Deeps has the most enriched $\delta^{18}\text{O}$ ratios followed by biotite from the Ashley and Mushuau intrusions. Biotite from the Eastern Deeps, Ovoid and Discovery Hill zones has depleted $\delta^{18}\text{O}$ relative to biotite from the

Western Deeps. Chilled margin biotite has the lowest $\delta^{18}\text{O}$ ratio and Mg# signature.

Figures 2-16 and 2-17 are representative down hole strip logs from individual drill holes with biotite $\delta^{18}\text{O}$ ratios; Figure 2-16 is for hole VB97368 in the Western Deeps and Figure 2-17 is from hole VB99528 in the Eastern Deeps.

With respect to VB97368, the highest biotite $\delta^{18}\text{O}$ ratio is 7.25 ‰ and is from troctolite in contact with Tasiuyak paragneiss. The paragneiss sample (JG-11-038) has a $\delta^{18}\text{O}$ ratio of 8.45 ‰. This suggests involvement of paragneiss with the troctolitic magma, which could have resulted in contamination of the magma parental to these rocks. With respect to VB99528, there is scatter among the biotite $\delta^{18}\text{O}$ ratios throughout the chamber. The highest $\delta^{18}\text{O}$ ratio in VB99528, 6.42 ‰, is in biotite from fragment-bearing troctolite. The lowest biotite $\delta^{18}\text{O}$ ratio is in feeder diorite. There are more consistent variations in biotite $\delta^{18}\text{O}$ at the deposit scale (west to east) as described above.

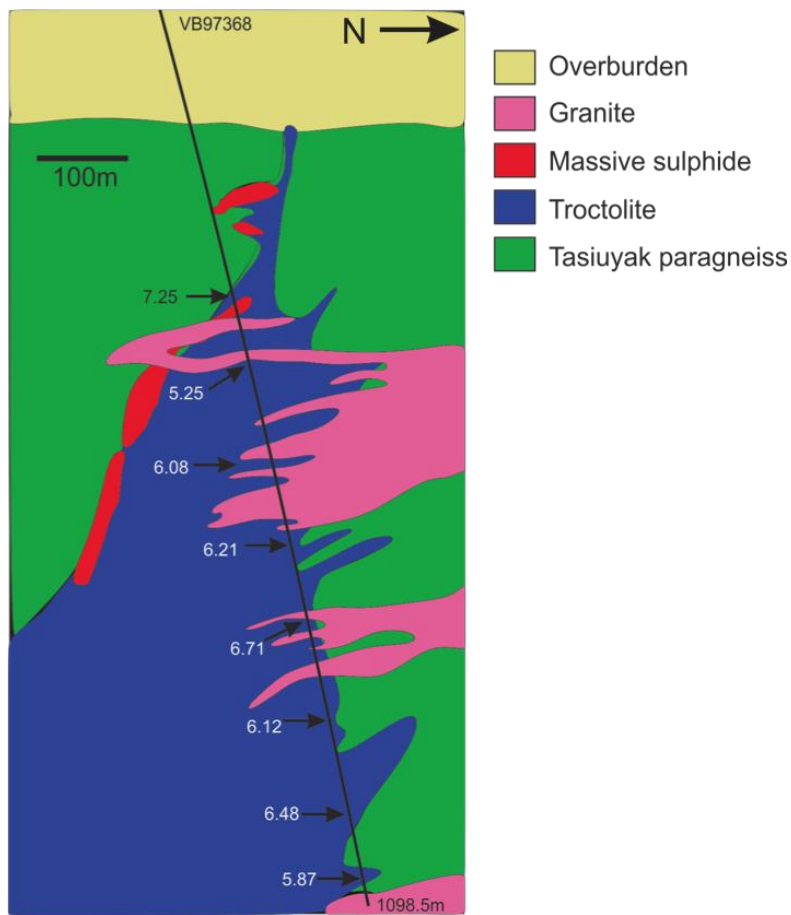


Fig. 2-16. $\delta^{18}\text{O}$ ratios of biotite in norite from the Western Deeps zone, VB97368. The highest $\delta^{18}\text{O}$ ratio (7.25) is from biotite in a mineralized norite breccia near the contact between the Western Deeps feeder dyke and the Tasiuyak paragneiss country rock. Biotite in the paragneiss country rock (sample JG-11-038) was analyzed and found to have a $\delta^{18}\text{O}$ ratio of 8.45‰.

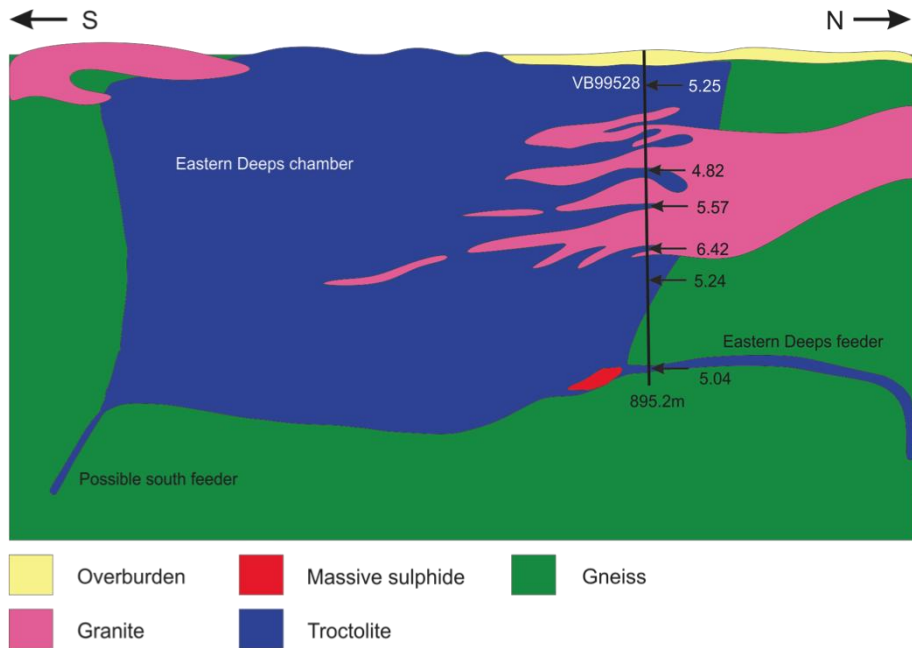


Fig. 2-17. $\delta^{18}\text{O}$ ratios of biotite from the Eastern Deeps, VB99528.

2.4. Discussion and conclusions

The main rock types of the VBI were emplaced via several pulses of mafic, and sulphide-bearing, magma. It is probable that the first magma pulses filled the Eastern Deeps chamber, the upper portion of the Western Deeps chamber (near where the dyke splays off the top of the chamber), and possibly the Ashley, Floodplain, and Kog Brook chambers, resulting in the weakly mineralized troctolites and olivine gabbro described above. A second pulse of magma would have exploited structures in the surrounding country rocks as dykes feeding into the more primitive troctolite- and olivine gabbro-filled magma chambers. This second pulse brought a mix of later, more-evolved magma, which both lacks modal olivine and contains significantly more pyroxene and partially assimilated fragments compared to the first pulse. This second pulse produced the

fragment-bearing troctolite, norite and diorite observed near the base of the Eastern Deep chamber, at the stratigraphic top of the Western Deep chamber, and where feeder dykes intersect these chambers. Feeder dykes are present at the base of the Eastern Deep, are splayed off the top of the Western Deep, feeding in to the Ovoid massive sulphide deposit, feeding the Discovery Hill zone, and within the South East extension. A final pulse of magma (or possibly a later discreet pulse associated with the second pulse mentioned above) brought brecciated feeder dyke material in to the system, depositing moderately to highly mineralized leopard texture troctolite and diorite, troctolite breccias and, of course, massive and semi-massive sulphide. This concept of different pulses of magma feeding the VBI (Evans-Lamswood et al., 2000) is substantiated by the variations seen in biotite major and trace element chemistry and oxygen isotope ratios.

This paper has evaluated both the distribution and geochemical characteristics of primary igneous biotite in mafic intrusives and chilled margins from the Voisey's Bay and Mushau intrusions. The major conclusions reached in this study are:

1. The mafic rock types associated with the NPS were identified via modal mineralogies obtained from MLA and include the following: troctolite, which primarily occurs in the Eastern Deep chamber and to a lesser degree in the Western Deep chamber and melatrotroctolite and leucotrotroctolite varieties which are present in the Mushau intrusion; diorite, which makes up feeder rocks from the eastern half of the intrusion (Eastern Deep and North Eastern Deep feeders, Discovery Hill dyke, Ovoid feeder, and the South East extension); norite and olivine norite, which occur in the feeder and chamber rocks associated with the

Western Deep intrusion, the Discovery Hill and Ovoid feeder dykes, and in the Floodplain intrusion; olivine gabbro, which makes up the bulk of the Ashley and Floodplain intrusions; and finally gabbronorite, which occurs as chilled marginal rocks throughout the VBI;

2. Biotite in the Voisey's Bay troctolites is a primary igneous mineral which suggests that water (hydroxyl) was present within the silicate melt structure of the magma parental to these rocks;
3. The highest concentration of biotite (>12 weight %) is in diorite feeder rocks and fragment-bearing troctolite (both with disseminated sulphide minerals) in the Eastern Deep. Biotite is spatially associated with disseminated sulphides and as such can be linked to a high temperature event associated with the formation of the Voisey's Bay ore;
4. Biotite major element chemistry is distinct across the VBI with variations occurring between the different deposits and between the different environments of formation (i.e. chamber vs feeder). Biotite with higher Mg/Mg+Fe ratios occurs in the Western Deep where the chamber and feeder dyke intersect and in the Eastern Deep chamber. Biotite with lower Mg/Mg+Fe ratios occurs in the Eastern Deep feeder rocks and the chilled margins;
5. The highest Ni values occur in moderately magnesian biotite from the Eastern Deep (fragment-bearing troctolite) and at the top of the Western Deep chamber where the feeder splay off. This biotite likely crystallized from a higher (Ni) tenor magma than the initial pulse which filled the large chambers;

6. There exist geochemical similarities (Mg/Mg+Fe, F and Ni) between biotite from the melatroctolite component of the Mushuau intrusion and biotite from the Western Deeps, Ashley, Floodplain, and Kog Brook intrusions. This suggests that biotite in these troctolite intrusions may have crystallized from geochemically similar pulses of magma;
7. All biotite $\delta^{18}\text{O}$ ratios plot within the normal range for igneous biotite and there is an increase in $\delta^{18}\text{O}$ ratios from east to west across the VBI. The higher Mg# biotite has relatively enriched $\delta^{18}\text{O}$ ratios and the lower Mg# biotite has relatively depleted $\delta^{18}\text{O}$ ratios. The differences in biotite $\delta^{18}\text{O}$ ratios are likely attributable to crystallization from geochemically distinct parental magmas (different pulses) containing hydroxyl (within the silicate structure of the high temperature melt) with different O¹⁸ and O¹⁶ ratios.
8. The geochemical variations seen in the biotite from the mafic intrusives of the VBI loosely fit with a multi-stage emplacement history for the VBI made up of at least two different pulses of mafic magma; the first pulse being a primitive, olivine-bearing, sulphide poor magma and the second pulse being a more evolved, fragment-bearing, olivine-poor magma followed by a fragment-rich, massive sulphide melt.

Table 2-5. Mean composition of biotite samples as determined by electron microprobe analysis.

JG-11-	1	3	6	12	16
Location	ED	ED	ED	ED	ED
Lithology	Troctolite	Troctolite	Troctolite	Troctolite	Troctolite
Wt % Biotite	2.04	2.01	2.52	4.15	5.82
SiO₂	37.45	37.66	36.5	37.73	36.93
Al₂O₃	15.46	15.9	15.2	15.1	16.07
TiO₂	5	4.21	5.14	4.77	3.83
V₂O₃	0.02	0.02	0.02	0.02	0
Cr₂O₃	0.12	0.06	0.01	0.07	0.02
FeO	9.12	9.21	12.54	9.57	11.98
MnO	0.04	0.02	0.04	0.04	0.03
MgO	17.98	18	15.32	17.53	16.35
NiO	0.07	0.07	0.17	0.1	0.11
K₂O	9.23	8.71	9.28	9.16	8.71
Na₂O	0.53	0.82	0.42	0.39	0.88
CaO	0.01	0.01	0.02	0.01	0.01
BaO	0.38	0.37	0.52	0.18	0.4
F	0.18	0.12	0.21	0.4	0.12
Cl	0.01	0.03	0.02	0.04	0.01
TOTAL	95.6	95.2	95.4	95.13	95.44
O≠F,Cl	0.08	0.06	0.09	0.17	0.05
Σ -X	95.52	95.14	95.31	94.95	95.39

Number of ions on the basis of 12 (O, OH, F) or 22 positive charges					
Si	5.46	5.49	5.44	5.53	5.45
Al	2.65	2.73	2.67	2.61	2.79
Ti	0.55	0.46	0.58	0.53	0.42
V	0	0	0	0	0
Cr	0.01	0.01	0	0.01	0
Fe	1.11	1.12	1.56	1.17	1.48
Mn	0	0	0	0.01	0
Mg	3.91	3.91	3.4	3.83	3.59
Ni	0.01	0.01	0.02	0.01	0.01
K	1.71	1.62	1.76	1.71	1.64
Na	0.15	0.23	0.12	0.11	0.25
Ca	0	0	0	0	0
Ba	0.02	0.02	0.03	0.01	0.02
Σ cations	15.57	15.58	15.56	15.53	15.65
F	0.08	0.05	0.1	0.18	0.05
Cl	0	0.01	0.01	0.01	0
Fe/FeMnMg	0.22	0.22	0.31	0.23	0.29
Al(IV)	2.54	2.51	2.56	2.47	2.55
Al(VI)	0.11	0.22	0.11	0.14	0.24
K/KNaBa	0.91	0.87	0.92	0.93	0.86

JG-11-	17	21	24	72	75
Location	ED	ED	ED	ED	ED
Lithology	LeopTroc	Troctolite	Troctolite	Diorite	Diorite
Wt % Biotite	4.07	12.34	2.54	13.01	12.71
SiO₂	37.28	37.5	37.76	36.93	36.93
Al₂O₃	15.53	15.81	16.1	14.99	15.78
TiO₂	4.12	3.28	3.96	3.87	3.35
V₂O₃	0	0	0.03	0	0
Cr₂O₃	0.01	0.05	0.04	0.02	0.02
FeO	12.35	12.19	9.28	17.27	15.64
MnO	0.07	0.04	0.03	0.06	0.04
MgO	16.35	16.54	18.24	13.2	14.15
NiO	0.07	0.15	0.1	0.02	0.04
K₂O	8.76	8.53	8.63	9.36	8.54
Na₂O	0.84	1	0.97	0.32	0.83
CaO	0.01	0	0.01	0.01	0.01
BaO	0.5	0.18	0.4	0.51	0.48
F	0.18	0.12	0.22	0.24	0.19
Cl	0.01	0.12	0.02	0.03	0.07
TOTAL	96.08	95.53	95.78	96.83	96.07
O≠F,Cl	0.08	0.08	0.1	0.11	0.1
Σ -X	96	95.45	95.69	96.72	95.97

Number of ions on the basis of 12 (O, OH, F) or 22 positive charges

Si	5.48	5.52	5.48	5.53	5.51
Al	2.69	2.74	2.75	2.65	2.77
Ti	0.46	0.36	0.43	0.44	0.38
V	0	0	0	0	0
Cr	0	0.01	0	0	0
Fe	1.52	1.5	1.13	2.16	1.95
Mn	0.01	0.01	0	0.01	0
Mg	3.58	3.63	3.94	2.95	3.15
Ni	0.01	0.02	0.01	0	0
K	1.64	1.6	1.6	1.79	1.63
Na	0.24	0.28	0.27	0.09	0.24
Ca	0	0	0	0	0
Ba	0.03	0.01	0.02	0.03	0.03
Σ cations	15.63	15.68	15.62	15.62	15.63
F	0.08	0.06	0.1	0.11	0.09
Cl	0	0.03	0	0.01	0.02
Fe/FeMnMg	0.3	0.29	0.22	0.42	0.38
Al(IV)	2.52	2.48	2.52	2.47	2.49
Al(VI)	0.17	0.26	0.23	0.18	0.28
K/KNaBa	0.86	0.84	0.84	0.94	0.86

JG-11-	100	102	130	153	32
Location	ED	ED	RP	NED	WD
Lithology	Gb norite	Gb norite	Gb norite	Diorite	Olv norite
Wt % Biotite	3.56	1.39	2.02	4.1	8.2
SiO₂	37.39	38.02	36.78	37.14	39.24
Al₂O₃	13.71	12.93	12.58	13.65	15
TiO₂	5.49	4.68	4.68	5.02	2.32
V₂O₃	0.17	0.03	0.13	0.1	0.04
Cr₂O₃	0.19	0	0.02	0.13	0.05
FeO	14.71	15.26	22.43	16.75	9.88
MnO	0.05	0.1	0.05	0.04	0.04
MgO	14.24	14.64	9.6	13.12	18.76
NiO	0.03	0.03	0.02	0.01	0.05
K₂O	9.77	9.88	9.23	9.5	8.35
Na₂O	0.02	0.06	0.01	0.1	1.06
CaO	0.03	0.04	0	0	0.01
BaO	0.46	0.33	0.48	0.41	0.32
F	0.69	1.68	0.84	0.24	1.55
Cl	0.03	0.09	0.44	0.08	0.12
TOTAL	96.98	97.76	97.28	96.3	96.8
O≠F,Cl	0.3	0.73	0.45	0.12	0.68
Σ -X	96.68	97.03	96.82	96.18	96.12

Number of ions on the basis of 12 (O, OH, F) or 22 positive charges

Si	5.57	5.68	5.69	5.59	5.7
Al	2.41	2.28	2.29	2.42	2.57
Ti	0.61	0.53	0.54	0.57	0.25
V	0.02	0	0.02	0.01	0
Cr	0.02	0	0	0.02	0.01
Fe	1.83	1.91	2.9	2.11	1.2
Mn	0.01	0.01	0.01	0.01	0.01
Mg	3.16	3.26	2.21	2.94	4.06
Ni	0	0	0	0	0.01
K	1.85	1.88	1.82	1.82	1.55
Na	0	0.02	0	0.03	0.3
Ca	0.01	0.01	0	0	0
Ba	0.03	0.02	0.03	0.02	0.02
Σ cations	15.5	15.58	15.49	15.52	15.66
F	0.32	0.79	0.41	0.11	0.71
Cl	0.01	0.02	0.12	0.02	0.03
Fe/FeMnMg	0.37	0.37	0.57	0.42	0.23
Al(IV)	2.43	2.32	2.31	2.41	2.3
Al(VI)	-0.03	-0.04	-0.02	0.01	0.27
K/KNaBa	0.98	0.98	0.98	0.97	0.83

JG-11-	033B	37	35	40	42
Location	WD	DH	WD	WD	WD
Lithology	Olv norite	Diorite	Troctolite	Norite	Troctolite
Wt % Biotite	5.34	8.98	3.58	7.68	3.31
SiO₂	39.7	36.24	39.01	39.12	39.4
Al₂O₃	15.3	15.87	14.7	14.12	14.24
TiO₂	2.32	2.91	3.78	3.48	4.41
V₂O₃	0.03	0	0.03	0.05	0.04
Cr₂O₃	0.14	0.02	0.07	0.16	0.04
FeO	7.49	15.48	7.72	11.16	8.16
MnO	0.01	0.07	0.02	0.03	0.03
MgO	20.46	15.23	19.88	17.66	19.3
NiO	0.05	0.07	0.05	0.09	0.03
K₂O	8.26	8.21	9.55	9.4	9.87
Na₂O	1.09	0.32	0.33	0.4	0.16
CaO	0.01	0.03	0.01	0	0.01
BaO	0.44	0.35	0.51	0.2	0.35
F	1.27	0.15	1.02	1.3	1.59
Cl	0.11	0.02	0.03	0.1	0.01
TOTAL	96.66	94.99	96.71	97.26	97.65
O≠F,Cl	0.56	0.07	0.43	0.57	0.67
Σ -X	96.1	94.92	96.28	96.69	96.98

Number of ions on the basis of 12 (O, OH, F) or 22 positive charges

Si	5.69	5.44	5.62	5.7	5.67
Al	2.58	2.81	2.5	2.43	2.41
Ti	0.25	0.33	0.41	0.38	0.48
V	0	0	0	0.01	0
Cr	0.02	0	0.01	0.02	0
Fe	0.9	1.95	0.93	1.36	0.98
Mn	0	0.01	0	0	0
Mg	4.37	3.41	4.27	3.84	4.14
Ni	0.01	0.01	0.01	0.01	0
K	1.51	1.57	1.76	1.75	1.81
Na	0.3	0.09	0.09	0.11	0.04
Ca	0	0.01	0	0	0
Ba	0.02	0.02	0.03	0.01	0.02
Σ cations	15.64	15.63	15.61	15.61	15.55
F	0.57	0.07	0.46	0.6	0.72
Cl	0.03	0.01	0.01	0.02	0
Fe/FeMnMg	0.17	0.36	0.18	0.26	0.19
Al(IV)	2.31	2.56	2.38	2.3	2.33
Al(VI)	0.28	0.25	0.12	0.13	0.08
K/KNaBa	0.82	0.93	0.94	0.93	0.97

JG-11-	44	47	78	80	89
Location	WD	WD	WD	WD	WD
Lithology	Troctolite	Troctolite	Olv norite	Olv norite	Diorite
Wt % Biotite	4.38	3.7	5.6	2.59	8.84
SiO₂	39.22	38.52	39.56	39.87	36.94
Al₂O₃	13.78	14.82	16.3	16.56	15.01
TiO₂	4.12	4.9	1.96	1.74	4.35
V₂O₃	0	0.02	0.01	0.02	0.05
Cr₂O₃	0.04	0.13	0.18	0.07	0.06
FeO	8.73	7.8	6.58	5.97	15.31
MnO	0.01	0.04	0.02	0.03	0.03
MgO	19.12	18.88	21.26	21.66	14.34
NiO	0.04	0.05	0.07	0.05	0.07
K₂O	9.82	9.82	7.23	7.07	8.81
Na₂O	0.24	0.35	1.75	1.67	0.66
CaO	0	0	0.02	0.02	0
BaO	0.47	0.36	0.26	0.41	0.4
F	1.71	0.8	0.79	0.98	0.18
Cl	0.05	0.01	0.09	0.02	0.03
TOTAL	97.34	96.49	96.06	96.14	96.24
O≠F,Cl	0.73	0.34	0.35	0.42	0.08
Σ -X	96.61	96.15	95.71	95.72	96.16

Number of ions on the basis of 12 (O, OH, F) or 22 positive charges

Si	5.69	5.57	5.62	5.64	5.5
Al	2.36	2.52	2.73	2.76	2.63
Ti	0.45	0.53	0.21	0.19	0.49
V	0	0	0	0	0.01
Cr	0	0.01	0.02	0.01	0.01
Fe	1.06	0.94	0.78	0.71	1.91
Mn	0	0	0	0	0
Mg	4.14	4.06	4.5	4.57	3.18
Ni	0.01	0.01	0.01	0.01	0.01
K	1.82	1.81	1.31	1.28	1.67
Na	0.07	0.1	0.48	0.46	0.19
Ca	0	0	0	0	0
Ba	0.03	0.02	0.01	0.02	0.02
Σ cations	15.59	15.57	15.67	15.63	15.6
F	0.79	0.36	0.35	0.44	0.08
Cl	0.01	0	0.02	0	0.01
Fe/FeMnMg	0.2	0.19	0.15	0.13	0.37
Al(IV)	2.31	2.43	2.38	2.36	2.5
Al(VI)	0.05	0.09	0.35	0.41	0.13
K/KNaBa	0.95	0.94	0.73	0.73	0.89

JG-11-	91	127	93	106	114
Location	OV	WD	DH	OV	WD
Lithology	Olv norite	Gb norite	Norite	Gb norite	Gb norite
Wt % Biotite	6.7	4.44	10.92	18.53	1.22
SiO₂	36.79	37.47	37.63	36.45	36.85
Al₂O₃	14.78	12.51	16.08	13.38	14.82
TiO₂	4.65	5.73	2.79	4.62	4
V₂O₃	0.09	0.07	0.06	0	0.14
Cr₂O₃	0.04	0.01	0.05	0.04	0.13
FeO	15.48	20.27	14.07	20.73	17.72
MnO	0.05	0.07	0.04	0.11	0.07
MgO	14.4	11.09	15.71	10.74	12.81
NiO	0.03	0.02	0.02	0.07	0.09
K₂O	9.25	9.03	8.07	9.06	9.14
Na₂O	0.4	0.37	0.93	0.06	0.32
CaO	0.03	0.08	0.01	0.03	0.02
BaO	0.41	0.25	0.15	0.26	0.12
F	0.24	0.75	0.16	0.4	0.22
Cl	0.02	0.1	0.02	0.2	0.02
TOTAL	96.67	97.81	95.78	96.15	96.47
O≠F,Cl	0.11	0.34	0.07	0.21	0.09
Σ -X	96.56	97.47	95.71	95.94	96.37

Number of ions on the basis of 12 (O, OH, F) or 22 positive charges

Si	5.47	5.66	5.54	5.61	5.53
Al	2.59	2.23	2.79	2.43	2.62
Ti	0.52	0.65	0.31	0.53	0.45
V	0.01	0.01	0.01	0	0.02
Cr	0.01	0	0.01	0.01	0.02
Fe	1.93	2.56	1.73	2.67	2.23
Mn	0.01	0.01	0.01	0.01	0.01
Mg	3.2	2.5	3.45	2.46	2.87
Ni	0	0	0	0.01	0.01
K	1.76	1.74	1.52	1.78	1.75
Na	0.12	0.11	0.26	0.02	0.09
Ca	0.01	0.01	0	0.01	0
Ba	0.02	0.01	0.01	0.02	0.01
Σ cations	15.61	15.48	15.63	15.52	15.6
F	0.11	0.36	0.07	0.19	0.1
Cl	0.01	0.03	0	0.05	0
Fe/FeMnMg	0.38	0.51	0.33	0.52	0.44
Al(IV)	2.53	2.34	2.46	2.39	2.47
Al(VI)	0.07	-0.11	0.33	0.03	0.16
K/KNaBa	0.93	0.93	0.85	0.98	0.95

JG-11-	59	61	68
Location	AF	AF	AF
Lithology	Norite	Olv gbr	Olv gbr
Wt % Biotite	11.29	3.34	2.23
SiO₂	38.43	38.5	39.59
Al₂O₃	14.51	14.33	13.78
TiO₂	1.52	4.65	3.66
V₂O₃	0.04	0.09	0.06
Cr₂O₃	0.04	0.11	0.44
FeO	13.11	9.55	6.36
MnO	0.03	0.04	0.03
MgO	17.32	18.08	20.87
NiO	0.03	0.04	0.02
K₂O	8.8	9.6	9.76
Na₂O	0.71	0.24	0.32
CaO	0.03	0.02	0.02
BaO	0.28	0.3	0.39
F	1.91	1.17	2.92
Cl	0.25	0.02	0.03
TOTAL	97.01	96.75	98.25
O≠F,Cl	0.86	0.5	1.24
Σ -X	96.15	96.25	97.02

Number of ions on the basis of 12 (O, OH, F) or 22 positive charges

Si	5.71	5.61	5.7
Al	2.54	2.46	2.34
Ti	0.17	0.51	0.4
V	0	0.01	0.01
Cr	0	0.01	0.05
Fe	1.63	1.16	0.77
Mn	0	0	0
Mg	3.83	3.92	4.48
Ni	0	0	0
K	1.67	1.78	1.79
Na	0.2	0.07	0.09
Ca	0	0	0
Ba	0.02	0.02	0.02
Σ cations	15.77	15.55	15.63
F	0.9	0.54	1.33
Cl	0.06	0.01	0.01
Fe/FeMnMg	0.3	0.23	0.15
Al(IV)	2.29	2.39	2.3
Al(VI)	0.25	0.07	0.04
K/KNaBa	0.88	0.95	0.94

JG-11-	69	134	137
Location	AF	MU	MU
Lithology	Olv gbr	MelaTroc	LeucoTroc
Wt % Biotite	3.73	0.18	1.95
SiO₂	38.56	38.25	37.14
Al₂O₃	14.01	14.74	15.28
TiO₂	3.22	5.41	3.09
V₂O₃	0.04	0.02	0.01
Cr₂O₃	0.14	0.05	0.03
FeO	11.95	9.58	15.08
MnO	0.05	0.04	0.05
MgO	17.13	17.76	14.83
NiO	0	0.06	0.06
K₂O	9.73	10.29	9.58
Na₂O	0.23	0.03	0.13
CaO	0.02	0.02	0.03
BaO	0.52	0.22	0.25
F	1.76	0.59	0.71
Cl	0.03	0.04	0.07
TOTAL	97.39	97.11	96.34
O≠F,Cl	0.75	0.26	0.32
Σ -X	96.65	96.85	96.02

Number of ions on the basis of 12 (O, OH, F) or 22 positive charges

Si	5.69	5.53	5.55
Al	2.43	2.51	2.69
Ti	0.36	0.59	0.35
V	0	0	0
Cr	0.02	0.01	0
Fe	1.48	1.16	1.89
Mn	0.01	0	0.01
Mg	3.76	3.83	3.31
Ni	0	0.01	0.01
K	1.83	1.9	1.83
Na	0.07	0.01	0.04
Ca	0	0	0.01
Ba	0.03	0.01	0.01
Σ cations	15.65	15.56	15.67
F	0.82	0.27	0.34
Cl	0.01	0.01	0.02
Fe/FeMnMg	0.28	0.23	0.36
Al(IV)	2.31	2.47	2.45
Al(VI)	0.12	0.05	0.24
K/KNaBa	0.95	0.99	0.97

Bibliography

- Ahrens, L. H. (1969). The use of ionization potentials in geochemistry. (pp. 144-154). Israel Program for Scientific Translations : Jerusalem, Israel U.S. Department of Commerce, Clearinghouse Fed. Sci. Tech. Inform. Retrieved from
<http://search.ebscohost.com/login.aspx?direct=true&AuthType=ip,url,uid&db=geh&AN=1970-011236&site=ehost-live&scope=site>
- Buerger, M. J. (1948). The role of temperature in mineralogy. *American Mineralogist*, 33 (3-4), 101-121. Retrieved from
<http://search.ebscohost.com/login.aspx?direct=true&AuthType=ip,url,uid&db=geh&AN=1949-021401&site=ehost-live&scope=site;>
http://www.minsocam.org/ammin/AM33/AM33_101.pdf
- Deer, W. A., Howie, R. A., & Zussman, J. (1962). *Rock-forming minerals* Longmans.
- Evans-Lamswood, D., Butt, D. P., Jackson, R. S., Lee, D. V., Muggridge, M. G., Wheeler, R. I., et al. (2000). Physical controls associated with the distribution of sulfides in the Voisey's Bay Ni-Cu-Co deposit, Labrador. *Economic Geology and the Bulletin of the Society of Economic Geologists*, 95 (4), 749-769. Retrieved from
<http://search.ebscohost.com/login.aspx?direct=true&AuthType=ip,url,uid&db=geh&AN=2000-054362&site=ehost-live&scope=site>; <http://www.segweb.org/journal.htm>
- Fleet, M. E. (2003). *Rock forming minerals, sheet silicates: Micas. volume 3A* (Second ed.). London: The Geological Society.
- Foster, M. D. (1960). *Interpretation of the composition of trioctahedral micas*. United States: U. S. Geological Survey : Reston, VA, United States. Retrieved from
<http://search.ebscohost.com/login.aspx?direct=true&AuthType=ip,url,uid&db=geh&AN=1960-008390&site=ehost-live&scope=site>
- Geological Survey Professional Paper. (1959). *Shorter contributions to general geology*. Washington: United States Government Printing Office.
- Guidotti, C. V. (1984). Micas in metamorphic rocks. *Reviews in Mineralogy*, 13, 357-467. Retrieved from
<http://search.ebscohost.com/login.aspx?direct=true&AuthType=ip,url,uid&db=geh&AN=1985-043368&site=ehost-live&scope=site>
- Hamilton, S. H. (1899). Exploration of the Delaware Valley. *Mineral Collector*, 6, 117-122.

- Le Bas, M. J., & Streckeisen, A. L. (1991). The IUGS systematics of igneous rocks. *Journal of the Geological Society of London*, 148, Part 5, 825-833. Retrieved from <http://search.ebscohost.com/login.aspx?direct=true&AuthType=ip,url,uid&db=geh&AN=1995-041857&site=ehost-live&scope=site>; <http://www.ingentaconnect.com/content/geol/jgs>
- Li, C., Lightfoot, P. C., Amelin, Y. V., & Naldrett, A. J. (2000). Contrasting petrological and geochemical relationships in the Voisey's Bay and Mushuau intrusions, Labrador, Canada; implications for ore genesis. *Economic Geology and the Bulletin of the Society of Economic Geologists*, 95(4), 771-799. Retrieved from <http://search.ebscohost.com/login.aspx?direct=true&AuthType=ip,url,uid&db=geh&AN=2000-054363&site=ehost-live&scope=site>; <http://www.segweb.org/journal.htm>
- Li, C., & Naldrett, A. J. (2000). Melting reactions of gneissic inclusions with enclosing magma at Voisey's Bay, Labrador, Canada; implications with respect to ore genesis. *Economic Geology and the Bulletin of the Society of Economic Geologists*, 95 (4), 801-814. Retrieved from <http://search.ebscohost.com/login.aspx?direct=true&AuthType=ip,url,uid&db=geh&AN=2000-054364&site=ehost-live&scope=site>; <http://www.segweb.org/journal.htm>
- Liese, H. C. (1963). Tetrahedrally coordinated aluminum in some natural biotites; an infrared absorption analysis. *American Mineralogist*, 48, 980-990. Retrieved from <http://search.ebscohost.com/login.aspx?direct=true&AuthType=ip,url,uid&db=geh&AN=1963-012872&site=ehost-live&scope=site>
- Lightfoot, P. C. (2012). Personal communication, *Phlogopite oxygen isotopes*
- Livi, K. J. T., & Veblen, D. R. (1985). Serpentine and phlogopite intergrowths in "eastonite" from Easton, Pennsylvania. *Geological Society of America Abstracts with Programs*, 17, 645.
- Mariga, J., Ripley, E. M., & Li, C. (2006). Oxygen isotopic studies of the interaction between xenoliths and mafic magma, Voisey's Bay Intrusion, Labrador, Canada. *Geochimica Et Cosmochimica Acta*, 70 (19), 4977-4996. doi: <http://dx.doi.org/10.1016/j.gca.2006.07.018>
- Miyano, T., & Miyano, S. (1982). Ferri-annite from the dales gorge member iron-formations, wittenoom area, western australia. *American Mineralogist*, 67 (11-12), 1179-1194. Retrieved from <http://search.ebscohost.com/login.aspx?direct=true&AuthType=ip,url,uid&db=geh&AN=1983-018419&site=ehost-live&scope=site>
- Munoz, J. L., & Ludington, S. D. (1974). Fluorine-hydroxyl exchange in biotite. *American Journal of Science*, 274, 396.

- Naldrett, A. J. (2010). From the mantle to the bank; the life of a Ni-Cu-PGE sulfide. *South African Journal of Geology*, 113(1), 1-32. doi: 10.2113/gssajg.113.1-1
- Naldrett, A. J., Asif, M., Krstic, S., & Li, C. (2000). The composition of mineralization of the Voisey's Bay Ni-Cu sulfide deposit, with special reference to platinum-group elements. *Economic Geology and the Bulletin of the Society of Economic Geologists*, 95(4), 845-865. Retrieved from <http://search.ebscohost.com/login.aspx?direct=true&AuthType=ip,url,uid&db=geh&AN=2000-054367&site=ehost-live&scope=site>; <http://www.segweb.org/journal.htm>
- Naldrett, A. J., Singh, J., Krstic, S., & Li, C. (2000). The mineralogy of the Voisey's Bay Ni-Cu-Co deposit, northern Labrador, Canada; influence of oxidation state on textures and mineral compositions. *Economic Geology and the Bulletin of the Society of Economic Geologists*, 95(4), 889-900. Retrieved from <http://search.ebscohost.com/login.aspx?direct=true&AuthType=ip,url,uid&db=geh&AN=2000-054369&site=ehost-live&scope=site>; <http://www.segweb.org/journal.htm>
- Nesse, W. D. (2004). *Introduction to optical mineralogy*. Oxford University Press.
- Ramberg, H. (1952). Chemical bonds and distribution of cations in silicates. *The Journal of Geology*, 60 (4), 331.
- Ripley, E. M., Park, Y., Li, C., & Naldrett, A. J. (2000). Oxygen isotope studies of the Voisey's Bay Ni-Cu-Co deposit, Labrador, Canada. *Economic Geology and the Bulletin of the Society of Economic Geologists*, 95(4), 831-844. Retrieved from <http://search.ebscohost.com/login.aspx?direct=true&AuthType=ip,url,uid&db=geh&AN=2000-054366&site=ehost-live&scope=site>; <http://www.segweb.org/journal.htm>
- Ryan, B. (1995). Anorthosite-granite (AMCG) suites. in The geology and mineral deposits of Labrador: A guide for the exploration geologist (compiled by R.J. Wardle and D.H.C. Wilton). In Newfoundland Department of Natural Resources - Centre for Earth Resources Research Report (Ed.), pp. 53
- Ryan, B. (2000). The Nain-Churchill boundary and the Nain Plutonic Suite; a regional perspective on the geologic setting of the Voisey's Bay Ni-Cu-Co deposit. *Economic Geology and the Bulletin of the Society of Economic Geologists*, 95 (4), 703-724. Retrieved from <http://search.ebscohost.com/login.aspx?direct=true&AuthType=ip,url,uid&db=geh&AN=2000-054360&site=ehost-live&scope=site>; <http://www.segweb.org/journal.htm>
- Slade, P. (2005). Rock-forming minerals. Volume 3A: Sheet silicates: Micas, 2nd ed. *Geological Magazine*, 142 (2), 219.

- Streckeisen, A. (1974). Classification and nomenclature of plutonic rocks recommendations of the IUGS subcommission on the systematics of igneous rocks. *Geologische Rundschau*, 63 (2), 773-786.
- Taylor, H. P., J., & Forester, R. W. (1979). An oxygen and hydrogen isotope study of the Skaergaard Intrusion and its country rocks; a description of a 55-m.y. old fossil hydrothermal system. *Journal of Petrology*, 20 (3), 355-419. Retrieved from <http://search.ebscohost.com/login.aspx?direct=true&AuthType=ip,url,uid&db=geh&AN=1980-018582&site=ehost-live&scope=site>
- Taylor, H. P. (1968). The oxygen isotope geochemistry of igneous rocks. *Contributions to Mineralogy and Petrology*, 19 (1), p.1-71
- Vale Newfoundland and Labrador. (2013). *Nineteenth year assessment report on geological, geophysical and geochemical exploration on claims in the Voisey's Bay area, northern Labrador*. St. John's: Department of Natural Resources, Government of Newfoundland and Labrador.
- Wardle, R. J. (1995). In Wilton D. H. C., et al (Eds.), *The geology and mineral deposits of Labrador: A guide for the exploration geologist*. Centre for Earth Resources Research, Memorial University of Newfoundland, St. John's: Geological Survey, Department of Natural Resources, Government of Newfoundland and Labrador.
- Wardle, R. J. (1990). In Mengel F. C. (Ed.), *Labrador segment of the trans-Hudson orogen; crustal development through oblique convergence and collision*. Geological Association of Canada : Toronto, ON, Canada. Retrieved from <http://search.ebscohost.com/login.aspx?direct=true&db=geh&AN=1991-033105&site=ehost-live&scope=site>
- Winchell, A. N. (1925). Studies in the mica group. *American Journal of Science*, 9 (52), 309-327. Retrieved from <http://search.ebscohost.com/login.aspx?direct=true&AuthType=ip,url,uid&db=geh&AN=1928-012172&site=ehost-live&scope=site>; http://www.minsocam.org/ammin/AM10/AM10_52.pdf

3. Chapter 3 – A petrographical and lithogeochemical evaluation of chilled marginal rocks from the Voisey’s Bay Intrusion, Labrador

ABSTRACT

The Voisey’s Bay nickel-copper-cobalt sulphide deposits are hosted by troctolite-norite-diorite intrusions of the Voisey’s Bay Intrusion (VBI), a minor component of the *ca.* 1.34-1.29 Ga Nain Plutonic Suite (NPS). Chilled margins are locally present as margins to the VBI and formed when hot magma was quenched against cold, solid rock. Mineral liberation analysis-scanning electron microscopy and petrography indicate that the chilled margins are gabbronorite, typically containing plagioclase (35-50 weight %), pyroxene (10-40 weight %), magnetite (<10 weight %), ilmenite (<5 weight %), and variable amounts of biotite and hornblende. The lack of olivine in these rocks suggests that the magma cooled at temperatures below the olivine solidus. Chilled margins occur in three settings within the VBI and can be subdivided into three groups based on rare earth element (REE) geochemistry; *i.* as chills on the margins of mafic feeder dykes, *ii.* as margins to brecciated, sulphide-bearing conduit rocks, and *iii.* as margins to large magma chambers. The gabbronorite “chills” contain 4.0-9.0 weight % MgO, 45-55 weight % SiO₂, 11-17 weight % Al₂O₃, and 8.0-15 weight % FeO*. The chilled margins of both Voisey’s Bay and Mushuau Ce/Yb ratios (22-27 and 12-17 respectively) suggests the possibility that there were two parental magmas of different compositions in the Voisey’s Bay region (i.e., VBI and Mushuau), that a single parental magma was contaminated by two different sources, or that some of the margins are true chills whereas others are simply contact margins or mafic dykes. Chills from settings *i* and *ii* show considerable

evidence of contamination (e.g., LREE and other HFSE-enrichments), likely from country rock. Chills from setting *iii* are not enriched in LREE and may in fact represent uncontaminated mafic magma emplaced as a later pulse.

3.1. Introduction

The Voisey's Bay Intrusion (VBI) comprises a group of gabbroic to troctolitic intrusives belonging to the 1.34 to 1.29 Ga Nain Plutonic Suite (NPS) of northern Labrador, that occur 45 km southwest of Nain (Li et al., 2000). The NPS straddles the 1.85 Ga collisional suture between garnet-bearing quartzofeldspathic paragneiss of the Proterozoic Churchill Province to the west and Archean Nain Province quartzofeldspathic orthogneiss in the east (Ryan, 1995) (Figure 3-1).

The VBI fills at least two magma chambers at depth connected by an overturning, steeply dipping, sheet-like dyke, which all together comprise the Voisey's Bay Complex (VBC). In detail, the VBC consists of four different environments, from east to west: (1) an upper magma chamber (the Eastern Deeps) with a barren troctolite cap overlying fragment-bearing, weakly mineralized troctolite; (2) the Ovoid and Mini Ovoid massive sulphide deposits; (3) an overturned troctolite sheet which is near-vertical in the Discovery Hill zone and steeply south-dipping in the Reid Brook zone; and (4) a lower troctolitic magma chamber (the Western Deeps) (Evans-Lamswood et al., 2000). The Ryan's Pond zone is located down dip and to the east of the Eastern Deeps deposit, most likely as a faulted off portion of the Eastern Deeps chamber. The Kog Brook zone is located to the southwest of the Western Deeps dyke, and consists of a large olivine gabbro magma chamber (likely associated with the Western Deeps chamber) cross cut by

Rapakivi granite. Figure 3-2 is a plan map (top) and north-facing section (bottom)

through the VBI illustrating the four different VBC environments.

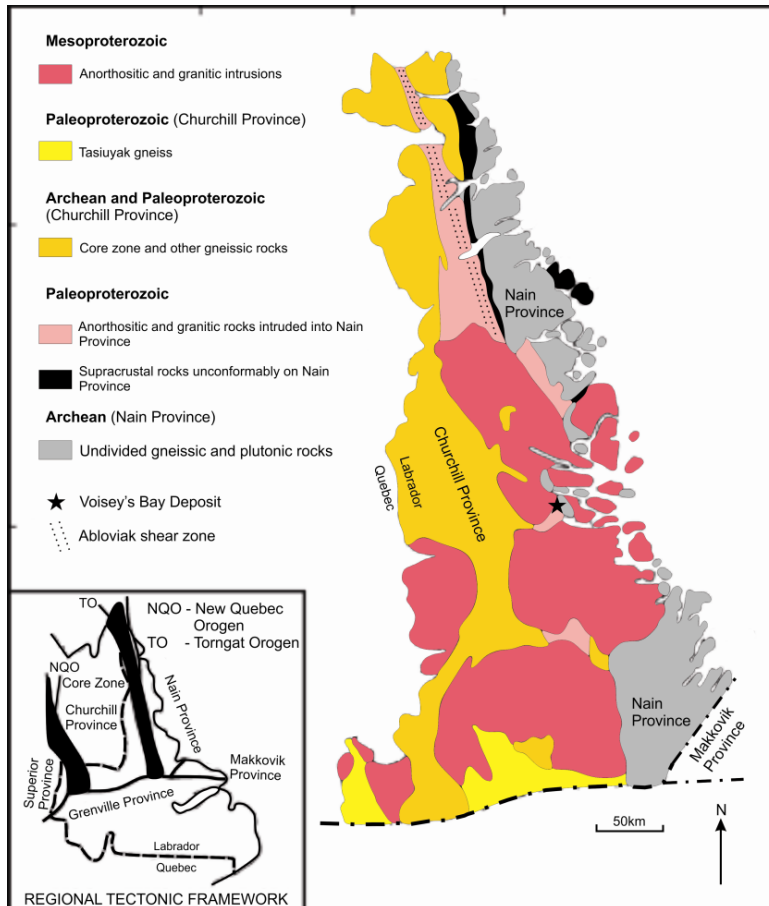


Fig. 3-1. A simplified geologic map of coastal Labrador. The Voisey's Bay mine site is indicated by the star on the map within the Mesoproterozoic Nain Plutonic Suite (NPS); this suite intruded along the suture between the Archean Nain Province (east) and the Proterozoic Churchill Province (west); modified after Ryan (1995). The Voisey's Bay deposits are hosted within the troctolite intrusions associated with the NPS.

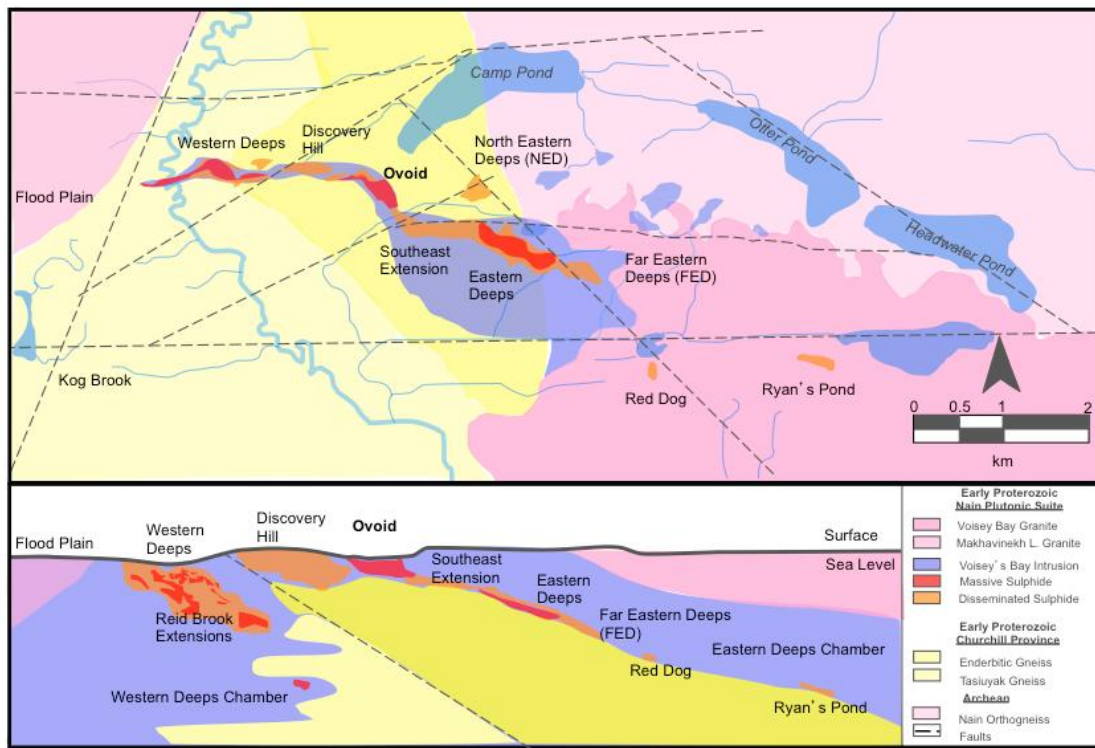


Fig. 3-2. Plan map (top) and north-facing section (bottom) through the Voisey's Bay Intrusion. Massive sulphide deposits are red and disseminated mineralization is shown in orange. Regional scale faults are plotted as dashed lines. Chilled margin samples were collected from the Kog Brook (to the west off-section on the north-facing cross section), Western Deeps, Discovery Hill, Ovoid, Eastern Deeps, and Ryan's Pond zones; map and section are modified from Li et al., 2000 (after Li and Naldrett, 1999; Lightfoot and Naldrett, 1999).

Nickeliferous massive sulphide mineralization (MASU) in the Eastern Deeps deposit occurs along the feeder entry line at the base of the magmatic chamber. The deposit is locally over 50 m thick and is typically haloed by a cloud of disseminated sulphides and brecciated troctolite. It is postulated that sulphide horizons at Ryan's Pond could be an extension of Eastern Deeps style mineralization, as a deposit of massive sulphide where a feeder enters at the base of the Eastern Deeps chamber (Vale, 2013). Moderately mineralized zones (15% leopard texture blebby sulphides and semi-massive veins) have been intersected during exploration drilling in Ryan's Pond, however, a

massive sulphide body comparable to an extension of the Eastern Deep has not yet been discovered. The Ovoid deposit occupies a basin-shaped depression in host enderbite gneiss that comprises up to 110 m vertical thickness of MASU overlying moderately mineralized troctolite and breccia (Naldrett et al., 2000). The Mini-Ovoid, located to the west of the Ovoid, is an accumulation of MASU within a swelling of the feeder dyke. The Discovery Hill zone contains disseminated and leopard texture sulphides (black clinopyroxene oikocrysts and large sulphide blebs in dyke material) and semi-massive to massive sulphide veins associated with the feeder dyke. Sulphides in this zone are concentrated in swells, where the diorite-norite dyke widens, which acted as hydrodynamic traps for the mineralization (Evans-Lamswood et al., 2000).

The form of mineralization in the Reid Brook zone is much more varied than in the other deposit environments as structural controls played an important role in the distribution of MASU bodies. Mineralization within the dyke is typically associated with leopard texture sulphides and feeder breccia sequences that contain tightly packed fragments. MASU deposits within the dyke occur where the dyke swells in thickness and subsequently flattens. Flattening of the dyke is believed to be associated with flat-lying north-south trending structures (fracturing and faulting). Thick intersections of MASU have also been encountered during drilling in the Churchill Province paragneiss country rock (Vale, internal data) at Reid Brook. The Kog Brook olivine gabbro contains trace fine-grained sulphide disseminations at irregular intervals.

3.2. Sampling

Sixteen chilled margins were sampled from drill core as summarized in Table 3-1. Because chills tend to be thin margins on more significant units (e.g., a thin chilled margin of gabbronorite on the margin of a larger troctolite chamber), some drill core samples were rather small. A minimum of 20 cm of halved-core was collected for each chilled interval. Each sample was cut for a polished thin section and a portion of each sample was crushed for whole rock lithogeochemistry. All sixteen chills were evaluated via petrographic analysis and ten of the samples (polished thin sections) were mapped using the mineral liberation analysis (MLA) software at Memorial University of Newfoundland. Six samples were evaluated as part of a biotite chemistry project and were analyzed using the electron microprobe at Carleton University (Chapter 2 of this thesis). Two of these samples (from the biotite study) were milled by mortar and pestle and sieved to a -40+60 mesh (0.422-0.251 mm) size fraction. The grain separates were eventually analyzed for oxygen isotope ratios at the Laboratory for Stable Isotope Science at the University of Western Ontario.

3.3. Description of chilled marginal rocks

Chilled margins form when hot magma contacts cold, solid rock and the heat flux from the magma cannot balance the initial conductive flux in the rock (Huppert and Sparks, 1989). This results in the rapid quenching of the magma and the crystallization of a fine-grained rock, finer than would be expected from normal plutonic cooling.

Table 3-1. Summary of chilled margin samples including sample and drillhole name, sample depth, rock type as determined by MLA (unless in italics which indicates that the sample had no MLA scan and was only examined petrographically), margin type, location of borehole, and occurrence. “Chill*” indicates chilled margins from a second, younger pulse of magma. These margins formed on contacts with younger granites and sulphide-bearing lithologies.

Sample	Drillhole	Depth	Lithology	Location	Occurrence	
JG11-116	VB07-820	From 167	To 167.6	Gabbro <i>norite</i>	Chill Western Deeps	Chills on diorite-norite feeder dykes except for one chill, sample JG11-127 that occurs as a margin on the upper contact of a thick sequence of olivine gabbro. These chills occur at the contact between dyke material and gneissic country rock; sample JG11-127 is in contact with Rapakivi granite.
JG11-127	VB09-897	371.6	372.2	Hornblende gabbro <i>norite</i>	Chill* Kog Brook	
JG11-130	VB01-555	251.7	253.6	Gabbro <i>norite</i>	Chill Ryan’s Pond	
JG11-106	OV09-028	33.9	34.2	Biotite gabbro <i>norite</i>	Chill Ovoid	
JG11-027	OV-09-038	87.0	87.6	Gabbro <i>norite</i>	Chill Ovoid	
JG11-109	OV09-066	57.8	58.0	Gabbro <i>norite</i>	Chill Ovoid	
JG11-099	VB04-619	212.0	212.8	Gabbro <i>norite</i>	Chill* Discovery Hill	Chilled magma associated with the injection of leopard texture troctolite and mineralized feeder breccia. Chills are within the Discovery Hill dyke and either within the basal breccia sequence in the Eastern Deeps or injected in to the country rock underlying the basal sequence.
JG11-140	VB04-619	210.9	211.9	Gabbro <i>norite</i>	Chill* Discovery Hill	
JG11-105	VB07-862	594.8	595.0	Hornblende gabbro <i>norite</i>	Chill* Eastern Deeps	
JG11-104	VB07-219A	796.5	797.4	Gabbro <i>norite</i>	Chill* Eastern Deeps	
JG11-101	VB04-630	522.1	523.1	Gabbro <i>norite</i>	Chill Eastern Deeps	
JG11-100	VB04-630	435.3	436.3	Gabbro <i>norite</i>	Chill Eastern Deeps	
JG11-102	VB04-630	534.15	534.8	Hornblende gabbro <i>norite</i>	Chill Eastern Deeps	
JG11-114	VB07-837	117.4	118.6	Hornblende gabbro <i>norite</i>	Chill* Western Deeps	Distribution of chills unclear; sample JG11-114 is chilled within dyke-hosted MASU and samples JG11-125 & 126 are chilled on margin of OGB chamber against Rapakivi granite.
JG11-126	VB09-897	182.9	183.9	Gabbro <i>norite</i>	Chill* Kog Brook	
JG11-125	VB09-897	170.1	171.1	Hornblende gabbro <i>norite</i>	Chill* Kog Brook	

It has been proposed that one can use the composition of chilled marginal rocks to assess the composition of the parental magma of a given system (Wager, 1960; Longhi et al., 1983; Hoover, 1989; Vander Auwera and Longhi, 1994). Within the VBI, chilled marginal rocks have been observed in the Eastern Deeps, Western Deeps, Ovoid, Discovery Hill, Kog Brook, and Ryan's Pond. A detailed description of the occurrence of the chilled margins within each zone is presented in the following section.

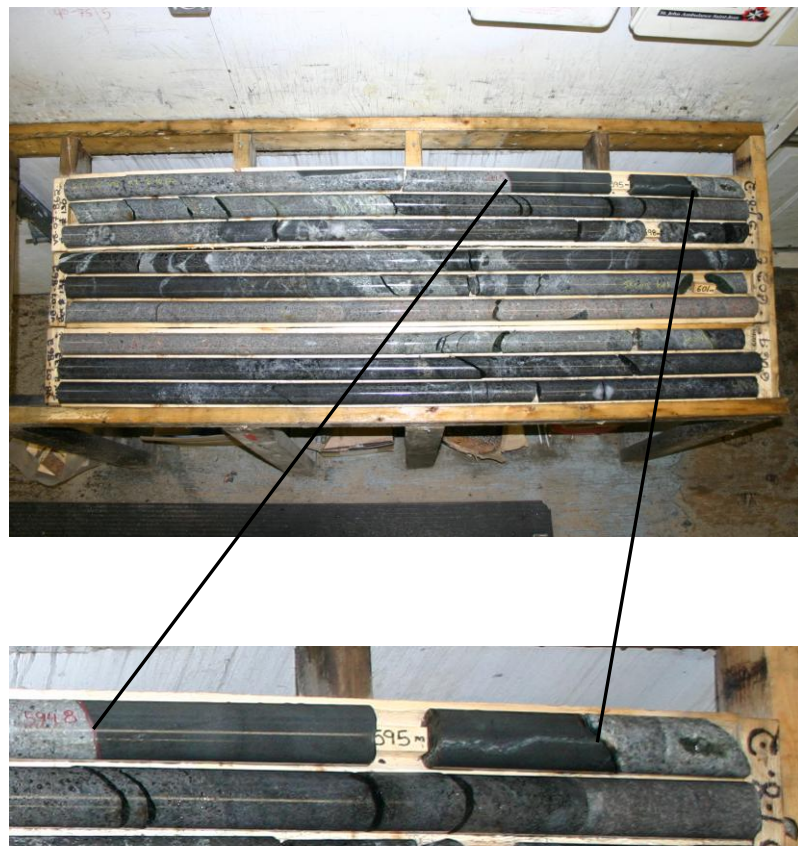


Fig. 3-3. A marginal hornblende gabbronorite from Eastern Deeps drill hole VB07-862 at 595.0 m below surface. This margin occurs between a thick package of fragment-bearing troctolite with granite slabs/dykes at various depths. This aphanitic interval is bounded by coarse-grained, homogeneous granite and may represent a younger pulse of mafic magma associated with the injection of mineralization from the Eastern Deeps feeder dyke. In this photo the granite is pale grey and pink, the fragment-bearing troctolite is dark purple-grey and the chilled margin is a dark bluish black and shown on the blowout photo.

In drill core, chilled margins can be distinguished from thin mafic dykes based on colour, grain size, and associated rock types (Figure 3-3). Chilled margins are typically bluish-black, whereas mafic dykes are dull brown. The aphanitic chills have very sharp black contacts and are spatially associated with troctolite-diorite-norite-olivine gabbro. VBI mafic dykes observed within the paragneiss country rock are locally weakly foliated and individual mineral grains can be visible in hand sample, unlike the chilled margins. The chills are aphanitic in drill core hence mineral identification is difficult. Petrographic examination reveals that the chills display ophitic textures wherein randomly oriented plagioclase laths form discontinuous frameworks around the interstitial mineral phases. Photomicrographs of the chilled margin sections constitute Appendix A. Consistent petrographic variations are not observed between the different chilled margins.

The typical mineral assemblage of the VBI chilled marginal rocks was determined by combining observations from petrography and the results of the MLA analyses. Using the MLA (Sylvester, 2012) grain boundaries are mapped via backscatter electron imaging (BSE) and grains are classified by comparison with elemental spectra.

MLA results for the chilled margin samples are summarized in Table 3-2; those samples omitted from Table 2 were not analyzed using the MLA. The typical mineral assemblage of the VBI chilled margins includes plagioclase (35-50 wt %), pyroxene (10-40 wt %), magnetite (<10 wt %), and ilmenite (<5 wt %), with variable amounts of biotite and hornblende. According to Streckeisen's (1974) classification scheme (Appendix A), the chilled margins would be classified as gabbronorite based on the MLA modal determinations.

3.4. Two generations of chilled margins

In the original drill core logging by Vale geologists all of these samples were recorded as chilled margins. With more detailed re-logging, however, it became apparent that only half (eight) of these samples are chilled against old, cold gneissic country rock. The other eight chilled margins are quenched against granitic rocks and mineralized troctolite and gabbro. This suggests that this second group of eight samples represent a younger pulse of gabbroic magma that quenched against the younger granitic intrusives. The granites had to be emplaced and cooling/partially cooled before the final pulse of gabbroic magma could quench against these granites. Chilled margin samples are listed on Tables 3-1 and 3-2 and the older chills are referred to simply as “Chills” while the younger chills are referred to as “Chills*”. The older group of chilled margins is in contact with orthogneiss and paragneiss country rock. The younger group of chilled margins is in contact with granite (predominantly Rapakivi), highly mineralized feeder material or massive sulphide; all of these units are younger or contemporaneous with the VBI troctolite-gabbro system. The distinction between the two groups of chilled margins appears to influence the micro-texture of the rock. Examples of the older versus younger chilled margin textures can be seen in Figure 3-4. Photomicrographs for the remaining chilled margins can be found in Appendix A. The mineral grains in the older chilled margins are equigranular, have anhedral boundaries, appear subrounded, and are weakly aligned (possibly related to flow direction of the parental magma). On the other hand, the younger chilled margins display bimodal grain sizes and individual minerals are ragged, giving the rock a felty appearance under petrographic microscope. These textural

differences may be attributable to differences in the temperature of formation of the different rocks. Specifically, the first generation of chilled margins would have crystallized rapidly as a result of contact with a cold gneissic rock whereas the second generation of chilled margins would have quenched against the younger granite intrusives in the VBI.

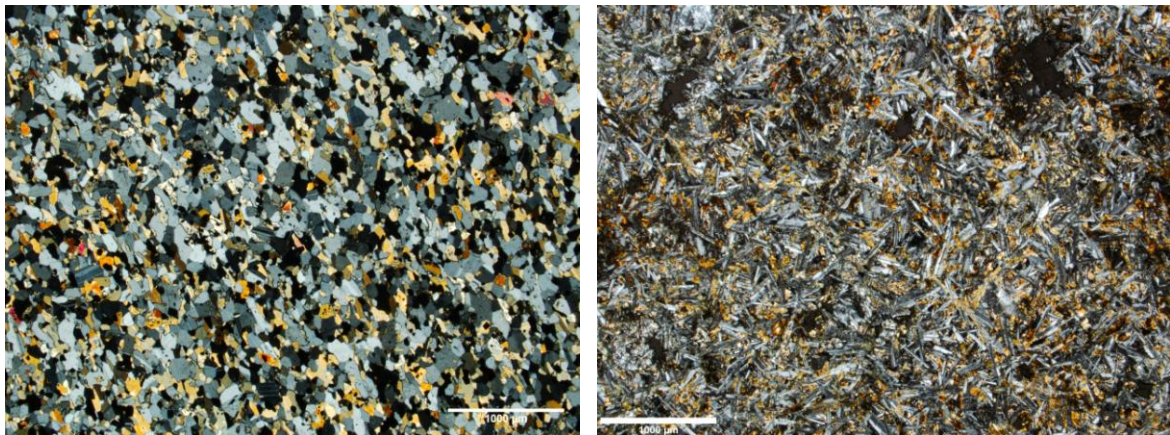


Fig. 3-4. Photomicrographs of micro-textures observed in the two generations of chilled margins. Left. JG-11-100. Chilled marginal gabbronorite from the Eastern Deeps: represents older generation of chilled margins. Grains have poorly defined crystal faces and display a weak fabric (possible indicator of flow direction). Grains are equigranular and plagioclase forms a discontinuous framework with fine, subrounded interstitial pyroxene and biotite (visible only under petrographic microscope). Right. JG-11-126. Chilled marginal gabbronorite from Kog Brook: represents younger generation of chilled margins. This margin formed when a younger, uncontaminated pulse of gabbroic magma quenched against a slab of Rapakivi granite. Note the felty, ragged appearance of individual grains and the bimodal grain sizes. Larger plagioclase laths form a discontinuous framework enclosing much finer grained interstitial pyroxene.

3.5. Occurrence of chilled margins

The occurrences of the chilled margins are briefly summarized in Table 3-1 and are described in detail below. The marginal rocks from the VBI occur in three distinct environments, which are defined by geochemical parameters that will be discussed in the following section. Although there are three geochemical varieties of chilled margins, the

chills from these three geochemical groups belong to the two different generations of chills described in section 3.4.

Group 1 chilled margins are developed on diorite-norite-troctolite feeder dykes and include chills at the base of the Ovoid dyke-hosted massive sulphide deposit (Fig. 3-5). These chills occur at the contact between dyke material and gneissic country rock. The chills formed when hot mafic magma quenched against cold country rock. One sample belonging to this group (JG-11-127, grouping based on whole rock geochemistry) is a chill that occurs as a margin on the upper contact of a thick sequence of olivine gabbro associated with the Kog Brook zone and occurs within one of two thick sequences of olivine gabbro emplaced in Kog Brook. The upper and lower sequences are separated by a thick package of paragneiss. The two olivine gabbro sequences likely represent distinct pulses of magma emplaced at different times.

Table 3-2. Modal mineralogies of the lithological units sampled from the Voisey's Bay and Mushauu intrusions. Locations are WD = Western Deeps, (N)ED = (north) Eastern Deeps, DH = Discovery Hill, OV = Ovoid, RP = Ryan's Pond, KB = Kog Brook. Margins that are omitted from this table were not analyzed using the MLA. JG-11-106 is in contact with enderbitic orthogneiss and the polished thin section was prepared along this contact. As such, part of the enderbite was captured in the MLA scan resulting in a high modal % of biotite.

Lithology	Sample	Mineralogy determined by MLA (weight percent)							Location	Depth	
		Plag	Olv	Opx	Cpx	Hbl	Biot	Sulph	Oxide		
Gabbro-norite	JG11-100	48.96	0.08	19.52	17.87	2.65	3.56	0.14	1.51	5.71	ED
	JG11-101	52.08	0.10	13.57	19.80	1.91	2.18	0.13	4.54	5.69	ED
	JG11-102	48.37	0.01	3.56	8.82	23.00	1.39	0.14	11.33	3.38	ED
	JG11-104	48.81	0.02	18.37	20.61	2.41	5.25	0.25	1.63	2.65	ED
	JG11-105	41.71	0.00	13.48	11.51	27.52	2.05	0.25	0.19	3.29	ED
	JG11-130	49.06	0.00	23.03*	12.21*	1.06	2.02	0.06	4.49	8.07	RP
	JG11-106	52.28	0.01	0.65	6.41	5.57	18.53	0.02	2.35	14.18	OV
	JG11-114	34.64	0.14	3.29	31.90	7.46	1.22	2.86	10.62	7.87	WD
	JG11-125	39.01	0.07	0.15	14.62	14.81	1.71	0.08	3.10	26.45	KB
	JG11-127	45.78	1.31	2.67	8.29	6.85	4.44	0.32	11.98	18.36	KB

Group 2 includes chilled margins associated with the injection of leopard texture troctolite, mineralized breccia and massive sulphide (Fig. 3-6). In the context of the VBI, this pulse of magma would follow the emplacement of barren, unmineralized, troctolite and gabbro, which initially filled large magma chambers. A later pulse of gabbroic magma, which succeeded the mineralization episode, may have followed the pulse of mineralized magma in to the Eastern Deeps chamber and Discovery Hill dyke. These two generations of magmas are parental to the Group 2 chilled margins. These chills occur within the Discovery Hill dyke and are in contact with weakly to moderately mineralized troctolite. Group 2 margins also occur in the Eastern Deeps either within the basal breccia sequence (in a similar fashion to those in the Discovery Hill dyke) or injected in to the country rock underlying the Eastern Deeps chamber. One Group 2 margin is in contact with a 20 m thick granitic intrusive (JG-11-105).

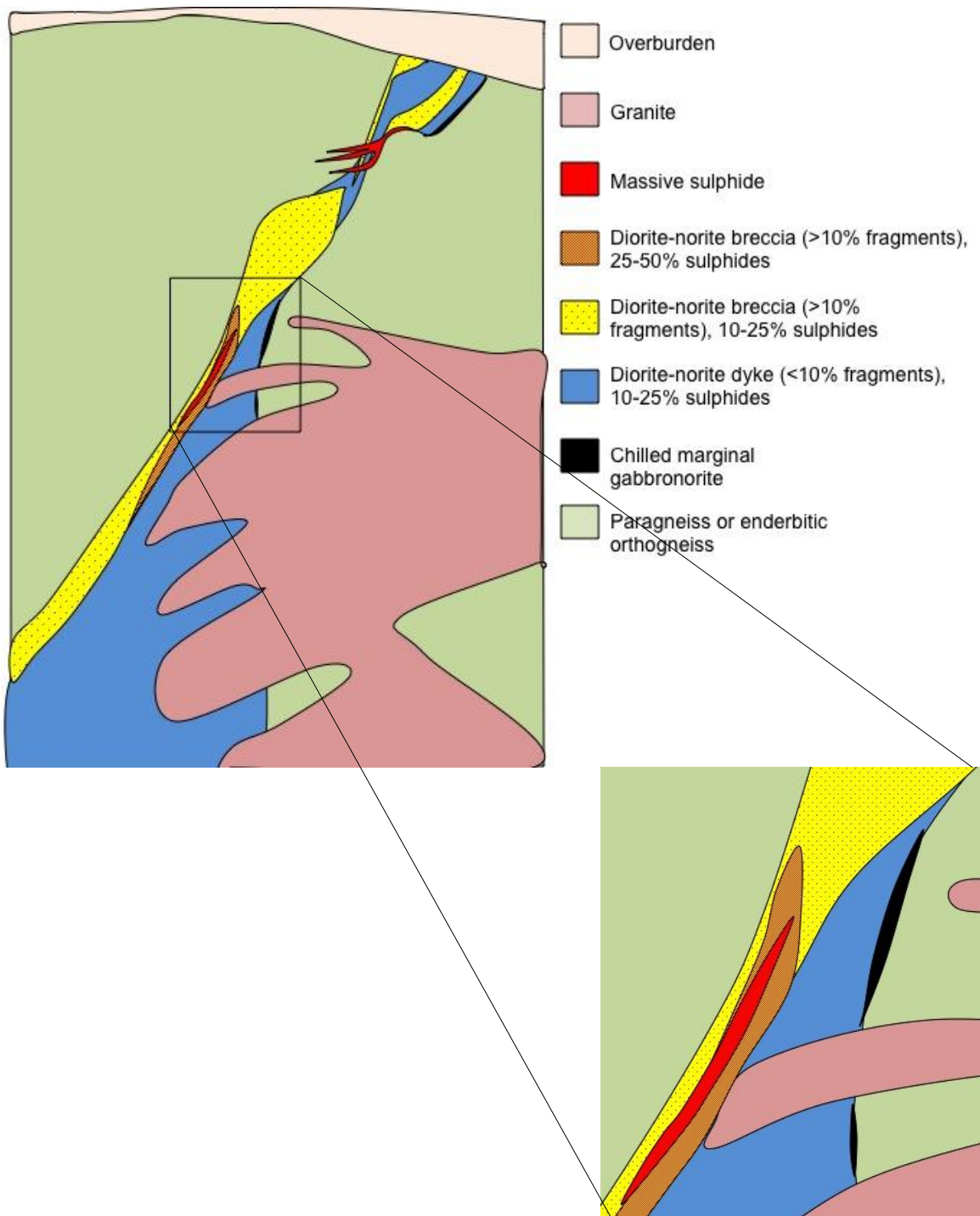


Fig. 3-5. West-facing schematic through the Reid Brook dyke (Western Deeps zone) showing the chilled margin along the contact between dyke and Tasiuyak paragneiss. Chilled margins in Group 1 also form at the base of the Ovoid (contact with underlying enderbite). Figure modified after Evans-Lamswood et al., (2000).

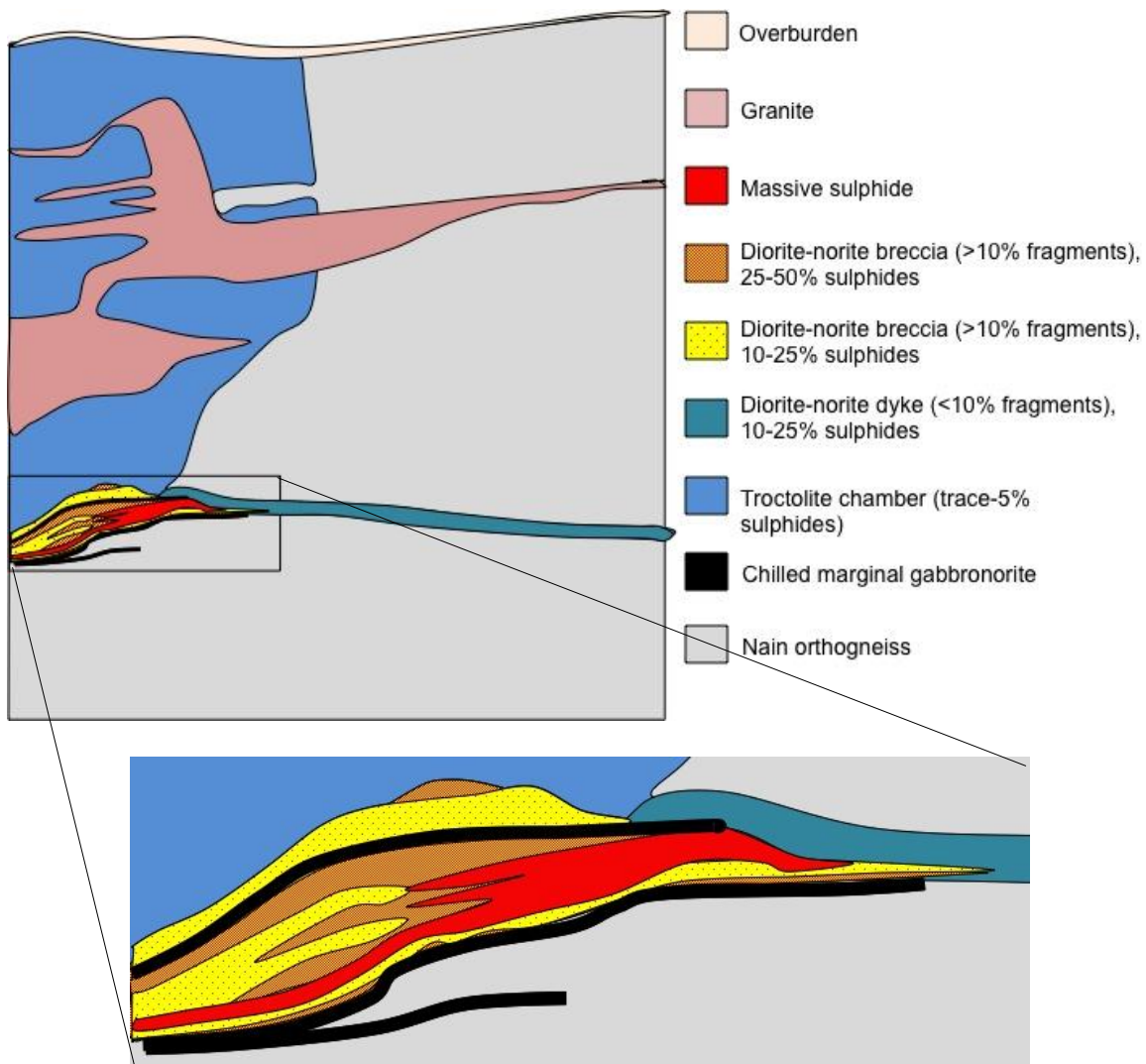


Fig. 3-6. West-facing schematic through the Eastern Deeps chamber. The chilled margin occurs either within the mineralized sequence at the base of the chamber, at the contact between the sulphide-bearing feeder and underlying Nain orthogneiss or injected directly into the orthogneiss. One Group 2 chilled margin occurs within the chamber in contact with a slab of granite. Figure modified after Evans-Lamswood et al., (2000).

The distribution of chilled margins belonging to Group 3 is not as well defined as Group 1 and 2 chills. JG-11-114 is in contact with massive sulphide within the feeder dyke in the Western Deeps. Samples JG-11-125 and JG-11-126 are in contact with Rapakivi granite that intruded into the Kog Brook zone. All three samples in this group

chilled against rocks younger than the main troctolite-gabbro of the VBI and must therefore represent a much younger magma, which intruded the system following the emplacement of granite and MASU.

3.6. Major and trace element whole rock lithogeochemistry

3.6.1. Major element chemistry of chilled margins

Variations in the major element chemistry of the marginal rocks are presented on Fig. 3-7. Chilled margins have magnesium number ($Mg/Mg+Fe$) values between 38 and 61 and contain between 45 and 55 weight percent (wt %) SiO_2 . Chills from Group 2 have higher (more primitive) Mg # values. Gabbronorite from all three geochemical groups contains between 11 and 17 wt % Al_2O_3 . Only one sample, JG-11-116, contains significantly less Al_2O_3 , with approximately 6 wt %. This difference could be attributed to JG-11-116 having chilled in contact with highly altered paragneiss, giving the chilled margin a different geochemical (contamination) signature. The chilled margins contain between 0 and 1.0 wt% K_2O , however two samples, JG-11-106 and JG-11-109 from the Ovoid, contain 2.2 and 1.7 wt% K_2O respectively. As with SiO_2 , Al_2O_3 and K_2O , FeO^* values do not vary greatly and typically range between 8.0 and 15 wt%. TiO_2 varies within Group 1 chilled margins, with values ranging between 1.9 and 3.9 wt%. Group 2 and 3 TiO_2 values are in the more confined range of 0.6 to 1.8 wt%. P_2O_5 values range between 0 and 1 wt% with the most variation occurring in the chilled rocks belonging to Group 1.

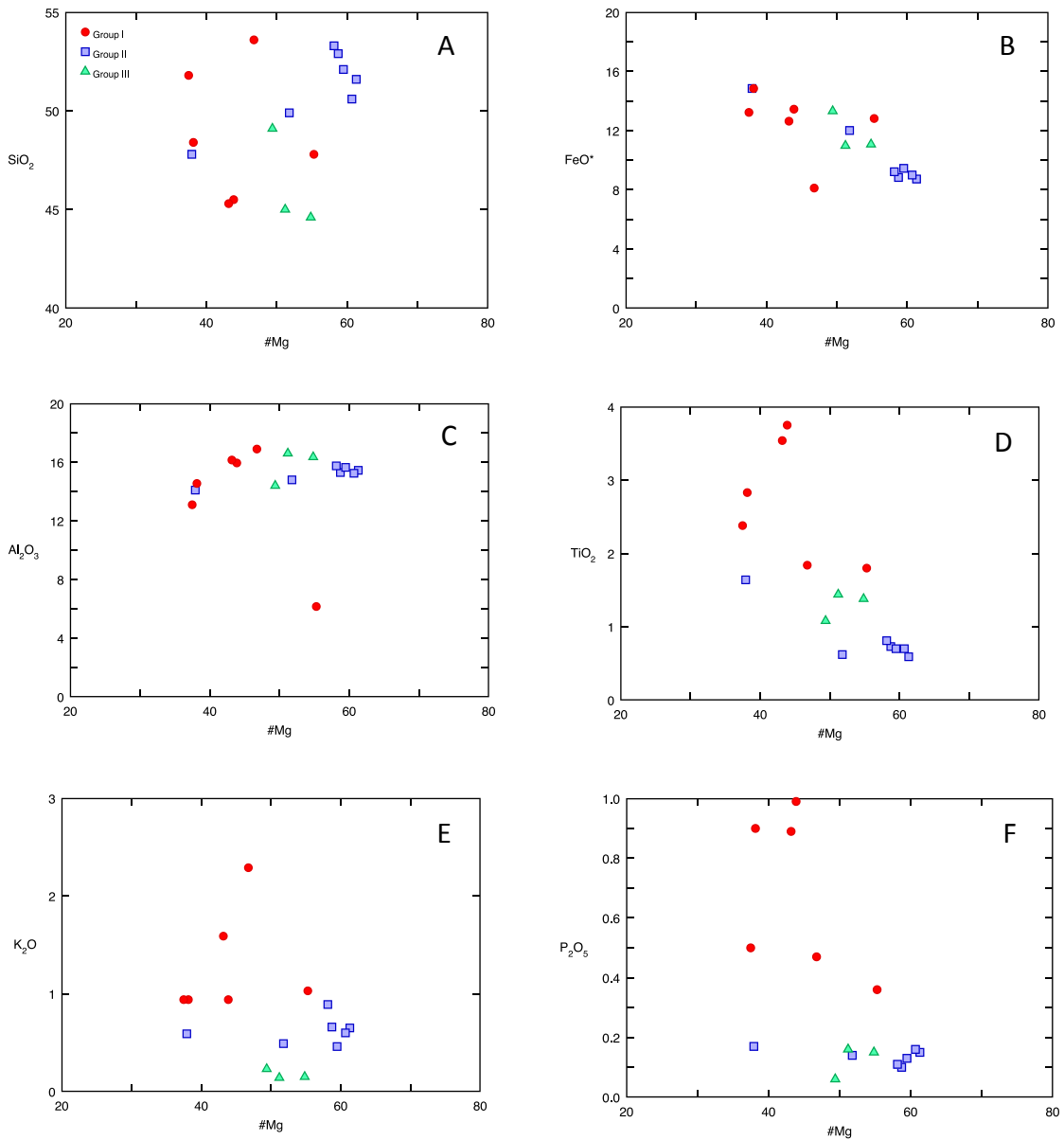


Fig. 3-7. Bi-variate major element plots for marginal rocks. Chills belong to Group 1 (red circles), Group 2 (blue squares) or Group 3 (green triangles). A. Mg # vs. SiO₂. B. Mg # vs. FeO*. C. Mg # vs. Al₂O₃. D. Mg # vs. TiO₂. E. Mg # vs. K₂O. F. Mg # vs. P₂O₅. Group 2 and 3 chills likely have a distinct source of contamination from the Group 1 chills.

Group 1 chilled gabbronorite shows the most variation in major element chemistry with slightly higher concentrations of K₂O, TiO₂ and P₂O₅ relative to chilled rocks in

Groups 2 and 3. Group 1 chemistry is most likely attributable to contamination from interaction with gneissic country rocks.

3.6.2. Trace element chemistry of chilled margins

Figures 3-8 & 3-9 are two basalt discrimination diagrams for chilled marginal rocks from the VBI. Figure 8 shows the chilled and contact margins plotted on Pearce and Norry's (1979) Zr versus Zr/Y basalt discrimination diagram. Chills from Group 1 (red circles) plot alone in the "within plate" field. For the most part, Group 2 and 3 chills plot within the "MORB" and "ARC" fields. Two Group 2 chills, JG-11-99 and JG-11-140, plot within the E-MORB field. These chills are from Discovery Hill and may preserve an E-MORB signature resulting from enderbitic orthogneiss contamination as the parental magma ascended from depth. The MORB-like signature observed in Group 2 and 3 chills implies that these chills originated from a fairly primitive magma. The within-plate signature observed in Group 1 chills suggests that these rocks crystallized from a more contaminated magma. One Group 3 chill, JG-11-114, plots within the volcanic arc field. This is the only marginal gabbro in direct contact with massive sulphide and the only chill containing trace sulphide minerals, thus the absolute concentrations of Zr and Y are diluted.

Figure 3-9 shows Floyd and Winchester's (1975) basalt discrimination diagram for marginal rocks from the VBI. The chilled margins plot in two groups; Group 1 chills plot near the alkaline/continental tholeiite basalt compositions and Group 2 and 3 margins plot toward the MORB composition, which is in agreement with the trends observed on Figure 3-8. Group 1 chilled margins record a contamination signature while Groups 2 and

3 chills record a more primitive magmatic signature. Group 1 chills have TiO_2 values between 1.9 and 3.9 wt %, whereas Group 2 and 3 chills have TiO_2 values between 0.5 and 0.8 wt %. Y/Nb ratios for Group 1 chills vary between 0.2 and 3.8 and Group 2 and 3 Y/Nb values range between 4.4 and 8.0.

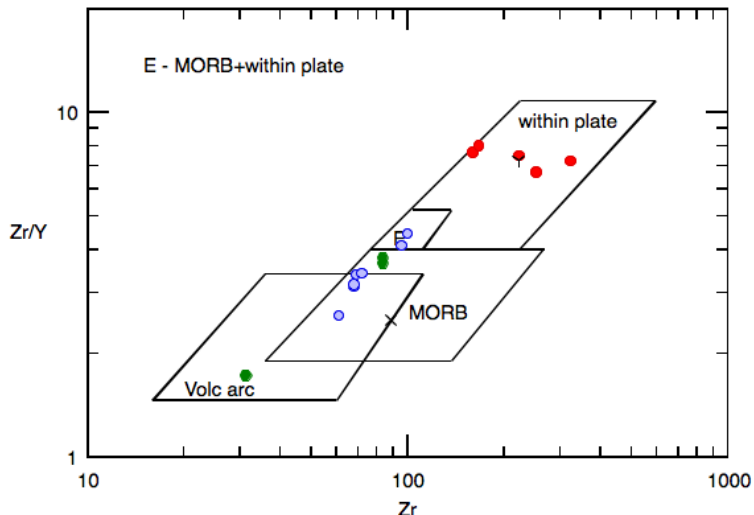


Fig. 3-8. Basalt discrimination plots after Pearce and Norry (1979). Chills from Group 1 plot in the “within plate” field (OIB indicated by symbol y). Chills from Groups 2 and 3 plot in the MORB field. One chill from Group 3 plots in the volcanic arc field. This chill is in contact with MASU.

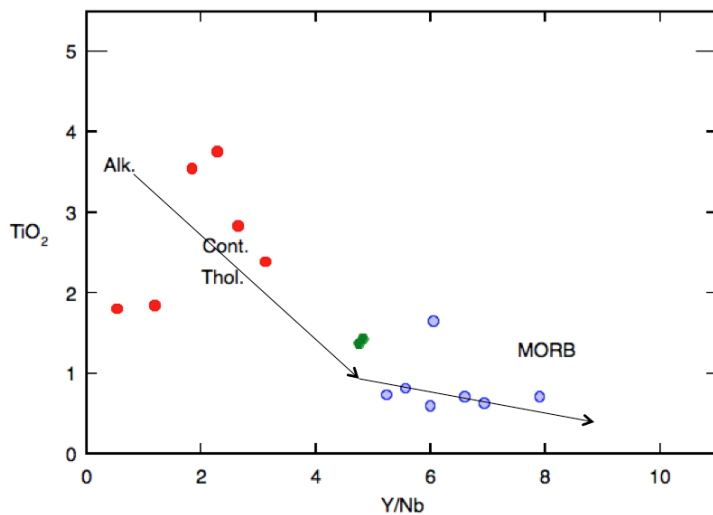


Fig. 3-9. Basalt discrimination plot after Floyd and Winchester (1975). Arrows show approximate trend from alkali basaltic composition (Group 1 chills) through to MORB composition (Group 2 and 3 chills). Group 1 chills are enriched in TiO_2 relative to Group 2 and 3. Groups 2 and 3 have higher Y/Nb ratios relative to Group 1.

3.7. Rare earth element lithogeochemistry of chilled margins

Figure 3-10 (A-D) is a plot of Ce vs. Yb (after Li et al., 2000) for troctolite and chilled marginal rocks from the VBI. The solid symbols represent the margin samples and are grouped as discussed above (Groups 1-3). The open symbols represent troctolite-diorite-norite-olivine gabbro from the VBI and colour is based upon which chilled margin grouping the troctolite could be associated with (for example, a troctolite from the Eastern Deep would be represented by a blue, open square as Group 2 chills are represented by solid blue squares and are also associated with the Eastern Deep). Troctolite sampled from the Mushau intrusion is plotted as purple diamonds. The data confirm that Voisey's Bay troctolite plots within the Voisey's Bay envelope as defined by Li et al. (2000) where $\text{Ce/Yb} = 22-27$. Each plot highlights the differences between marginal rocks and "regular" troctolite sampled from the deposit.

Figure 3-10A is a plot of data for rocks associated with Group 1 chilled margins. There is scatter among the data for Group 1 rocks which is likely attributable to country rock contamination. Samples from Groups 2 and 3, on the other hand, (Fig. 3-10B & 3-10C) plot along two trends. Chilled margins from Groups 2 and 3 plot closer to the Mushau trend ($\text{Ce/Yb} < 17$) whereas chamber and feeder rocks from these groups plot along the Voisey's Bay trend ($\text{Ce/Yb} > 22$). This could be attributable to the fact that all of the Group 3 margins and four of the Group 2 margins are representative of a younger pulse of less-contaminated magma that quenched against the granitic dykes and mineralized troctolite. Figure 3-10D shows the Ce vs. Yb plot for only chilled margins and Mushau troctolite.

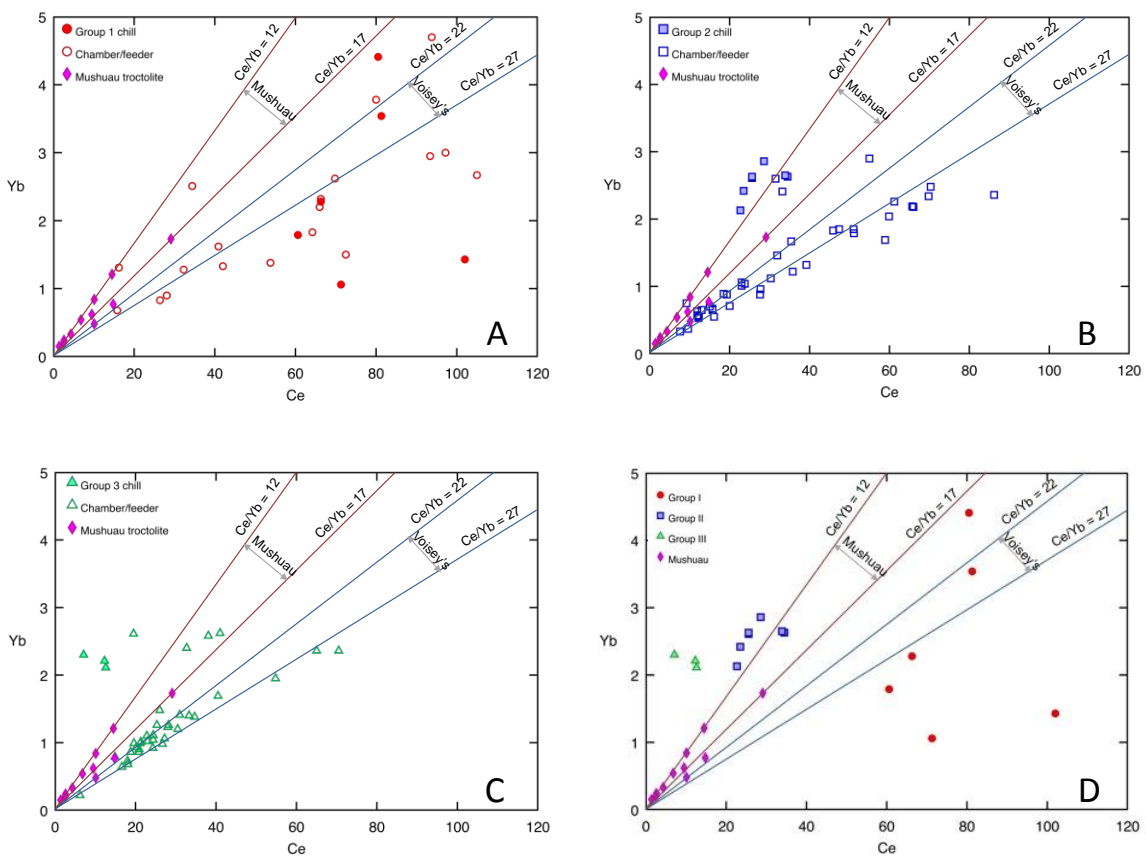


Fig. 3-10. Bivariant plots showing Ce vs. Yb for chilled marginal rocks and mafic intrusive rocks associated with the chills. Ce/Yb lines show the ranges for Mushuau ($\text{Ce}/\text{Yb} = 12-17$) and Voisey's Bay ($\text{Ce}/\text{Yb} = 22-27$) troctolite (from Li et al., 2000). A. Group I chills plotted with Mushuau troctolite and troctolite-diorite-norite from the same depositional zone as the Group 1 chills. B. Group 2 chills plotted with Mushuau and Eastern Deep troctolite and Discovery Hill diorite-norite. C. Group 3 chills plotted with Mushuau troctolite and troctolite-olivine gabbro-norite from the Western Deep and Kog Brook. D. Plot of all chills and Mushuau troctolite.

Figure 3-11 shows a chondrite-normalized REE plot of chilled margin samples (McDonough and Sun, 1989). Chills belonging to Group 1 are enriched relative to C1 chondrites and are light rare earth element (LREE) enriched. Group 1 chilled margins are enriched in Sr, K, Rb, and Ba (mobile, large ion lithophile (LIL) elements) (Fig. 3-12). This is likely a contamination signature with the LIL elements originating in the

surrounding country rock, as these elements would not be present in uncontaminated mafic magmas.

As with Group 1 chills, Group 2 chills are LREE-enriched. These two geochemical groups of chilled margins plot subparallel on the chondrite-normalized diagrams. Group 2 chilled margins are also enriched in mobile LILs picked up from country rock probably as gneissic fragments in the brecciated troctolite associated with these chilled margins.

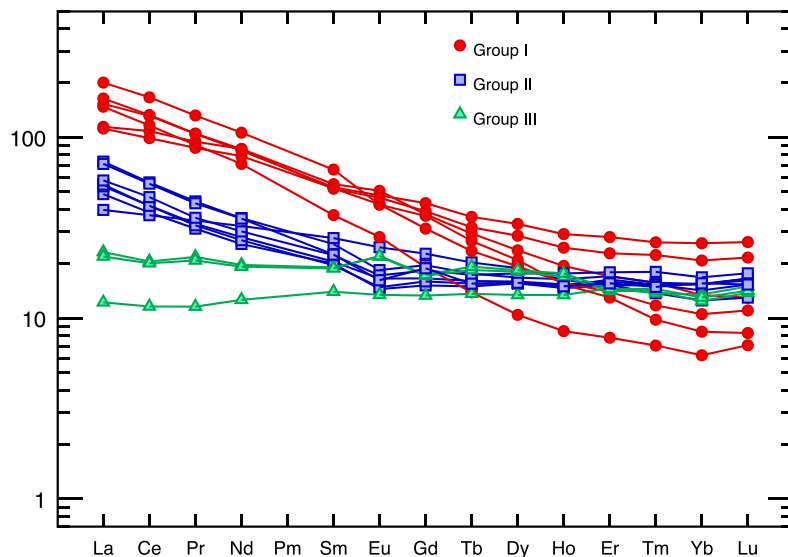


Fig. 3-11. Chondrite-normalized (C1 normalization factors from McDonough and Sun, 1989) rare earth element (REE) plot of chilled margin samples from the VBI.

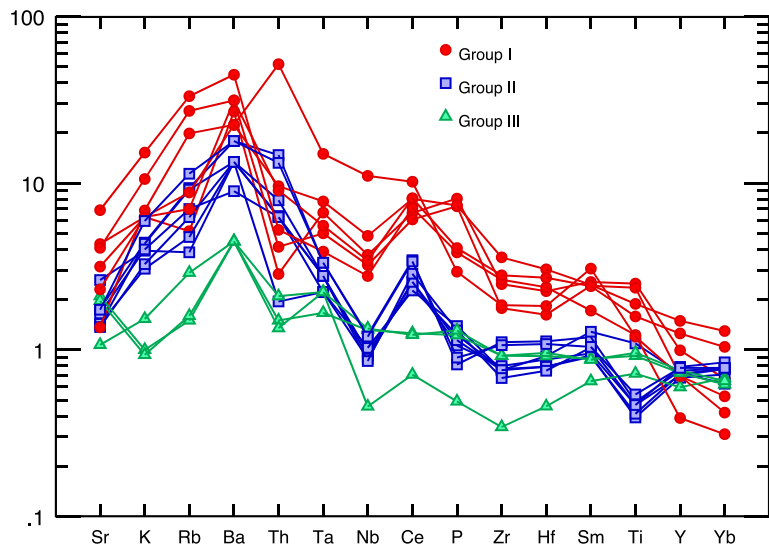


Fig. 3-12. MORB-normalized rare earth element multielement plot of chilled margins from the VBI, (MORB normalization factors from Pearce, 1983).

Group 3 chilled margins are flat-lying on multielement diagrams and are not enriched in LREE. JG-11-114, which is confined to the feeder dyke and is in contact with massive sulphide, may represent an uncontaminated sample from depth transported closer to surface contemporaneous with massive sulphide or it may represent a younger, uncontaminated troctolitic component injected in to the system following the main episode of mineralization. The chills belonging to this group do not show contamination signatures like the chills in Groups 1 and 2 and may have crystallized from a residual magma associated with sulphide segregation. The two chilled margins from Kog Brook would have formed when their parental magma quenched against Rapakivi granite dykes and their chemistries are likely to be representative of the parental magma composition of a younger, uncontaminated troctolitic-gabbroic magma.

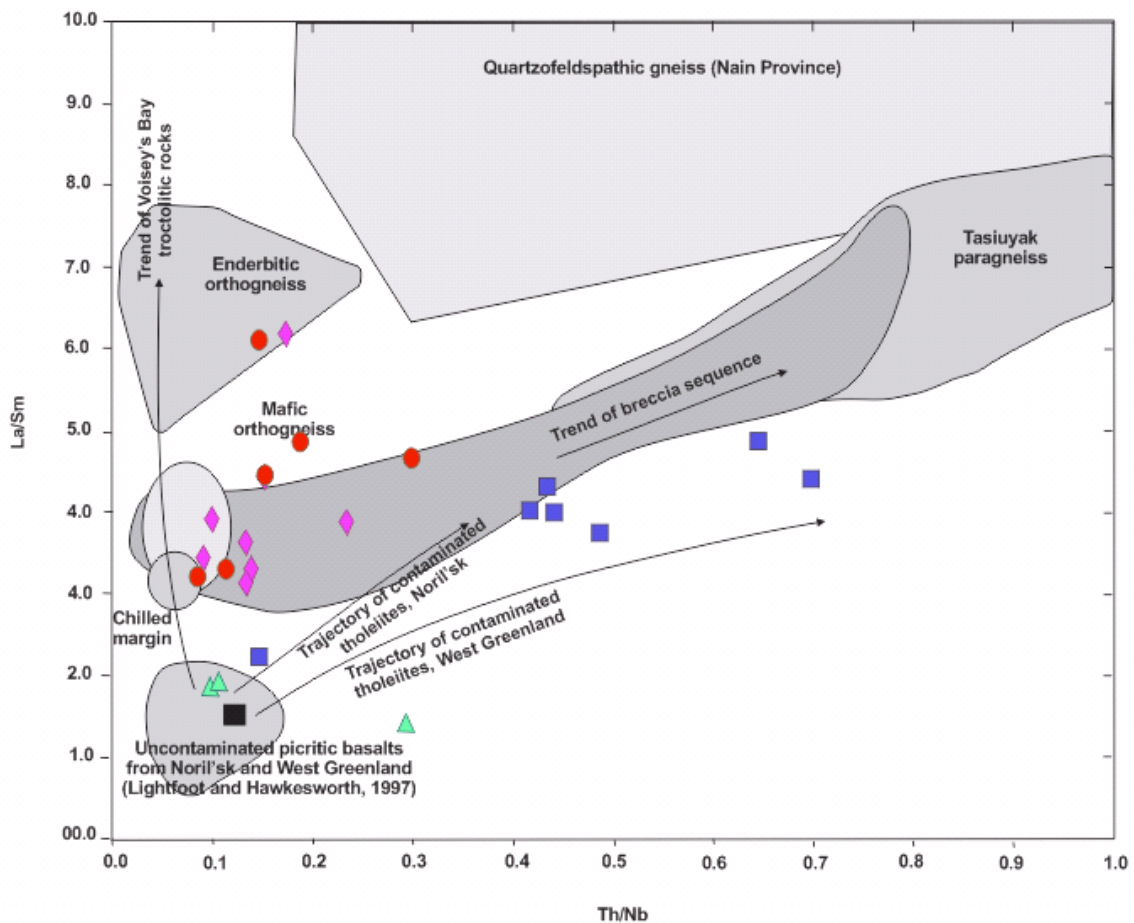


Fig. 3-13. Plot of La/Sm vs. Th/Nb in chilled marginal rocks from the VBI and troctolite from the Mushuau intrusion. Fields and trend lines are from Li et al. (2000). Red circles indicate chills from Group 1, blue squares indicate chills from Group 2 and green triangles indicate chills from Group 3. Purple diamonds indicate Mushuau troctolite. The black square in the lower left corner indicates the composition of the primitive mantle (composition from Sun and McDonough, 1989) and is within the field defined by uncontaminated picritic basalts.

On the plot of Th/Nb vs. La/Sm (Fig. 3-13), chilled margins belonging to Group 1 plot in a trend parallel to the Voisey's Bay troctolite but with higher Th/Nb ratios. These chills are most likely contaminated by both orthogneiss and paragneiss. The Mushuau troctolite plots near the mafic orthogneiss and chilled margin fields defined by Li et al. (2000). Group 2 chilled margins, which are spatially associated with feeder dyke brecciated sequences, plot along the “trend of breccia sequence” and likely represent a

non-mineralized component of an early ore-bearing pulse into the VBI chamber and feeder dyke complex. Group 2 chills appear to be contaminated mainly by paragneiss Group 3 margins plot near the field of uncontaminated picritic basalts for Noril'sk and West Greenland (composition from Lightfoot and Hawkesworth, 1997 in Li et al., 2000) and the primitive mantle composition (after Sun and McDonough, 1989). Group 3 chilled margins appear to have crystallized from a primitive, uncontaminated mafic magma

3.8. Discussion and significance

Chilled marginal rocks may represent a quenched magma, parental to the ore-bearing Voisey's Bay troctolite intrusion. Chilled margins are found throughout the VBI and occur in three different environments, which can be summarized as follows: *i.* on the margins of diorite-norite feeder dykes; *ii.* spatially associated with leopard texture troctolite and mineralized breccia in the Eastern Deeps and Discovery Hill zones, and; *iii.* on large olivine gabbro magma chambers intruded by granite sheets. There are three geochemically distinct groups of chilled marginal rocks that correlate with the three different environments in which the margins are found (as summarized above). The chills in Group 1 are enriched in LREEs and in LILs, a contamination signature picked up from the surrounding country rock. Group 2 chilled margins are also enriched in LREEs and LILs and are injected into sulphide-bearing troctolite breccia or the country rock underlying the brecciated sequence. Group 3 margins are not enriched in LREEs or LILs and are chilled margins on the Kog Brook olivine gabbro chamber. JG-11-114 is a margin associated with a massive sulphide body in the Western Deeps.

Chills from Groups 1 (and, to a lesser degree, Group 2) plot parallel to the trend for Voisey's Bay troctolite, however; it should be noted that they likely inherited a geochemical signature from the country rocks (via direct contact and the incorporation of fragments). The samples in Group 3 may represent a much younger, less contaminated mafic magma. JG-11-114 is anomalous and its spatial association with massive sulphide in the Western Deeps feeder dyke suggests it may be armoured from the effects of country rock contamination and late-intruding granites.

These observations are important in that they suggest that two mafic magmas of differing ages may have fed the Voisey's Bay system. It can be postulated that the older chilled margins in contact with old, cold country represent one of the early pulses of magma that fed the VBI. The chilled margins in contact with granite and highly mineralized troctolite and MASU represent a younger pulse of magma, younger even than the Rapikivi granites. This magma would have been emplaced at a time of high heat flow and are chemically similar to the younger Mushauau intrusion. These chilled margins also represent a more primitive (less contaminated) pulse of mafic magma.

The first pulse of magma to the VBC likely produced the barren normal troctolite, which overlies the Eastern Deeps deposit. The second pulse of magma produced a more evolved troctolite, troctolite breccias and sulphide breccias. This second pulse is represented by Group 1 chilled margins and was contaminated by gneissic country rock. The third pulse of magma produced the granites in the VBC and occurred during a period of continued high heat flow. The final pulse of mafic magma followed the emplacement of the granites. This younger pulse is more primitive and has a geochemical signature

more akin to Mushuau troctolite. The chills belonging to Groups 2 and 3 represent this last pulse. The first, second and third pulses of magma are part of a mega pulse, which brought the early troctolite and sulphide mineralization to shallower depths and emplaced them in the framework of the VBC. The fourth and final pulse of magma intruded the VBC as a new mega pulse but unfortunately neither sulphide mineralization nor even granite intrusives have been associated with this younger, uncontaminated magma.

Bibliography

- Evans-Lamswood, D., Butt, D. P., Jackson, R. S., Lee, D. V., Muggridge, M. G., Wheeler, R. I., et al. (2000). Physical controls associated with the distribution of sulfides in the Voisey's Bay Ni-Cu-Co deposit, Labrador. *Economic Geology and the Bulletin of the Society of Economic Geologists*, 95 (4), 749-769. Retrieved from <http://search.ebscohost.com/login.aspx?direct=true&AuthType=ip,url,uid&db=geh&AN=2000-054362&site=ehost-live&scope=site>; <http://www.segweb.org/journal.htm>
- Floyd, P. A., & Winchester, J. A. (1975). Magma type and tectonic setting discrimination using immobile elements. *Earth and Planetary Science Letters*, 27 (2), 211-218. Retrieved from <http://search.ebscohost.com/login.aspx?direct=true&AuthType=ip,url,uid&db=geh&AN=1976-007461&site=ehost-live&scope=site>; <http://www.sciencedirect.com/science/journal/0012821X>
- Helz, R. T. (2009). Processes active in mafic magma chambers: The example of Kilauea Iki lava lake, Hawaii. *Lithos*, 111 (1–2), 37-46. doi:<http://dx.doi.org/10.1016/j.lithos.2008.11.007>
- Hoover, J. D. (1989). The chilled marginal gabbro and other contact rocks of the Skaergaard Intrusion. *Journal of Petrology*, 30 (2), 441-476. Retrieved from <http://search.ebscohost.com/login.aspx?direct=true&AuthType=ip,url,uid&db=geh&AN=1989-071559&site=ehost-live&scope=site>
- Huminicki, M. A. E., Sylvester, P. J., Lastra, R., Cabri, L. J., Evans-Lamswood, D., & Wilton, D. H. C. (2008). First report of platinum-group minerals from a hornblende gabbro dyke in the vicinity of the southeast extension zone of the Voisey's Bay Ni-Cu-Co deposit, Labrador. *Mineralogy and Petrology*, 92 (1-2), 129-164. doi: 10.1007/s00710-007-0205-5
- Huppert, H. E., & Sparks, R. S. (1989). Chilled margins in igneous rocks. *Earth and Planetary Science Letters*, 92 (3-4), 397-405. Retrieved from <http://search.ebscohost.com/login.aspx?direct=true&AuthType=ip,url,uid&db=geh&AN=1989-045216&site=ehost-live&scope=site>; <http://www.sciencedirect.com/science/journal/0012821X>
- Latypov, R., Chistyakova, S., & Alapieti, T. (2007). Revisiting problem of chilled margins associated with marginal reversals in mafic-ultramafic intrusive bodies. *Lithos*, 99 (3-4), 178-206. doi: 10.1016/j.lithos.2007.05.008
- Lesher, C. M., Wilton, D. H. C., & Lightfoot, P. C. (2008). In Evans-Lamswood D. (Ed.), *Geology of the Voisey's Bay Ni-Cu-Co deposit, guidebook to field trip B1* (Joint

Annual Meeting ed.). Quebec: Geological Association of Canada - Mineralogical Association of Canada.

Li, C., Lightfoot, P. C., Amelin, Y. V., & Naldrett, A. J. (2000). Contrasting petrological and geochemical relationships in the Voisey's Bay and Mushuau intrusions, Labrador, Canada; implications for ore genesis. *Economic Geology and the Bulletin of the Society of Economic Geologists*, 95 (4), 771-799. Retrieved from <http://search.ebscohost.com/login.aspx?direct=true&AuthType=ip,url,uid&db=geh&AN=2000-054363&site=ehost-live&scope=site>; <http://www.segweb.org/journal.htm>

Li, C., & Naldrett, A. J. (1999). Geology and petrology of the Voisey's Bay intrusion; reaction of olivine with sulfide and silicate liquids. *Lithos*, 47 (1-2), 1-31. Retrieved from <http://search.ebscohost.com/login.aspx?direct=true&AuthType=ip,url,uid&db=geh&AN=1999-043476&site=ehost-live&scope=site>; <http://www.sciencedirect.com/science/journal/00244937>

Lightfoot, P. C., & Hawkesworth, C. J. (1997). Flood basalts and magmatic Ni, Cu, and PGE sulphide mineralization; comparative geochemistry of the Noril'sk (Siberian traps) and west Greenland sequences. *Geophysical Monograph*, 100, 357-380. Retrieved from <http://search.ebscohost.com/login.aspx?direct=true&AuthType=ip,url,uid&db=geh&AN=1998-050388&site=ehost-live&scope=site>

Lightfoot, P. C., & Naldrett, A. J. (1999). Geological and geochemical relationships in the Voisey's Bay intrusion, Nain Plutonic Suite, Labrador, Canada. *Short Course Notes - Geological Association of Canada*, 13, 1-30. Retrieved from <http://search.ebscohost.com/login.aspx?direct=true&AuthType=ip,url,uid&db=geh&AN=2001-058741&site=ehost-live&scope=site>

Longhi, J., Wooden, J. L., & Coppinger, K. D. (1983). The petrology of high-Mg dikes from the Beartooth Mountains, Montana; a search for the parent magma of the Stillwater Complex. *Journal of Geophysical Research*, 88, Suppl., 53-69. doi: 10.1029/JB088iS01p00B53

Naldrett, A. J., Asif, M., Kristic, S., & Li, C. (2000). The composition of mineralization of the Voisey's Bay Ni-Cu sulfide deposit, with special reference to platinum-group elements. *Economic Geology and the Bulletin of the Society of Economic Geologists*, 95 (4), 845-865. Retrieved from <http://search.ebscohost.com/login.aspx?direct=true&AuthType=ip,url,uid&db=geh&AN=2000-054367&site=ehost-live&scope=site>; <http://www.segweb.org/journal.htm>

Pearce, J. A. (1983). Role of the sub-continental lithosphere in magma genesis at active continental margins. Shiva geology series. (pp. 230-249). United Kingdom: Shiva

Publ: Nantwich, United Kingdom. Retrieved from
<http://search.ebscohost.com/login.aspx?direct=true&AuthType=ip,url,uid&db=geh&AN=1986-079640&site=ehost-live&scope=site>

Pearce, J. A., & Norry, M. J. (1979). Petrogenetic implications of Ti, Zr, Y, and Nb variations in volcanic rocks. *Contributions to Mineralogy and Petrology*, 69 (1), 33-47. Retrieved from
<http://search.ebscohost.com/login.aspx?direct=true&AuthType=ip,url,uid&db=geh&AN=1982-048666&site=ehost-live&scope=site>

Ryan, B. (1995). Anorthosite-granite (AMCG) suites. *in* the geology and mineral deposits of Labrador: A guide for the exploration geologist (compiled by R.J. Wardle and D.H.C. Wilton). In Newfoundland Department of Natural Resources - Centre for Earth Resources Research Report (Ed.), pp. 53

Ryan, B. (2000). The Nain-Churchill boundary and the Nain Plutonic Suite; a regional perspective on the geologic setting of the Voisey's Bay Ni-Cu-Co deposit. *Economic Geology and the Bulletin of the Society of Economic Geologists*, 95 (4), 703-724. Retrieved from
<http://search.ebscohost.com/login.aspx?direct=true&AuthType=ip,url,uid&db=geh&AN=2000-054360&site=ehost-live&scope=site>; <http://www.segweb.org/journal.htm>

Streckeisen, A. (1974). Classification and nomenclature of plutonic rocks recommendations of the IUGS subcommission on the systematics of igneous rocks. *Geologische Rundschau*, 63 (2), 773-786.

Sun, S. S., & McDonough, W. F. (1989). Chemical and isotopic systematics of oceanic basalts; implications for mantle composition and processes. *Geological Society Special Publications*, 42, 313-345. Retrieved from
<http://search.ebscohost.com/login.aspx?direct=true&AuthType=ip,url,uid&db=geh&AN=1991-026033&site=ehost-live&scope=site>

Sun, S. S., & McDonough, W. F. (1989). Chemical and isotopic systematics of oceanic basalts; implications for mantle composition and processes. *Geological Society Special Publications*, 42, 313-345. Retrieved from
<http://search.ebscohost.com/login.aspx?direct=true&AuthType=ip,url,uid&db=geh&AN=1991-026033&site=ehost-live&scope=site>

Sylvester, P. J. (2012). Use of the mineral liberation analyzer (MLA) for mineralogical studies of sediments and sedimentary rocks. *Mineralogical Association of Canada*, (Short Course 42), 1-16.

Vander Auwera, J., & Longhi, J. (1994). Experimental study of a jotunite (hypersthene monzodiorite); constraints on the parent magma composition and crystallization

conditions (P, T, F, O₂) of the Bjerkreim-Sokndal layered intrusion (Norway). *Contributions to Mineralogy and Petrology*, 118 (1), 60-78. Retrieved from <http://search.ebscohost.com/login.aspx?direct=true&AuthType=ip,url,uid&db=geh&AN=1995-021529&site=ehost-live&scope=site>

Wager, L. R. (1960). The major element variation of the layered series of the Skaergaard intrusion (Greenland) and a re-estimation of the average composition of the hidden layered series and of the successive residual magmas. *Journal of Petrology*, 1 (3), 364-398. Retrieved from

<http://search.ebscohost.com/login.aspx?direct=true&AuthType=ip,url,uid&db=geh&AN=1960-005876&site=ehost-live&scope=site>

4. Chapter 4 - Summary

This study has documented petrographical, mineralogical and geochemical characteristics of the mafic intrusive rocks of the Voisey's Bay Intrusion in view. A new classification scheme is utilized to differentiate rocks from different parts of the deposit and the detailed mineral chemical study of biotite substantiates the observation that there are notable differences between chamber and feeder rocks from the intrusion. Furthermore, the study of the chilled margins from the deposit has allowed for an important distinction between two generations of chilled margins. The major conclusions from this study are summarized below.

Chapter 2: Major, trace and oxygen isotope geochemistry of biotite in troctolite from the Voisey's Bay Ni-Cu-Co deposit and Mushuau intrusion, Labrador

1. Troctolite was previously believed to occupy the bulk of the VBI, however, a detailed mineralogical evaluation of mafic rocks from across the deposit has indicated that troctolite is confined to the large magma chambers of the VBI. Troctolite occurs largely within the Eastern Deep chamber and to a lesser extent within the Western Deep chamber. Melatrotroctolite and leucotrotroctolite varieties are present in the Mushuau intrusion. Diorite comprises the feeder rocks in the eastern half of the intrusion, including feeders to the Eastern Deep, Discovery Hill, the Ovoid, and the southeast extension. Norite and olivine norite are present as feeder dykes to the Western Deep (including the Reid Brook dyke) and as lesser amounts in the Discovery Hill and Ovoid zones and in the Floodplain intrusion.

Olivine gabbro makes up the bulk of the Ashley and Floodplain magma chambers.

Gabbronorite is present as chilled marginal rocks throughout the VBI;

2. Biotite in the mafic rocks from the VBI is a primary igneous mineral and its presence indicates that water (hydroxyl) was present within the silicate melt structure of the magma parental to these rocks.;
3. Biotite major element chemistry is distinct across the VBI with the most important variations occurring between the different environments (i.e. chamber vs. feeder). The most primitive (higher magnesium number) biotite occurs in the Western Deep where the chamber and feeder intersect and within the Eastern Deep chamber troctolite. More evolved biotite occurs in the Eastern Deep feeder rocks and the chilled margins. These variations in biotite chemistry probably represent two different pulses/ages of mafic magma;
4. The highest Ni values occur in moderately magnesian biotite of fragment-bearing troctolite from the Eastern Deep and in troctolite at the top of the Western Deep chamber. This biotite, with its moderate magnesium number, likely crystallized from a more evolved, higher (Ni) tenor magma than the initial pulse of primitive magma which filled the chambers;
5. There is a positive correlation between magnesium number and the $\delta^{18}\text{O}$ ratio of biotite, with more primitive biotite having relatively enriched $\delta^{18}\text{O}$ ratios.

Chapter 3: A petrographical and lithogeochemical evaluation of chilled marginal rocks from the Voisey's Bay Intrusion, Labrador

1. Chilled margins are found in three different environments in the VBI: *i.* on the margins of diorite-norite feeder dykes: *ii.* spatially associated with leopard texture troctolite and mineralized breccia in the Eastern Deeps and Discovery Hill zones; and *iii.* on large olivine gabbro magma chambers;
2. The three geochemically distinct groups of marginal rocks correlate to the three environments in which the margins are found: *i.* Group 1 are enriched in LREEs and LILs, indicative of a contamination signature picked up from the surrounding country rock: *ii.* Group 2 margins are also enriched in LREEs and LILs: and *iii.* Group 3 margins are not enriched in either LREEs or LILs and are exclusively associated with the Western Deeps and Kog Brook intrusions;
3. Marginal rocks from Groups 1 and 2 display gneissic contamination signatures and are unlikely to provide an accurate representation of the parental magma composition for the VBI. Group 1 chilled margins are most likely contaminated by both orthogneiss and paragneiss whereas Group 2 chilled margins appear to be contaminated mainly by paragneiss. Group 3 chilled margins appear uncontaminated and may represent a more primitive magma composition.

Biotite chemistry differs notably between chamber and feeder rocks. This change in mineral chemistry and crystallization environment must co-incide with a change in magma chemistry between the emplacement of the chamber and feeder environments. An

initial pulse of magma likely removed material from a lower staging chamber and injected it in to the Western Deeps chamber and later the Eastern Deeps chamber. The magma remaining in the source continued to differentiate and when it was injected in to the feeder environments of the VBC it retained it's more evolved, contaminated signature.

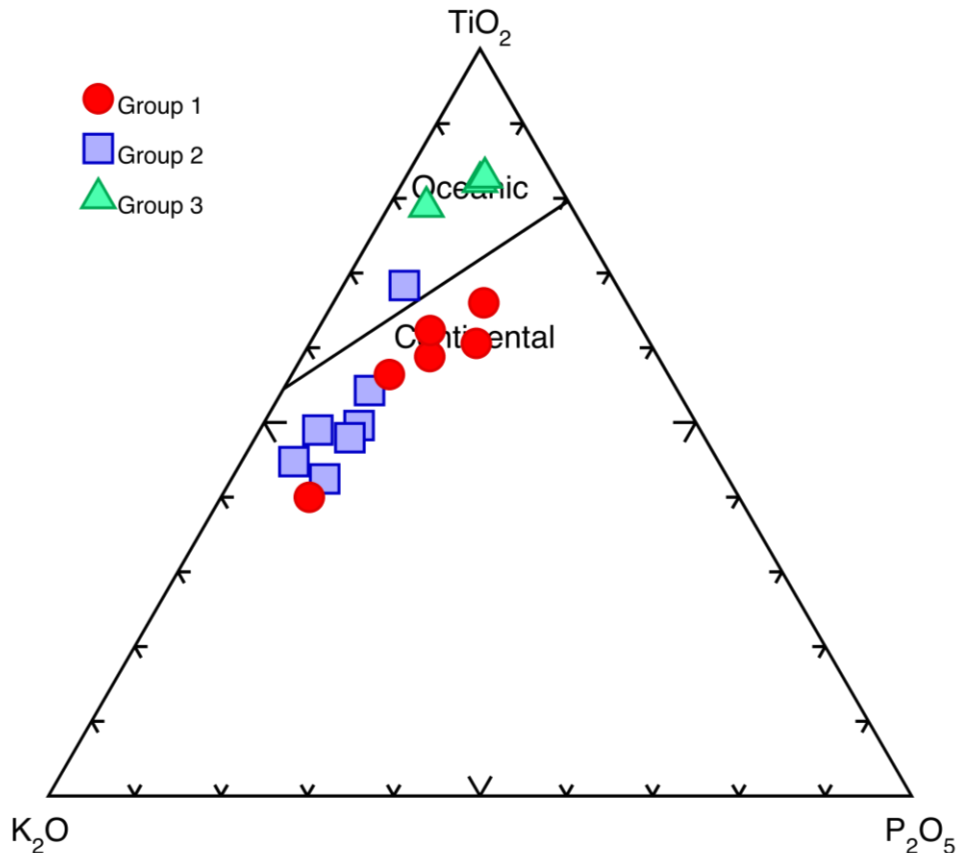


Fig. 4-1. TiO_2 - K_2O - P_2O_5 discrimination diagram for chilled margins from the Voisey's Bay Intrusion (after Pearce et al., 1975).

Evidence from the chilled margins support this theory and address the question of system contaminants more directly. The least contaminated marginal rocks occur within the large, primitive magma chamber (Western Deeps) and are represented by Group 3 chilled margins (Fig. 4-1). The margins associated with the feeder-dykes and brecciated diorite and troctolite display contamination signatures and are represented by Group 1 and

two chills. Furthermore, chills in these feeder environments are more commonly associated with mineralization, linking mineralization to the contamination evidenced in the chilled margins. These contaminated margins are more evolved than their uncontaminated counterparts and likely represent a different pulse of magma that fed the VBC. Figure 4-1 highlights the differences seen in contamination signatures between the three groups of chilled margins. Chills from Group 3 plot toward the TiO_2 apex, away from the K_2O and P_2O_5 appices, signatures likely inherited from country rock contamination.

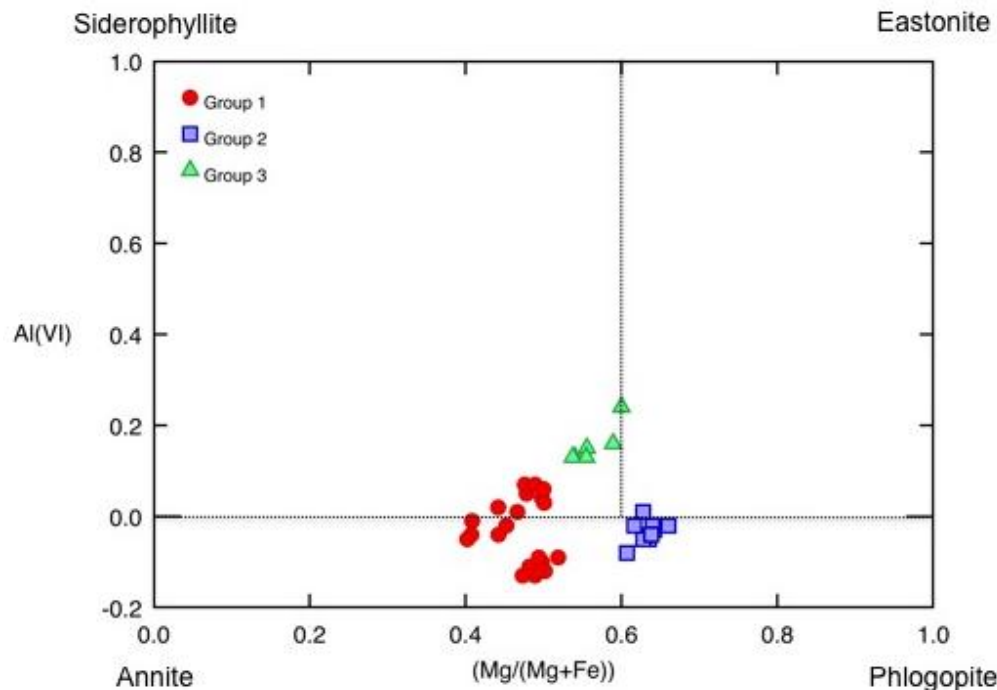


Fig. 4-2. Composition of biotite in chilled margins. Biotite from Group 1 chills is indicated by red circles. Group 2 biotite is indicated by blue squares. Group 3 biotite is indicated by green triangles.

It should be recalled from Chapter 2 that aluminum could occur in both tetrahedral (IV) and octahedral (VI) coordination in naturally occurring minerals. It normally occurs in tetrahedral coordination in high temperature minerals, in octahedral coordination in

low temperature minerals and it may have both four- and six-fold coordination in intermediate temperature minerals (i.e. biotite). This suggests the amount of aluminum in tetrahedral coordination is a function of the temperature of formation. Aluminum in tetrahedral coordination in biotite in chilled margins suggests this mineral crystallized at a higher temperature, specifically, when the hot parental magma quenched and cooled quickly.

Aluminum in biotite from Group 1 and Group 2 chilled margins straddles the boundary of tetrahedral and octahedral coordination but aluminum in biotite from Group 3 chilled margins is in octahedral coordination (Fig. 4-2). Margins in Groups 1 are believed to have quenched from an initial mega pulse of magma, which fed the VBI. This older, hotter, more contaminated pulse of magma was likely parental to the Group 1 chills and hence crystallized biotite with aluminum in mostly tetrahedral and lesser octahedral coordination. The cluster of biotite from Group I chills with $\text{Al(VI)} < 0$ is from the Kog Brook intrusion where the cluster with $\text{Al(VI)} > 0$ is from the Ovoid and Ryan's Pond deposits. Margins in Group 2 and 3 are possibly associated with a second, younger, less contaminated mega pulse of magma more intimately associated with the Mushuau intrusion and the Western Deeps zone of the VBI. This pulse of magma crystallized biotite in tetrahedral coordination (some from Group 2) and octahedral coordination (Group 2 and Group 3). The aluminum in octahedral coordination from the Group 3 chill indicates this magma was emplaced at a cooler temperature than the magma parental to the Group 1 chills.

Furthermore, the biotite in chilled margins from Group 1 has lower Mg/Mg+Fe values (as seen on Figure 4-2) than biotite in the other chilled margins. This likely reflects that they crystallized from a magma that was less magnesium rich than that which produced the Group 2 and 3 margins. The lower Mg values are likely attributed to the fact that the magma parental to Group 1 chills is more contaminated (Fig. 4-1) than the mega pulse parental to Groups 2 and 3 chills.

The geochemical variations seen in biotite and chilled margins from the mafic intrusive rocks of the VBI can be explained by this multi-stage emplacement history that includes at least two different mega-pulses of mafic magma. A more primitive, uncontaminated magma could have been initially injected into the VBC. This initial pulse would have preceded the important contamination episode, which then triggered the precipitation of sulphide minerals. The idea of a multi-stage emplacement history for the VBI fits with observations by others (e.g. Evans-Lamswood et al., 2000) and continued detailed study of this concept will allow for a better understanding of the processes important to each step of emplacement and help to constrain the timing of contamination versus mineralization.

Bibliography

- Ahrens, L. H. (1969). The use of ionization potentials in geochemistry. (pp. 144-154). Israel Program for Scientific Translations : Jerusalem, Israel. U.S. Department of Commerce, Clearinghouse Fed. Sci. Tech. Inform. Retrieved from
<http://search.ebscohost.com/login.aspx?direct=true&AuthType=ip,url,uid&db=geh&AN=1970-011236&site=ehost-live&scope=site>
- Amelin, Y. V., Li, C., Valeyev, O., & Naldrett, A. J. (2000). Nd-Pb-Sr isotope systematics of crustal assimilation in the Voisey's bay and Mushauau intrusions, Labrador, Canada. *Economic Geology and the Bulletin of the Society of Economic Geologists*, 95 (4), 815-830. Retrieved from
<http://search.ebscohost.com/login.aspx?direct=true&AuthType=ip,url,uid&db=geh&AN=2000-054365&site=ehost-live&scope=site>; <http://www.segweb.org/journal.htm>
- Bedard, J. H. (2001). Parental magmas of the Nain Plutonic Suite anorthosites and mafic cumulates; a trace element modelling approach. *Contributions to Mineralogy and Petrology*, 141 (6), 747-771. Retrieved from
<http://search.ebscohost.com/login.aspx?direct=true&AuthType=ip,url,uid&db=geh&AN=2002-005252&site=ehost-live&scope=site>:
- Berg, J. H., Emslie, R. F., Hamilton, M. A., Morse, S. A., Ryan, A. B., & Wiebe, R. A. (1994). *Anorthositic, granitoid, and related rocks of the Nain Plutonic Suite. Guidebook to a field excursion to the Nain area. August 4-10.* International Geological Correlation Program Projects #290 and #315.
- Berg, J. H., & Briegel, J. S. (1983). Geology of the Jonathon Intrusion and associated rocks. *Contribution - Geology Department, University of Massachusetts*, 40, 42-50. Retrieved from
<http://search.ebscohost.com/login.aspx?direct=true&AuthType=ip,url,uid&db=geh&AN=1988-072807&site=ehost-live&scope=site>
- Buerger, M. J. (1948). The role of temperature in mineralogy. *American Mineralogist*, 33 (3-4), 101-121. Retrieved from
<http://search.ebscohost.com/login.aspx?direct=true&AuthType=ip,url,uid&db=geh&AN=1949-021401&site=ehost-live&scope=site>;
http://www.minsocam.org/ammin/AM33/AM33_101.pdf
- Clayton, R. N., & Mayeda, T. K. (1963). The use of bromine pentafluoride in the extraction of oxygen from oxides and silicates for isotopic analysis. *Geochimica Et Cosmochimica Acta*, 27 (1), 43-52. Retrieved from
<http://search.ebscohost.com/login.aspx?direct=true&AuthType=ip,url,uid&db=geh&>

[AN=1963-014328&site=ehost-live&scope=site;
http://www.sciencedirect.com/science/journal/00167037](http://www.sciencedirect.com/science/journal/00167037)

Deer, W. A., Howie, R. A., & Zussman, J. (1962). *Rock-forming minerals*. Longmans.

Emslie, R. F., & Loveridge, W. D. (1992). Fluorite-bearing early and middle Proterozoic granites, Okak Bay area, Labrador; geochronology, geochemistry and petrogenesis. *Lithos*, 28 (2), 87-109. Retrieved from
<http://search.ebscohost.com/login.aspx?direct=true&AuthType=ip,url,uid&db=geh&AN=1993-036065&site=ehost-live&scope=site;>
<http://www.sciencedirect.com/science/journal/00244937>

Emslie, R. F., & Russell, W. J. (1988). Umiakovik Lake batholith and other felsic intrusions, Okak Bay area, Labrador. *Paper - Geological Survey of Canada*, 88-1C, 27-32. Retrieved from
<http://search.ebscohost.com/login.aspx?direct=true&AuthType=ip,url,uid&db=geh&AN=1988-027710&site=ehost-live&scope=site>

Emslie, R. F., & Stirling, J. A. R. (1993). Rapakivi and related granitoids of the Nain Plutonic Suite; geochemistry, mineral assemblages and fluid equilibria. *Canadian Mineralogist*, 31, Part 4, 821-847. Retrieved from
<http://search.ebscohost.com/login.aspx?direct=true&AuthType=ip,url,uid&db=geh&AN=1998-023167&site=ehost-live&scope=site>

Evans-Lamswood, D., Butt, D. P., Jackson, R. S., Lee, D. V., Mugridge, M. G., Wheeler, R. I., et al. (2000). Physical controls associated with the distribution of sulfides in the Voisey's Bay Ni-Cu-Co deposit, Labrador. *Economic Geology and the Bulletin of the Society of Economic Geologists*, 95 (4), 749-769. Retrieved from
<http://search.ebscohost.com/login.aspx?direct=true&AuthType=ip,url,uid&db=geh&AN=2000-054362&site=ehost-live&scope=site>; <http://www.segweb.org/journal.htm>

Fleet, M. E. (2003). *Rock forming minerals, sheet silicates: Micas. volume 3A* (Second ed.). London: The Geological Society.

Floyd, P. A., & Winchester, J. A. (1975). Magma type and tectonic setting discrimination using immobile elements. *Earth and Planetary Science Letters*, 27 (2), 211-218. Retrieved from
<http://search.ebscohost.com/login.aspx?direct=true&AuthType=ip,url,uid&db=geh&AN=1976-007461&site=ehost-live&scope=site>;
<http://www.sciencedirect.com/science/journal/0012821X>

Foster, M. D. (1960). *Interpretation of the composition of trioctahedral micas*. United States: U. S. Geological Survey : Reston, VA, United States. Retrieved from

<http://search.ebscohost.com/login.aspx?direct=true&AuthType=ip,url,uid&db=geh&AN=1960-008390&site=ehost-live&scope=site>

Geological Survey Professional Paper. (1959). *Shorter contributions to general geology*. Washington: United States Government Printing Office.

Gower, C. F., Flanagan, M. J., Kerr, A., & Bailey, D. G. (1982). Geology of the Kaipokok Bay - Big River Area, Central Mineral Belt, Labrador. *Report - Province of Newfoundland. Dept.of Mines and Energy. Mineral Development Division*, 82-7 Retrieved from

<http://search.ebscohost.com/login.aspx?direct=true&AuthType=ip,url,uid&db=geh&AN=1983-023740&site=ehost-live&scope=site>

Guidotti, C. V. (1984). Micas in metamorphic rocks. *Reviews in Mineralogy*, 13, 357-467. Retrieved from

<http://search.ebscohost.com/login.aspx?direct=true&AuthType=ip,url,uid&db=geh&AN=1985-043368&site=ehost-live&scope=site>

Hamilton, S. H. (1899). Exploration of the Delaware valley. *Mineral Collector*, 6, 117-122.

Hamilton, M. A., Emslie, R. F., & Roddick, J. C. (1994). *Detailed emplacement chronology of basic magmas of the mid-Proterozoic Nain Plutonic Suite, Labrador; insights from U-Pb systematics in zircon and baddeleyite*. U. S. Geological Survey : Reston, VA, United States. Retrieved from

<http://search.ebscohost.com/login.aspx?direct=true&AuthType=ip,url,uid&db=geh&AN=1998-060619&site=ehost-live&scope=site>

Helz, R. T. (2009). Processes active in mafic magma chambers: The example of Kilauea Iki lava lake, Hawaii. *Lithos*, 111 (1-2), 37-46.

Hoover, J. D. (1989). The chilled marginal gabbro and other contact rocks of the Skaergaard Intrusion. *Journal of Petrology*, 30 (2), 441-476. Retrieved from
<http://search.ebscohost.com/login.aspx?direct=true&AuthType=ip,url,uid&db=geh&AN=1989-071559&site=ehost-live&scope=site>

Huminicki, M. A. E., Sylvester, P. J., Lastra, R., Cabri, L. J., Evans-Lamswood, D., & Wilton, D. H. C. (2008). First report of platinum-group minerals from a hornblende gabbro dyke in the vicinity of the southeast extension zone of the Voisey's Bay Ni-Cu-Co deposit, Labrador. *Mineralogy and Petrology*, 92 (1-2), 129-164.

Huppert, H. E., & Sparks, R. S. (1989). Chilled margins in igneous rocks. *Earth and Planetary Science Letters*, 92 (3-4), 397-405. Retrieved from
<http://search.ebscohost.com/login.aspx?direct=true&AuthType=ip,url,uid&db=geh&AN=1989-071559&site=ehost-live&scope=site>

[AN=1989-045216&site=ehost-live&scope=site;
http://www.sciencedirect.com/science/journal/0012821X](http://www.sciencedirect.com/science/journal/0012821X)

Lambert, D. D., Frick, L. R., Foster, J. G., Li, C., & Naldrett, A. J. (2000). Re-Os isotope systematics of the Voisey's Bay Ni-Cu-Co magmatic sulfide system, Labrador, Canada; II, implications for parental magma chemistry, ore genesis, and metal redistribution. *Economic Geology and the Bulletin of the Society of Economic Geologists*, 95 (4), 867-888. Retrieved from
<http://search.ebscohost.com/login.aspx?direct=true&AuthType=ip,url,uid&db=geh&AN=2000-054368&site=ehost-live&scope=site;> <http://www.segweb.org/journal.htm>

Latypov, R., Chistyakova, S., & Alapieti, T. (2007). Revisiting problem of chilled margins associated with marginal reversals in mafic-ultramafic intrusive bodies. *Lithos*, 99 (3-4), 178-206.

Le Bas, M. J., & Streckeisen, A. L. (1991). The IUGS systematics of igneous rocks. *Journal of the Geological Society of London*, 148, Part 5, 825-833. Retrieved from
<http://search.ebscohost.com/login.aspx?direct=true&AuthType=ip,url,uid&db=geh&AN=1995-041857&site=ehost-live&scope=site;>
<http://www.ingentaconnect.com/content/geol/jgs>

Lesher, C. M., Wilton, D. H. C., & Lightfoot, P. C. (2008). In Evans-Lamswood D. (Ed.), *Geology of the Voisey's Bay Ni-Cu-Co deposit, guidebook to field trip B1* (Joint Annual Meeting ed.). Quebec: Geological Association of Canada - Mineralogical Association of Canada.

Li, C., Lightfoot, P. C., Amelin, Y. V., & Naldrett, A. J. (2000). Contrasting petrological and geochemical relationships in the Voisey's Bay and Mushuau intrusions, Labrador, Canada; implications for ore genesis. *Economic Geology and the Bulletin of the Society of Economic Geologists*, 95 (4), 771-799. Retrieved from
<http://search.ebscohost.com/login.aspx?direct=true&AuthType=ip,url,uid&db=geh&AN=2000-054363&site=ehost-live&scope=site;> <http://www.segweb.org/journal.htm>

Li, C., & Naldrett, A. J. (1999). Geology and petrology of the Voisey's Bay Intrusion; reaction of olivine with sulfide and silicate liquids. *Lithos*, 47 (1-2), 1-31. Retrieved from
<http://search.ebscohost.com/login.aspx?direct=true&AuthType=ip,url,uid&db=geh&AN=1999-043476&site=ehost-live&scope=site;>
<http://www.sciencedirect.com/science/journal/00244937>

Li, C., & Naldrett, A. J. (2000). Melting reactions of gneissic inclusions with enclosing magma at Voisey's Bay, Labrador, Canada; implications with respect to ore genesis. *Economic Geology and the Bulletin of the Society of Economic Geologists*, 95 (4), 801-814. Retrieved from

<http://search.ebscohost.com/login.aspx?direct=true&AuthType=ip,url,uid&db=geh&AN=2000-054364&site=ehost-live&scope=site>; <http://www.segweb.org/journal.htm>

Liese, H. C. (1963). Tetrahedrally coordinated aluminum in some natural biotites; an infrared absorption analysis. *American Mineralogist*, 48, 980-990. Retrieved from <http://search.ebscohost.com/login.aspx?direct=true&AuthType=ip,url,uid&db=geh&AN=1963-012872&site=ehost-live&scope=site>

Lightfoot, P. C. (2012). Personal correspondance, *Phlogopite oxygen isotopes*

Lightfoot, P. C., & Hawkesworth, C. J. (1997). Flood basalts and magmatic Ni, Cu, and PGE sulphide mineralization; comparative geochemistry of the Noril'sk (Siberian traps) and west Greenland sequences. *Geophysical Monograph*, 100, 357-380. Retrieved from <http://search.ebscohost.com/login.aspx?direct=true&AuthType=ip,url,uid&db=geh&AN=1998-050388&site=ehost-live&scope=site>

Lightfoot, P. C., Keays, R. R., Evans-Lamswood, D., & Wheeler, R. (2012). S saturation history of Nain Plutonic Suite mafic intrusions; origin of the Voisey's Bay Ni-Cu-Co sulfide deposit, Labrador, Canada. *Mineralium Deposita*, 47 (1-2), 23-50.

Lightfoot, P. C., & Naldrett, A. J. (1999). Geological and geochemical relationships in the Voisey's Bay Intrusion, Nain Plutonic Suite, Labrador, Canada. *Short Course Notes - Geological Association of Canada*, 13, 1-30. Retrieved from <http://search.ebscohost.com/login.aspx?direct=true&AuthType=ip,url,uid&db=geh&AN=2001-058741&site=ehost-live&scope=site>

Livi, K. J. T., & Veblen, D. R. (1985). Serpentine and phlogopite intergrowths in "eastonite" from Easton, Pennsylvania. *Geological Society of America Abstracts with Programs*, 17, 645.

Longhi, J., Wooden, J. L., & Coppinger, K. D. (1983). The petrology of high-Mg dikes from the Beartooth Mountains, Montana; a search for the parent magma of the Stillwater Complex. *Journal of Geophysical Research*, 88, Suppl., 53-69.

Mariga, J., Ripley, E. M., & Li, C. (2006). Oxygen isotopic studies of the interaction between xenoliths and mafic magma, Voisey's Bay Intrusion, Labrador, Canada. *Geochimica Et Cosmochimica Acta*, 70 (19), 4977-4996. doi: <http://dx.doi.org/10.1016/j.gca.2006.07.018>

Miyano, T., & Miyano, S. (1982). Ferri-annite from the Dales Gorge member iron-formations, Wittenoom area, western Australia. *American Mineralogist*, 67 (11-12), 1179-1194. Retrieved from

<http://search.ebscohost.com/login.aspx?direct=true&AuthType=ip,url,uid&db=geh&AN=1983-018419&site=ehost-live&scope=site>

Morse, S. A. (1969). The Kiglapait layered intrusion, Labrador. *Memoir - Geological Society of America*, 112. Retrieved from
<http://search.ebscohost.com/login.aspx?direct=true&AuthType=ip,url,uid&db=geh&AN=1970-027350&site=ehost-live&scope=site>

Munoz, J. L., & Ludington, S. D. (1974). Fluorine-hydroxyl exchange in biotite. *American Journal of Science*, 274, 396.

Naldrett, A. J. (2010). From the mantle to the bank; the life of a Ni-Cu-PGE sulfide. *South African Journal of Geology*, 113 (1), 1-32. doi: 10.2113/gssajg.113.1-1

Naldrett, A. J., Keats, H., Sparkes, K., & Moore, R. (1996). Geology of the Voisey's Bay Ni-Cu-Co deposit, Labrador, Canada. *Exploration and Mining Geology*, 5, 169.

Naldrett, A. J., & Li, C. (2007). *The Voisey's Bay Deposit, Labrador, Canada. Special publication no. 5*. Geological Association of Canada, Mineral Deposits Division.

Naldrett, A. J., Asif, M., Krstic, S., & Li, C. (2000). The composition of mineralization of the Voisey's Bay Ni-Cu sulfide deposit, with special reference to platinum-group elements. *Economic Geology and the Bulletin of the Society of Economic Geologists*, 95 (4), 845-865. Retrieved from
<http://search.ebscohost.com/login.aspx?direct=true&AuthType=ip,url,uid&db=geh&AN=2000-054367&site=ehost-live&scope=site>; <http://www.segweb.org/journal.htm>

Naldrett, A. J., Li, C., Krstic, S., & Amelin, Y. (1997). Geology and genesis of the Voisey's Bay Ni-Cu-Co deposit, Labrador, Canada. *EOS, Transactions, American Geophysical Union*, 78 (46), 810. Retrieved from
<http://search.ebscohost.com/login.aspx?direct=true&AuthType=ip,url,uid&db=geh&AN=1999-001470&site=ehost-live&scope=site>

Naldrett, A. J., Singh, J., Krstic, S., & Li, C. (2000). The mineralogy of the Voisey's Bay Ni-Cu-Co deposit, northern Labrador, Canada; influence of oxidation state on textures and mineral compositions. *Economic Geology and the Bulletin of the Society of Economic Geologists*, 95 (4), 889-900. Retrieved from
<http://search.ebscohost.com/login.aspx?direct=true&AuthType=ip,url,uid&db=geh&AN=2000-054369&site=ehost-live&scope=site>; <http://www.segweb.org/journal.htm>

Nesse, W. D. (2004). *Introduction to optical mineralogy*. Oxford University Press.

Pearce, J. A. (1983). Role of the sub-continental lithosphere in magma genesis at active continental margins. Shiva geology series. (pp. 230-249). United Kingdom: Shiva

Publ: Nantwich, United Kingdom. Retrieved from
<http://search.ebscohost.com/login.aspx?direct=true&AuthType=ip,url,uid&db=geh&AN=1986-079640&site=ehost-live&scope=site>

Pearce, J. A., & Norry, M. J. (1979). Petrogenetic implications of Ti, Zr, Y, and Nb variations in volcanic rocks. *Contributions to Mineralogy and Petrology*, 69 (1), 33-47. Retrieved from
<http://search.ebscohost.com/login.aspx?direct=true&AuthType=ip,url,uid&db=geh&AN=1982-048666&site=ehost-live&scope=site>

Pearce, T. H., Gorman, B. E., & Birkett, T. C. (1975). The $\text{TiO}_2\text{-K}_2\text{O-P}_2\text{O}_5$ diagram: A method of discriminating between oceanic and non-oceanic basalts. *Earth and Planetary Science Letters*, 24 (3), 419-426. Retrieved from
<http://search.ebscohost.com/login.aspx?direct=true&AuthType=ip,url,uid&db=geh&AN=1975-009843&site=ehost-live&scope=site>; <http://www.sciencedirect.com/science/journal/0012821X>

Ramberg, H. (1952). Chemical bonds and distribution of cations in silicates. *The Journal of Geology*, 60 (4), 331.

Ripley, E. M., Park, Y., Li, C., & Naldrett, A. J. (2000). Oxygen isotope studies of the Voisey's Bay Ni-Cu-Co deposit, Labrador, Canada. *Economic Geology and the Bulletin of the Society of Economic Geologists*, 95 (4), 831-844. Retrieved from
<http://search.ebscohost.com/login.aspx?direct=true&AuthType=ip,url,uid&db=geh&AN=2000-054366&site=ehost-live&scope=site>; <http://www.segweb.org/journal.htm>

Ryan, B. (1995). Anorthosite-granite (AMCG) suites. *in* the geology and mineral deposits of Labrador: A guide for the exploration geologist (compiled by R.J. Wardle and D.H.C. Wilton). Newfoundland Department of Natural Resources - Centre for Earth Resources Research Report (Ed.), pp. 53

Ryan, B. (1984). Regional geology of the central part of the central mineral belt, Labrador. *Memoir - Government of Newfoundland and Labrador, Department of Mines and Energy, Mineral Development Division*, 3. Retrieved from
<http://search.ebscohost.com/login.aspx?direct=true&AuthType=ip,url,uid&db=geh&AN=1985-075383&site=ehost-live&scope=site>

Ryan, B. (1991). Makhavinekh Lake pluton, Labrador, Canada; geological setting, subdivisions, mode of emplacement, and a comparison with Finnish rapakivi granites. *Precambrian Research*, 51 (1-4), 193-225. Retrieved from
<http://search.ebscohost.com/login.aspx?direct=true&AuthType=ip,url,uid&db=geh&AN=1993-000835&site=ehost-live&scope=site>; <http://www.sciencedirect.com/science/journal/03019268>

- Ryan, B. (1997). The Mesoproterozoic Nain plutonic suite in eastern Canada, and the setting of the Voisey's Bay Ni-Cu-Co sulphide deposit. *Geoscience Canada*, 24 (4), 173-188. Retrieved from
<http://search.ebscohost.com/login.aspx?direct=true&AuthType=ip,url,uid&db=geh&AN=1998-022986&site=ehost-live&scope=site;>
<http://www.gac.ca/JOURNALS/geocan.html>
- Ryan, B. (2000). The Nain-Churchill boundary and the Nain Plutonic Suite; a regional perspective on the geologic setting of the Voisey's Bay Ni-Cu-Co deposit. *Economic Geology and the Bulletin of the Society of Economic Geologists*, 95 (4), 703-724. Retrieved from
<http://search.ebscohost.com/login.aspx?direct=true&AuthType=ip,url,uid&db=geh&AN=2000-054360&site=ehost-live&scope=site;> <http://www.segweb.org/journal.htm>
- Scoates, J. S., & Mitchell, J. N. (2000). The evolution of troctolitic and high Al basaltic magmas in Proterozoic anorthosite plutonic suites and implications for the Voisey's Bay massive Ni-Cu sulfide deposit. *Economic Geology and the Bulletin of the Society of Economic Geologists*, 95 (4), 677-701. Retrieved from
<http://search.ebscohost.com/login.aspx?direct=true&AuthType=ip,url,uid&db=geh&AN=2000-054359&site=ehost-live&scope=site;> <http://www.segweb.org/journal.htm>
- Simmons, K. R., Wiebe, R. A., Snyder, G. A., & Simmons, E. C. (1986). U-Pb zircon age for the Newark Island layered intrusion, Nain Anorthosite Complex. [Abstract]. *Geological Society of America*, 18. 751.
- Slade, P. (2005). Rock-forming minerals. Volume 3A: Sheet silicates: Micas, 2nd ed. *Geological Magazine*, 142 (2), 219.
- Streckeisen, A. (1976). To each plutonic rock its proper name. *Earth-Science Reviews*, 12(1; 1), 1-33. Retrieved from
<http://search.ebscohost.com/login.aspx?direct=true&AuthType=ip,url,uid&db=geh&AN=1976-028023&site=ehost-live&scope=site;>
<http://www.sciencedirect.com/science/journal/00128252>
- Streckeisen, A. (1974). Classification and nomenclature of plutonic rocks recommendations of the IUGS subcommission on the systematics of igneous rocks. *Geologische Rundschau*, 63 (2), 773-786.
- Sun, S. S., & McDonough, W. F. (1989). Chemical and isotopic systematics of oceanic basalts; implications for mantle composition and processes. *Geological Society Special Publications*, 42, 313-345. Retrieved from
<http://search.ebscohost.com/login.aspx?direct=true&AuthType=ip,url,uid&db=geh&AN=1991-026033&site=ehost-live&scope=site>

- Sylvester, P. J. (2012). Use of the mineral liberation analyzer (MLA) for mineralogical studies of sediments and sedimentary rocks. *Mineralogical Association of Canada*, (Short Course 42), 1-16.
- Taylor, H. P., J., & Forester, R. W. (1979). An oxygen and hydrogen isotope study of the Skaergaard Intrusion and its country rocks; a description of a 55-m.y. old fossil hydrothermal system. *Journal of Petrology*, 20 (3), 355-419. Retrieved from <http://search.ebscohost.com/login.aspx?direct=true&AuthType=ip,url,uid&db=geh&AN=1980-018582&site=ehost-live&scope=site>
- Taylor, H. P. (1968). The oxygen isotope geochemistry of igneous rocks. *Contributions to Mineralogy and Petrology*, 19 (1), 1-71.
- Vale Newfoundland and Labrador. (2013). *Nineteenth year assessment report on geological, geophysical and geochemical exploration on claims in the Voisey's Bay area, northern Labrador*. St. John's: Department of Natural Resources, Government of Newfoundland and Labrador.
- Vander Auwera, J., & Longhi, J. (1994). Experimental study of a jotunite (hypersthene monzodiorite); constraints on the parent magma composition and crystallization conditions (P, T, F, O₂) of the Bjerkreim-Sokndal layered intrusion (Norway). *Contributions to Mineralogy and Petrology*, 118 (1), 60-78. Retrieved from <http://search.ebscohost.com/login.aspx?direct=true&AuthType=ip,url,uid&db=geh&AN=1995-021529&site=ehost-live&scope=site>
- Wager, L. R. (1960). The major element variation of the layered series of the Skaergaard Intrusion (Greenland) and a re-estimation of the average composition of the hidden layered series and of the successive residual magmas. *Journal of Petrology*, 1 (3), 364-398. Retrieved from <http://search.ebscohost.com/login.aspx?direct=true&AuthType=ip,url,uid&db=geh&AN=1960-005876&site=ehost-live&scope=site>
- Wardle, R. J. (1995). In Wilton D. H. C., et al. (Eds.), *The geology and mineral deposits of Labrador: A guide for the exploration geologist*. Centre for Earth Resources Research, Memorial University of Newfoundland, St. John's: Geological Survey, Department of Natural Resources, Government of Newfoundland and Labrador.
- Wardle, R. J., Gower, C. F., Ryan, B., Nunn, G. A. G., James, D. T., & Kerr, A. (1997). *Geological map of Labrador; 1: 1 million scale*. (Geological Survey, Map 97-07 ed.) Government of Newfoundland and Labrador, Department of Mines and Energy.
- Wardle, R. J. (1990). In Mengel F. C. (Ed.), *Labrador segment of the trans-Hudson orogen; crustal development through oblique convergence and collision*. Geological Association of Canada, Toronto, ON, Canada. Retrieved from

<http://search.ebscohost.com/login.aspx?direct=true&db=geh&AN=1991-033105&site=ehost-live&scope=site>

Winchell, A. N. (1925). Studies in the mica group. *American Journal of Science*, 9 (52), 309-327. Retrieved from
<http://search.ebscohost.com/login.aspx?direct=true&AuthType=ip,url,uid&db=geh&AN=1928-012172&site=ehost-live&scope=site>;
http://www.minsocam.org/ammin/AM10/AM10_52.pdf

Yu, Y., & Morse, S. A. (1993). $^{40}\text{Ar}/^{39}\text{Ar}$ chronology of the Nain anorthosites, Canada. *Canadian Journal of Earth Sciences, Revue Canadienne Des Sciences De La Terre*, 30 (6), 1166-1178. Retrieved from
<http://search.ebscohost.com/login.aspx?direct=true&AuthType=ip,url,uid&db=geh&AN=1993-046004&site=ehost-live&scope=site>

Appendix A

Photomicrographs of individual thin sections and Streckeisen's classification diagrams.

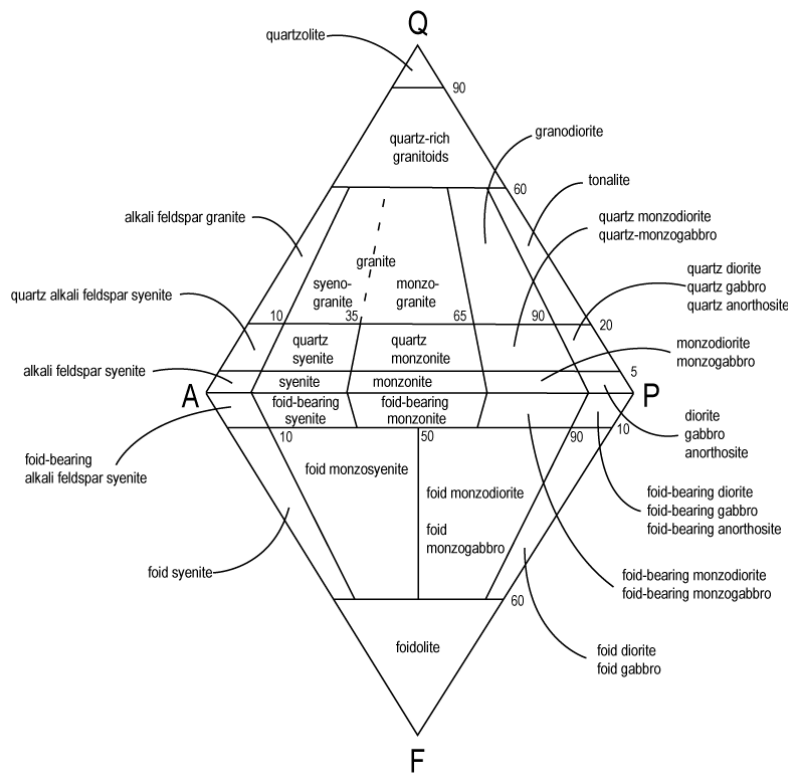


Fig. A-1. QAPF diagram for classification of igneous rocks. Modified after Streckeisen, 1974.

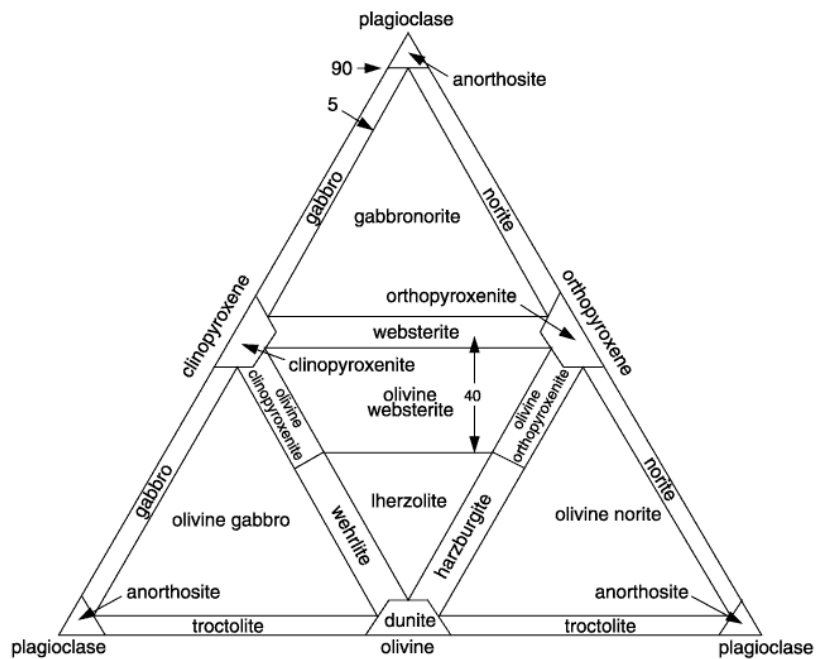


Fig. A-2. Classification and nomenclature of mafic-ultramafic rocks. Modified after Streckeisen (1974).

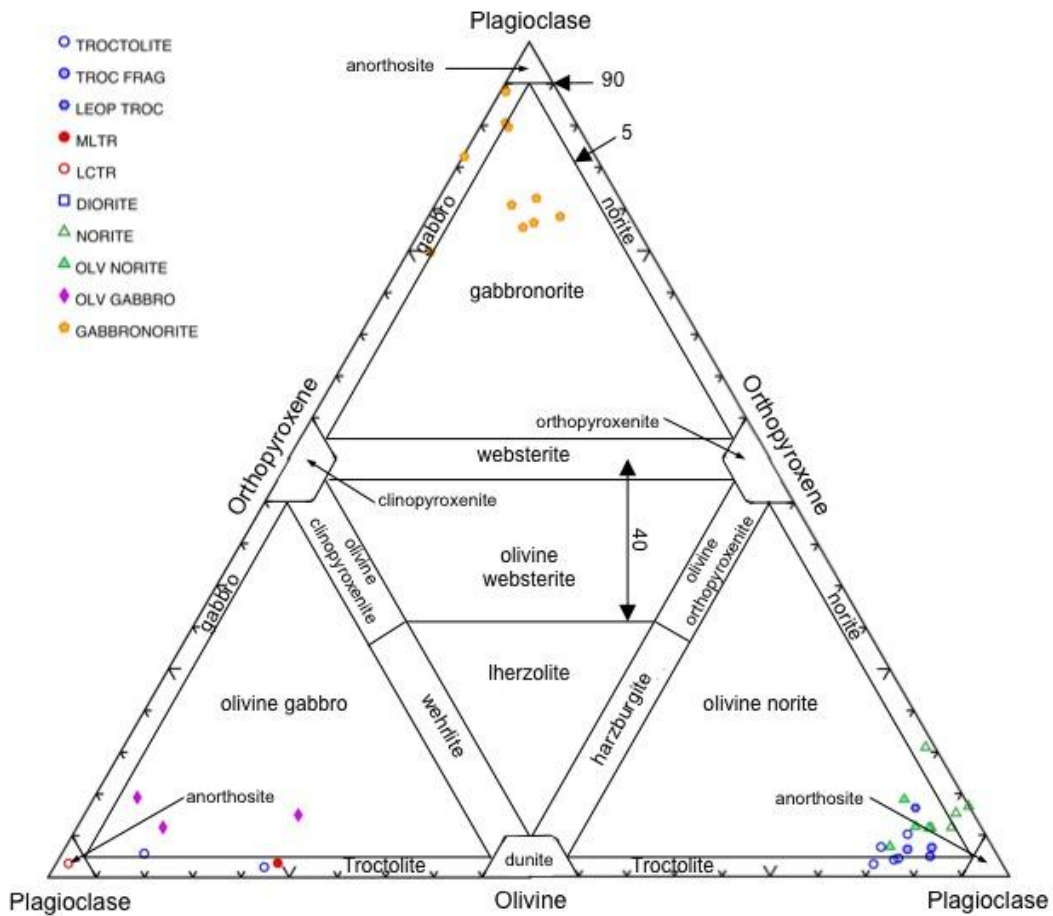


Fig. A-3. Selected samples (where MLA analyses were completed) from this study plotted on Streckeisen's (1974) classification scheme for mafic-ultramafic rocks. Samples plotted on this diagram are samples which were run on the MLA and classifications above are based on (normalized) modal mineralogies determined from MLA analyses. Modal mineralogies for each individual sample are presented in Chapter 2 (Table 2-1). Rock types and symbols are noted in the upper left corner and rocks types are as follows: troctolite, troctolite with fragments, leopard texture troctolite, melatrotroctolite, leucotroctolite, diorite, norite, olivine norite, olivine gabbro, and gabbronorite. Modified after Streckeisen (1974).

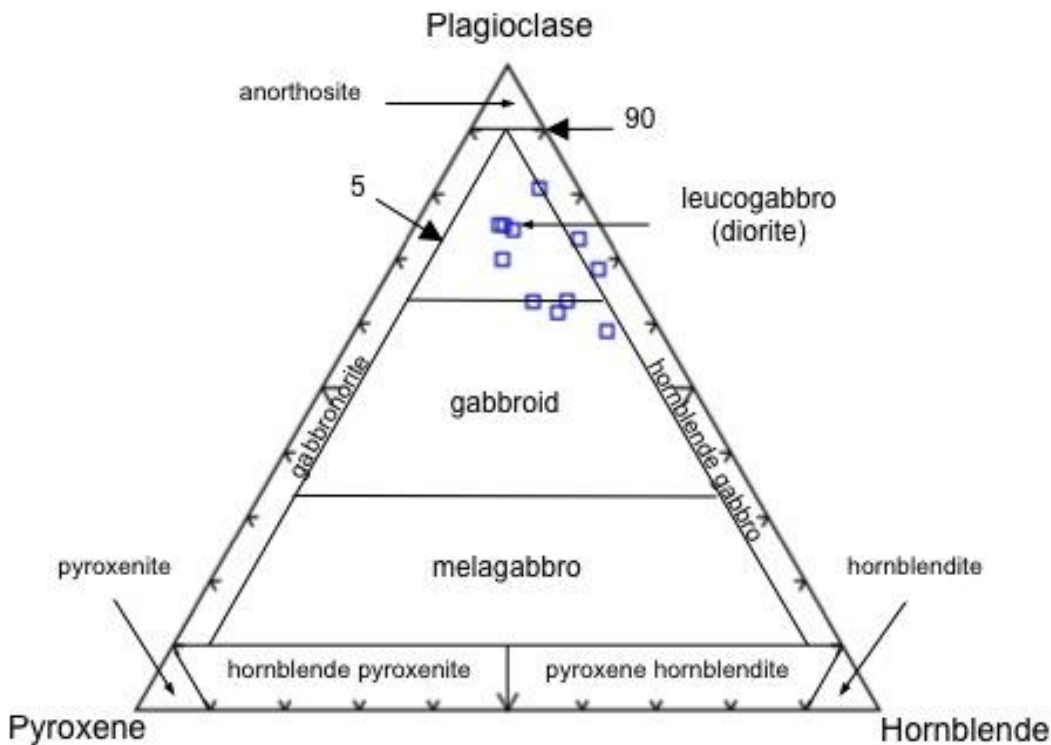
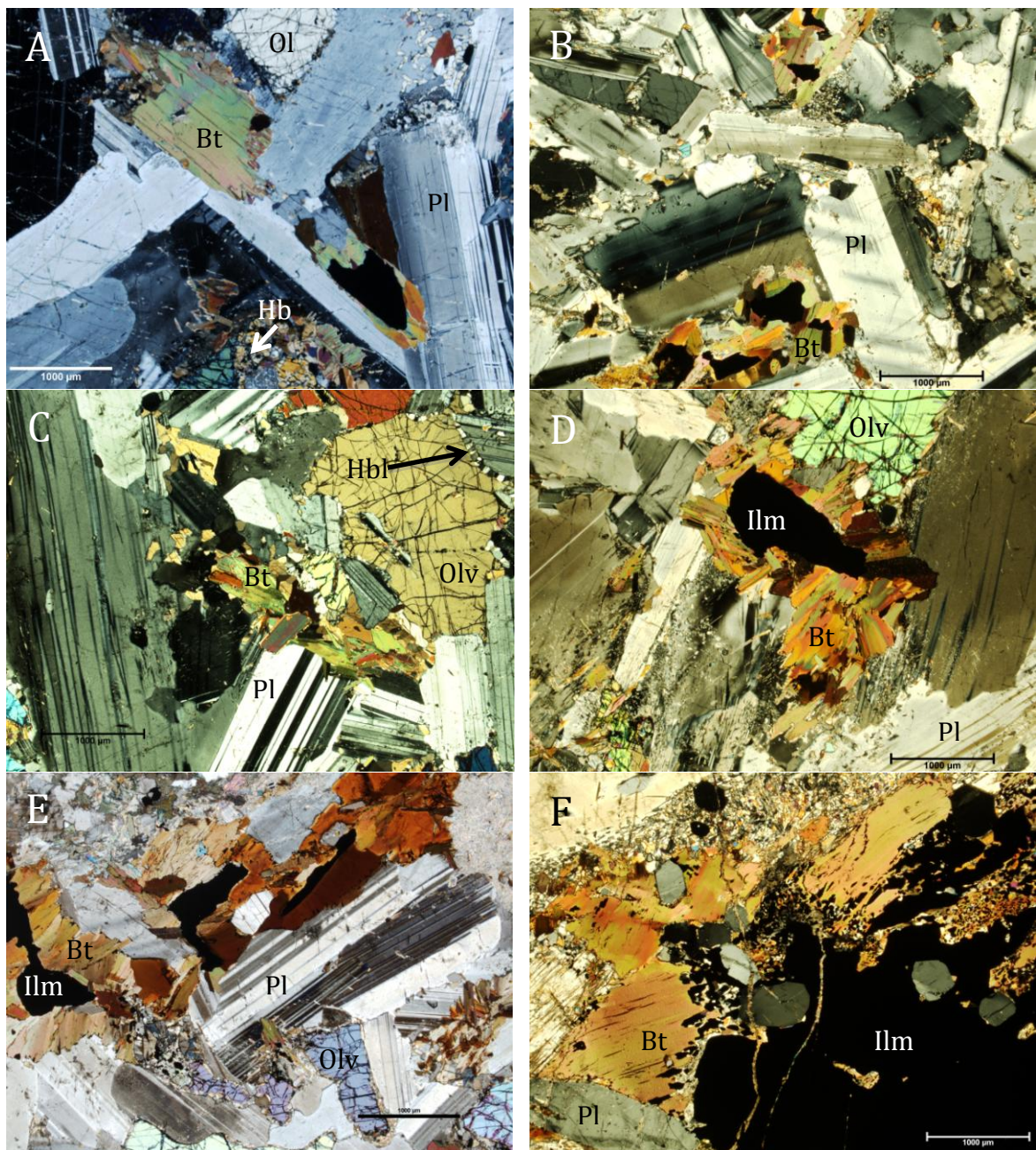


Fig. A-4. Selected samples from this study plotted on Streckeisen's (1976) classification scheme for gabbroic rocks. This nomenclature and classification scheme is based on the proportions of plagioclase, pyroxene (orthopyroxene plus clinopyroxene) and hornblende. Open blue squares represent samples that were classified as diorite based on modal mineralogy as determined via MLA. Modified after Streckeisen (1976).



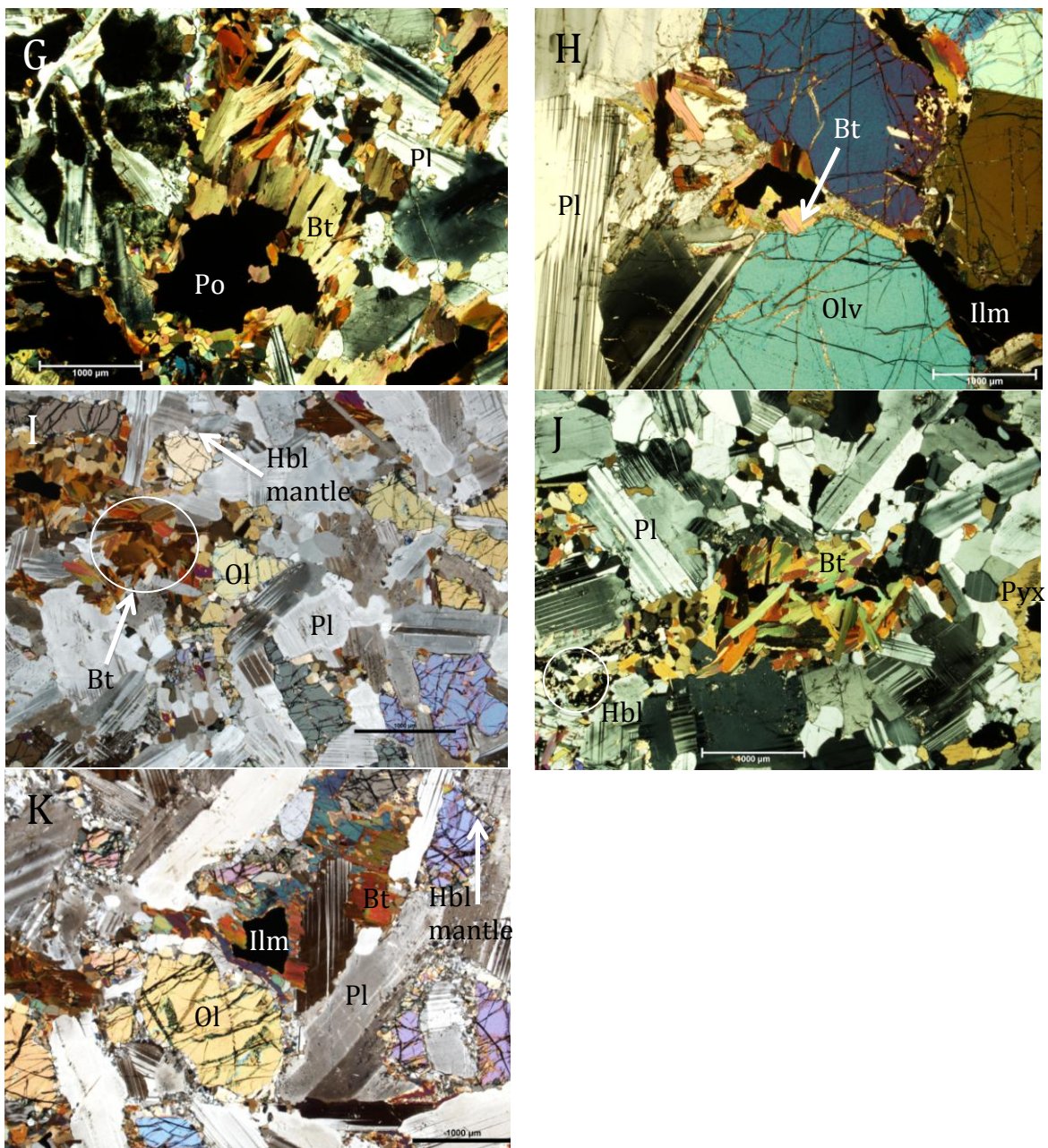


Fig. A-5. Photomicrographs A-K (above) show the different varieties of troctolite from the Voisey's Bay Intrusion (VBI). A. JG-11-001. Troctolite from the Eastern Deeps chamber. Note elongate, euhedral plagioclase laths with interstitial olivine and biotite. Hornblende forms a discontinuous reaction rim around olivine grain at the bottom of the picture, just left of centre. B. JG-11-035. Troctolite from the Western Deeps chamber. Fine-grained interstitial ilmenite grains (opaque) are enclosed by platy, fine-grained biotite. C. JG-11-003. Coarse-grained, inequigranular troctolite from the Eastern Deeps chamber. Note the cluster of fine-grained, platy biotite at the centre of the photomicrograph. The coarse olivine grain right of centre is mantled by fine-grained

hornblende grains. D. JG-11-042. Coarse-grained troctolite from the Western Deeps chamber. Note plagioclase is weakly saussuritized indicating a possible reaction between residual fluids from late-stage magmatic crystallization and previously formed plagioclase. E. JG-11-012. Troctolite from the Eastern Deeps chamber. Euhedral plagioclase laths are coarse-grained and enclose interstitial, mantled olivine and interstitial biotite. Biotite forms coronas around ilmenite grains. F. JG-11-044. Troctolite from the Western Deeps chamber. The large ilmenite oikocryst in the bottom right of the picture encloses several rounded plagioclase crystals. Moderately saussuritized plagioclase is visible in the upper left portion of the picture and is separated from the ilmenite by coarse-grained, strained biotite. Biotite likely crystallized as a late, interstitial phase from residual magmatic fluids, which also altered previously formed plagioclase grains. G. JG-11-017. Leopard texture troctolite from the base of the Eastern Deeps chamber. Blebby interstitial sulphides are mantled by fine-grained biotite and hornblende. Anhedral, stubby plagioclase grained are enclosed in pyroxene oikocrysts (as seen in the upper left corner of the photomicrograph). H. JG-11-047. Coarse-grained cumulate plagioclase and olivine in troctolite from the Western Deeps chamber. Interstitial biotite mantles fine-grained ilmenite and is associated with the saussuritization of plagioclase. I-K. JG-11-006, JG-11-016, JG-11-024. Coarse-grained, fragment-bearing troctolite from the Eastern Deeps chamber. Fragments of gneissic country rock are not visible in these photos. Plagioclase laths enclose interstitial clusters of medium-grained, platy biotite mantling ilmenite grains. Olivine is rimmed with pyroxene and hornblende from incomplete reactions with late-stage magmatic liquid.

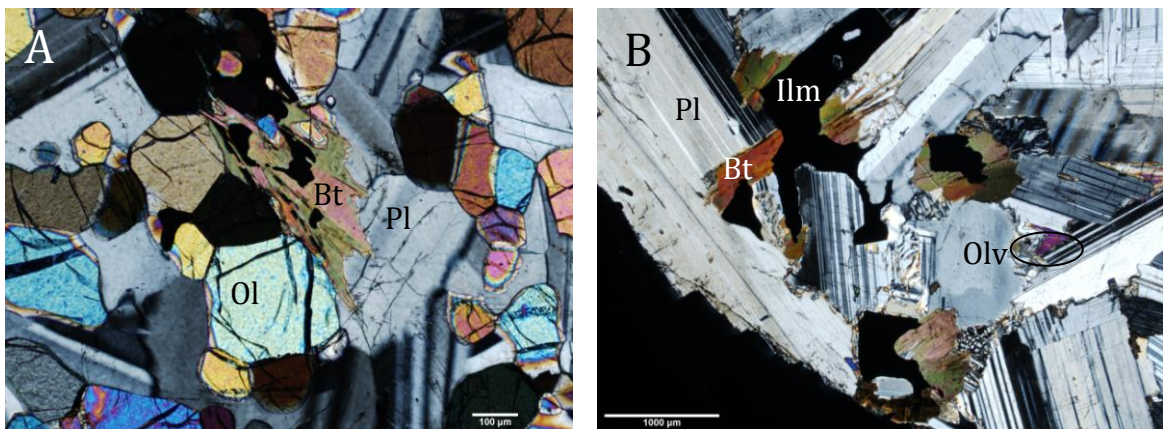
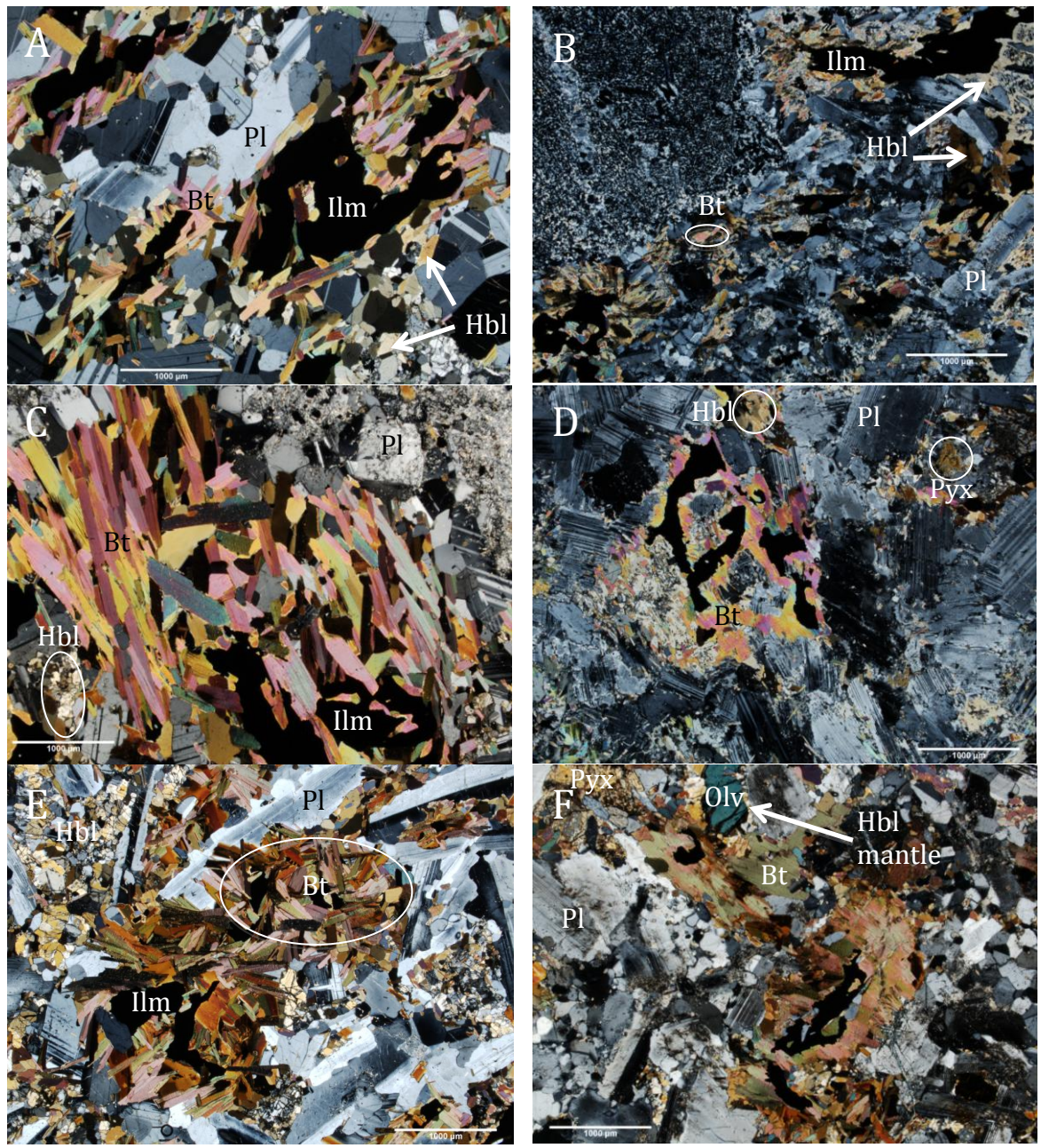


Fig. A-6. Photomicrographs A-B (above) show the different varieties of troctolite in the Mushuau intrusion. A. JG-11-134. Meltroctolite from the Mushuau intrusion. Fine grained, cumulate plagioclase and olivine enclose interstitial ilmenite and with trace very fine grained interstitial biotite. B. JG-11-137. Leucotroctolite from the Mushuau intrusion. Medium to coarse grained plagioclase laths enclose fine grained interstitial biotite and disseminated ilmenite. Trace, very fine grained olivine present.



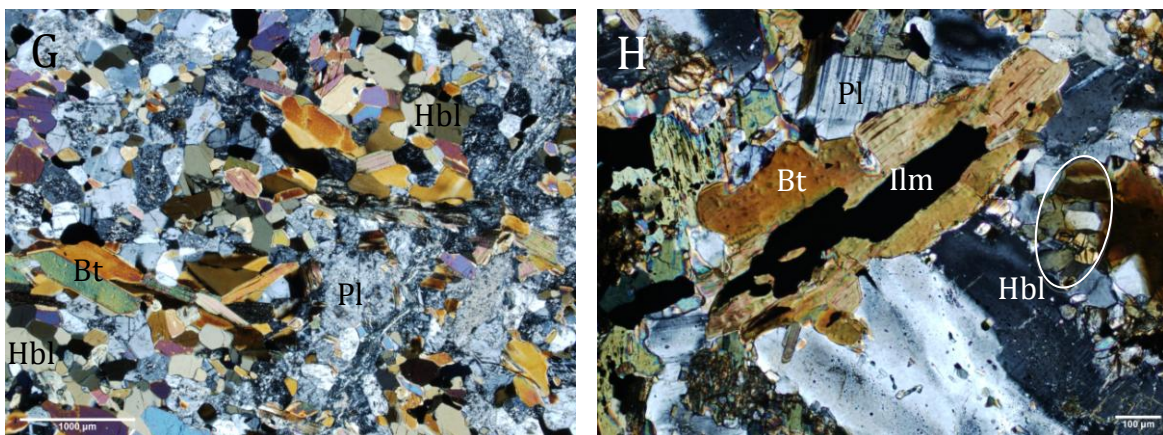
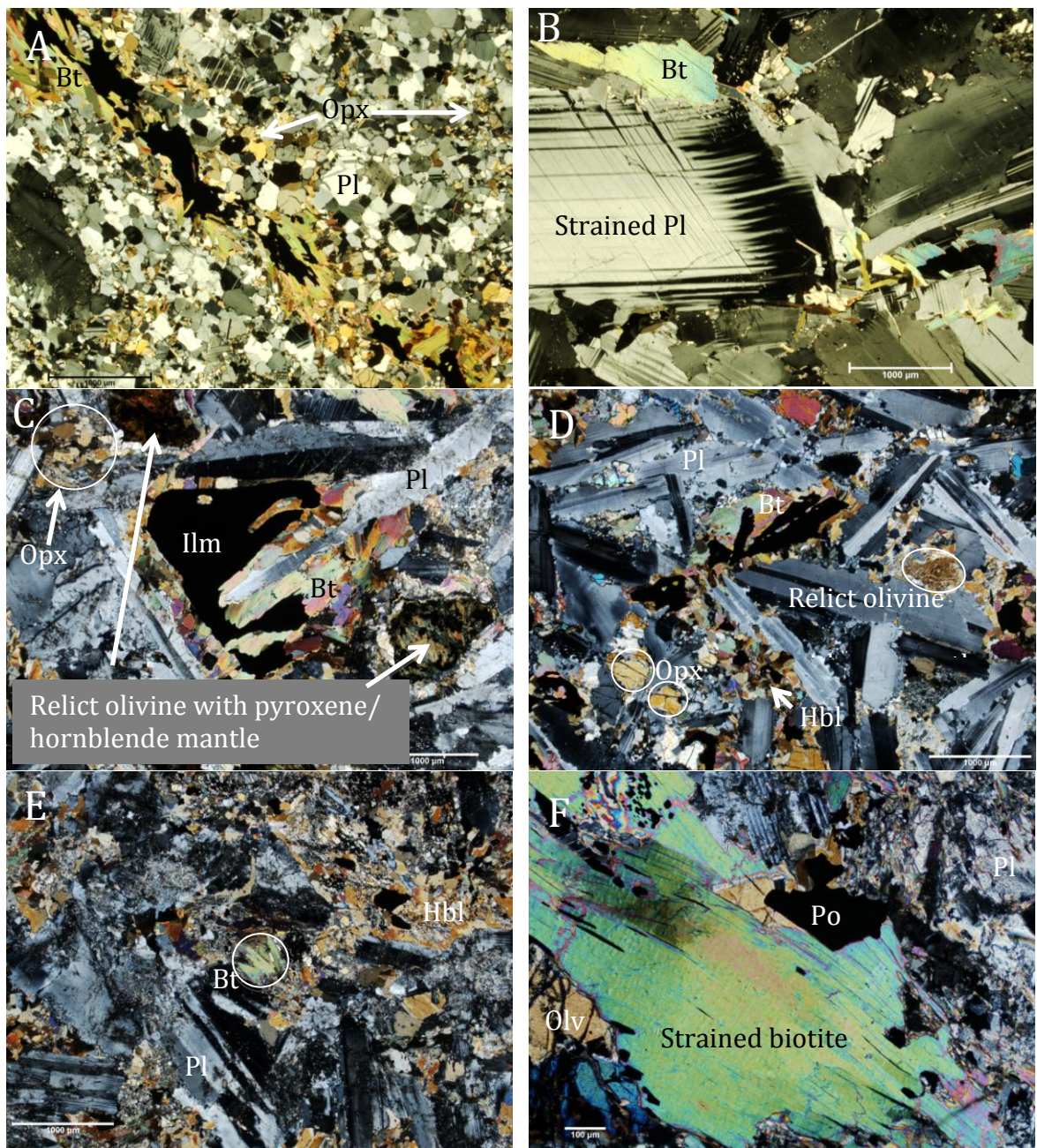


Fig. A-7. Photomicrographs A-H (above) show the different varieties of diorite from the VBI. A. JG-11-072. Diorite from the feeder to the Eastern Deeps. Medium grained cumulus plagioclase with interstitial hornblende, biotite and ilmenite. Plagioclase and biotite display euhedral grain boundaries. Ilmenite and hornblende have anhedral grain boundaries. B. JG-11-037. Moderately saussuritized diorite from the Discovery Hill dyke. Fine to medium grained plagioclase forms framework around interstitial hornblende, which is concentrated along the grain boundaries between ilmenite and plagioclase. Large plagioclase grain in upper left corner displays sieve-like texture. C. JG-11-075. Diorite from the feeder to the Eastern Deeps. Weakly saussuritized anhedral cumulus plagioclase with interstitial biotite (displaying weak alignment) and ilmenite. Small cluster of fine grained, interstitial hornblende in lower left corner. D. JG-11-088. Weakly altered diorite from south-east extension zone. Medium grained plagioclase with clusters of interstitial biotite, pyroxene and hornblende. Fine grained biotite forms complete rims around isotropic oxide minerals. E. JG-11-076. Diorite from feeder to the Eastern Deeps. Subhedral, unaltered cumulus plagioclase framework with large clusters of hydrous interstitial mineral phases including biotite and hornblende. Trace fine ilmenite disseminations. F. JG-11-089. Diorite from the south-east extension zone. Anhedral plagioclase encloses interstitial feathery biotite. Single olivine grain rimmed by fine grained hornblende visible near the top of the photomicrograph. G. JG-11-086. Diorite from north Eastern Deeps feeder. Fine grained saussuritized plagioclase with fine surrounded interstitial hornblende grains. H. JG-11-124. Medium grained, weakly altered diorite from the base of the Ovoid. Interstitial ilmenite is rimmed by subhedral biotite. Cluster of surrounded interstitial hornblende visible at right side of photomicrograph. Medium grained plagioclase displays subhedral grain boundaries.



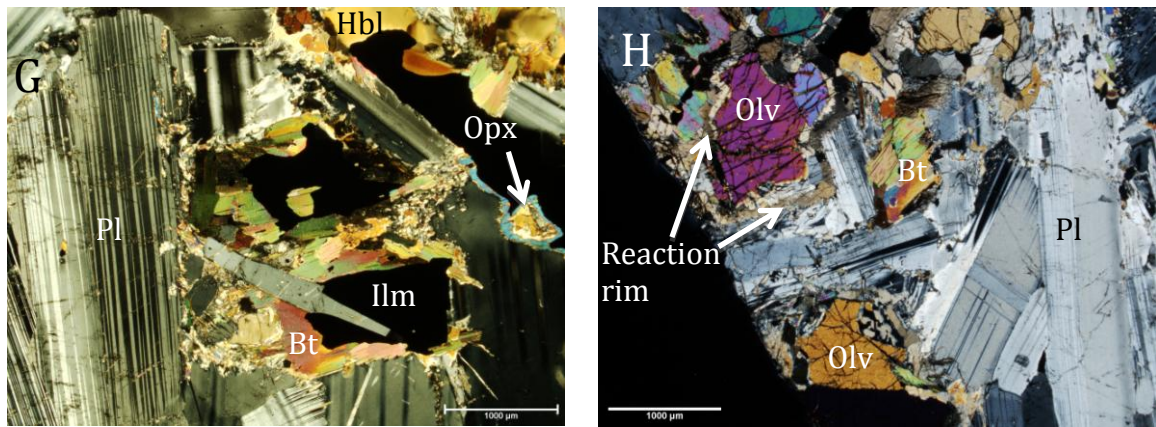


Fig. A-8. Photomicrographs A-H (above) show the different varieties of norite from the VBI and the Floodplain intrusion. A. JG-11-040. Fine grained norite from the feeder to the Eastern Deeps. Subhedral cumulus plagioclase forms a continuous framework around interstitial orthopyroxene. Fine grained veinlet of ilmenite with a thin margin of biotite crosscuts the photomicrograph. B. JG-11-032. Olivine norite from the Western Deeps chamber. Coarse grained cumulus plagioclase with fine interstitial biotite is visible in this sample. Large plagioclase grain on left side of photomicrograph shows evidence of strain or deformation. C. JG-11-093. Weakly pervasively altered norite from Discovery Hill dyke. Saussuritized cumulus plagioclase with interstitial clusters of fine grained orthopyroxene. Biotite rims the coarse ilmenite grains in the centre of the photo. A relict olivine with a pyroxene + hornblende mantle is visible toward the lower right hand corner of the photomicrograph. D. JG-11-091. Olivine norite from the Ovoid zone. Plagioclase framework encloses anhedral pyroxene and hornblende. Trace disseminated oxide minerals are rimmed with biotite. E. JG-11-097. Norite from the Discovery Hill dyke. Pervasively altered plagioclase cumulate with interstitial hornblende and minor biotite. F. JG-11-078. Olivine norite from the Western Deeps dyke. Small grain of pyrrhotite is visible near the centre of the photomicrograph and is bounded by a coarse grain of strained biotite. Plagioclase is pervasively saussuritized. G. JG-11-059. Norite from the Floodplain intrusion. Coarse grained, unaltered, euhedral plagioclase laths enclose interstitial hornblende and minor pyroxene. Interstitial ilmenite is partially rimmed by biotite and some fine grained pyroxene grains are partially enclosed by a biotite mantle resulting from an incomplete reaction with late-stage magmatic liquid. H. JG-11-080. Olivine norite from the Western Deeps dyke. Coarse, euhedral plagioclase laths as seen in the lower right corner with interstitial hornblende and minor biotite. Coarse olivine grain toward upper left corner is mantled with a pyroxene reaction rim.

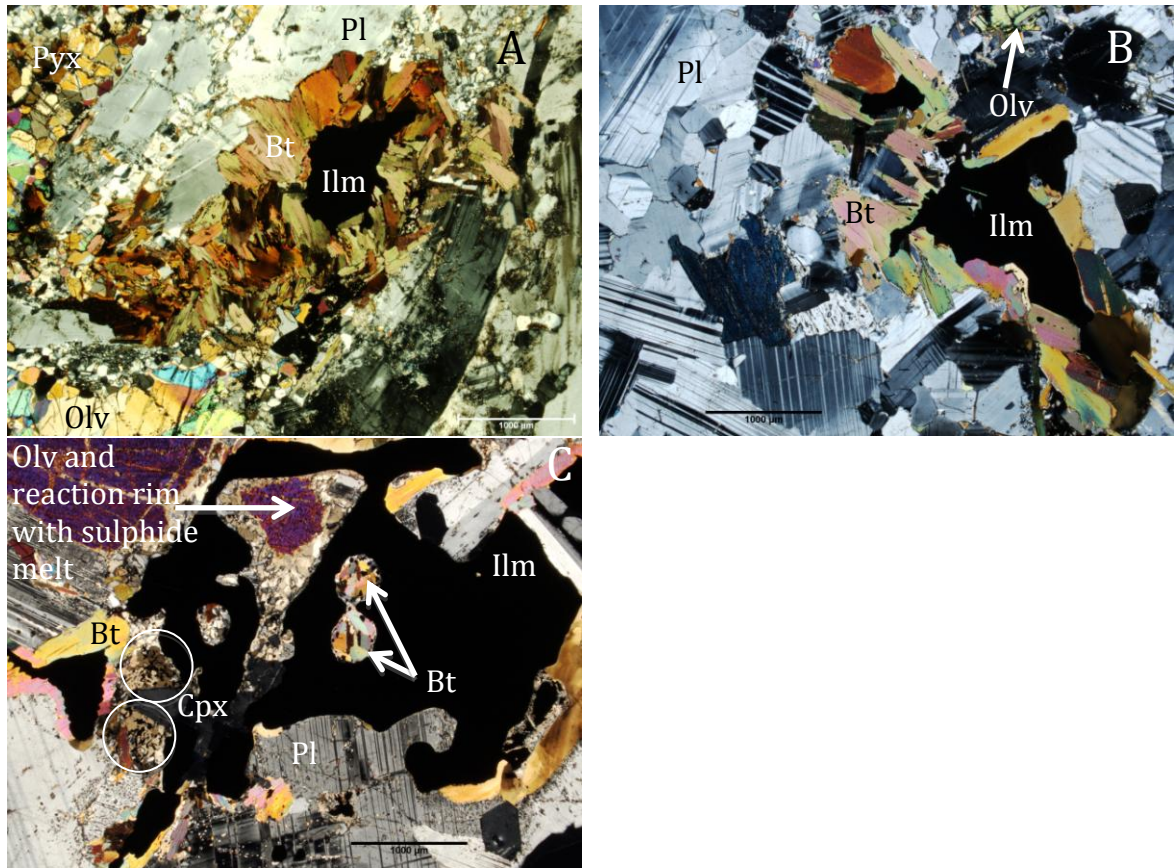


Fig. A-9. Photomicrographs A-C (above) show the different varieties of olivine gabbro from the Ashley and Floodplain intrusions. A. JG-11-061. Olivine gabbro from the Floodplain intrusion. Ragged, coarse grained anhedral plagioclase cumulate with interstitial pyroxene and olivine. Minor ilmenite mantled by biotite. B. JG-11-069. Olivine gabbro from the Ashley intrusion. Unaltered, cumulus plagioclase visible in the left corner of the photomicrograph. Fine grained interstitial biotite is present in clusters around oxide minerals. Small grain of olivine visible near upper edge of photo. C. JG-11-068. Olivine gabbro from the Ashley intrusion. Plagioclase grains enclose large bleb of ilmenite. Olivine oikocryst enclosed within ilmenite has a pyroxene mantle, likely a reaction rim from interaction with melt. Two small blebs of biotite are visible near the centre of the photo and are probably either rims around very fine disseminated sulphide grains or results from incomplete late stage reactions between magmatic liquid and partially crystallized minerals.

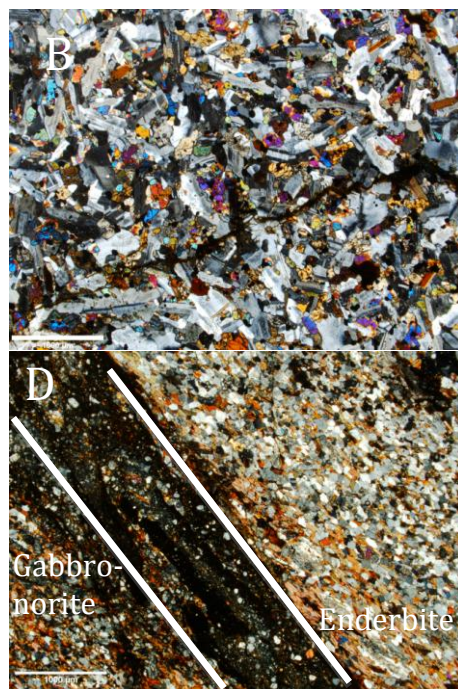
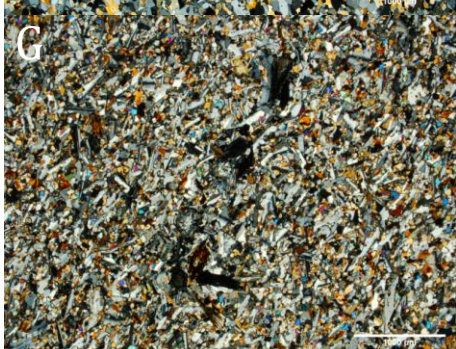
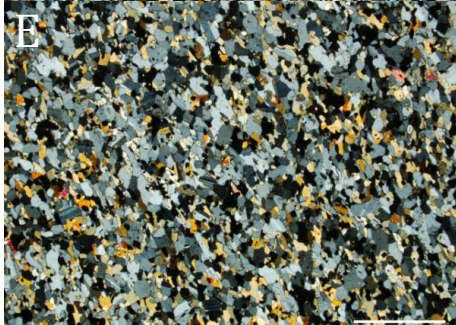




Fig. A-10. Photomicrographs A-J (above) show chilled marginal gabbronorite from various locations within the VBI. A. JG-11-100, from the Eastern Deep chamber. Note inequigranular grain sizes and felty appearance of the elongate plagioclase grains, which form a discontinuous framework around very fine grained interstitial pyroxene grains. B. JG-11-130, from the Ryan's Pond zone. Inequigranular, anhedral grains. The pyroxene species in this chill are notably different from chills elsewhere in the VBI; clinopyroxene is present as hedenbergite, which is a rare pyroxene typically found in contact metamorphic rocks and orthopyroxene is present as ferrosilite, a variety of orthopyroxene commonly seen in ultramafic igneous rocks. C. JG-11-101, from the Eastern Deep chamber. Weak alignment of individual grains, possibly due to flow banding. D. JG-11-106, from the base of the Ovoid deposit. The actual contact between gabbronorite and enderbitic country rock is visible across the centre of this photomicrograph. Gabbronorite is visible in the lower left corner and enderbitic gneiss is visible in the upper right corner. E. JG-11-102, from the Eastern Deep chamber. Weak flow banding visible. F. JG-11-114, from the Western Deep feeder dyke. Grains have anhedral boundaries and grain size is equigranular overall. G. JG-11-104, from the Eastern Deep chamber. Inequigranular, felty texture. H. JG-11-125, from the Kog Brook zone. I. JG-11-105, from the Eastern Deep chamber. J. JG-11-127, from the Kog Brook zone.

Appendix B

Master sample list, map showing drill hole locations and MLA mineral grain boundary maps.

Table B-1. Master sample list with sample name, borehole name, depth (from and to), lithology, and the location and environment of each sample. All samples were collected from drill core. TROC = troctolite, TROC(F) = troctolite with fragments, LEOP = leopard troctolite, TRBX = troctolite breccia, MLTR = melatroctolite, LCTR = leucotroctolite, ORGN = orthogneiss, ENGN = enderbitic orthogneiss, NOG = Nain orthogneiss, GPGN = garnetiferous paragneiss, DIOR = diorite, NOR = norite, GBNO = gabbronorite, OVNO = olivine norite, OVGB = olivine gabbro, MFdk = mafic dyke, RPGR = rapakivi granite, QM = quartz monzonite, C. ROCK = country rock.

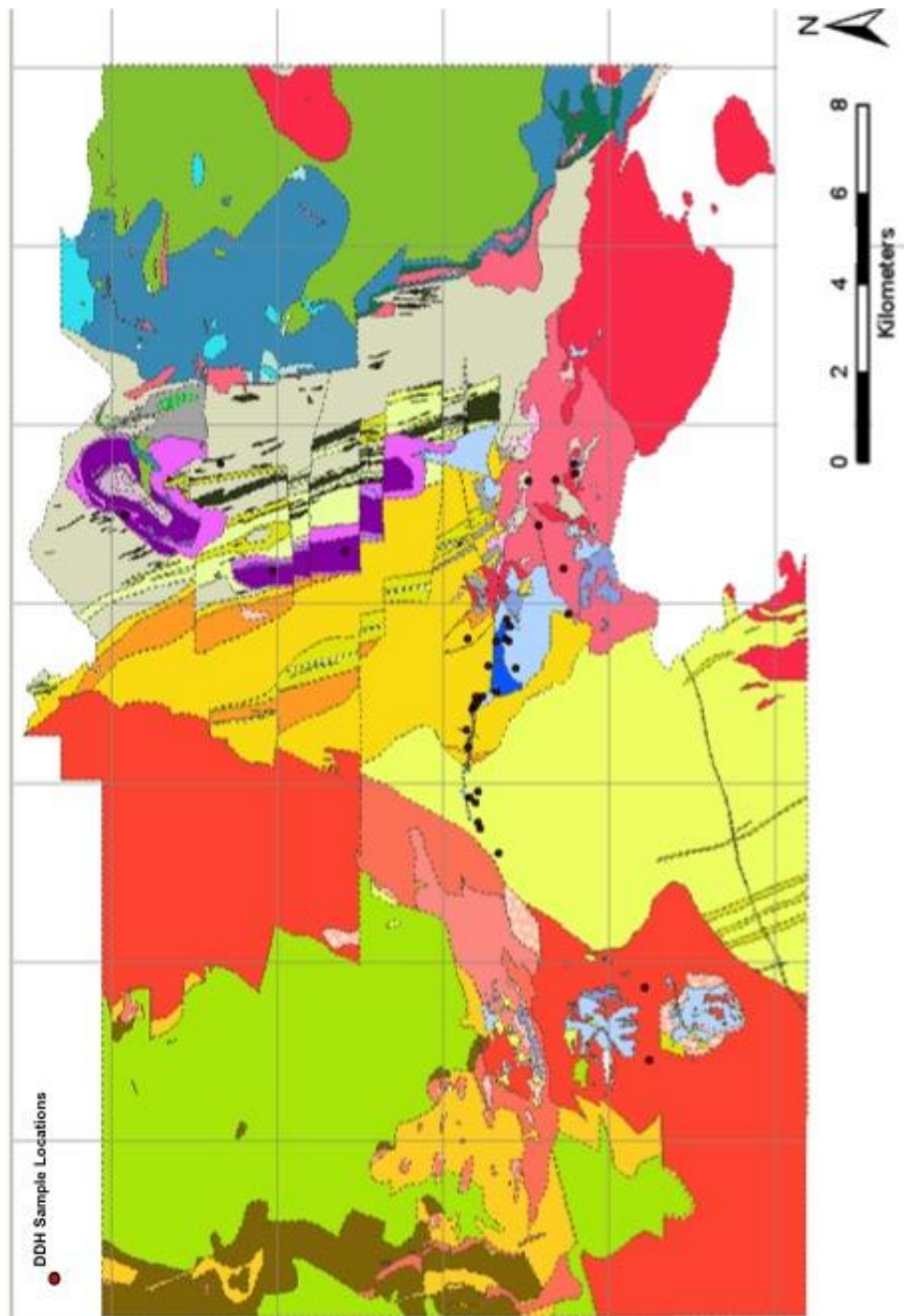
Sample	BH ID	From	To	Lithology	Location	Enviro
JG-11-001	VB-99-528	101	102	TROC	EASTERN DEEPS	CHAMBER
JG-11-002	VB-99-528	208	208.9	TROC	EASTERN DEEPS	CHAMBER
JG-11-003	VB-99-528	298	298.7	TROC	EASTERN DEEPS	CHAMBER
JG-11-004	VB-99-528	400	401	TROC	EASTERN DEEPS	CHAMBER
JG-11-005	VB-99-528	519.1	519.5	TROC(F)	EASTERN DEEPS	CHAMBER
JG-11-006	VB-99-528	601	601.8	TROC(F)	EASTERN DEEPS	CHAMBER
JG-11-007	VB-99-528	700.4	701.4	ENGN	EASTERN DEEPS	CHAMBER
JG-11-008	VB-99-528	800	801	ENGN	EASTERN DEEPS	CHAMBER
JG-11-009	VB-99-528	890.4	891.2	ORGN	EASTERN DEEPS	C. ROCK
JG-11-010	VB-08-871	100	101	TROC	EASTERN DEEPS	CHAMBER
JG-11-011	VB-08-871	200	200.8	TROC	EASTERN DEEPS	CHAMBER
JG-11-012	VB-08-871	300	300.8	TROC	EASTERN DEEPS	CHAMBER
JG-11-013	VB-08-871	400	401	QM	EASTERN DEEPS	CHAMBER
JG-11-014	VB-08-871	493	493.9	TROC	EASTERN DEEPS	CHAMBER
JG-11-015	VB-08-871	599	600	TROC	EASTERN DEEPS	CHAMBER
JG-11-016	VB-08-871	700	700.8	TROC(F)	EASTERN DEEPS	CHAMBER
JG-11-017	VB-08-871	800	801	LEOP	EASTERN DEEPS	CHAMBER
JG-11-018	VB-08-871	900	901	ENGN	EASTERN DEEPS	C. ROCK
JG-11-019	VB-99-526	100	101	TROC	EASTERN DEEPS	CHAMBER
JG-11-020	VB-99-526	200	200.8	TROC	EASTERN DEEPS	CHAMBER
JG-11-021	VB-99-526	306	307	DIOR	EASTERN DEEPS	CHAMBER
JG-11-022	VB-99-526	400	401	TROC	EASTERN DEEPS	CHAMBER
JG-11-023	VB-99-526	500	501	TROC(F)	EASTERN DEEPS	CHAMBER
JG-11-024	VB-99-526	600	601	TROC(F)	EASTERN DEEPS	CHAMBER
JG-11-025	VB-99-526	700	701	ENGN	EASTERN DEEPS	CHAMBER
JG-11-026	VB-99-526	800	801	ENGN	EASTERN DEEPS	CHAMBER
JG-11-027	OV-09-038	87	87.6	GBNO	OVOID	CHILL
JG-11-028	OV-09-038	88.4	88.8	MFdk	OVOID	FEEDER
JG-11-029	VB-97-368	306	307	TRBX	WESTERN DEEPS	CHAMBER
JG-11-030	VB-97-368	401.8	402.8	OVNO	WESTERN DEEPS	CHAMBER
JG-11-031	VB-97-368	512	513	OVNO	WESTERN DEEPS	CHAMBER
JG-11-032	VB-97-368	609	610	OVNO	WESTERN DEEPS	CHAMBER
JG-11-033	VB-97-368	700	701	OVNO	WESTERN DEEPS	CHAMBER
JG-11-034	VB-97-368	800	801	TROC	WESTERN DEEPS	CHAMBER
JG-11-035	VB-97-368	900	901	TROC	WESTERN DEEPS	CHAMBER
JG-11-036	VB-97-368	990	990.9	TROC	WESTERN DEEPS	CHAMBER
JG-11-037	VB-04-619	225.5	226.3	DIOR	DISCOVERY HILL	FEEDER
JG-11-038	VB-97-407	101	101.9	GPGN	WESTERN DEEPS	C. ROCK
JG-11-039	VB-97-407	200	201	GPGN	WESTERN DEEPS	C. ROCK
JG-11-040	VB-97-407	303	304	NOR	WESTERN DEEPS	CHAMBER
JG-11-041	VB-97-407	400	401	NOR	WESTERN DEEPS	CHAMBER

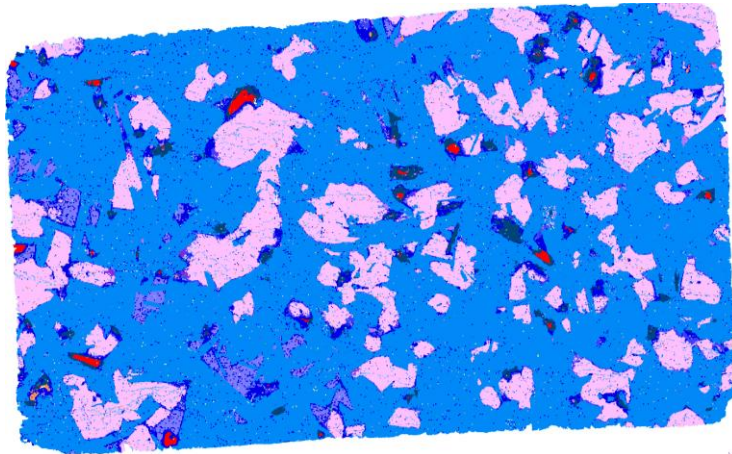
JG-11-042	VB-97-407	500	501	TROC	WESTERN DEEPS	CHAMBER
JG-11-043	VB-97-407	592	593	TROC	WESTERN DEEPS	CHAMBER
JG-11-044	VB-97-407	700	700.9	TROC	WESTERN DEEPS	CHAMBER
JG-11-045	VB-97-407	808	808.9	TROC	WESTERN DEEPS	CHAMBER
JG-11-046	VB-97-407	900	901	TROC	WESTERN DEEPS	CHAMBER
JG-11-047	VB-97-407	1000	1001	TROC	WESTERN DEEPS	CHAMBER
JG-11-048	VB-97-407	1100	1101	RPGR	WESTERN DEEPS	CHAMBER
JG-11-049	VB-97-407	1179	1180	RPGR	WESTERN DEEPS	CHAMBER
JG-11-050	VB-09-891	81.2	82.3	TROC(F)	MUSHUAU	CHAMBER
JG-11-051	VB-09-891	100.4	101	NOG	MUSHUAU	CHAMBER
JG-11-052	S-99-013	100	101	MLTR	MUSHUAU	CHAMBER
JG-11-053	S-99-013	200	201	MLTR	MUSHUAU	CHAMBER
JG-11-054	S-99-013	300	301	ORGN	MUSHUAU	CHAMBER
JG-11-055	S-99-013	397	398	ORGN	MUSHUAU	CHAMBER
JG-11-056	VB-09-894	100	101	GPGN	FLOODPLAIN	C. ROCK
JG-11-057	VB-09-894	200	201	GPGN	FLOODPLAIN	C. ROCK
JG-11-058	VB-09-894	325.3	326.6	NOR	FLOODPLAIN	CHAMBER
JG-11-059	VB-09-894	440.5	441.5	NOR	FLOODPLAIN	CHAMBER
JG-11-060	VB-09-894	500.6	501.6	NOR	FLOODPLAIN	CHAMBER
JG-11-061	VB-09-894	600	601	OVGB	FLOODPLAIN	CHAMBER
JG-11-062	VB-09-894	700	701	OVGB	FLOODPLAIN	CHAMBER
JG-11-063	VB-09-894	800	801.1	OVGB	FLOODPLAIN	CHAMBER
JG-11-064	VB-09-894	900	901	RPGR	FLOODPLAIN	CHAMBER
JG-11-065	VB-09-895	119.2	120.2	TROC	ASHLEY	CHAMBER
JG-11-066	VB-09-895	199.2	199.8	TROC	ASHLEY	CHAMBER
JG-11-067	VB-09-895	300	300.9	TROC(F)	ASHLEY	CHAMBER
JG-11-068	VB-09-895	408	409	OVGB	ASHLEY	CHAMBER
JG-11-069	VB-09-895	512	513	OVGB	ASHLEY	CHAMBER
JG-11-070	VB-09-895	600	601	OVGB	ASHLEY	CHAMBER
JG-11-071	VB-09-895	682	683	OVGB	ASHLEY	CHAMBER
JG-11-072	VB-99-528	846.1	847	DIOR	EASTERN DEEPS	FEEDER
JG-11-073	VB-99-528	850.8	851.8	DIOR	EASTERN DEEPS	FEEDER
JG-11-074	VB-99-521	728.5	729.5	DIOR	EASTERN DEEPS	FEEDER
JG-11-075	VB-99-521	740	741	DIOR	EASTERN DEEPS	FEEDER
JG-11-076	VB-99-526	734.6	735.6	DIOR	EASTERN DEEPS	FEEDER
JG-11-077	VB-99-526	747.5	748.5	DIOR	EASTERN DEEPS	FEEDER
JG-11-078	VB-07-826	238.7	239.7	OVNO	WESTERN DEEPS	FEEDER
JG-11-079	VB-07-826	279.4	280.2	OVNO	WESTERN DEEPS	FEEDER
JG-11-080	VB-07-826	296	296.8	OVNO	WESTERN DEEPS	FEEDER
JG-11-081	VB-07-841	591	591.8	OVNO	WESTERN DEEPS	FEEDER
JG-11-082	VB-07-841	593.8	594.5	OVNO	WESTERN DEEPS	FEEDER
JG-11-083	VB-07-841	618.6	619	OVNO	WESTERN DEEPS	FEEDER
JG-11-084	VB-10-920	434	435	DIOR	NORTHEASTERN DEEPS	FEEDER
JG-11-085	VB-10-920	451	452	DIOR	NORTHEASTERN DEEPS	FEEDER
JG-11-086	VB-10-920	454.4	455.4	DIOR	NORTHEASTERN DEEPS	FEEDER
JG-11-087	VB-10-920	460.3	461.1	DIOR	NORTHEASTERN DEEPS	FEEDER
JG-11-088	VB-09-879	30	31	DIOR	SOUTHEAST EXTENSION	FEEDER
JG-11-089	VB-09-879	120	121	DIOR	SOUTHEAST EXTENSION	FEEDER
JG-11-090	VB-09-879	134	135	DIOR	SOUTHEAST EXTENSION	FEEDER
JG-11-091	VB-95-205	227.7	228.7	OVNO	OVOID	FEEDER
JG-11-092	VB-95-205	238.1	239.1	OVNO	OVOID	FEEDER

JG-11-093	VB-03-607	9.5	10	NOR	DISCOVERY HILL	FEEDER
JG-11-094	VB-03-607	74	74.5	NOR	DISCOVERY HILL	FEEDER
JG-11-095	VB-03-607	84.8	85.6	NOR	DISCOVERY HILL	FEEDER
JG-11-096	VB-04-619	210	210.9	NOR	DISCOVERY HILL	FEEDER
JG-11-097	VB-04-619	213.5	214.5	NOR	DISCOVERY HILL	FEEDER
JG-11-098	VB-04-619	207	208	NOR	DISCOVERY HILL	FEEDER
JG-11-099	VB-04-619	212	212.8	GBNO	DISCOVERY HILL	CHILL
JG-11-100	VB-04-630	435.3	436.3	GBNO	EASTERN DEEPS	CHILL
JG-11-101	VB-04-630	522.1	523.1	GBNO	EASTERN DEEPS	CHILL
JG-11-102	VB-04-630	534.1	534.8	GBNO	EASTERN DEEPS	CHILL
JG-11-103	VB-04-630	564	564.1	TROC	EASTERN DEEPS	CHAMBER
JG-11-104	VB-07-219A	796.5	797.4	GBNO	EASTERN DEEPS	CHILL
JG-11-105	VB-07-862	594.8	595	GBNO	EASTERN DEEPS	CHILL
JG-11-106	OV-09-028	33.9	34.2	GBNO	OVOID	CHILL
JG-11-107	OV-09-045	57.8	59	NOR	OVOID	FEEDER
JG-11-108	OV-09-082	78.6	79.4	NOR	OVOID	FEEDER
JG-11-109	OV-09-066	57.8	58	GBNO	OVOID	CHILL
JG-11-110	VB-07-818	147.4	148.3	NOR	WESTERN DEEPS	FEEDER
JG-11-111	VB-07-818	149.5	150.6	NOR	WESTERN DEEPS	FEEDER
JG-11-112	VB-07-823	147.7	148.4	NOR	WESTERN DEEPS	FEEDER
JG-11-113	VB-07-823	149	149.7	NOR	WESTERN DEEPS	FEEDER
JG-11-114	VB-07-837	117.4	118.6	GBNO	WESTERN DEEPS	CHILL
JG-11-115	VB-07-837	121.4	123.5	NOR	WESTERN DEEPS	FEEDER
JG-11-116	VB-07-820	167	167.6	GBNO	WESTERN DEEPS	CHILL
JG-11-117	VB-07-820	192.8	193.8	MFDK	WESTERN DEEPS	FEEDER
JG-11-118	VB-07-820	195.2	195.8	MFDK	WESTERN DEEPS	FEEDER
JG-11-119	VB-07-820	240.5	240.9	MFDK	WESTERN DEEPS	FEEDER
JG-11-120	VB-09-901	450.3	451.3	TROC	RED DOG	CHAMBER
JG-11-121	VB-09-901	456.2	457.2	TROC	RED DOG	CHAMBER
JG-11-122	VB-09-901	473.2	474.2	TROC	RED DOG	CHAMBER
JG-11-123	VB-09-901	476	477	TROC	RED DOG	CHAMBER
JG-11-124	VB-95-205	236.4	237.2	DIOR	OVOID	FEEDER
JG-11-125	VB-09-897	170.1	171.1	GBNO	KOG BROOK	CHILL
JG-11-126	VB-09-897	182.9	183.9	GBNO	KOG BROOK	CHILL
JG-11-127	VB-09-897	371.6	372.2	GBNO	KOG BROOK	CHILL
JG-11-128	VB-99-529	737.5	737.9	MFDK	RYAN'S POND	CHAMBER
JG-11-129	VB-01-554	1391.2	1391.6	TROC	RYAN'S POND	CHAMBER
JG-11-130	VB-01-555	251.7	253.6	GBNO	RYAN'S POND	CHILL
JG-11-131	VB-99-514	1114.1	1115	MFDK	RYAN'S POND	CHAMBER
JG-11-132	VB-09-886	7	8	MLTR	MUSHUAU	CHAMBER
JG-11-133	VB-09-886	107.1	108	MLTR	MUSHUAU	CHAMBER
JG-11-134	VB-09-886	203	204	MLTR	MUSHUAU	CHAMBER
JG-11-135	VB-09-889	545	546	MLTR	MUSHUAU	CHAMBER
JG-11-136	VB-09-889	643	643.9	LCTR	MUSHUAU	CHAMBER
JG-11-137	VB-09-889	745	746	LCTR	MUSHUAU	CHAMBER
JG-11-138	VB-09-889	843	844	LCTR	MUSHUAU	CHAMBER
JG-11-139	VB-09-889	918.7	919.7	MLTR	MUSHUAU	CHAMBER
JG-11-140	VB-04-619	210.9	211.9	GBNO	DISCOVERY HILL	CHILL
JG-11-141	VB-99-504	1282.4	1283.4	ORGN	RYAN'S POND	C. ROCK
JG-11-142	VB-09-897	459.2	460.2	OVGB	KOG BROOK	CHAMBER
JG-11-153	VB-98-471	920.8	922.2	MFDK	NORTHEASTERN DEEPS	FEEDER

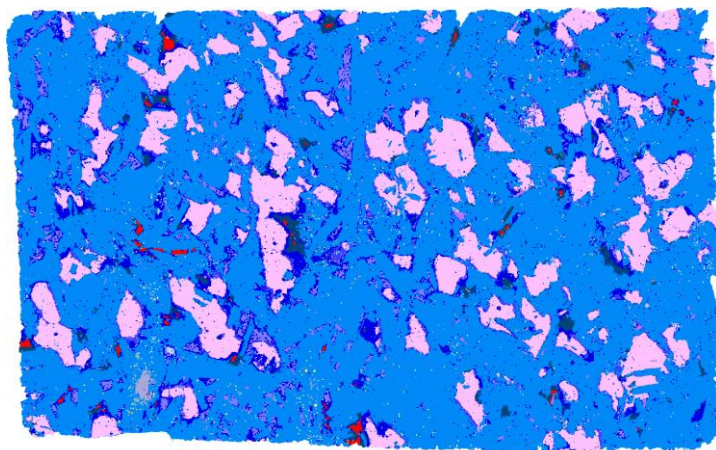
JG-11-154	VB-98-454	1256	1257	TROC	RED DOG	CHAMBER
JG-11-155	VB-10-920	460.3	461.1	MFDK	NORTHEASTERN DEEPS	FEEDER
JG-11-156	VB-10-920	468	468.6	MFDK	NORTHEASTERN DEEPS	FEEDER

Fig. B-1. Plan map showing borehole locations.

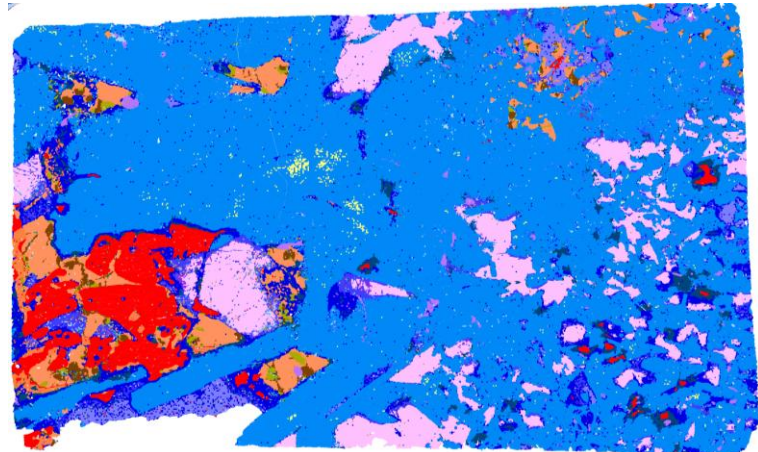




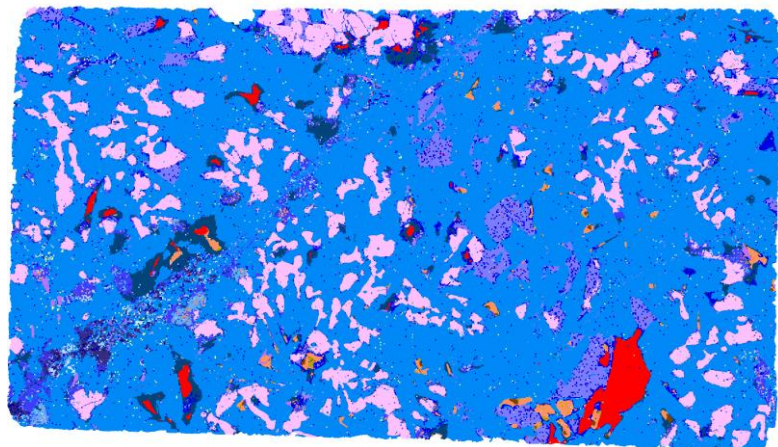
JG-11-001.



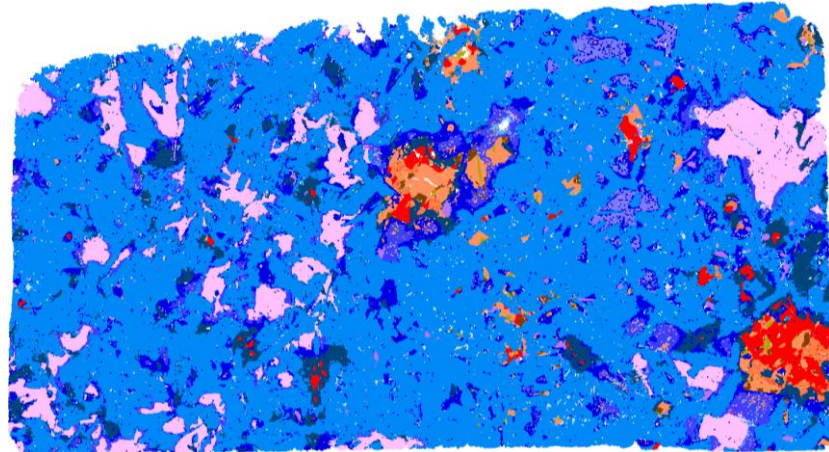
JG-11-003.



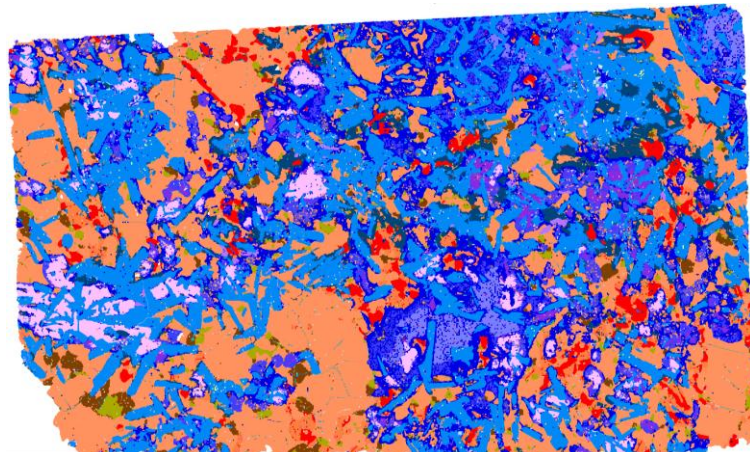
JG-11-006.



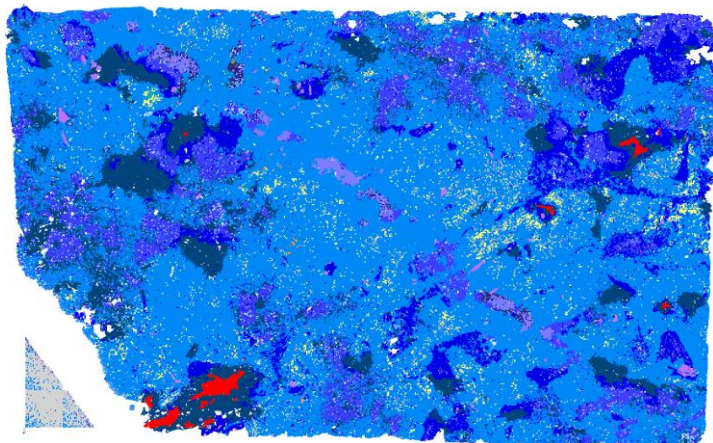
JG-11-012.



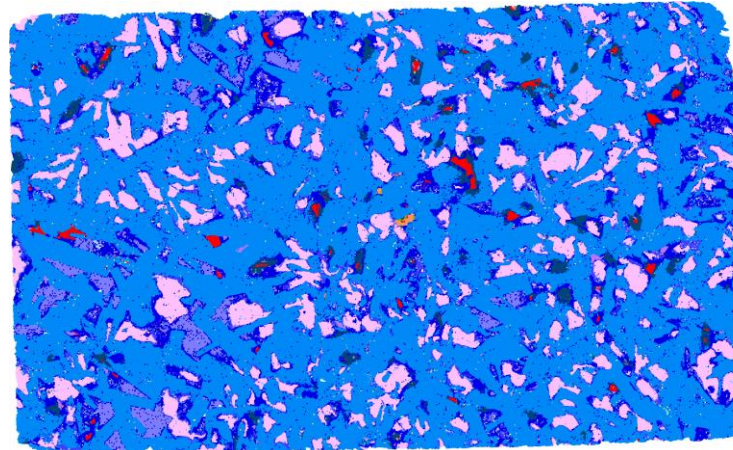
JG-11-016.



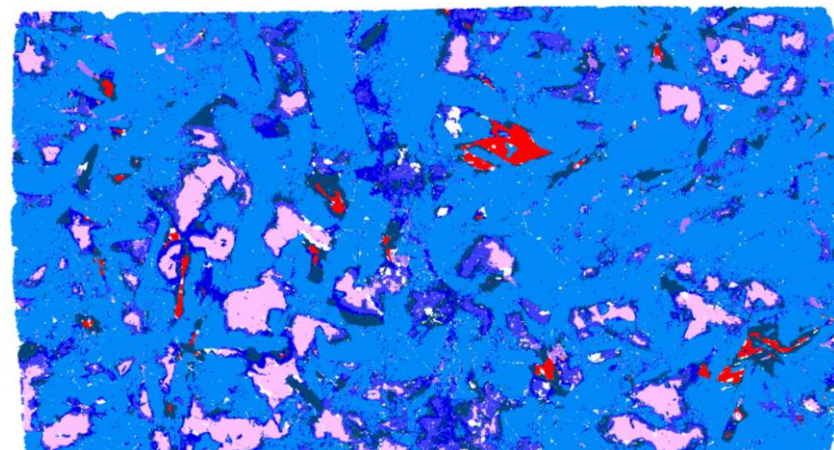
JG-11-017.



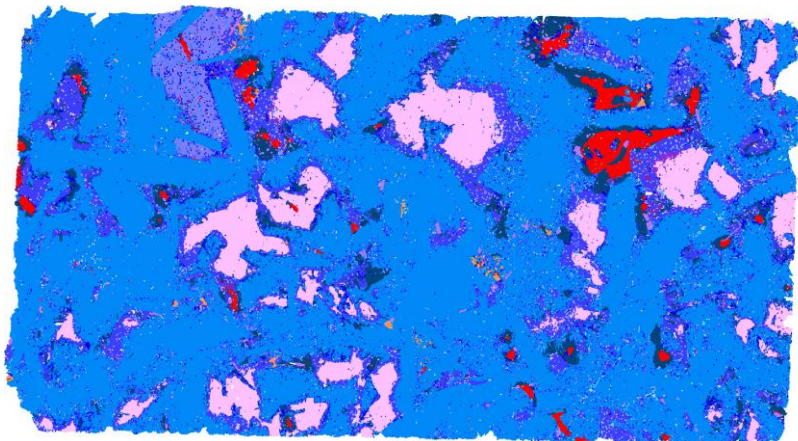
JG-11-021.



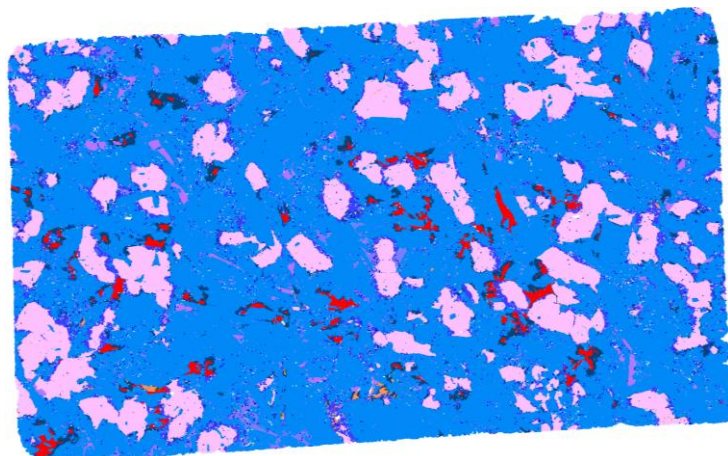
JG-11-024.



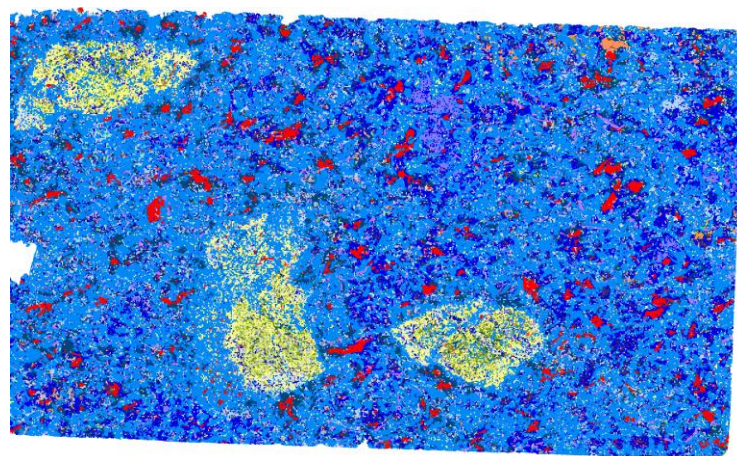
JG-11-032.



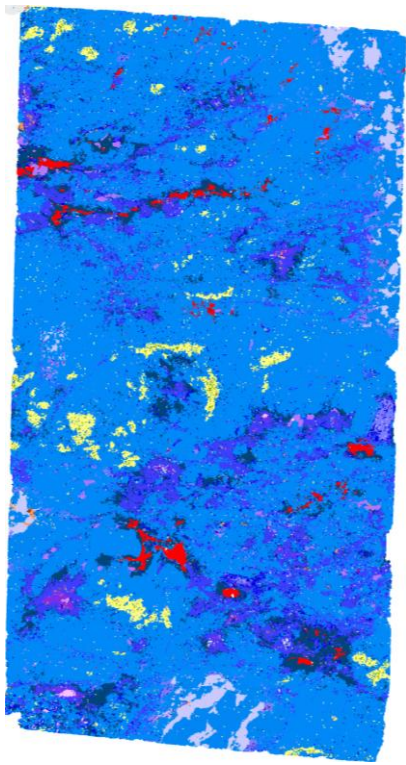
JG-11-033.



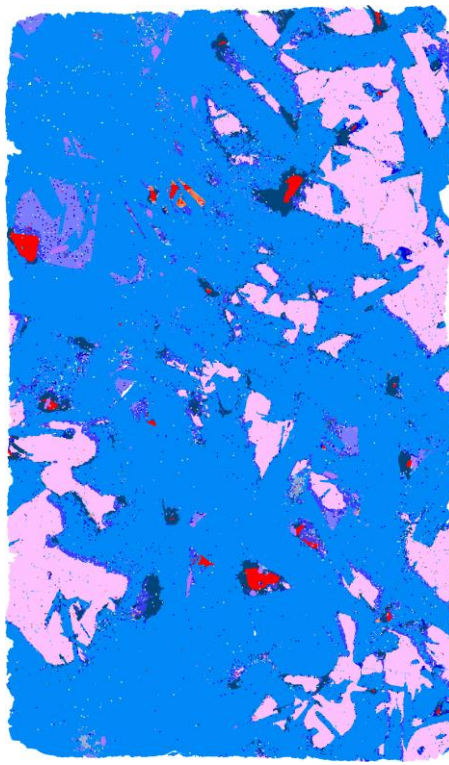
JG-11-035.



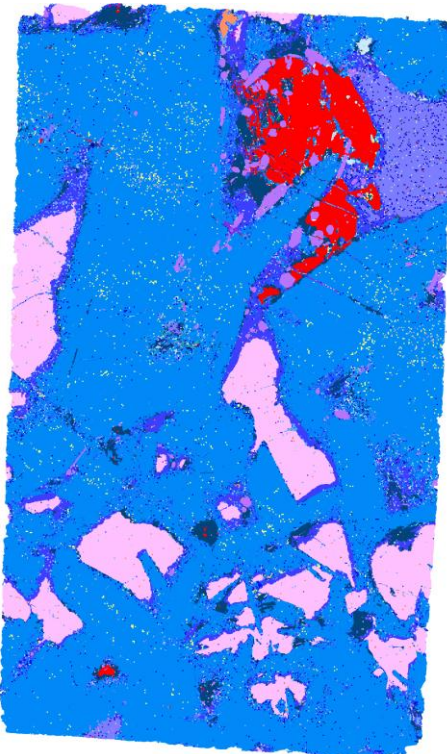
JG-11-037.



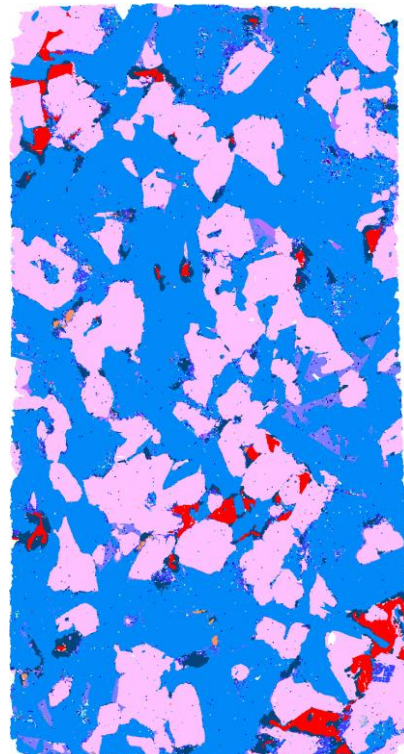
JG-11-040.



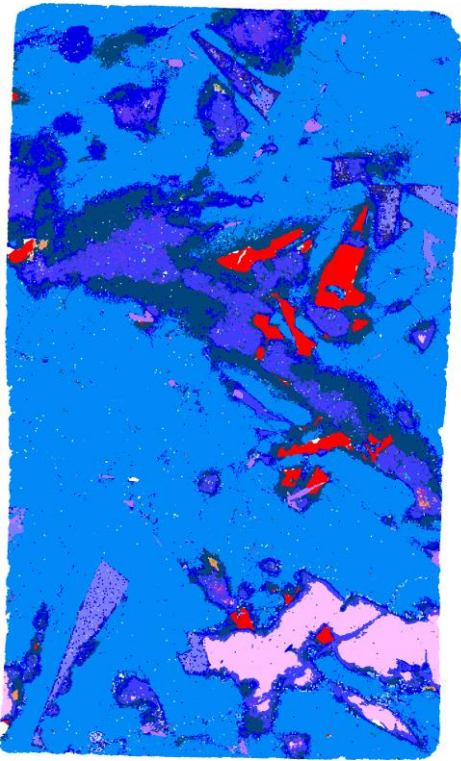
JG-11-042.



JG-11-044.



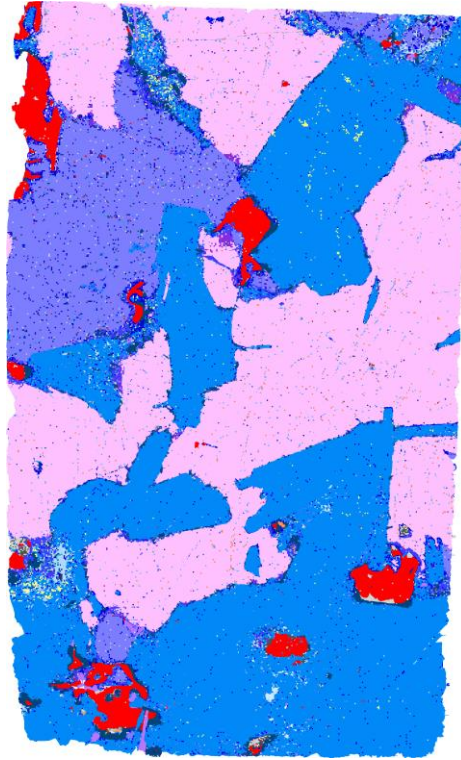
JG-11-047.



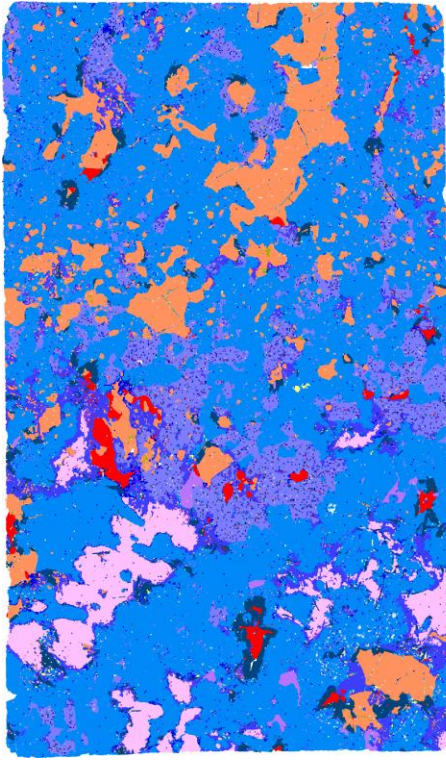
JG-11-059.



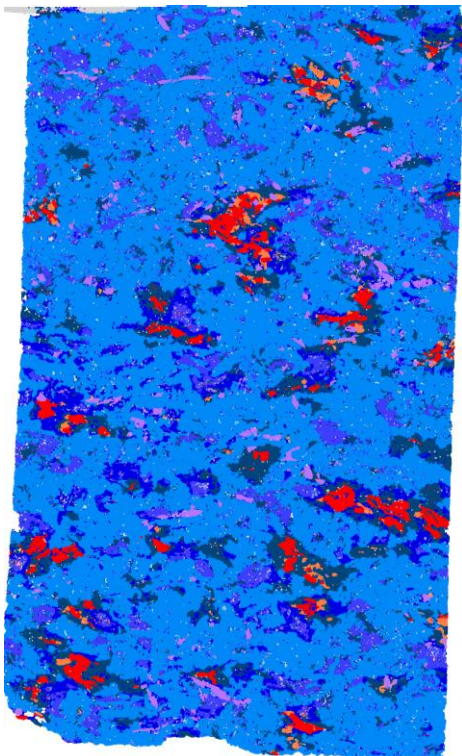
JG-11-061.



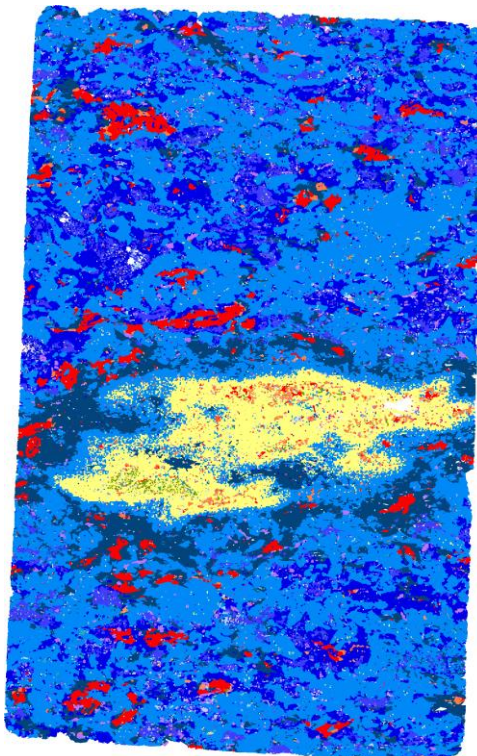
JG-11-068.



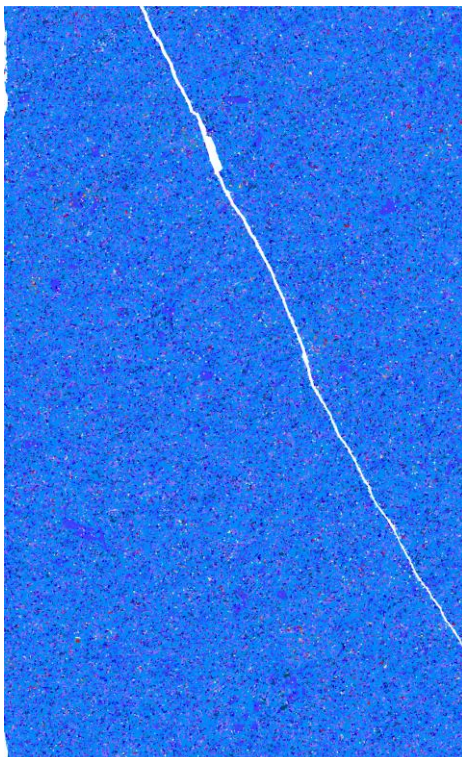
JG-11-069.



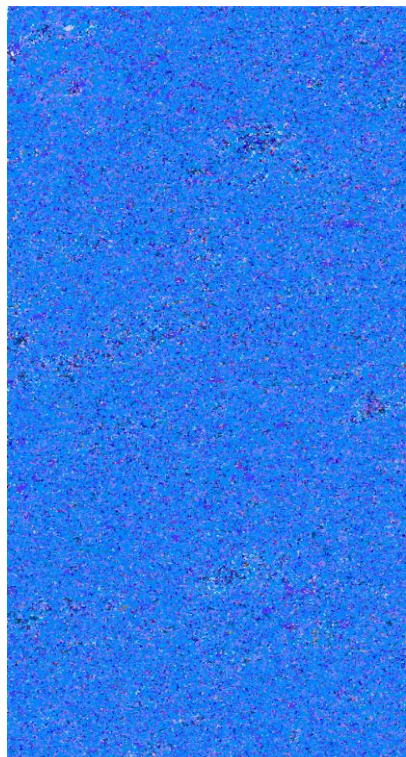
JG-11-072.



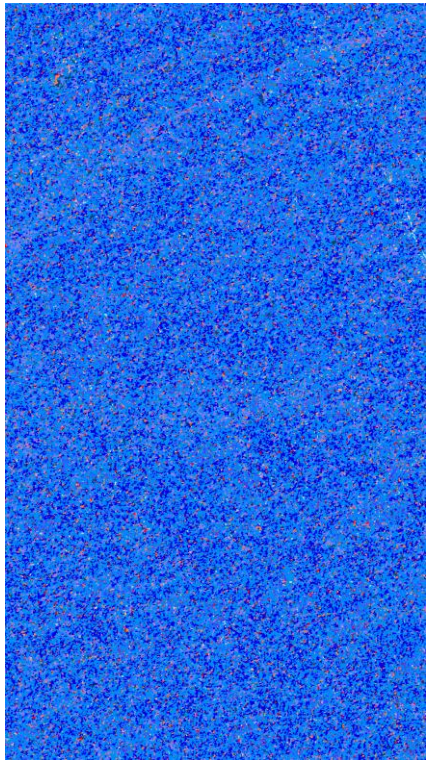
JG-11-075.



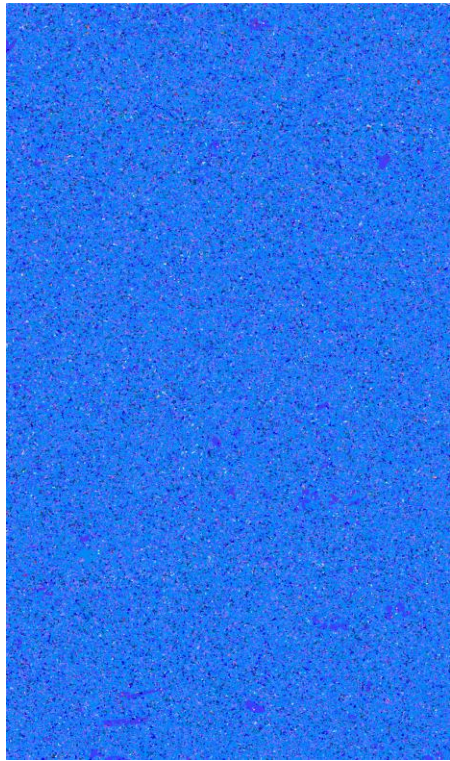
JG-11-100.



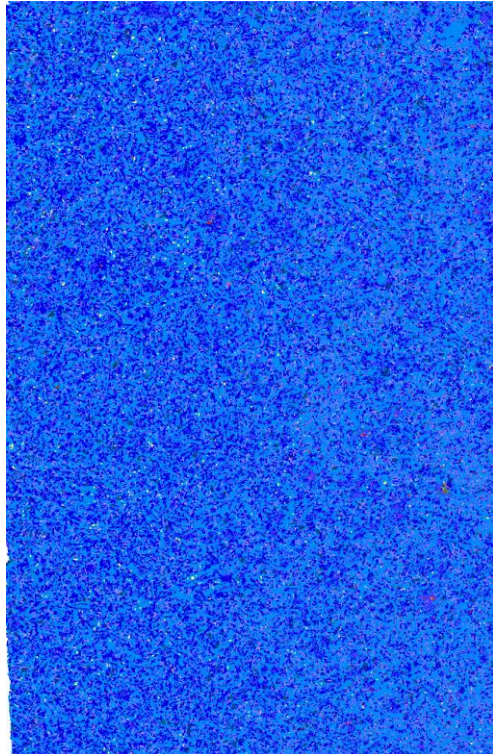
JG-11-101.



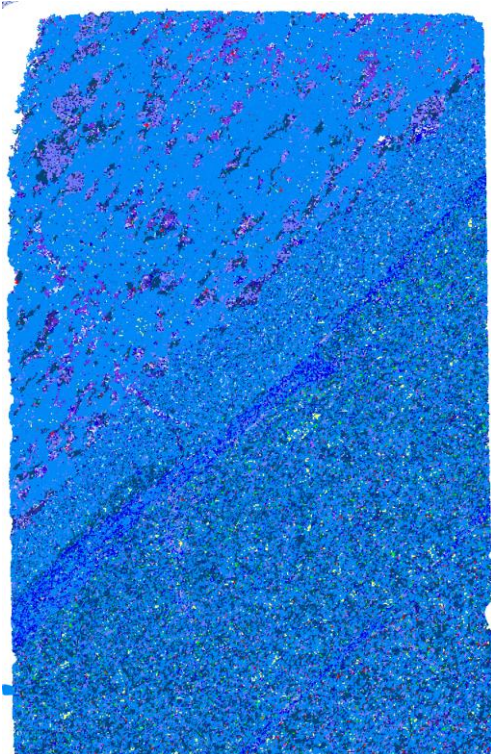
JG-11-102.



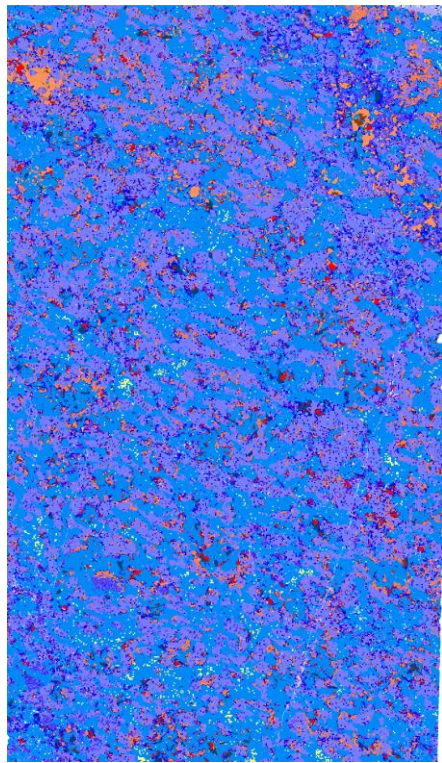
JG-11-104.



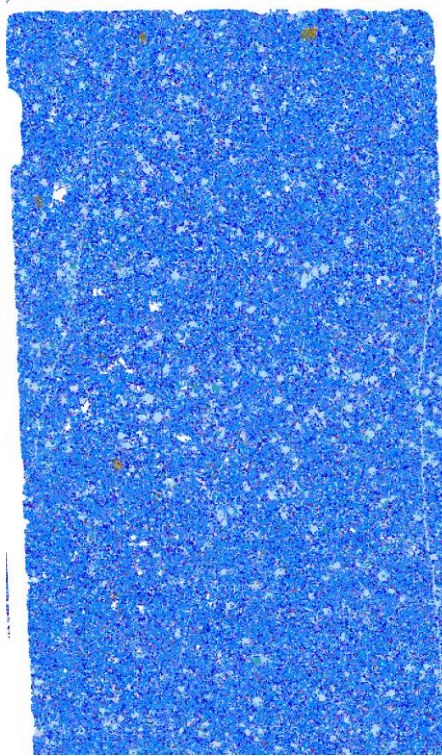
JG-11-105.



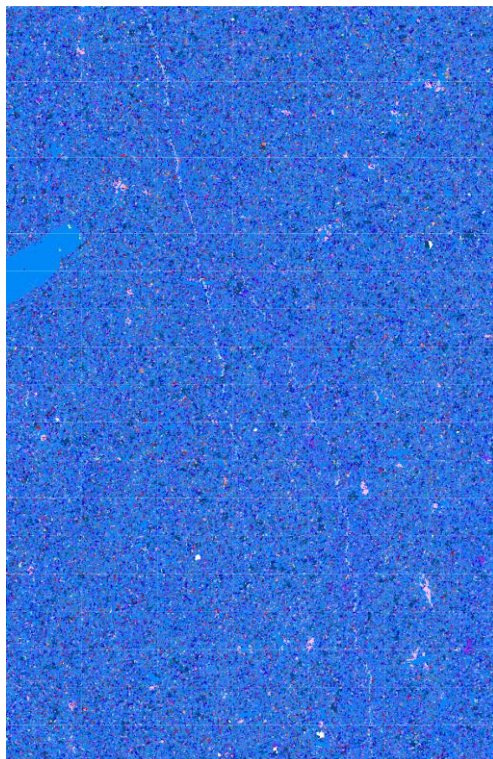
JG-11-106.



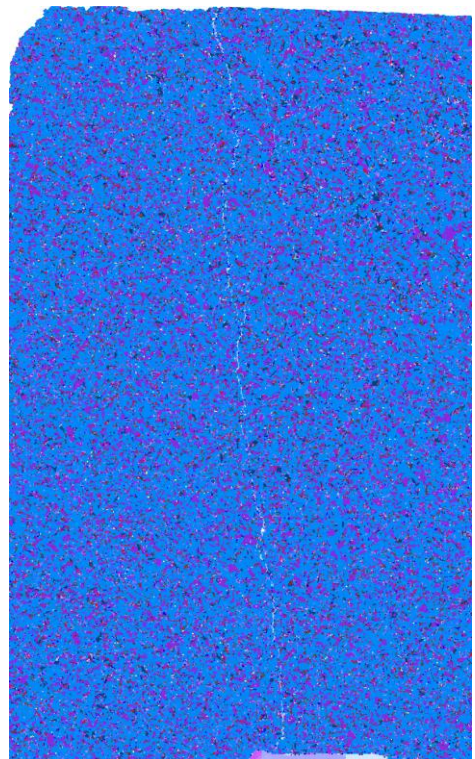
JG-11-114.



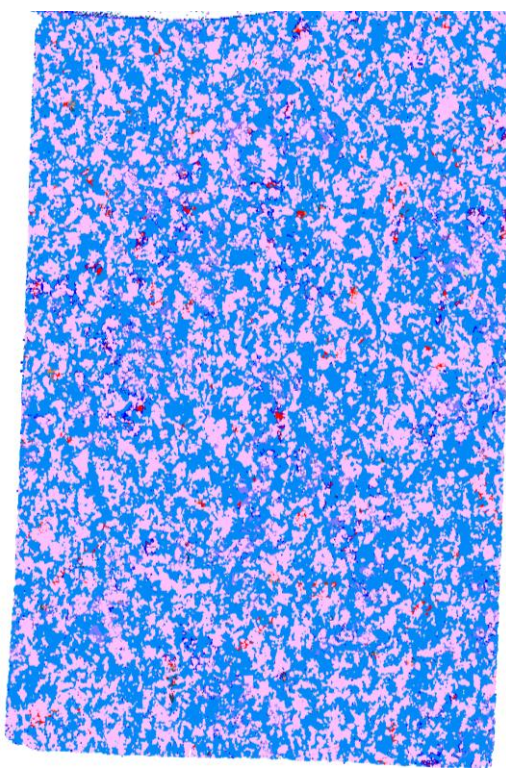
JG-11-125.



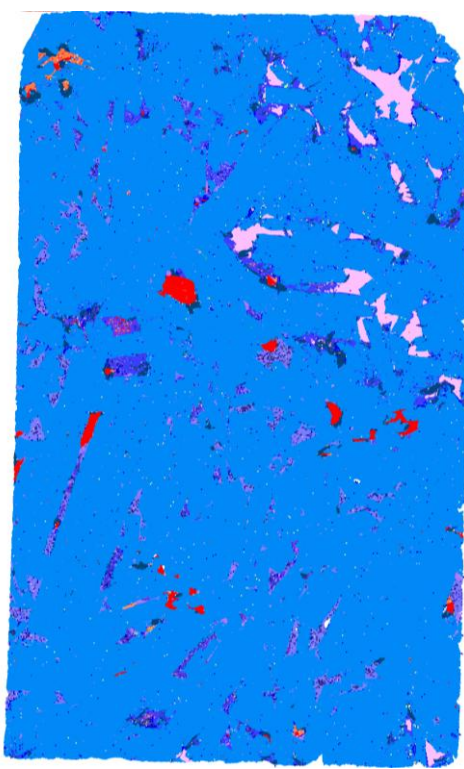
JG-11-127.



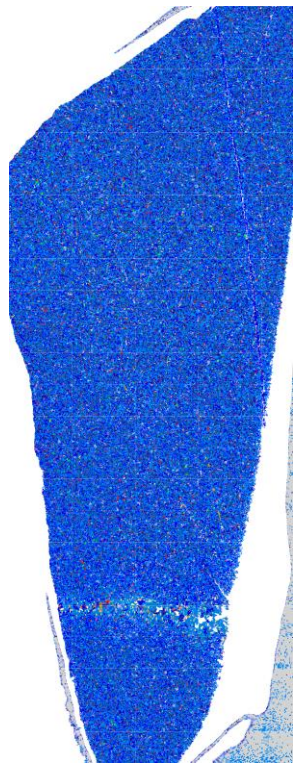
JG-11-130.



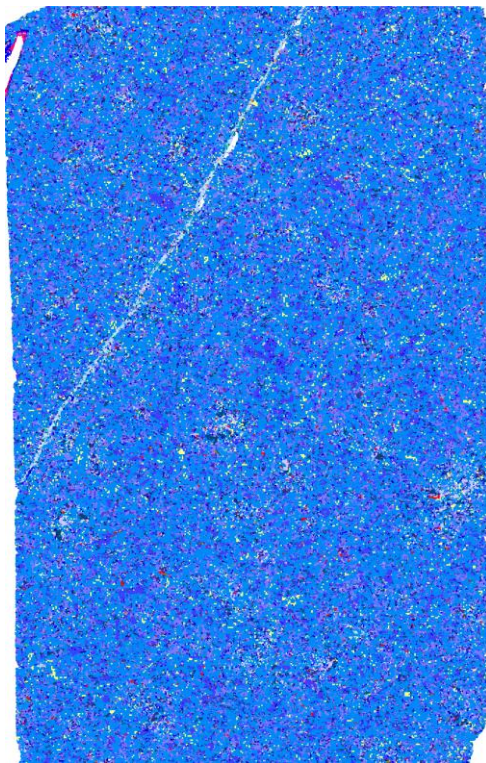
JG-11-134.



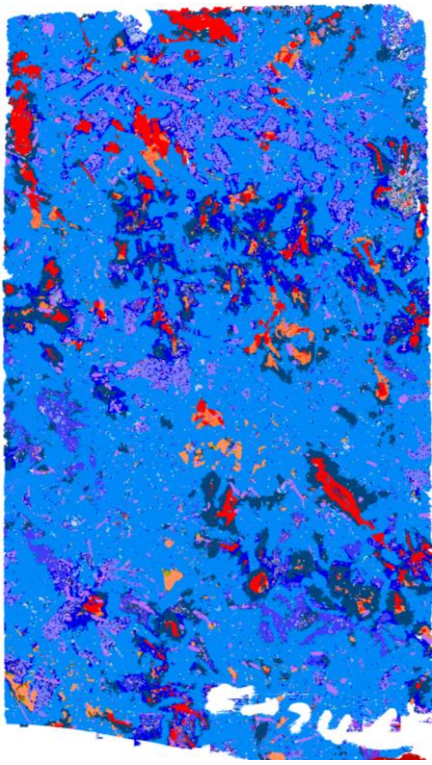
JG-11-137.



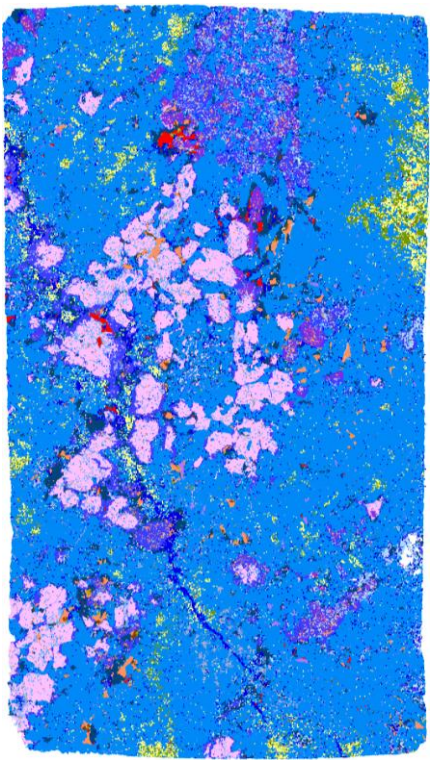
JG-11-150.



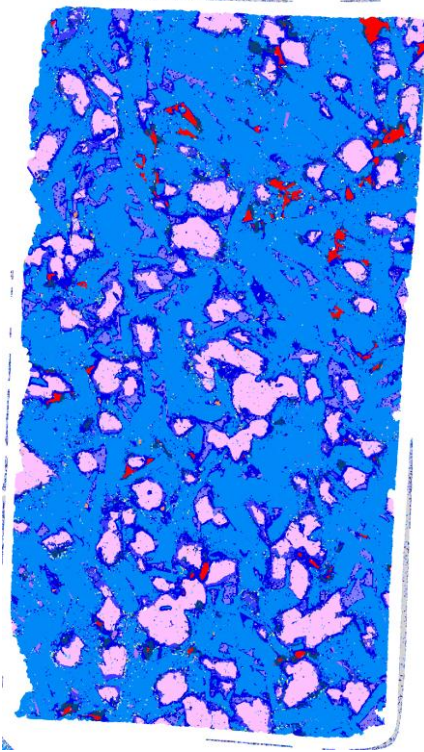
JG-11-153.



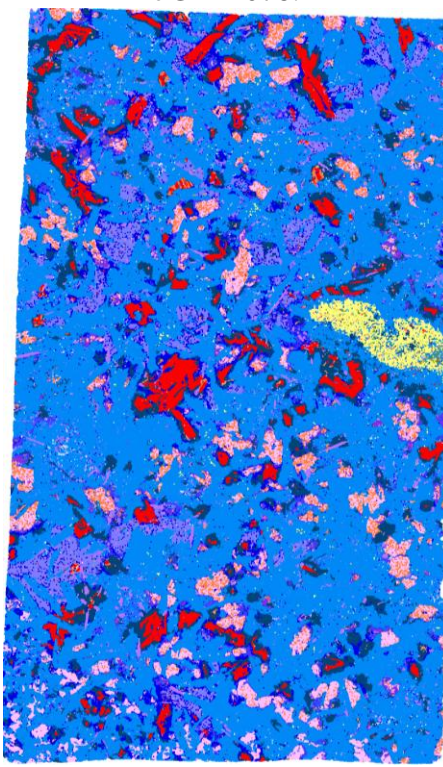
JG-11-076.



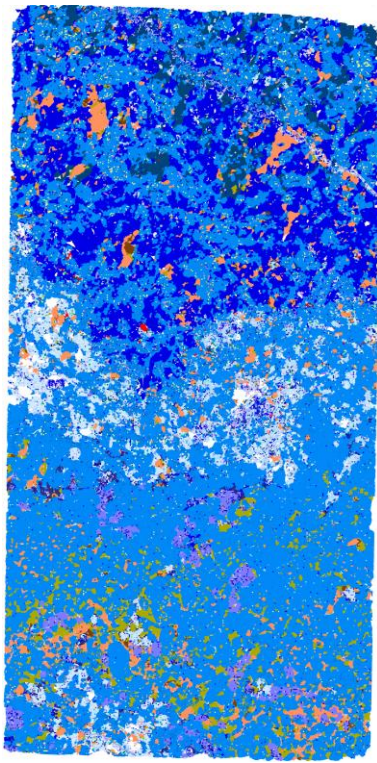
JG-11-078.



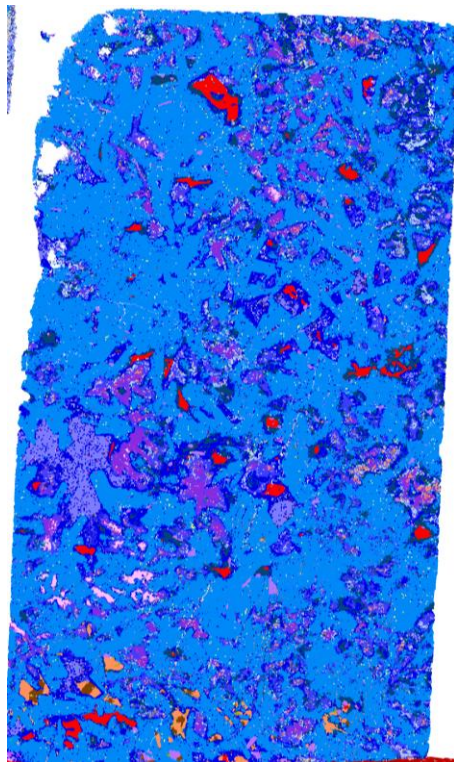
JG-11-080.



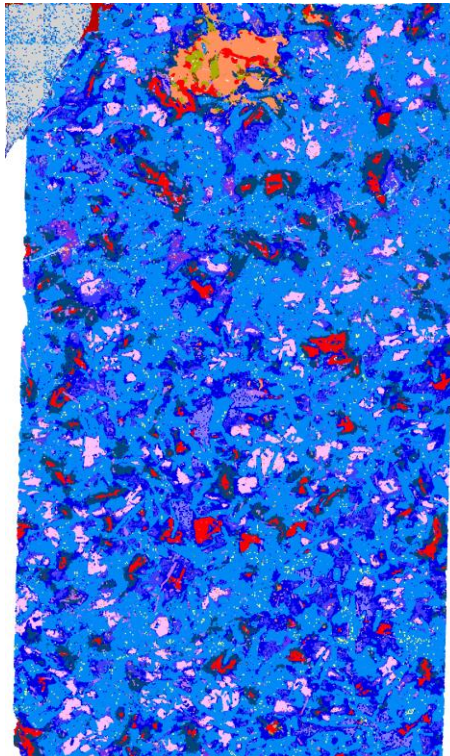
JG-11-084.



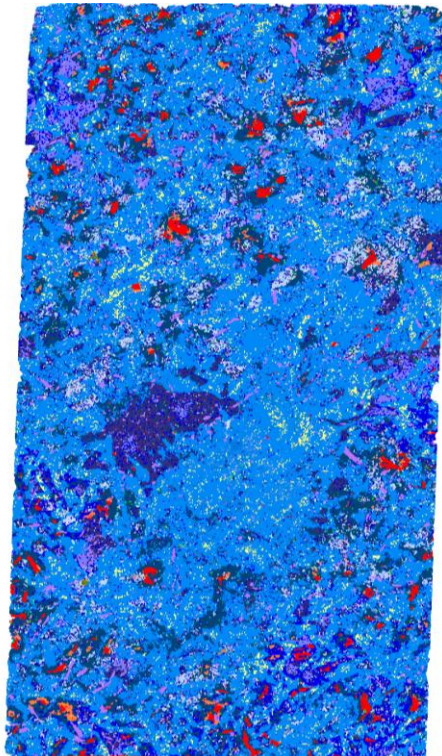
JG-11-086.



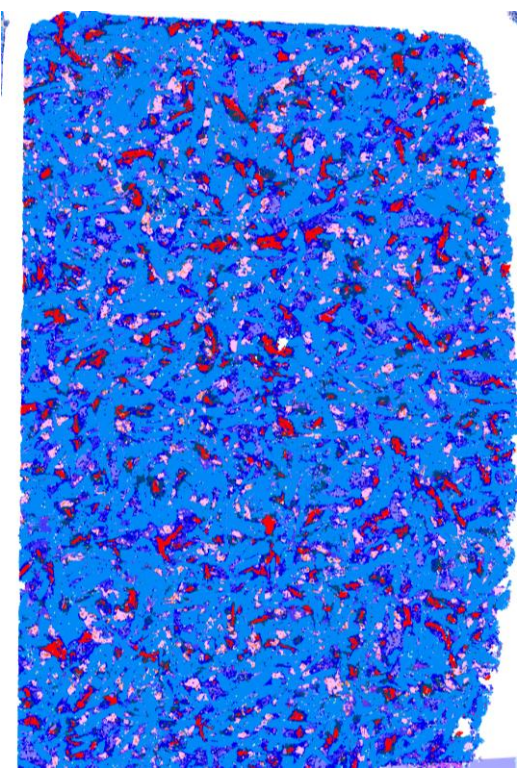
JG-11-088.



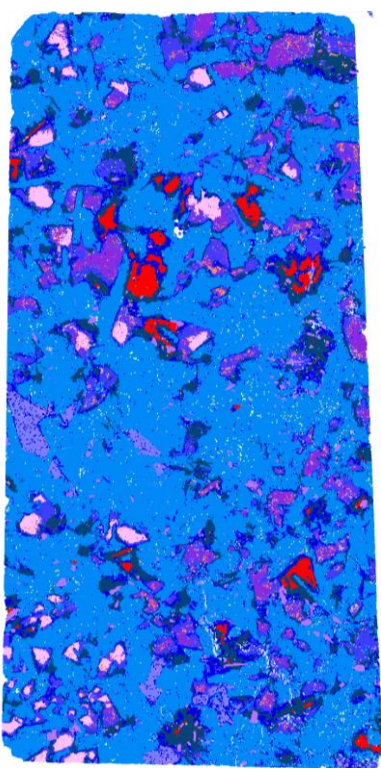
JG-11-089.



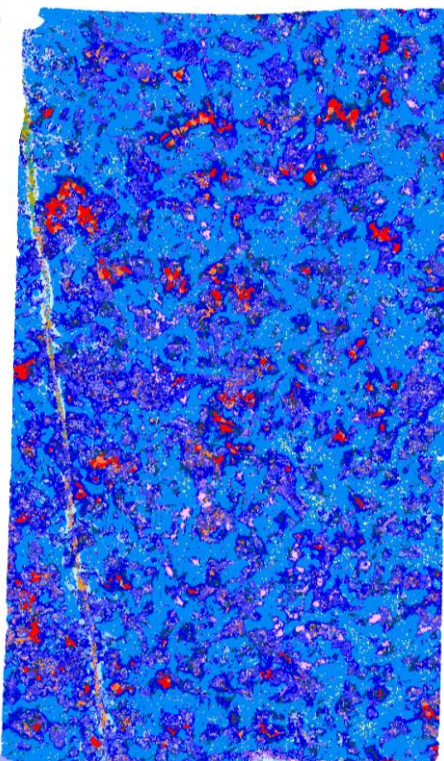
JG-11-090.



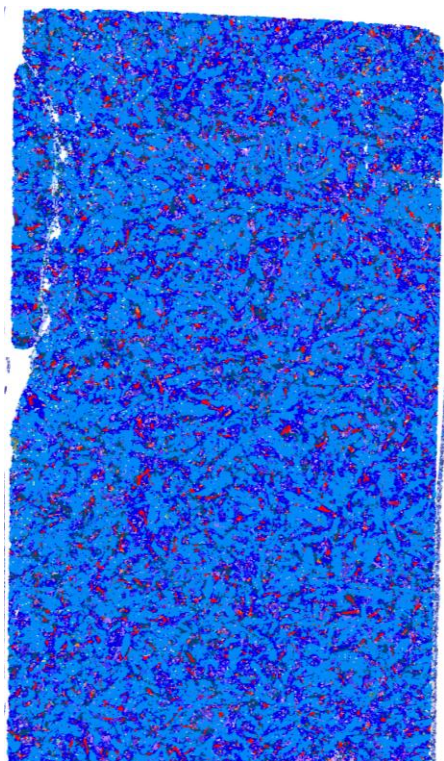
JG-11-091.



JG-11-093.



JG-11-097.



JG-11-124.

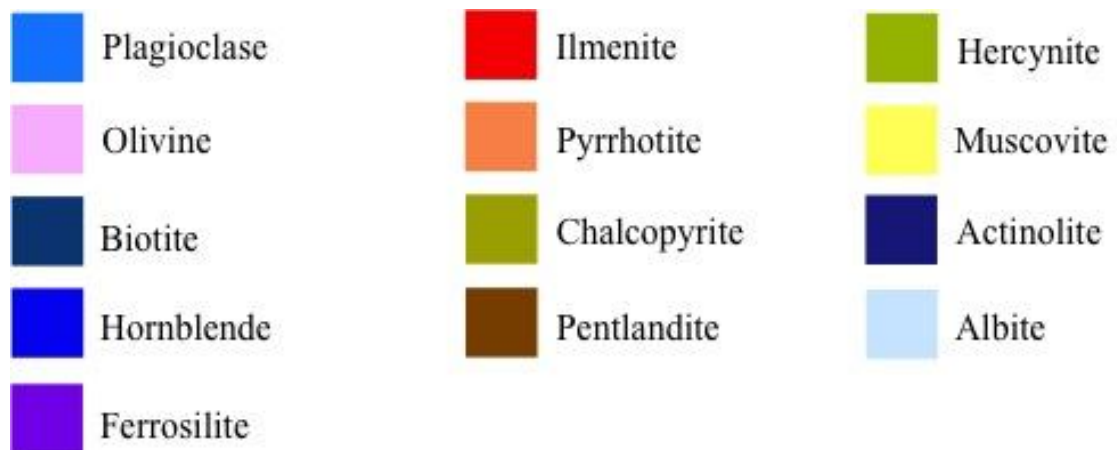
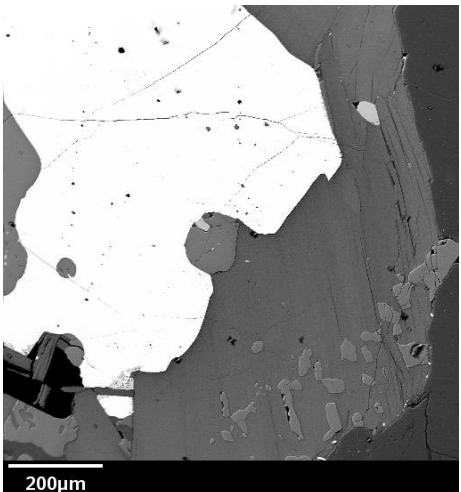


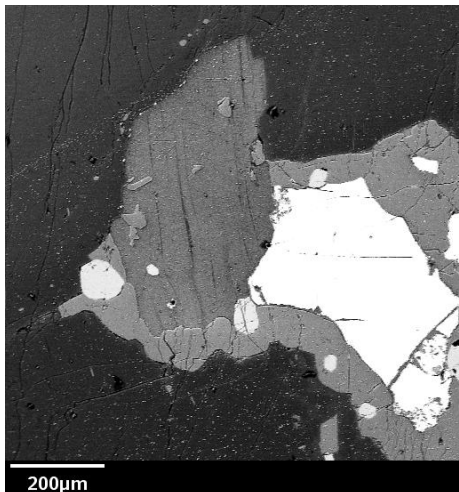
Fig. B-2. Legend for MLA grain boundary maps.

Appendix C

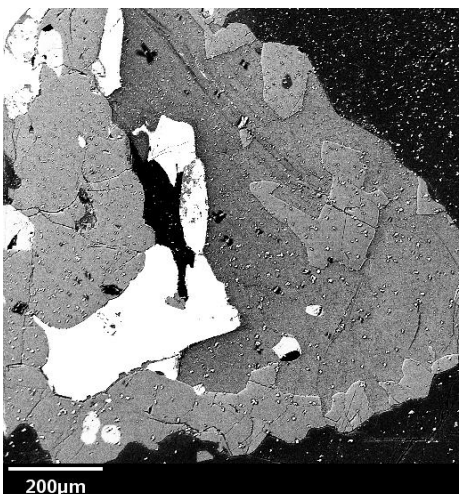
Electron microprobe digital backscatter electron images of individual biotite grains probed.



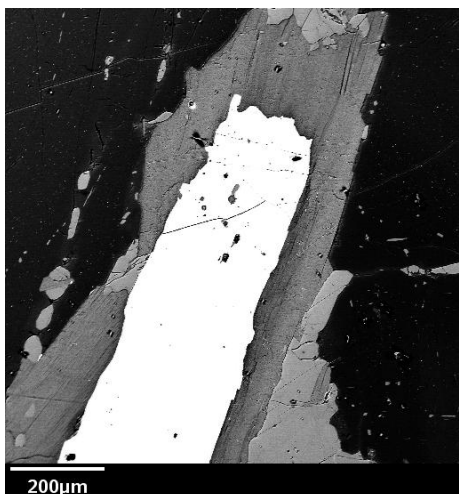
JG-11-001.



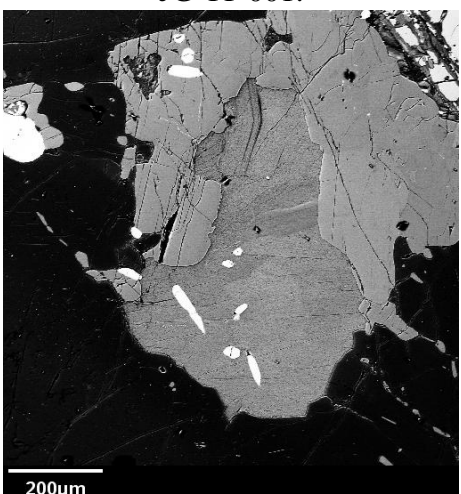
JG-11-001.



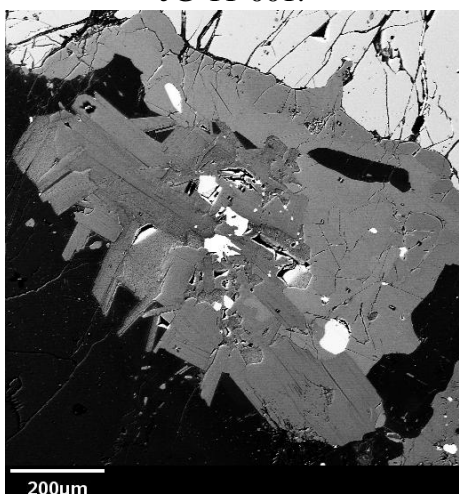
JG-11-001.



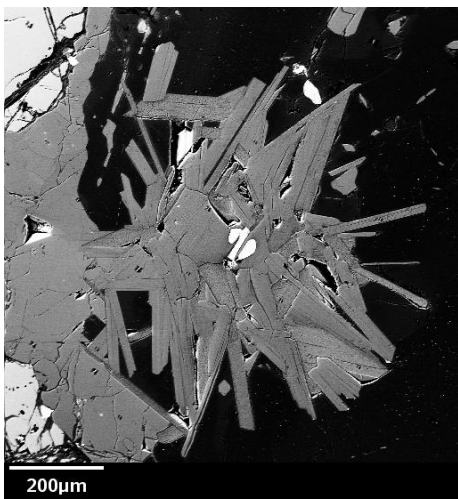
JG-11-001.



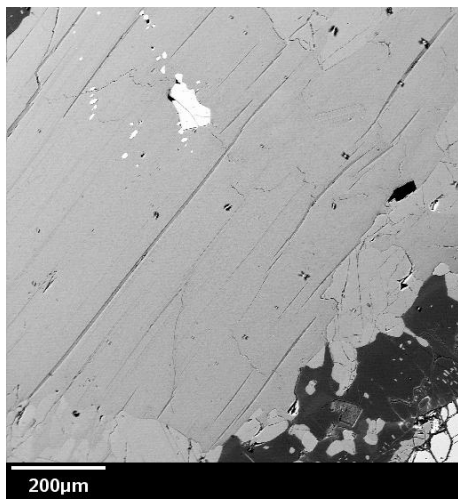
JG-11-001.



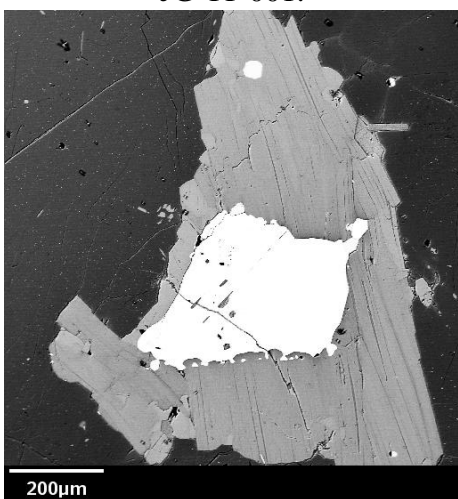
JG-11-001.



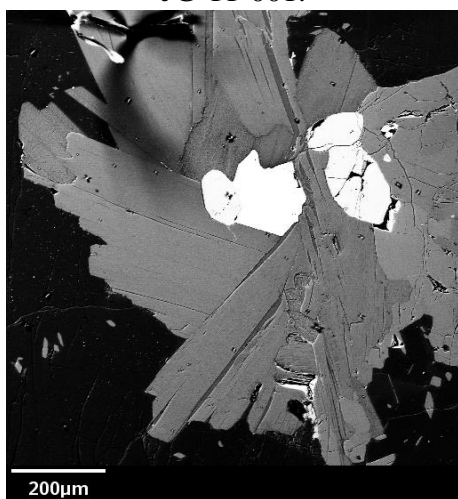
JG-11-001.



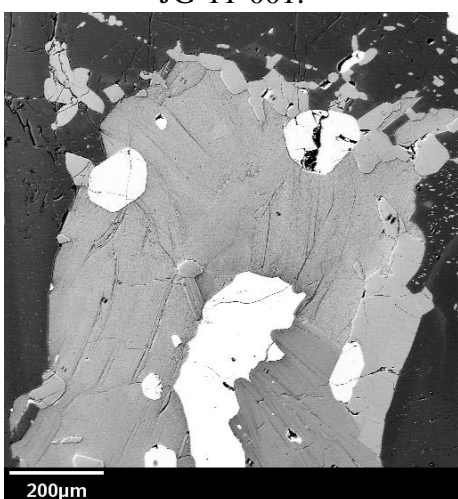
JG-11-001.



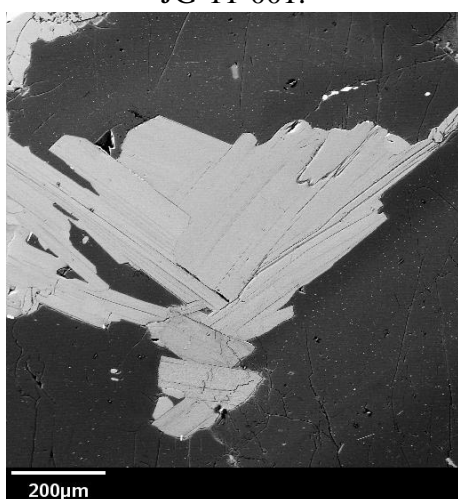
JG-11-001.



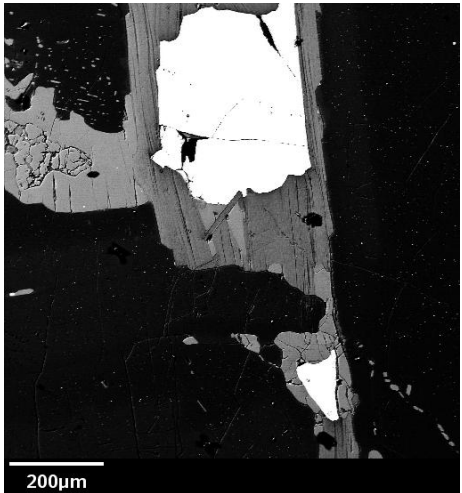
JG-11-001.



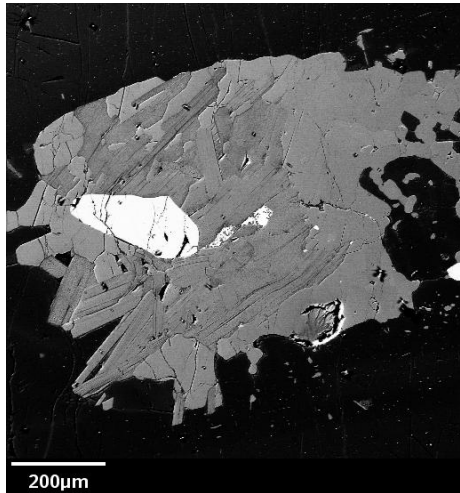
JG-11-001.



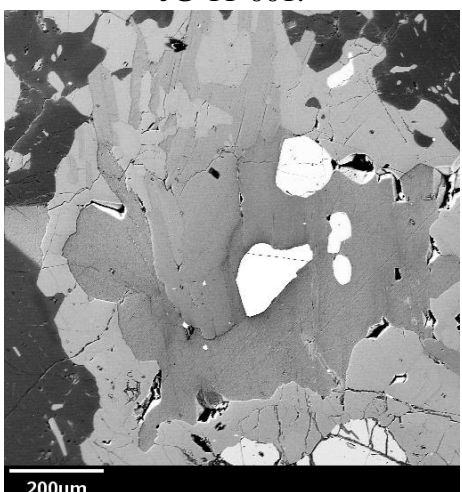
JG-11-001.



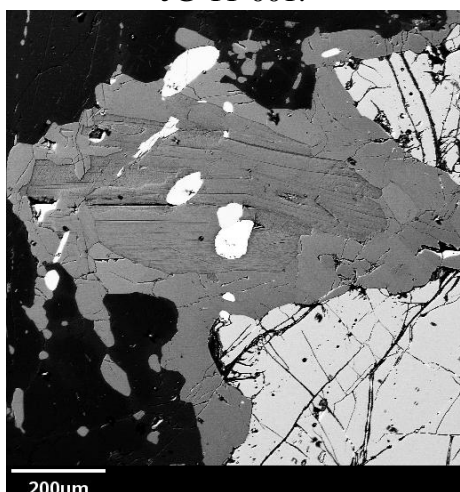
JG-11-001.



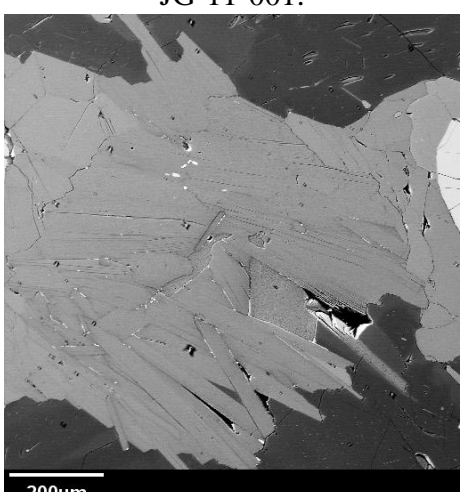
JG-11-001.



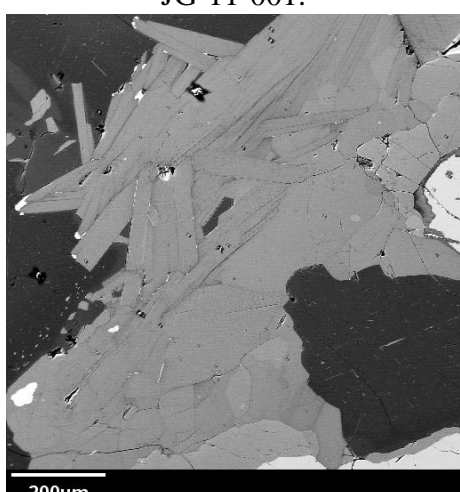
JG-11-001.



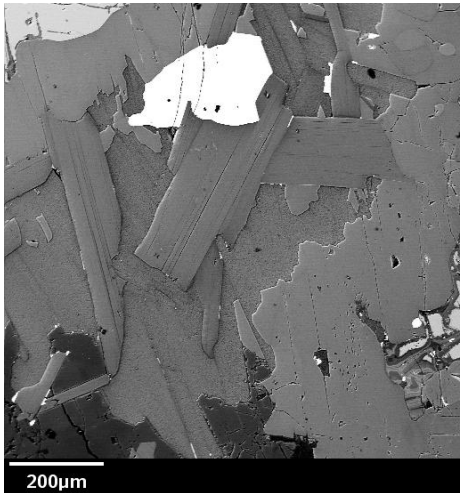
JG-11-001.



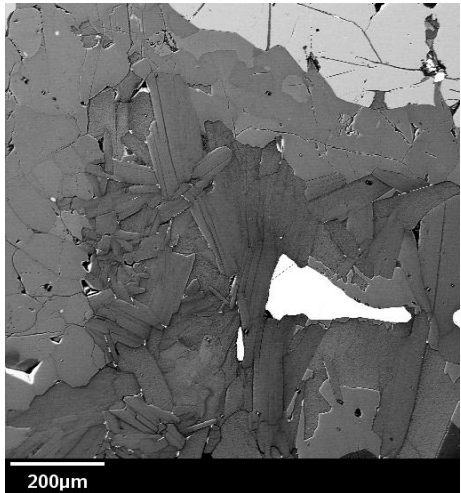
JG-11-003.



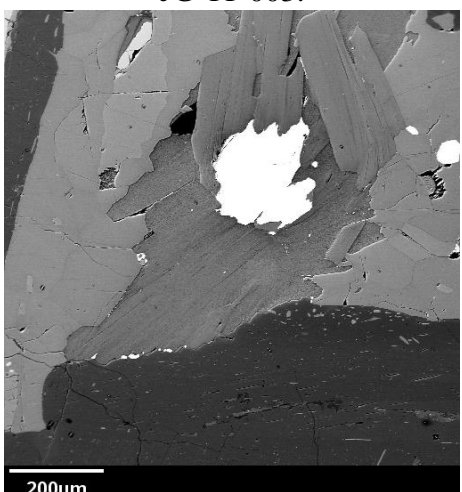
JG-11-003.



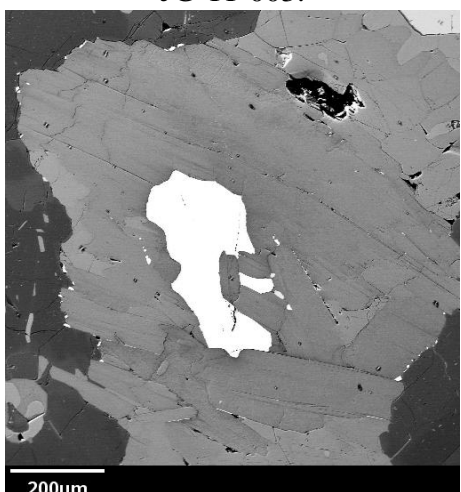
JG-11-003.



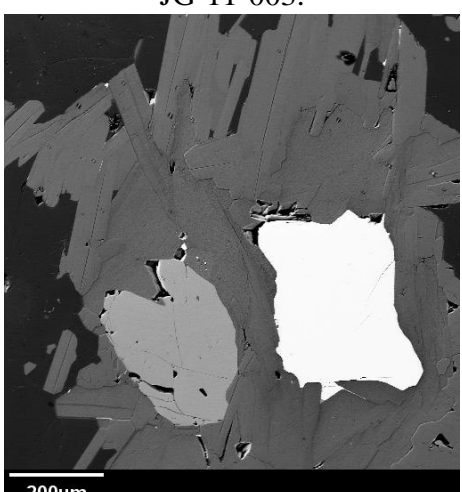
JG-11-003.



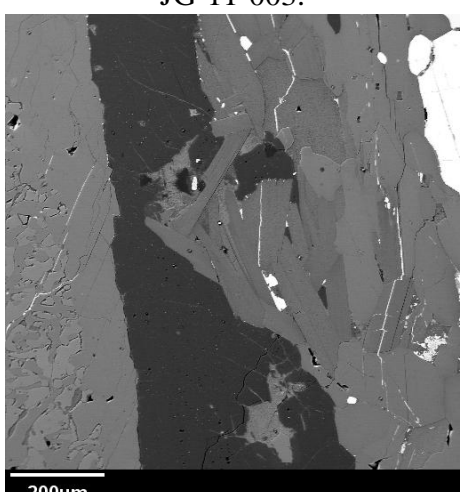
JG-11-003.



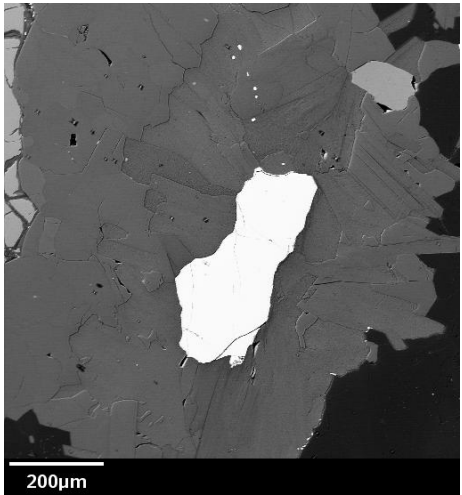
JG-11-003.



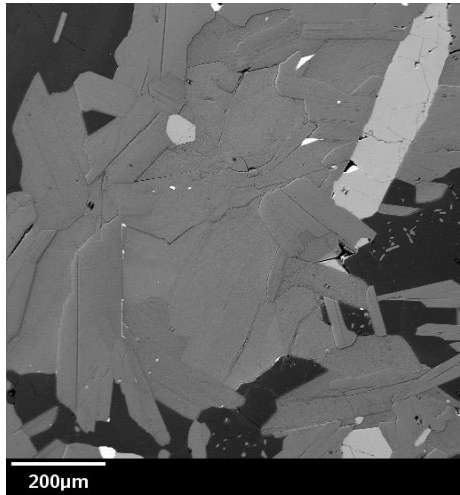
JG-11-006.



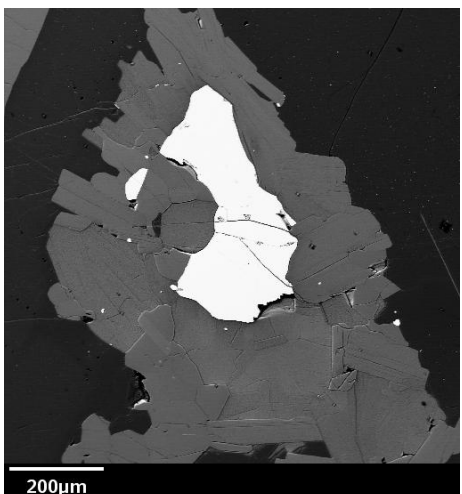
JG-11-006.



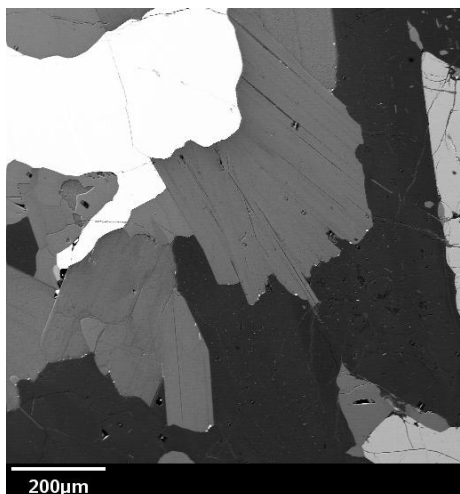
JG-11-006.



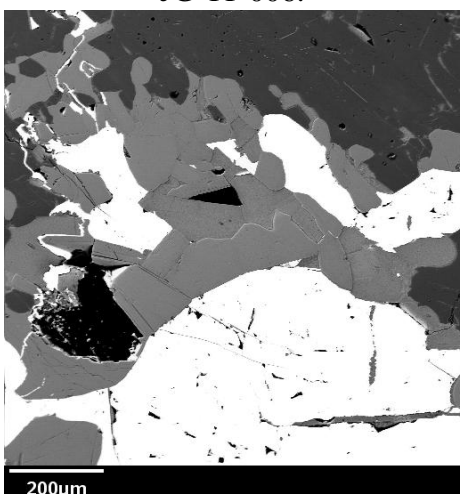
JG-11-006.



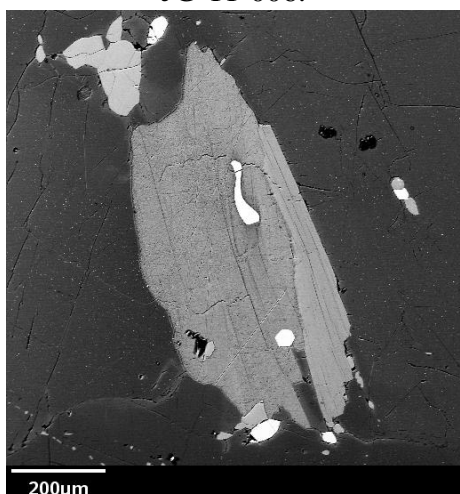
JG-11-006.



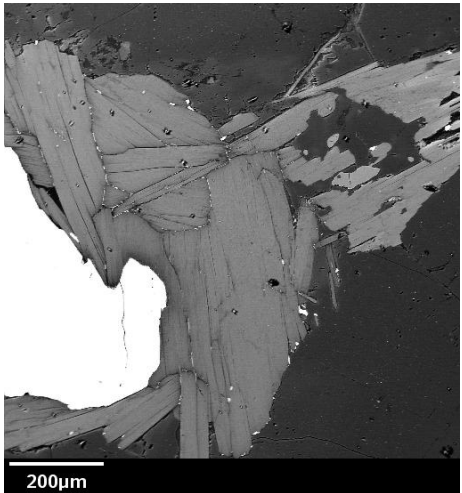
JG-11-006.



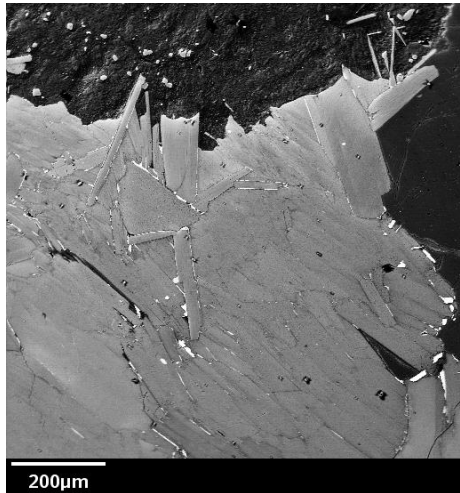
JG-11-006.



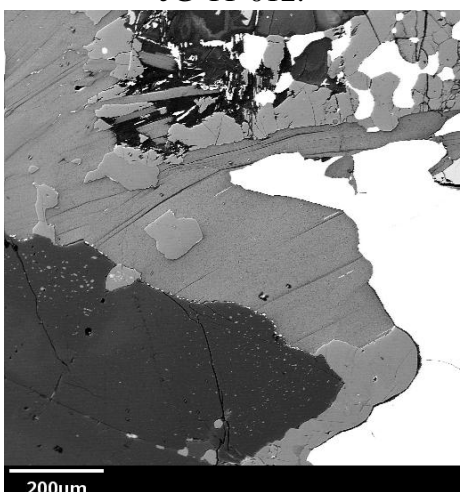
JG-11-011.



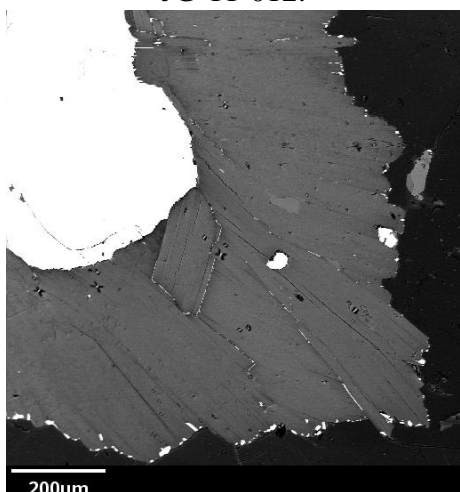
JG-11-012.



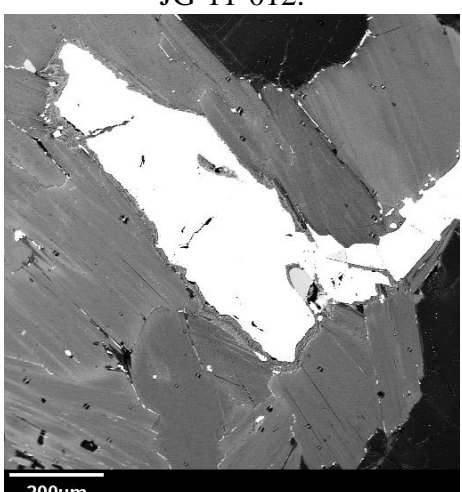
JG-11-012.



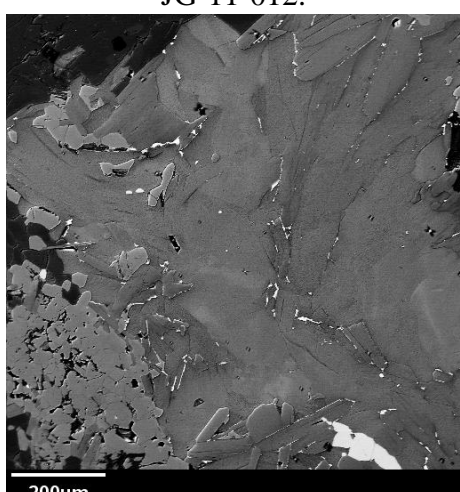
JG-11-012.



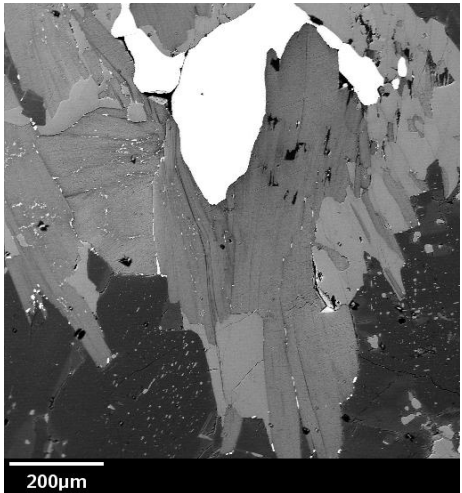
JG-11-012.



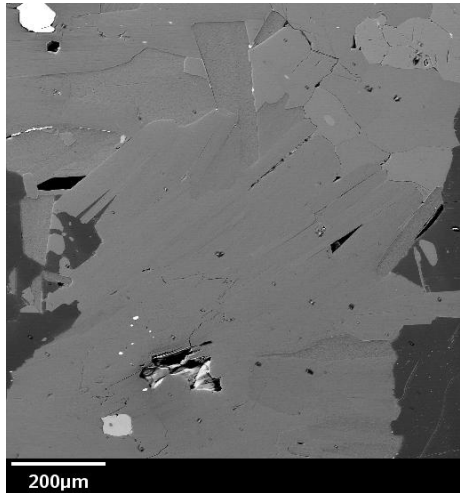
JG-11-012.



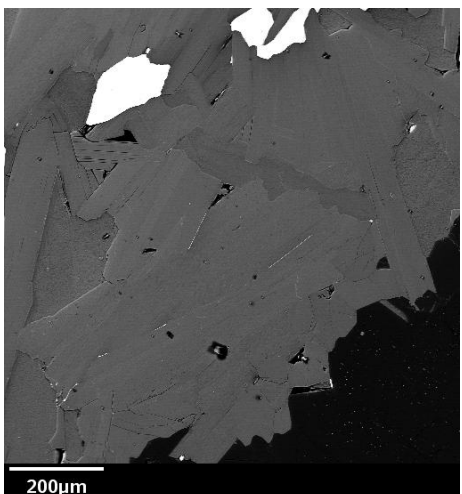
JG-11-012.



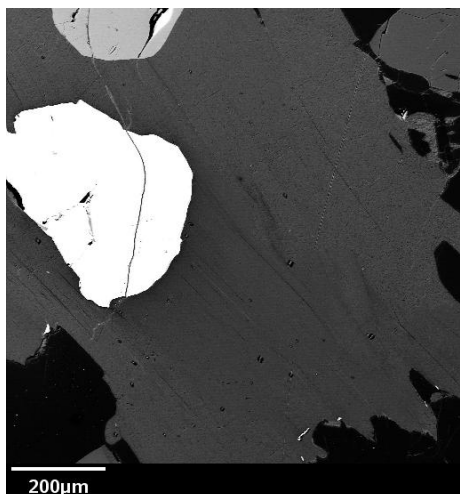
JG-11-012.



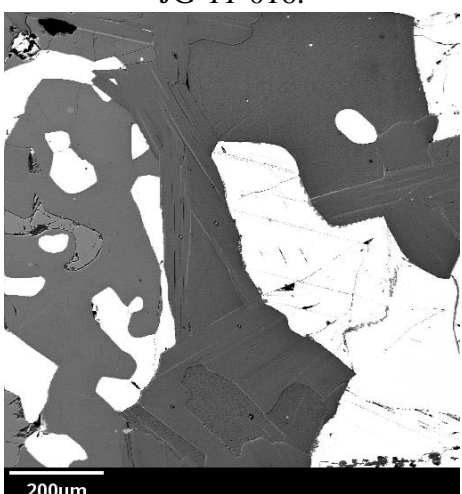
JG-11-016.



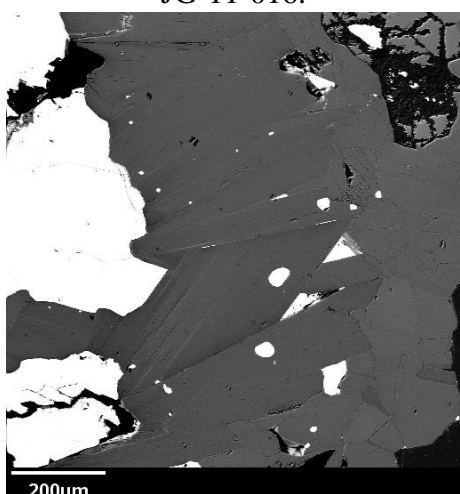
JG-11-016.



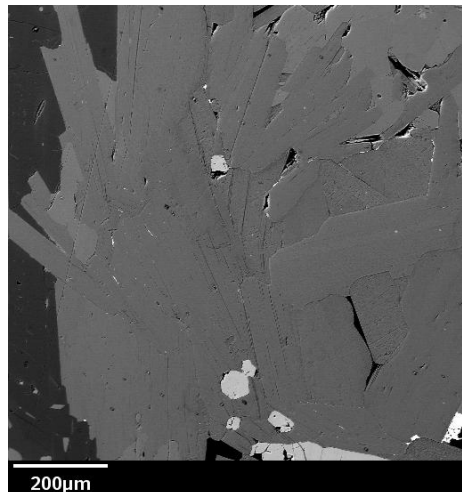
JG-11-016.



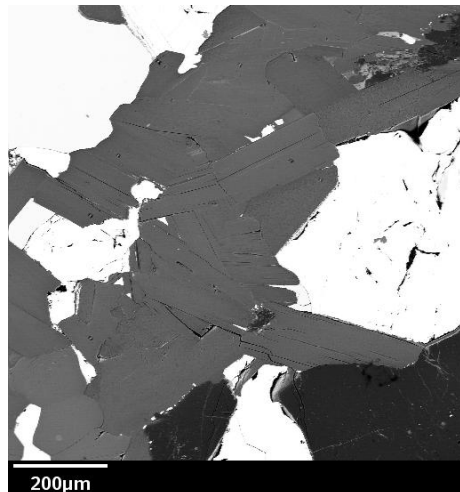
JG-11-016.



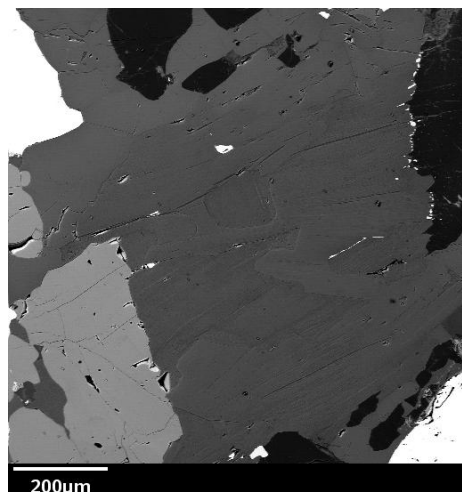
JG-11-016.



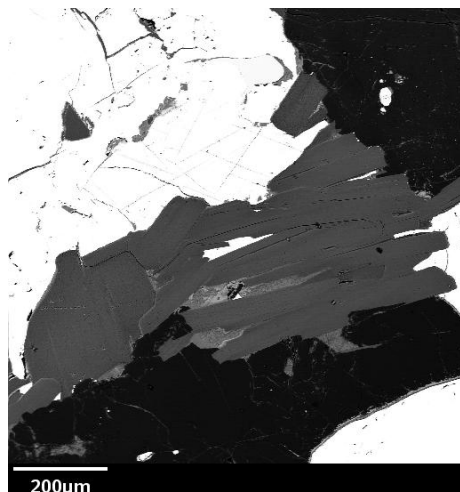
JG-11-016.



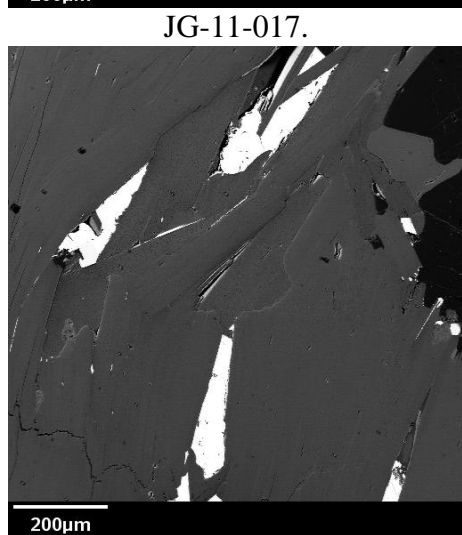
JG-11-017.



JG-11-017.



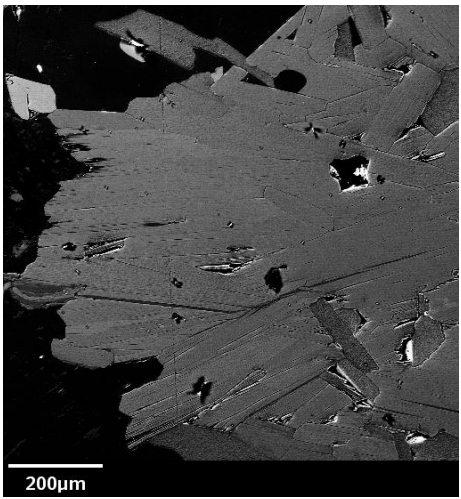
JG-11-017.



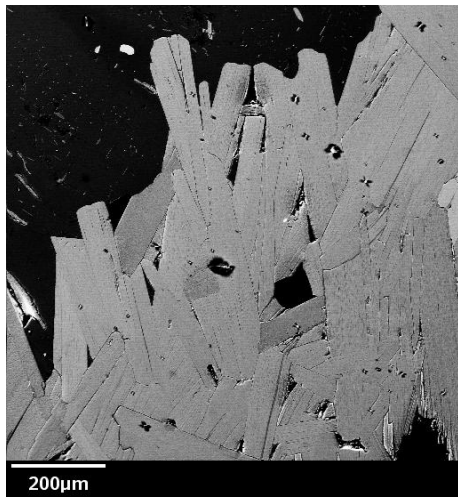
JG-11-017.



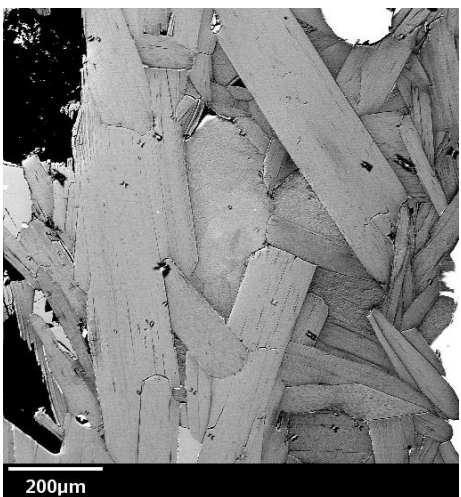
JG-11-017.



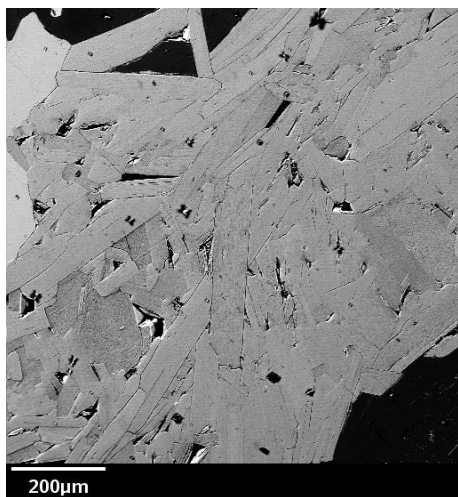
JG-11-021.



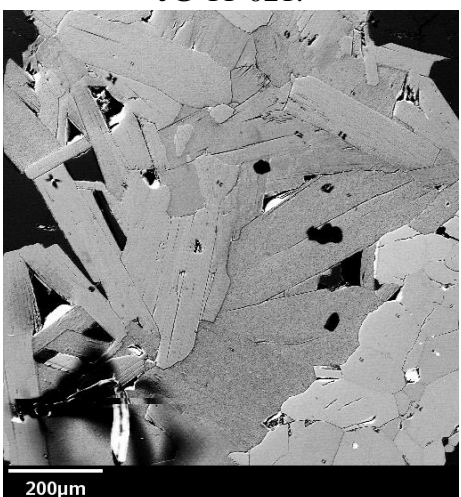
JG-11-021.



JG-11-021.



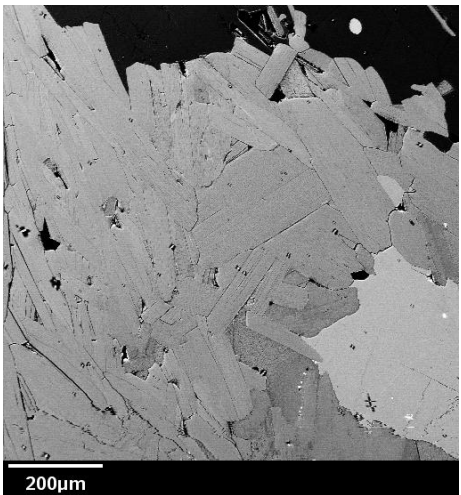
JG-11-021.



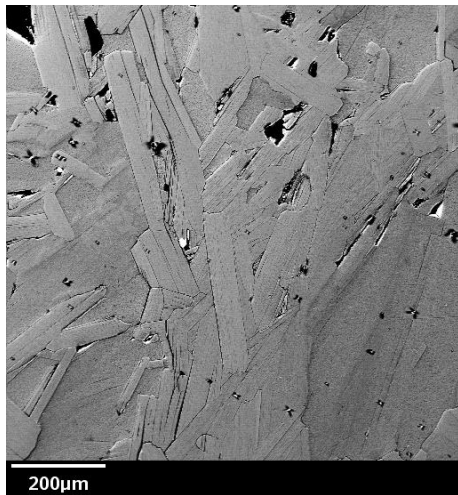
JG-11-021.



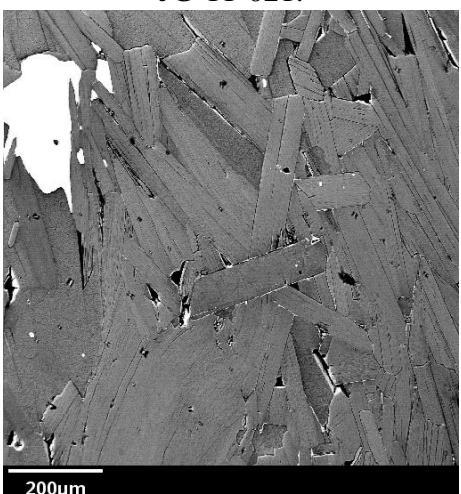
JG-11-021.



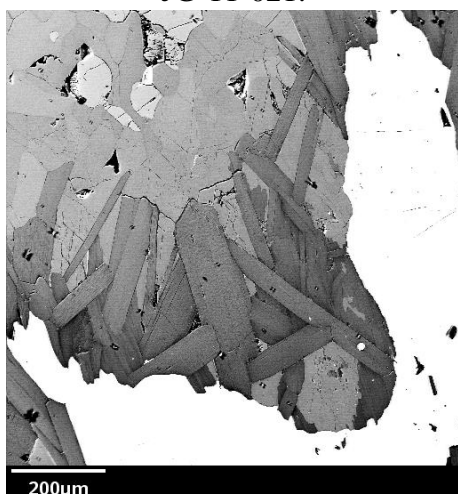
JG-11-021.



JG-11-021.



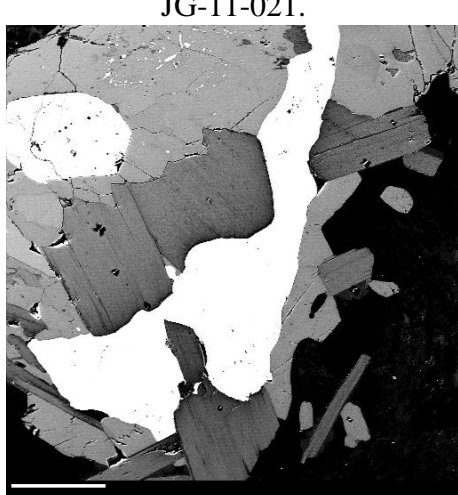
JG-11-021.



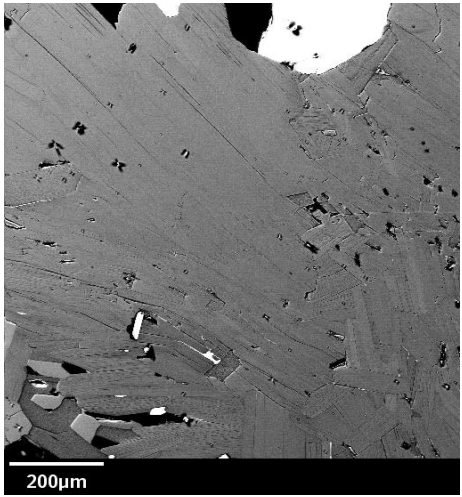
JG-11-021.



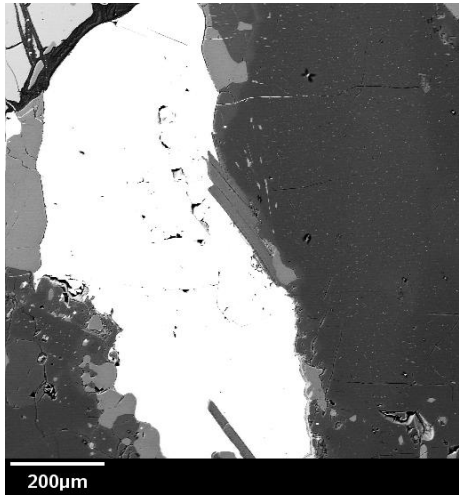
JG-11-021.



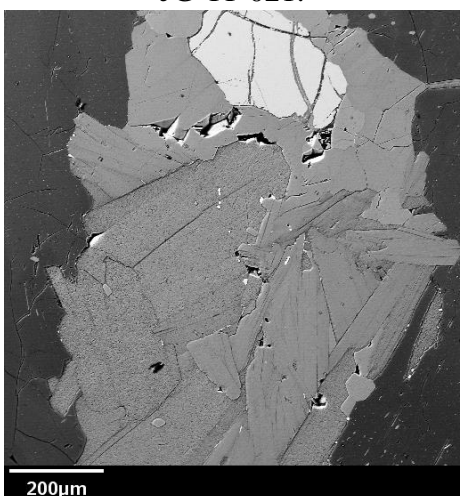
JG-11-021.



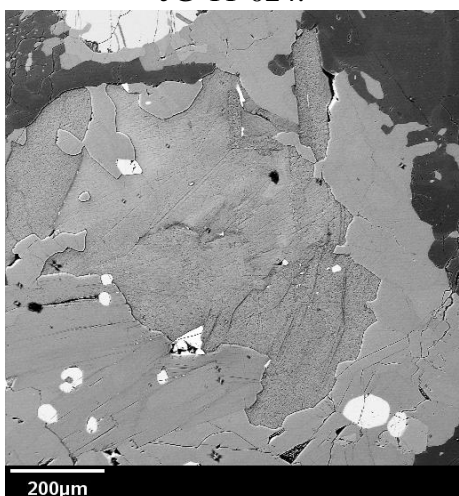
JG-11-021.



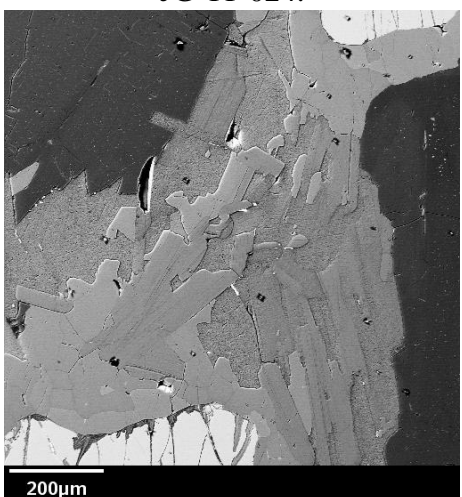
JG-11-024.



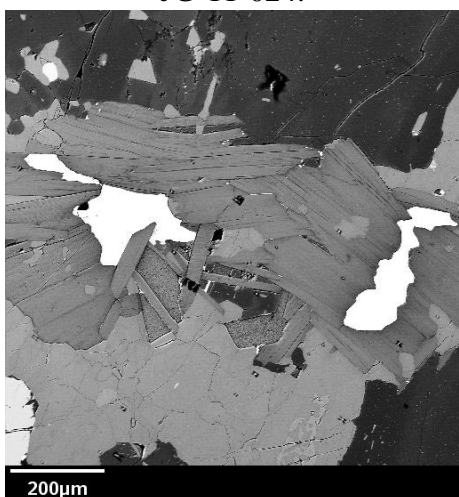
JG-11-024.



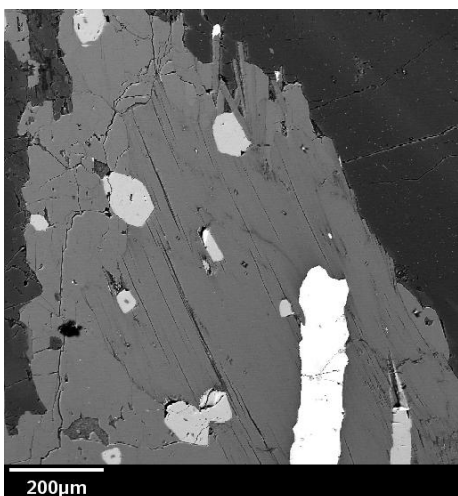
JG-11-024.



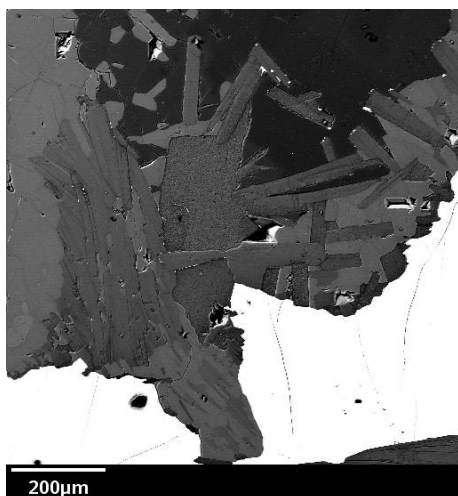
JG-11-024.



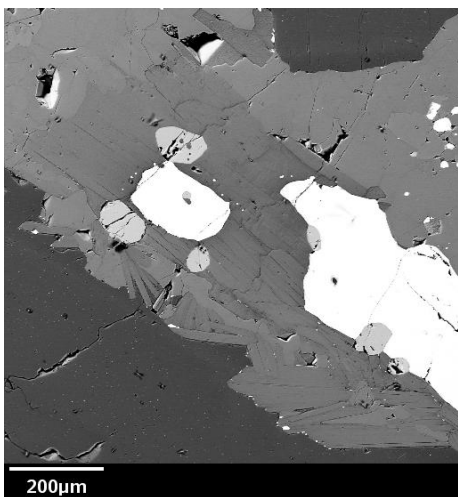
JG-11-024.



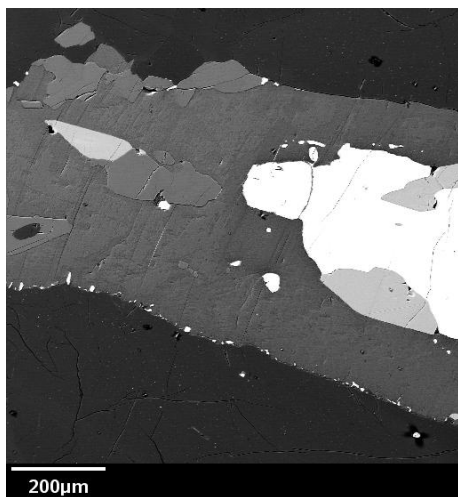
JG-11-024.



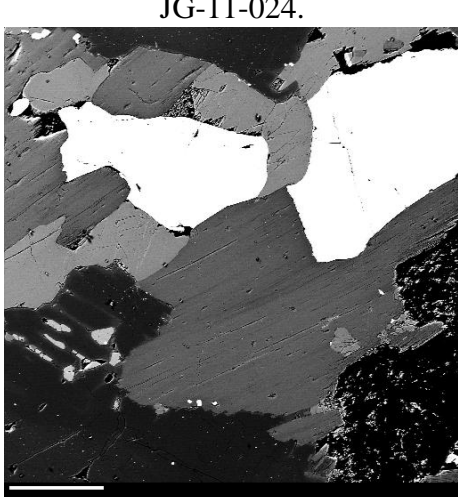
JG-11-024.



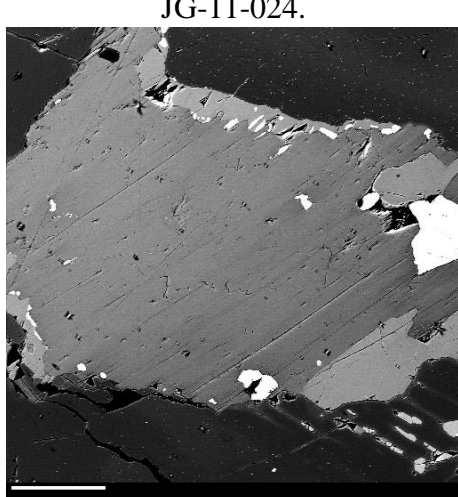
JG-11-024.



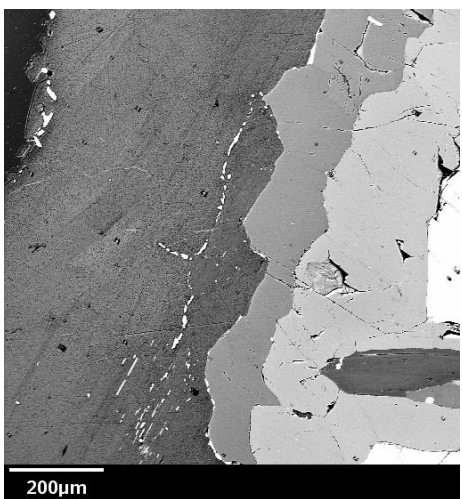
JG-11-024.



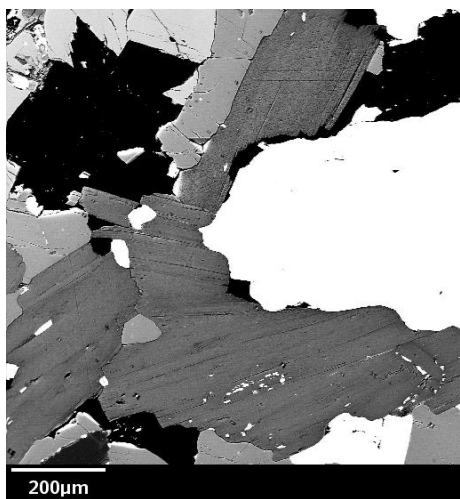
JG-11-032.



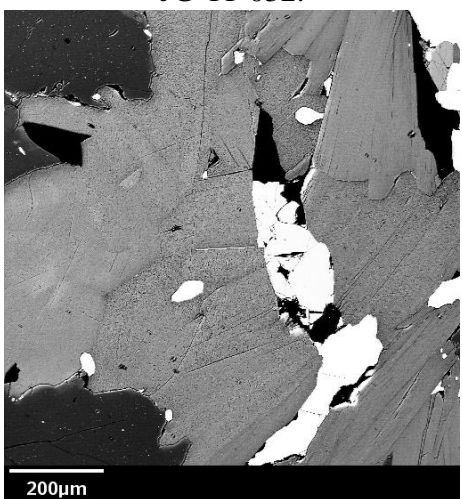
JG-11-032.



JG-11-032.



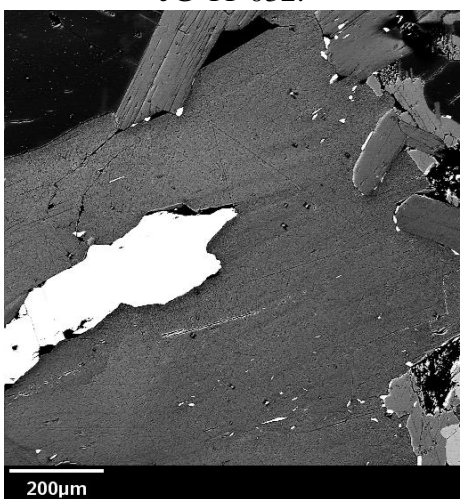
JG-11-032.



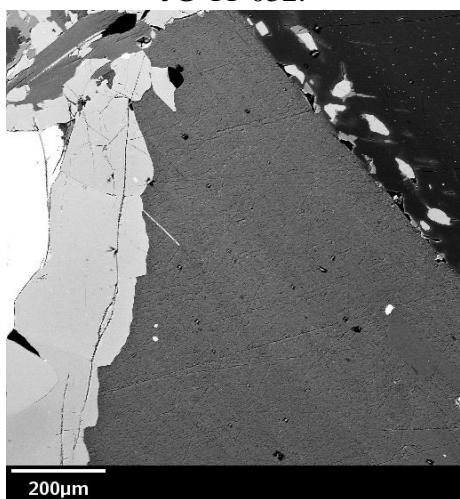
JG-11-032.



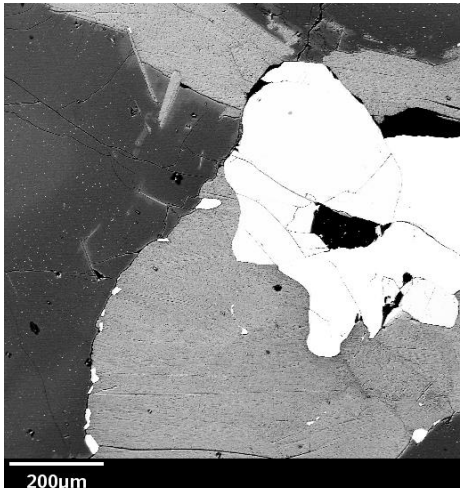
JG-11-032.



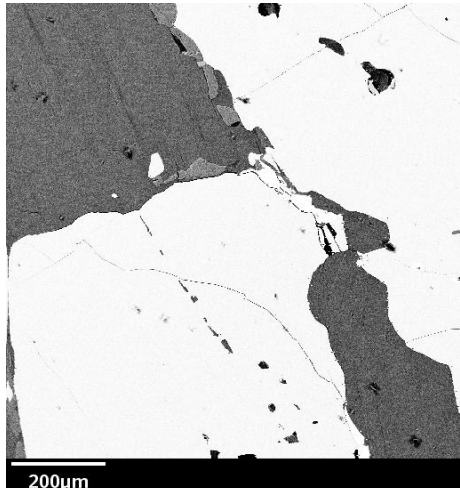
JG-11-032.



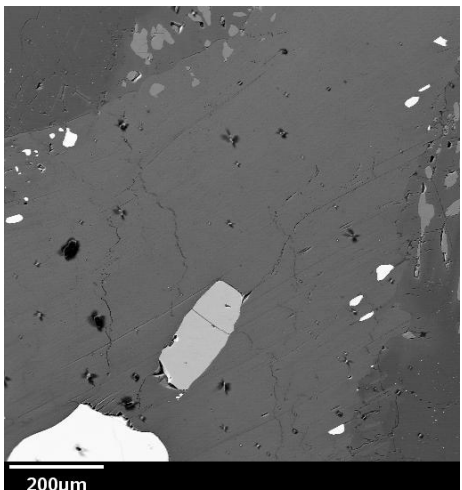
JG-11-032.



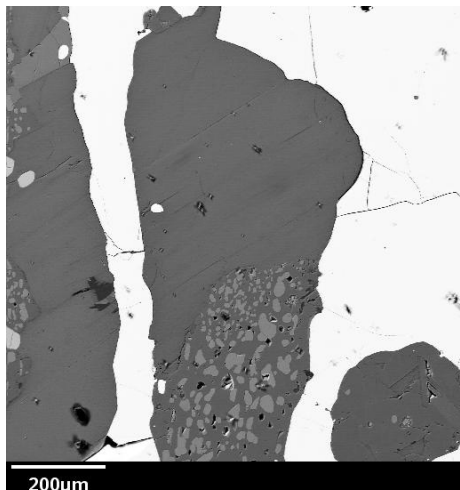
JG-11-032.



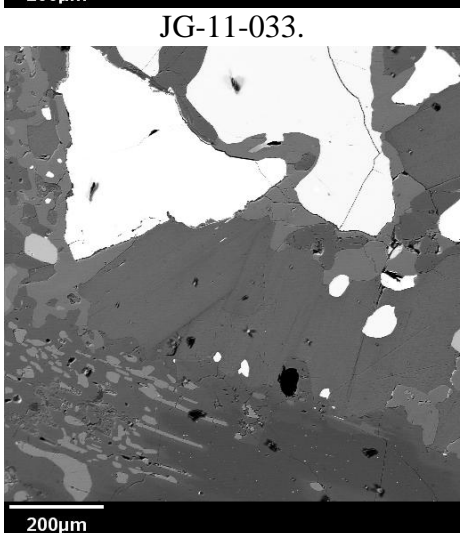
JG-11-033.



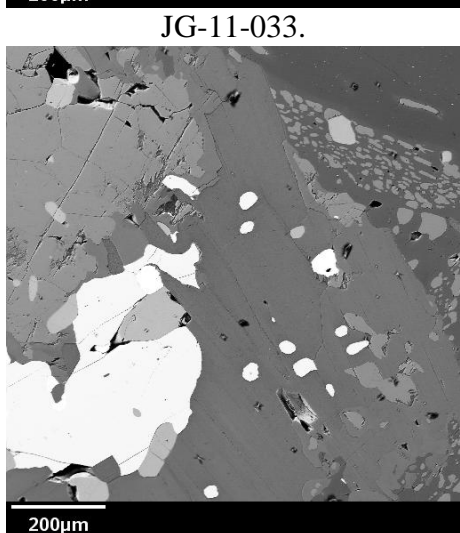
JG-11-033.



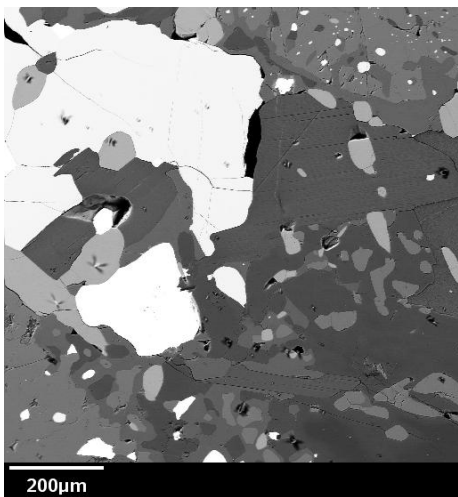
JG-11-033.



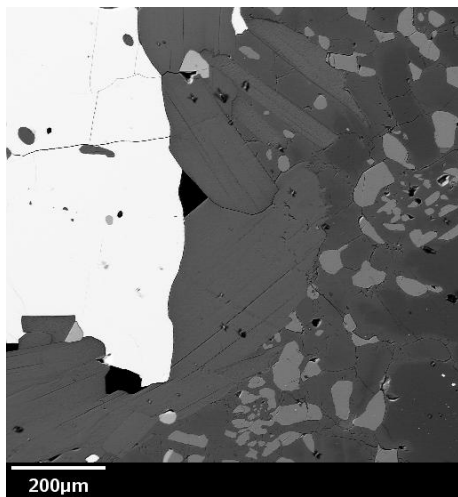
JG-11-033.



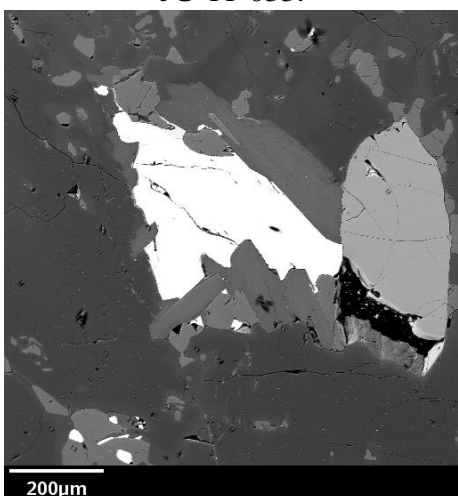
JG-11-033.



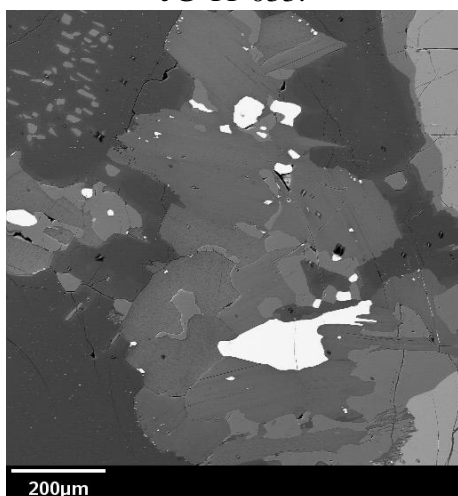
JG-11-033.



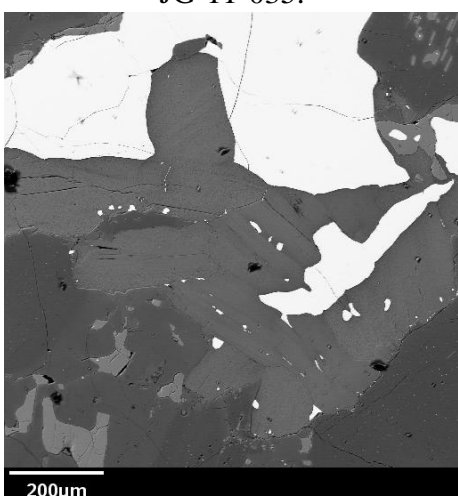
JG-11-033.



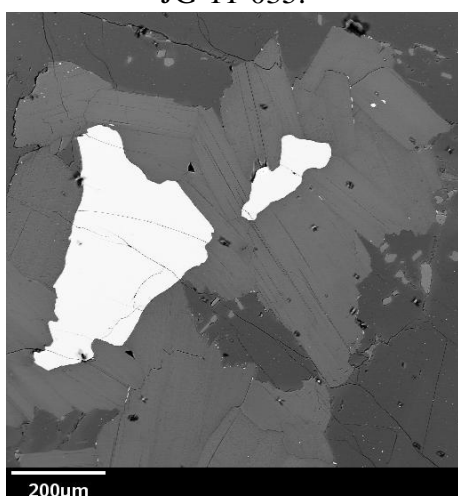
JG-11-035.



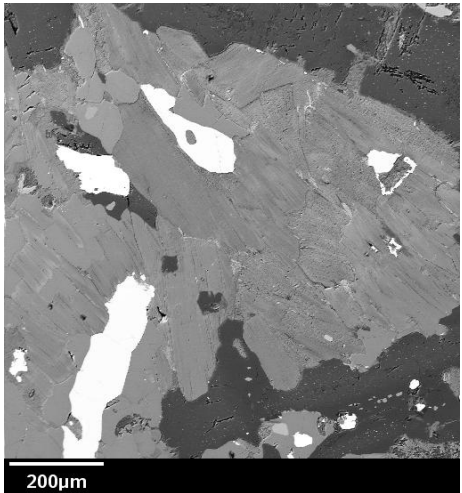
JG-11-035.



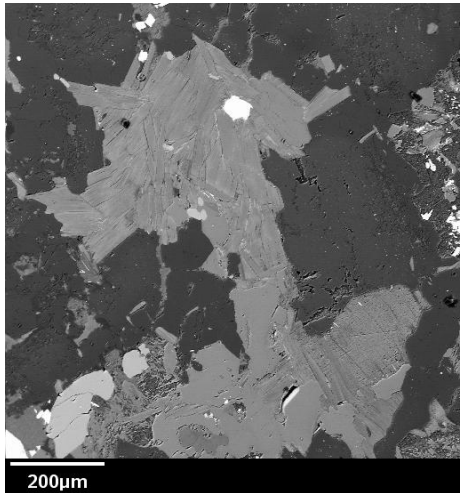
JG-11-035.



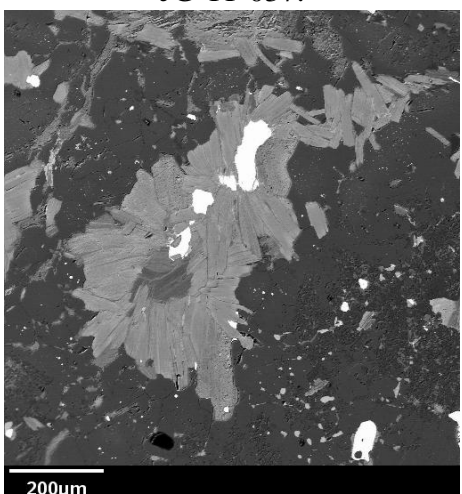
JG-11-035.



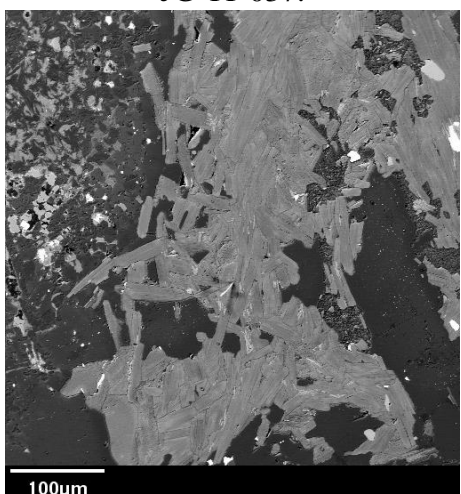
JG-11-037.



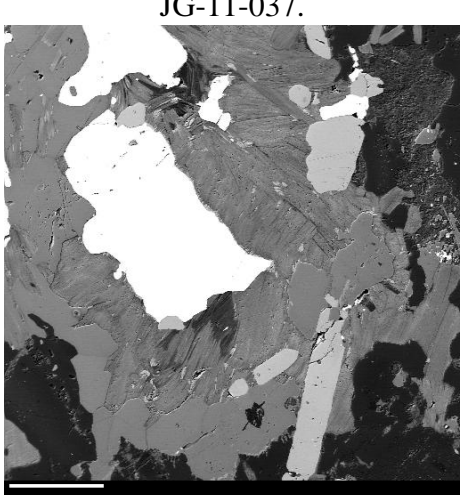
JG-11-037.



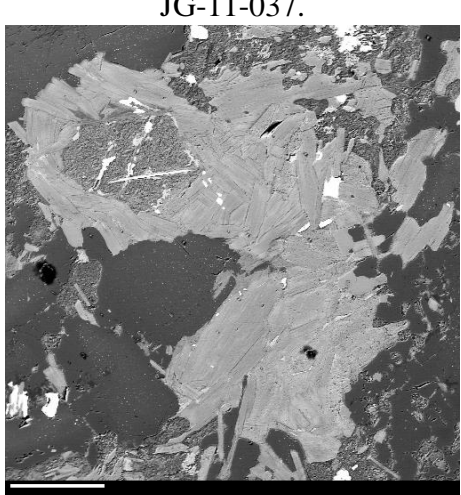
JG-11-037.



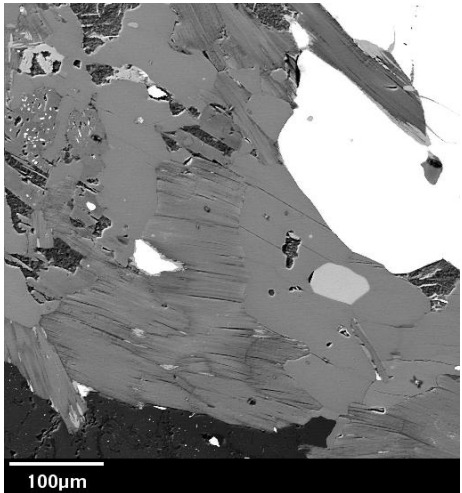
JG-11-037.



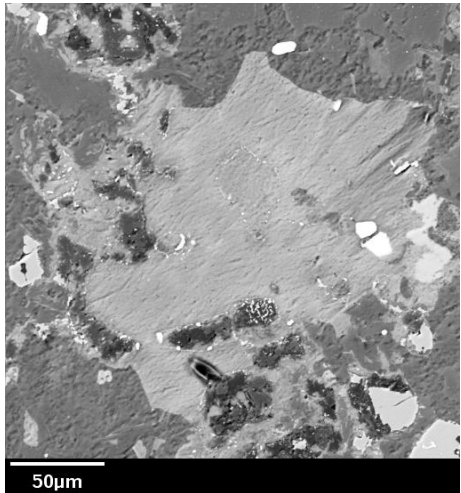
JG-11-037.



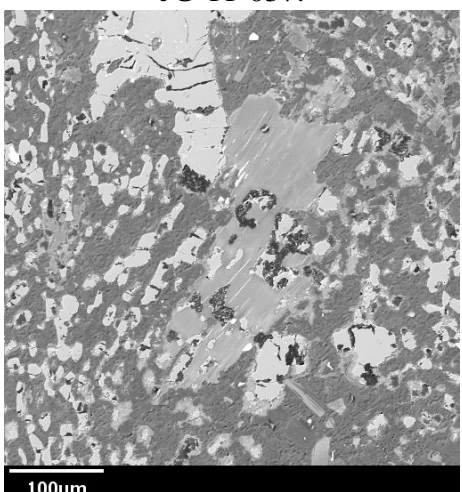
JG-11-037.



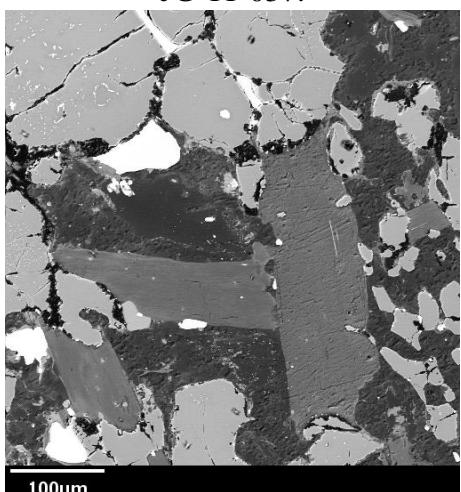
JG-11-037.



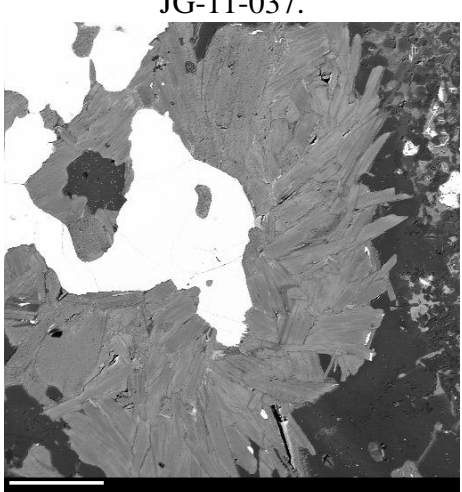
JG-11-037.



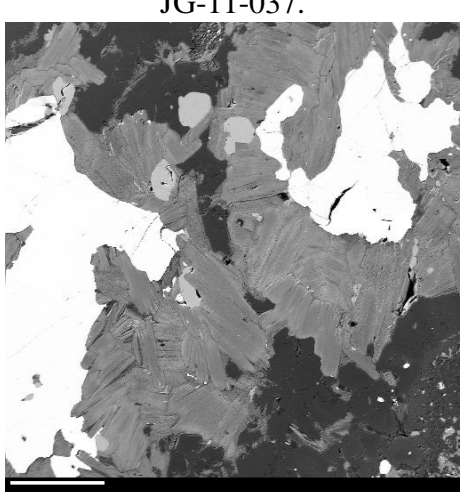
JG-11-037.



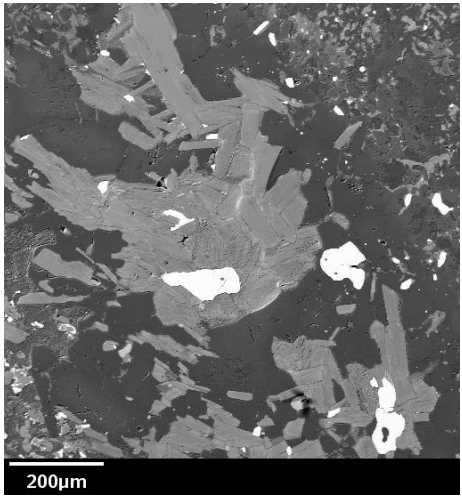
JG-11-037.



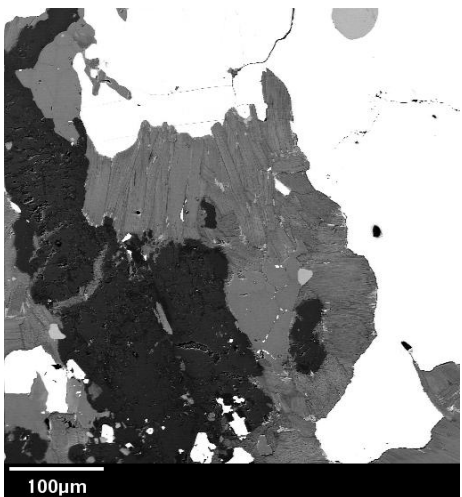
JG-11-037.



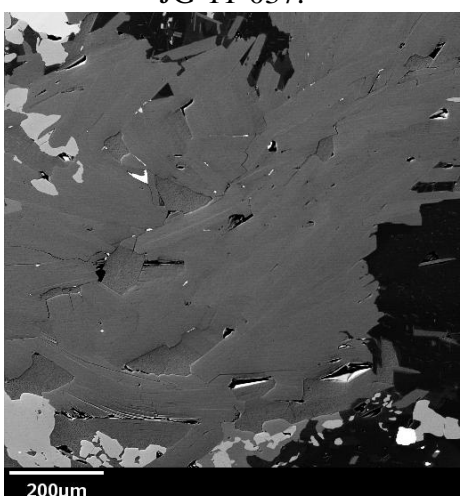
JG-11-037.



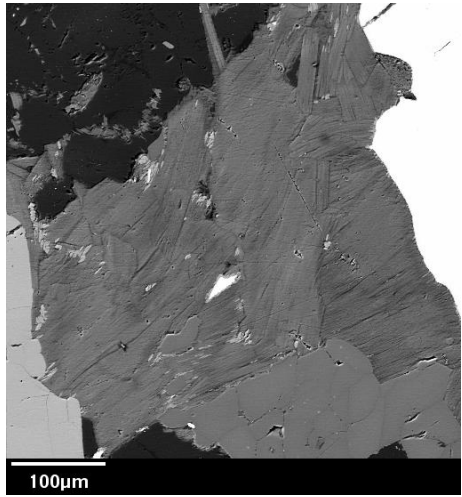
JG-11-037.



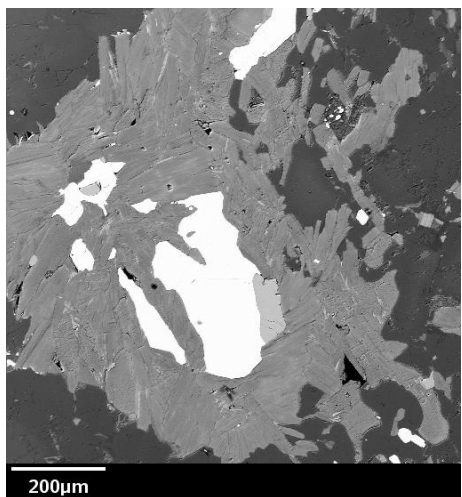
JG-11-037.



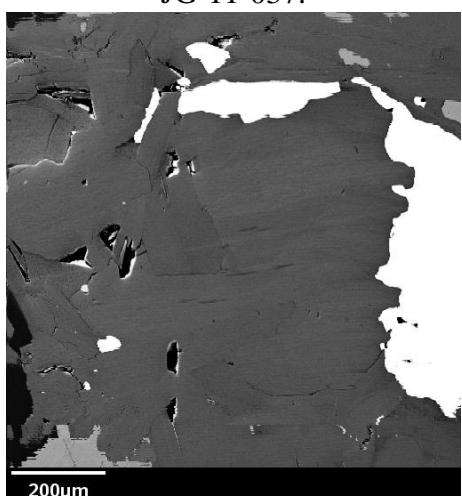
JG-11-040.



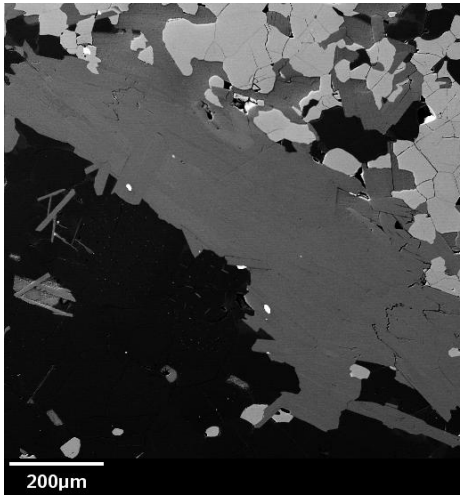
JG-11-037.



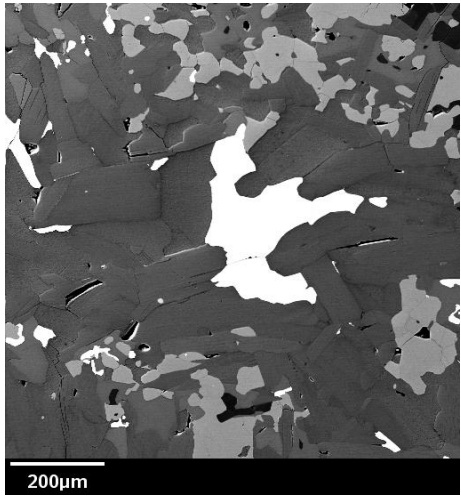
JG-11-037.



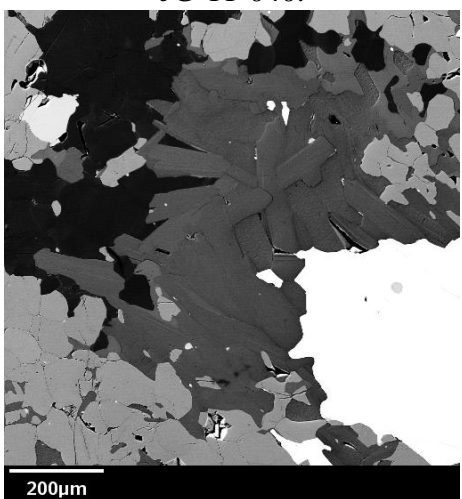
JG-11-040.



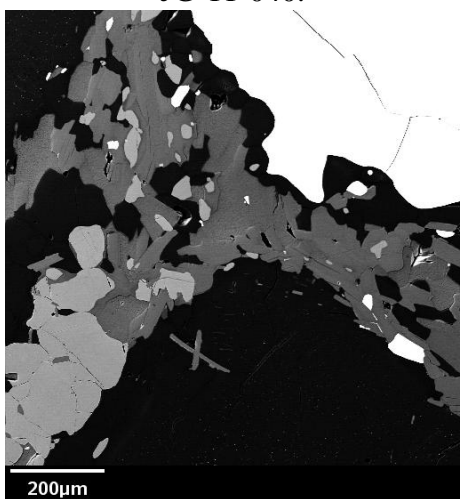
JG-11-040.



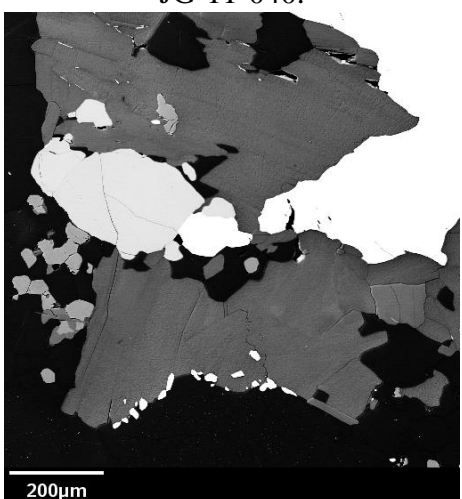
JG-11-040.



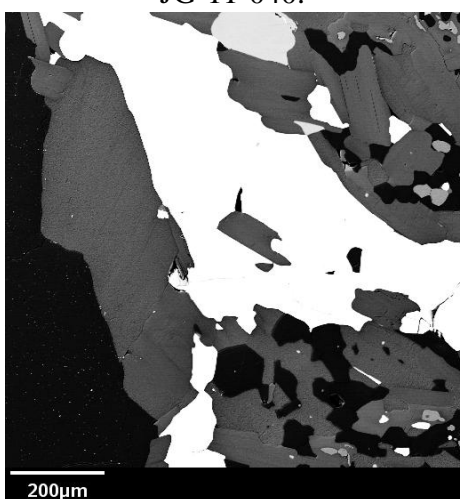
JG-11-040.



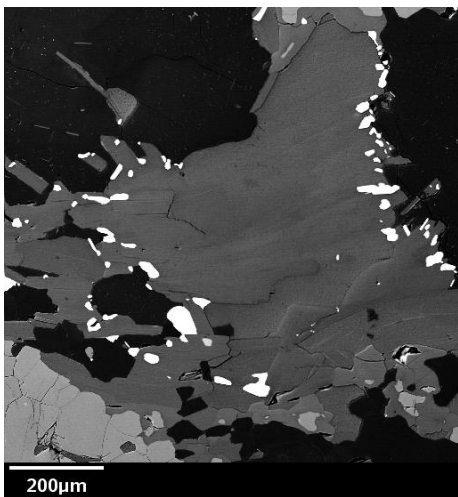
JG-11-040.



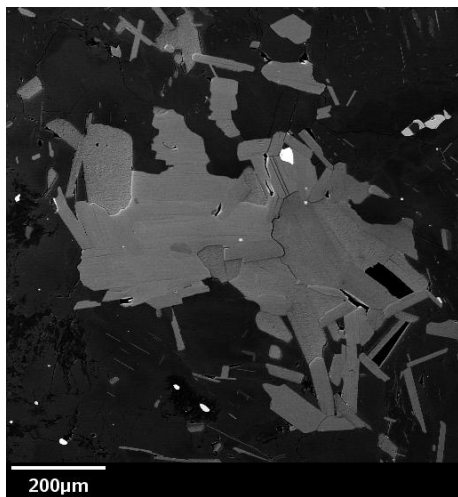
JG-11-040.



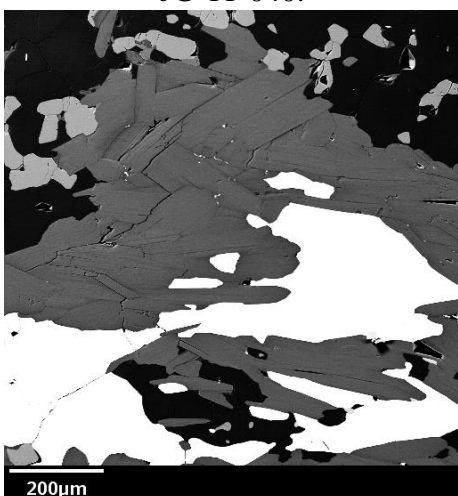
JG-11-040.



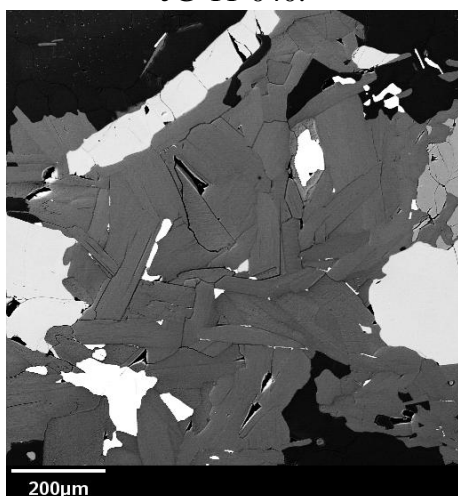
JG-11-040.



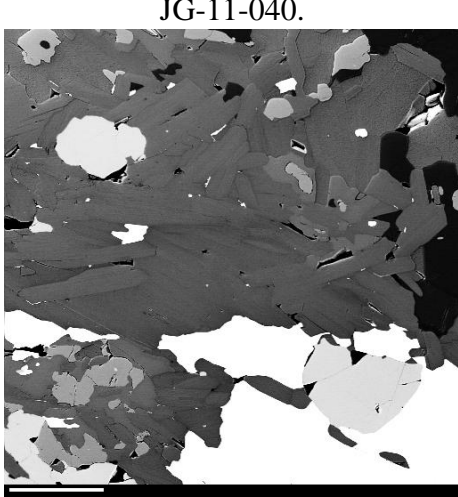
JG-11-040.



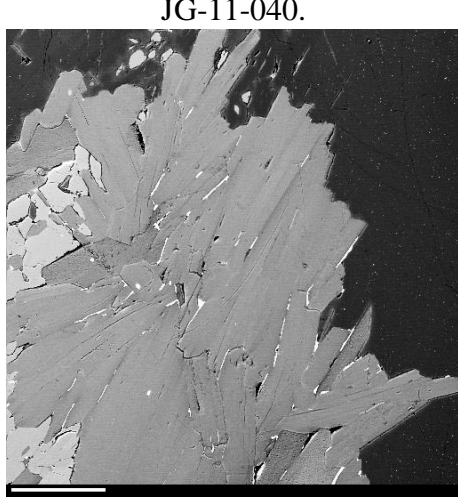
JG-11-040.



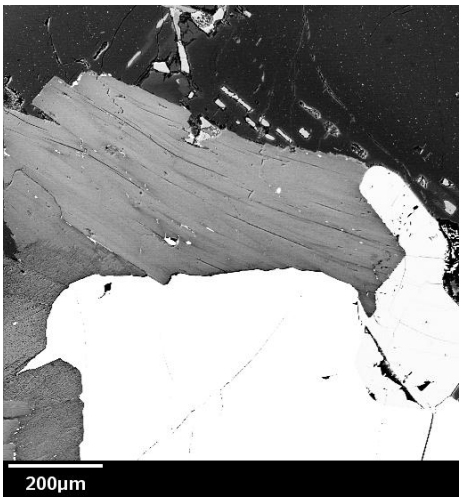
JG-11-040.



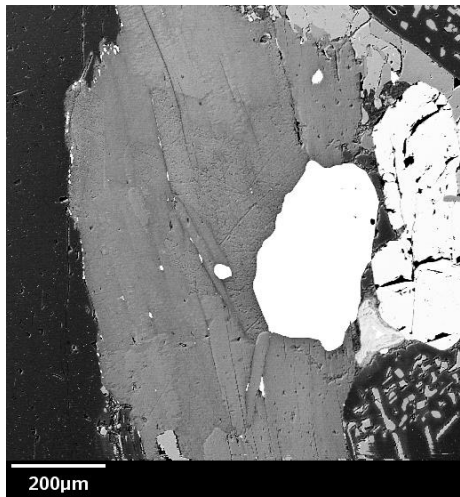
JG-11-040.



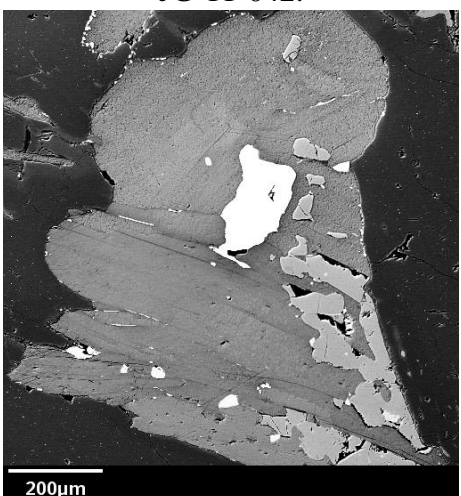
JG-11-042.



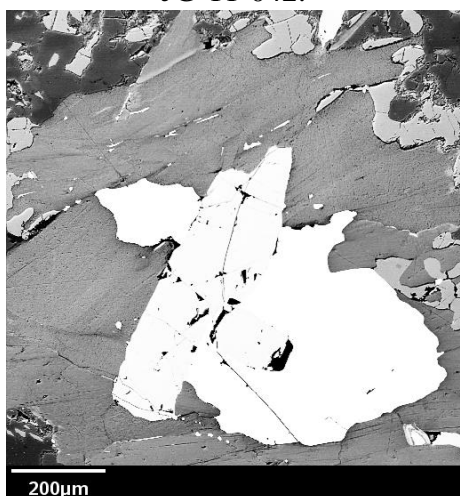
JG-11-042.



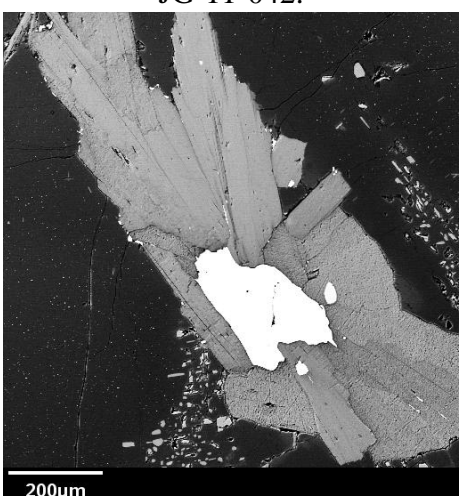
JG-11-042.



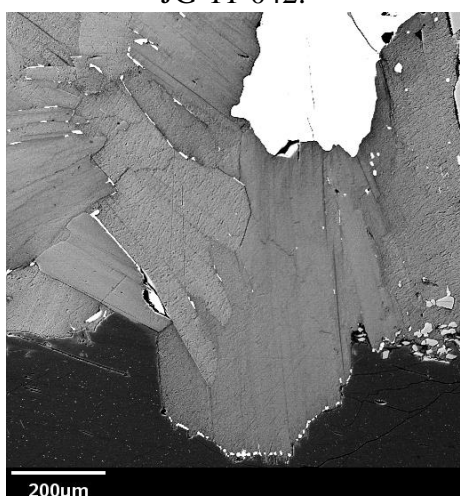
JG-11-042.



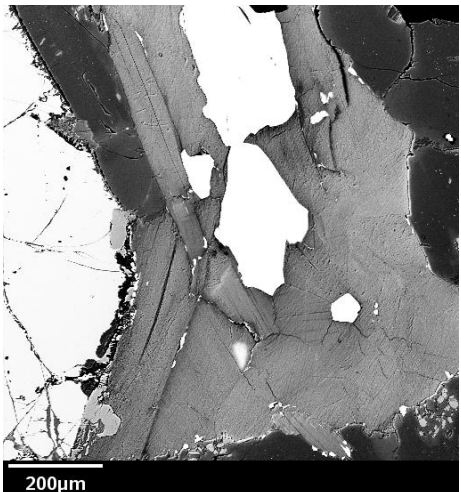
JG-11-042.



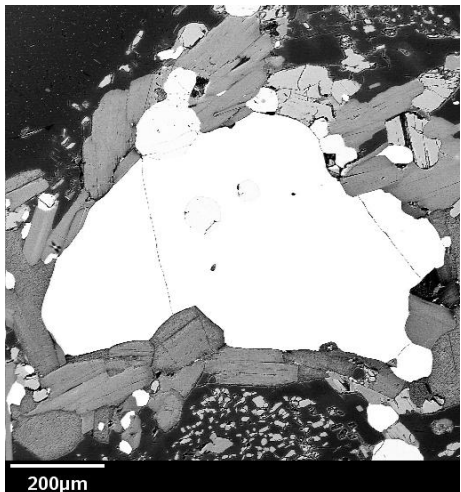
JG-11-042.



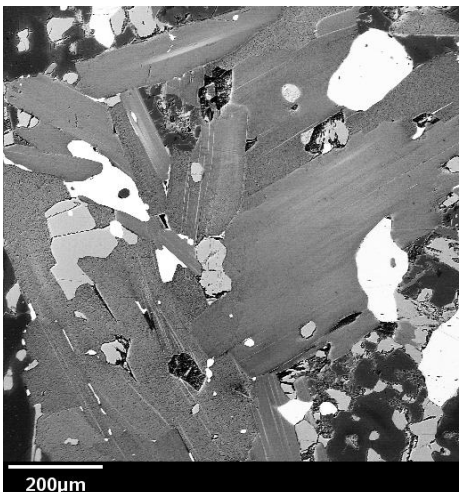
JG-11-042.



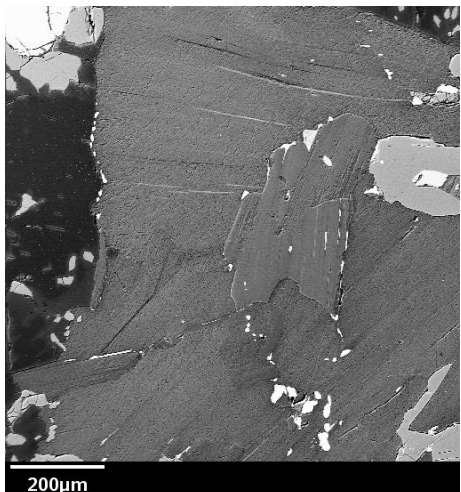
JG-11-042.



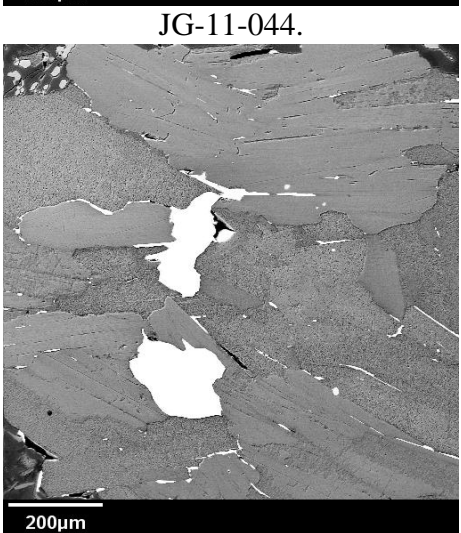
JG-11-044.



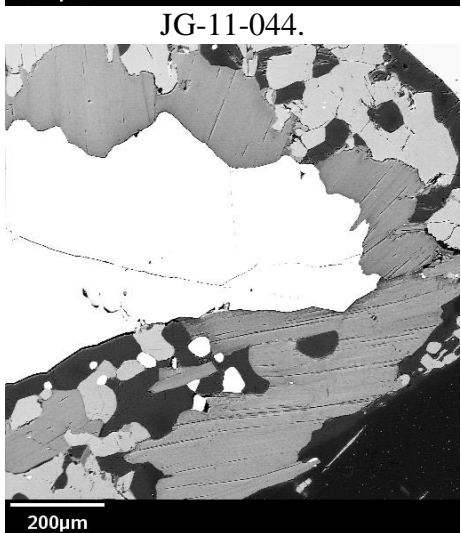
JG-11-044.



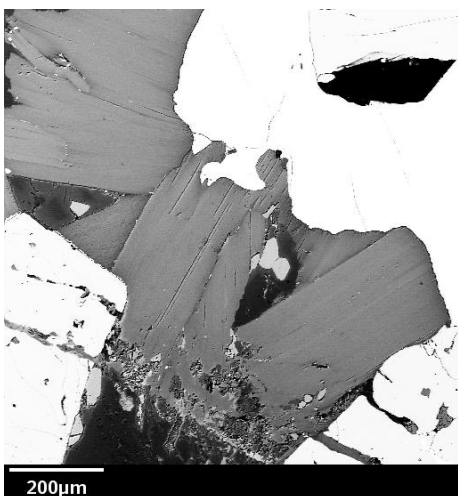
JG-11-044.



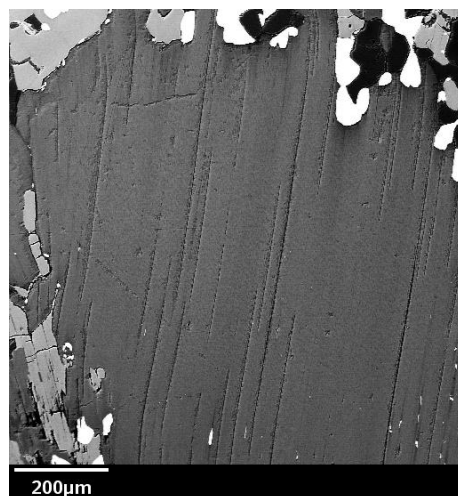
JG-11-044.



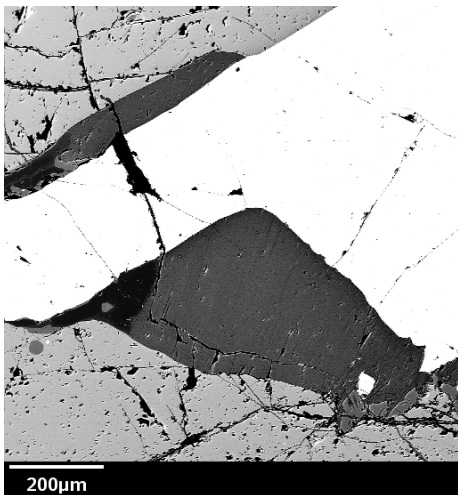
JG-11-044.



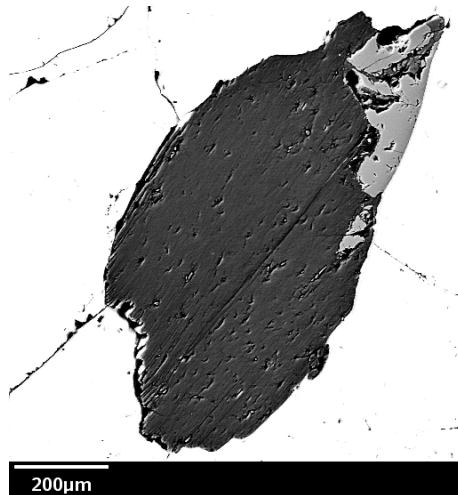
JG-11-044.



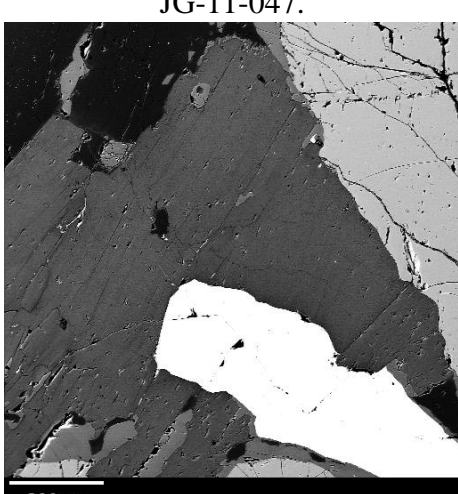
JG-11-044.



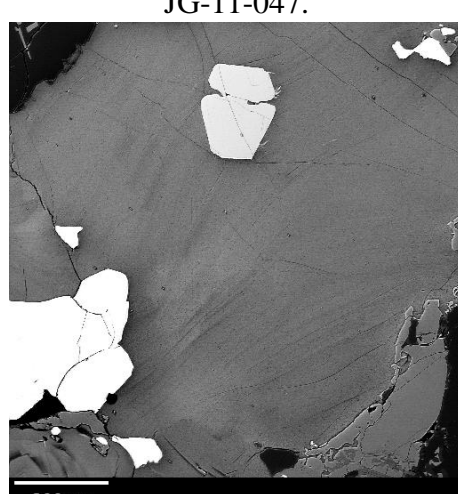
JG-11-047.



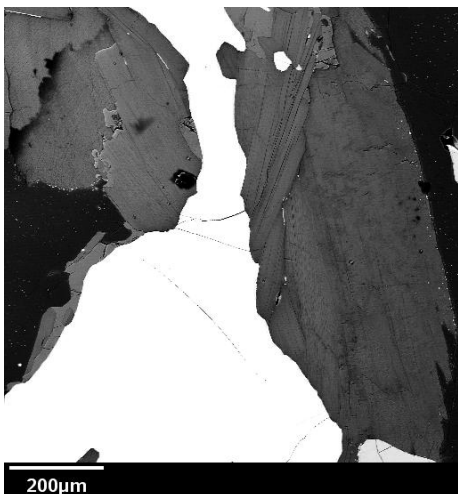
JG-11-047.



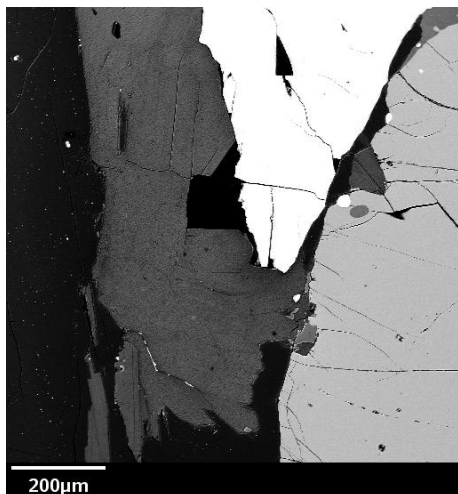
JG-11-047.



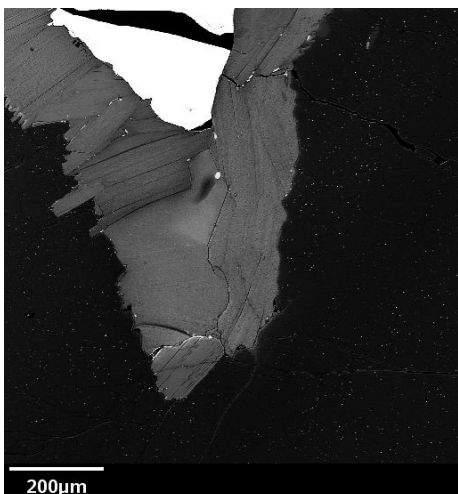
JG-11-047.



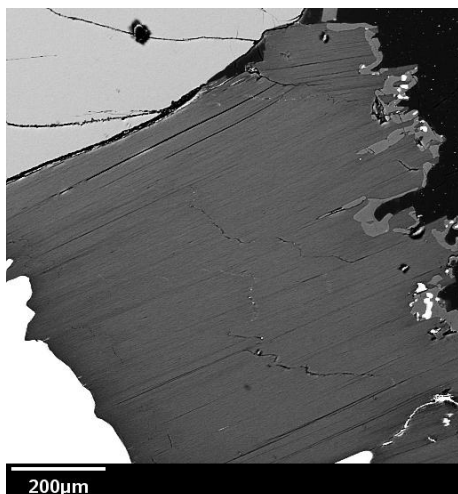
JG-11-047.



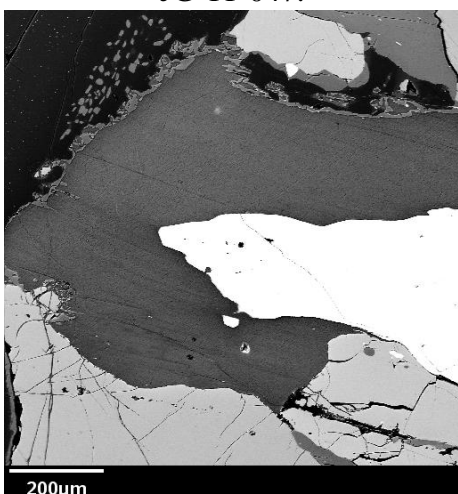
JG-11-047.



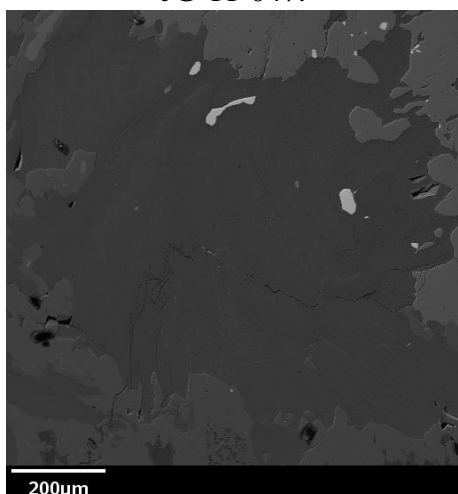
JG-11-047.



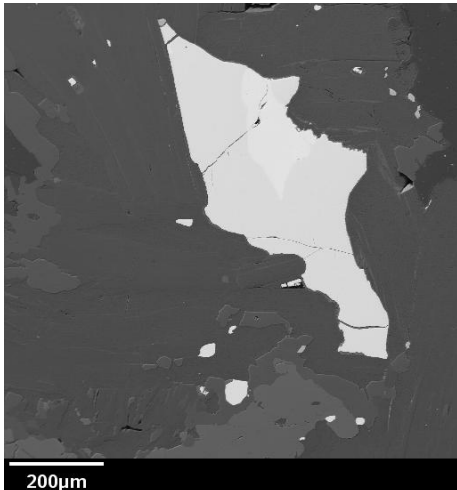
JG-11-047.



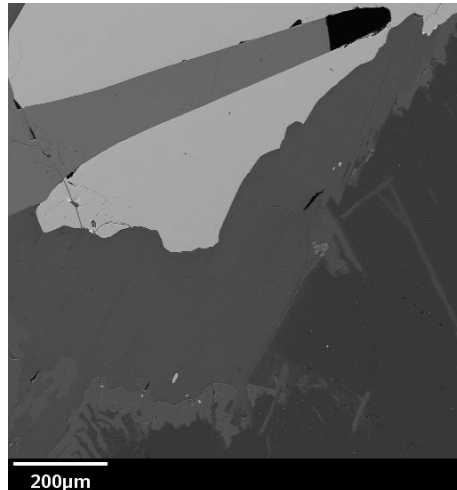
JG-11-047.



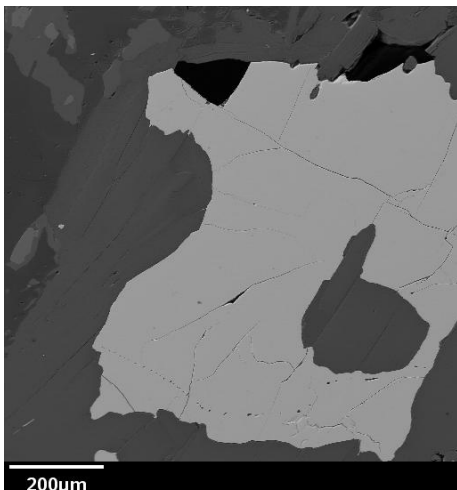
JG-11-059.



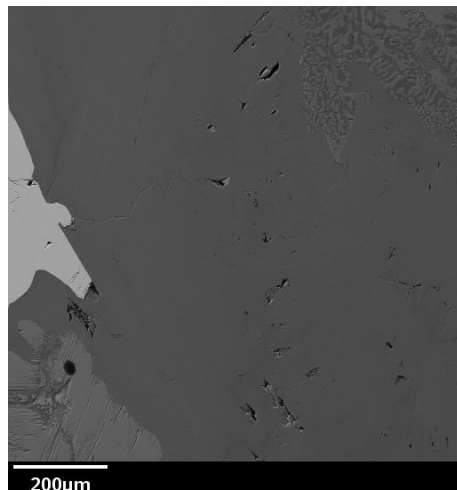
JG-11-059.



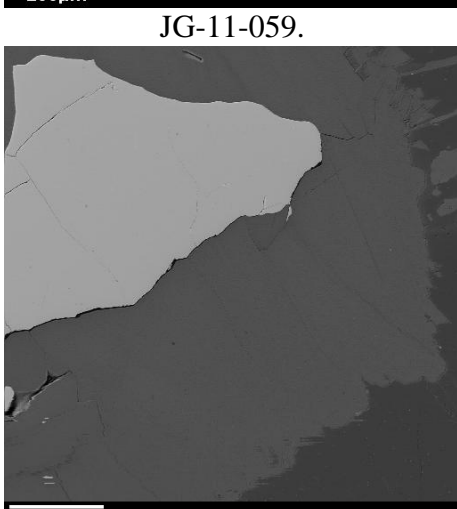
JG-11-059.



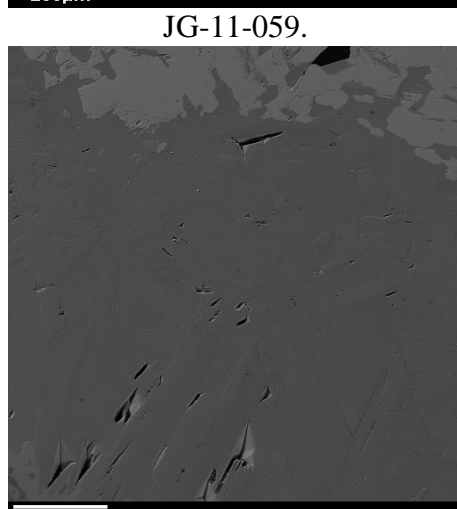
JG-11-059.



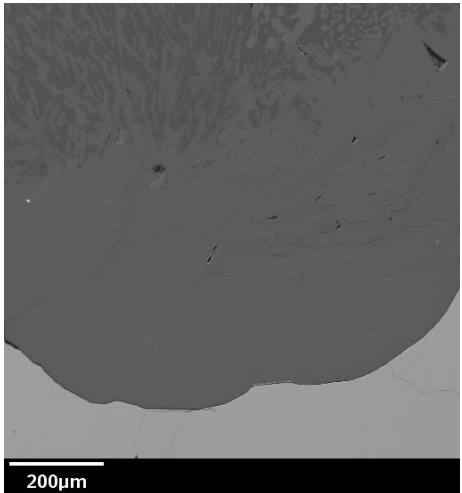
JG-11-059.



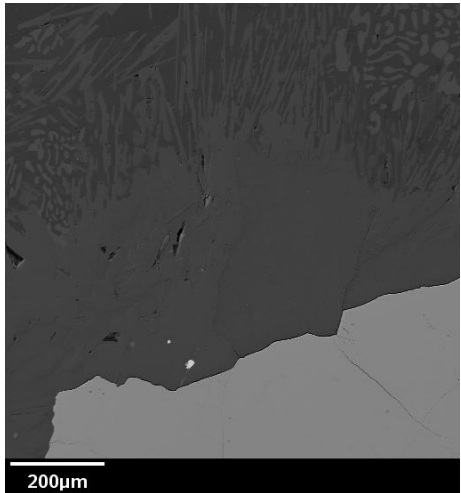
JG-11-059.



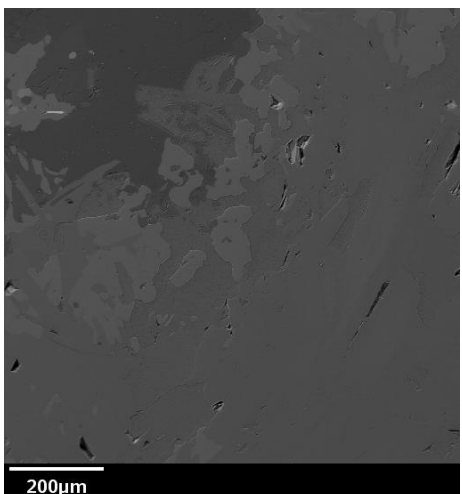
JG-11-059.



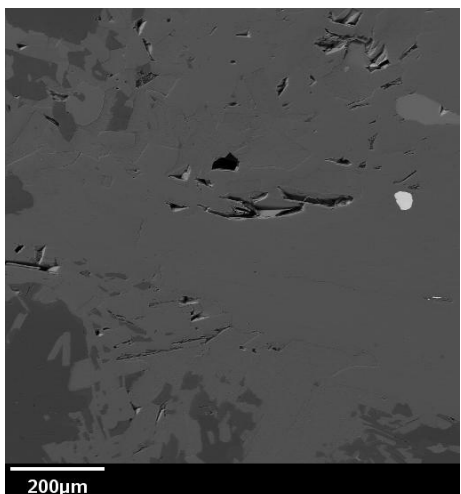
JG-11-059.



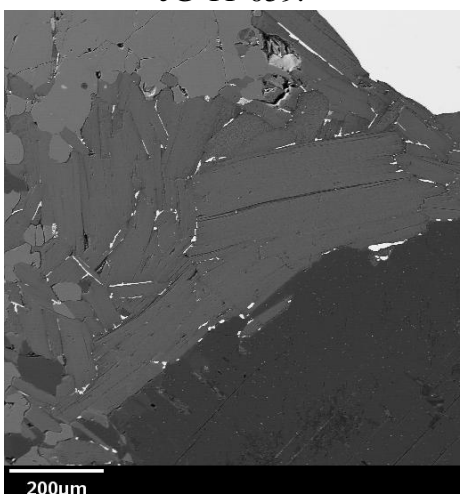
JG-11-059.



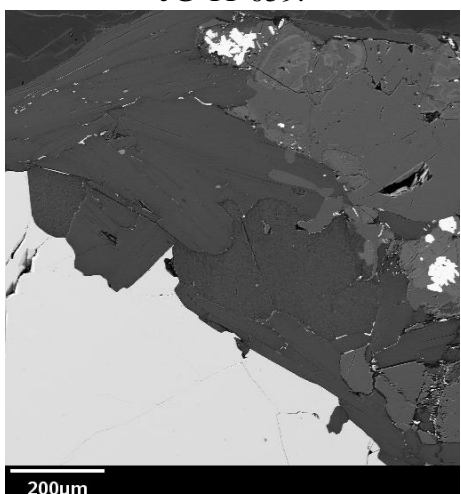
JG-11-059.



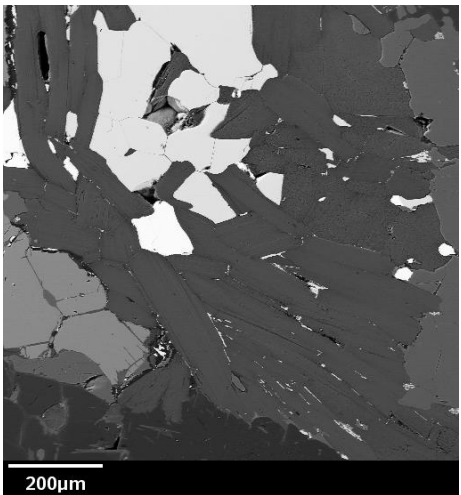
JG-11-059.



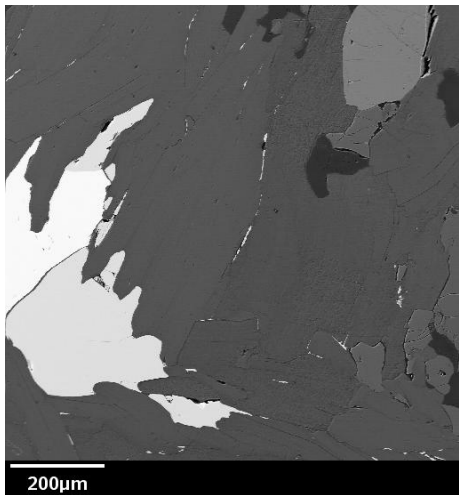
JG-11-061.



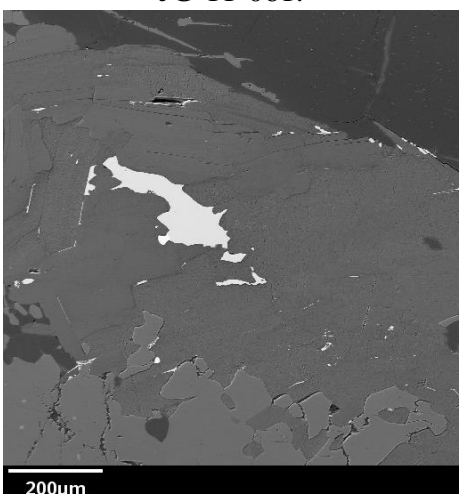
JG-11-061.



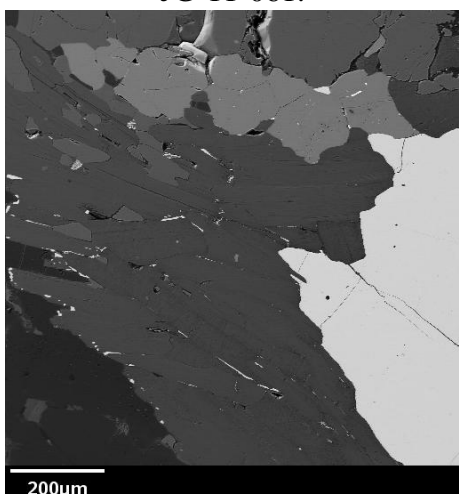
JG-11-061.



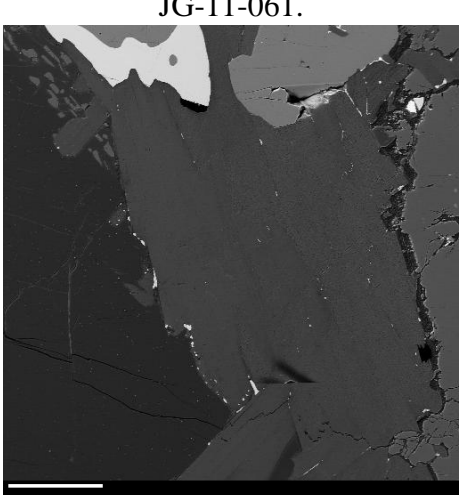
JG-11-061.



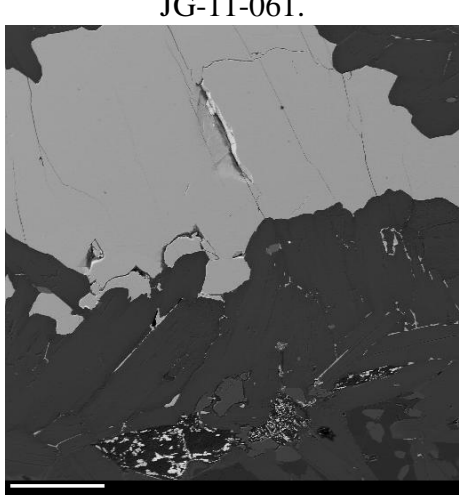
JG-11-061.



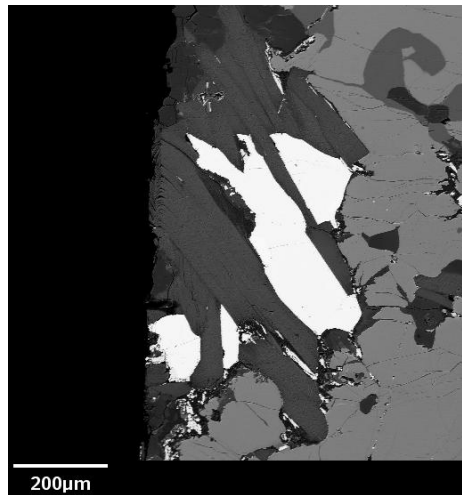
JG-11-061.



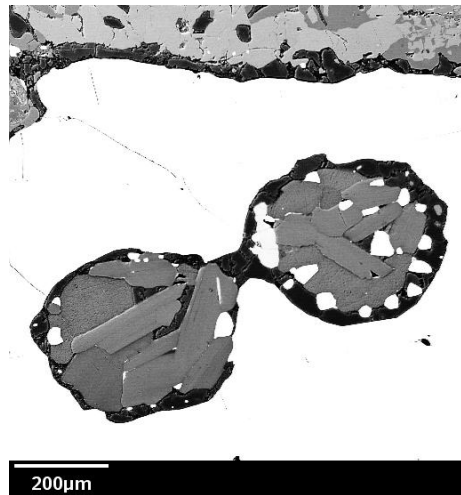
JG-11-061.



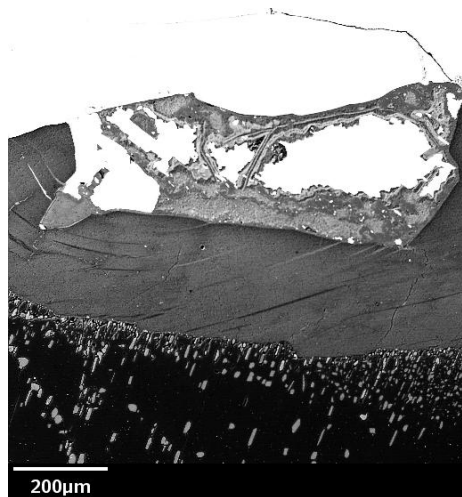
JG-11-061.



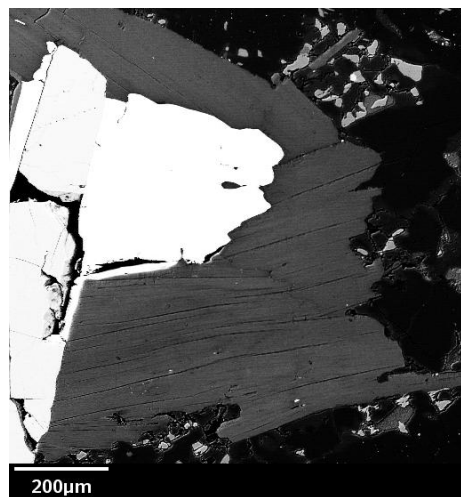
JG-11-061.



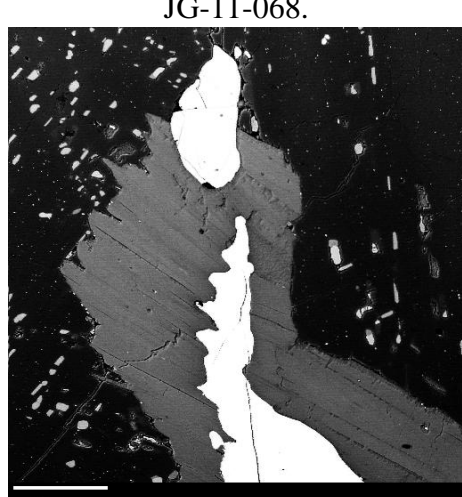
JG-11-068.



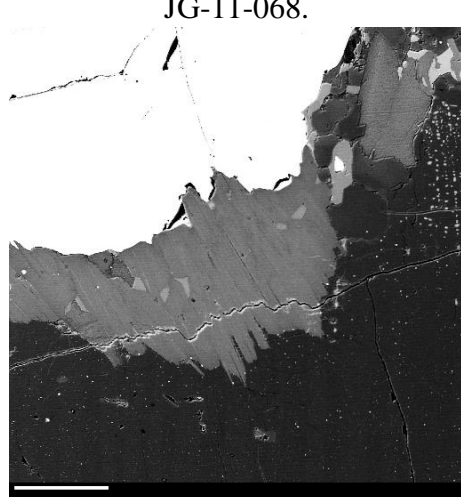
JG-11-068.



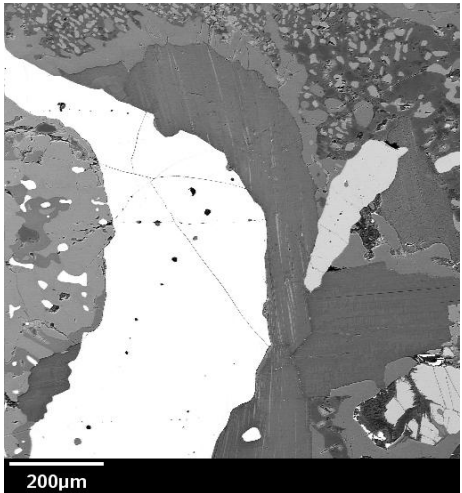
JG-11-068.



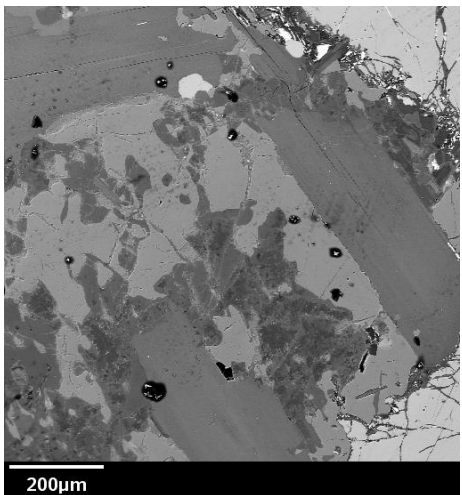
JG-11-068.



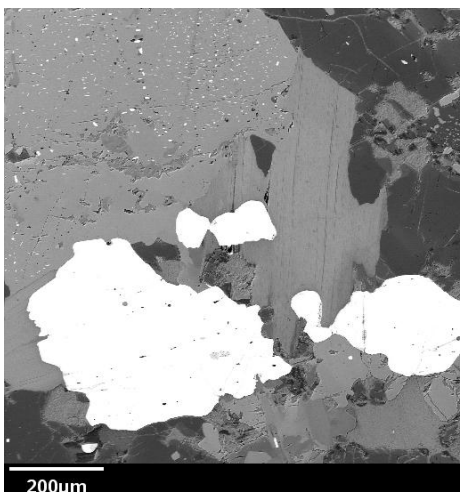
JG-11-068.



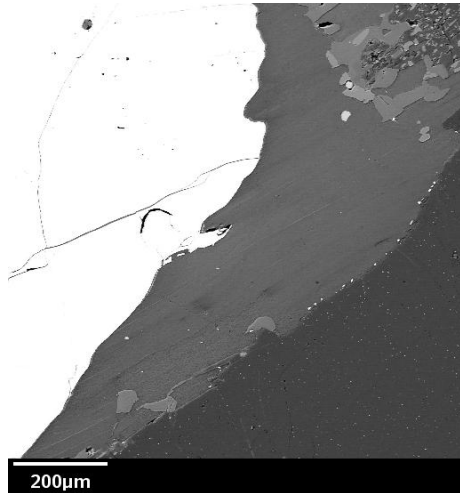
JG-11-068.



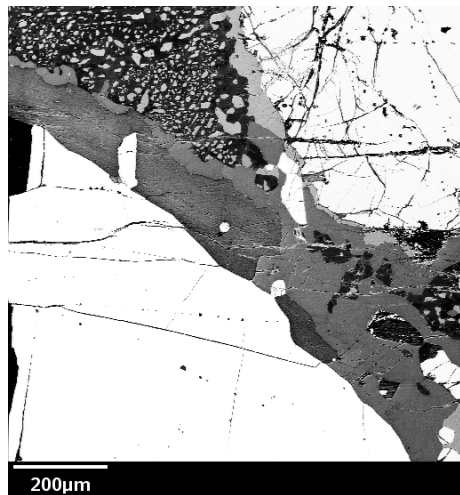
JG-11-068.



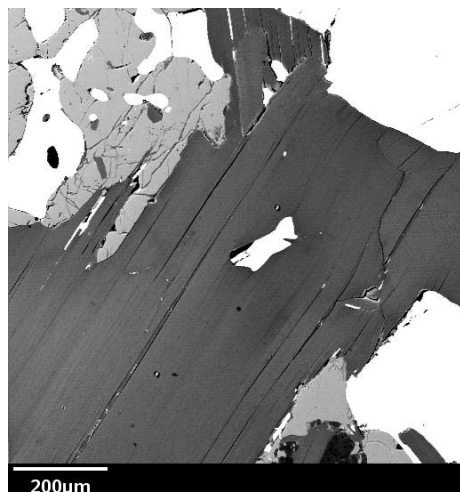
JG-11-068.



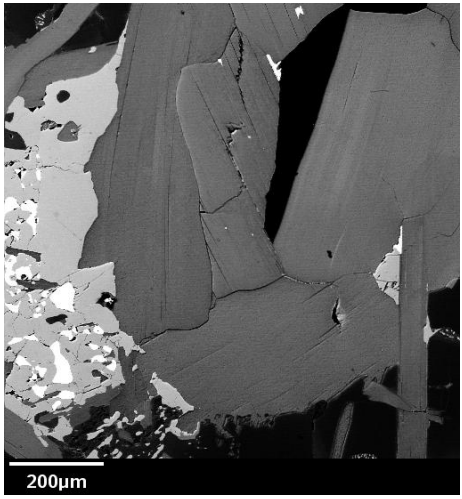
JG-11-068.



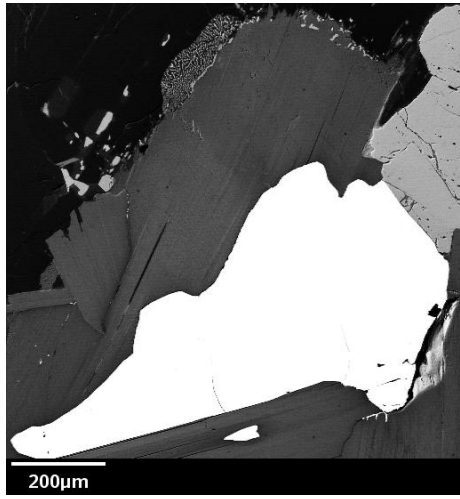
JG-11-068.



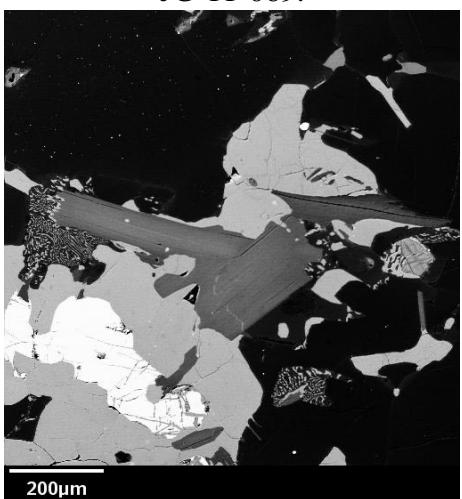
JG-11-069.



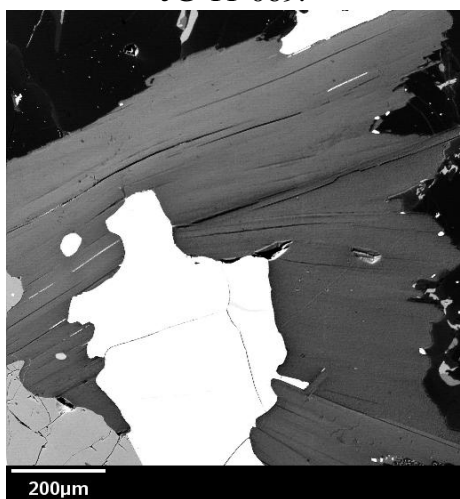
JG-11-069.



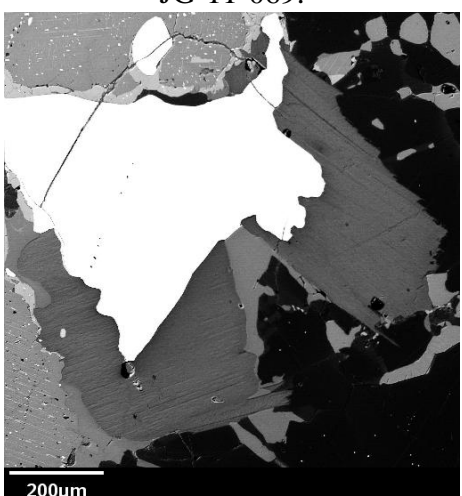
JG-11-069.



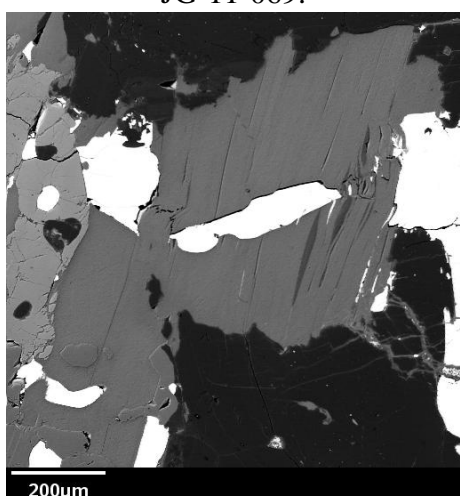
JG-11-069.



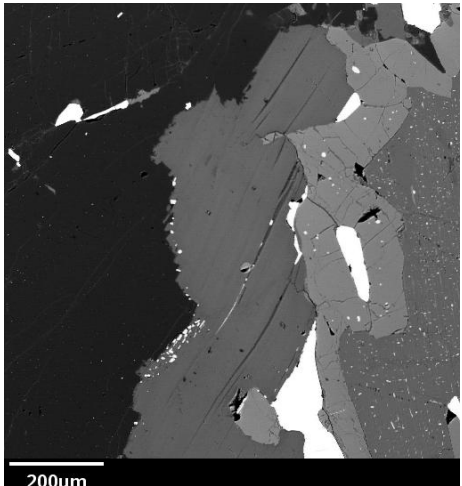
JG-11-069.



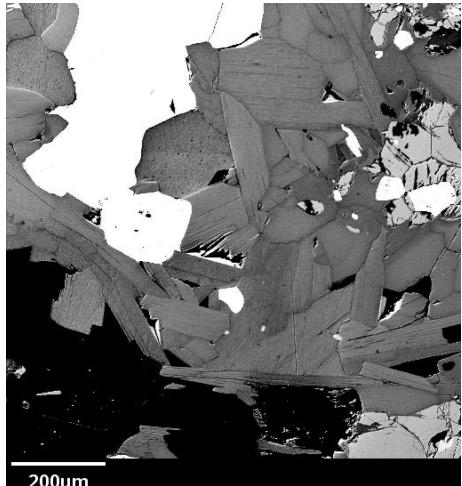
JG-11-069.



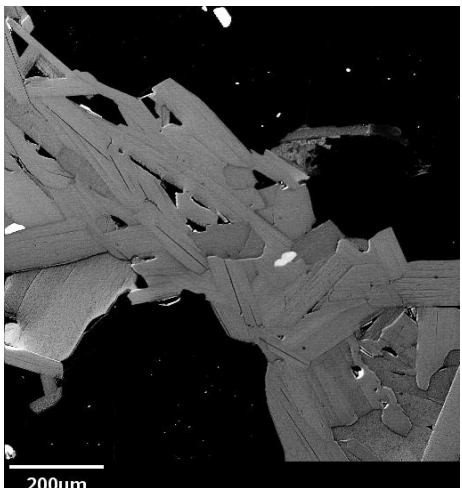
JG-11-069.



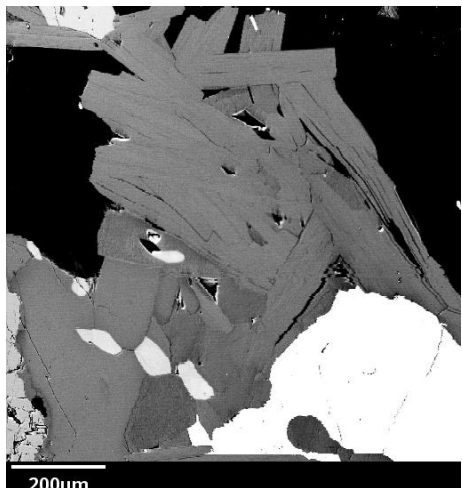
JG-11-069.



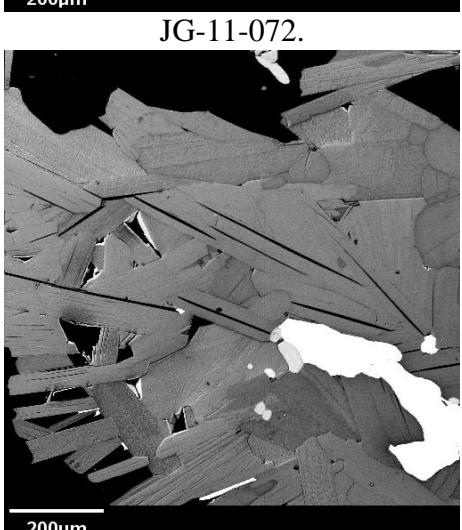
JG-11-072.



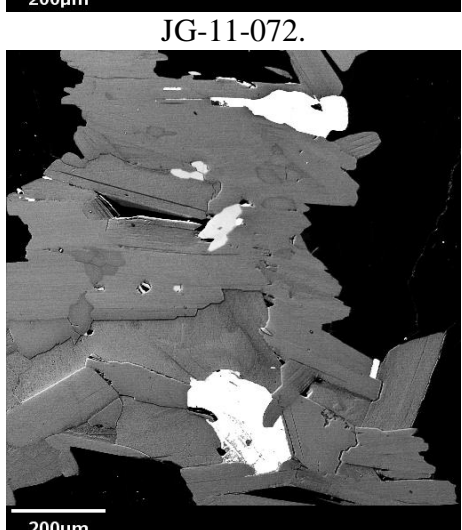
JG-11-072.



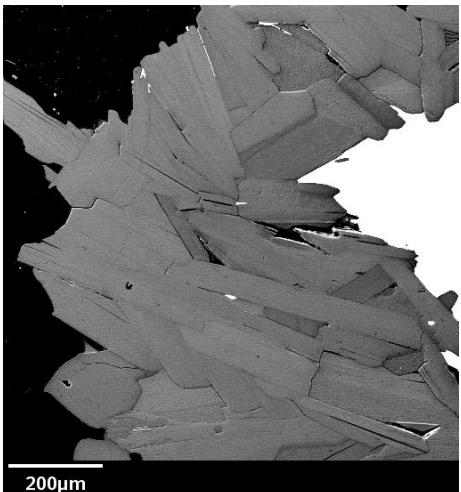
JG-11-072.



JG-11-072.

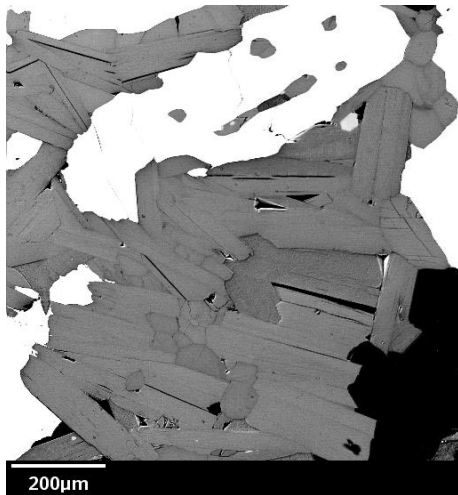


JG-11-072.



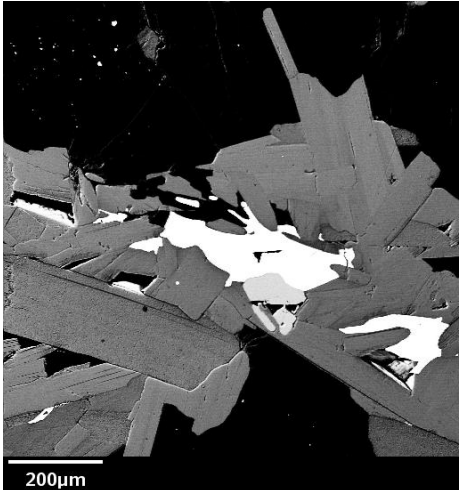
200µm

JG-11-072.



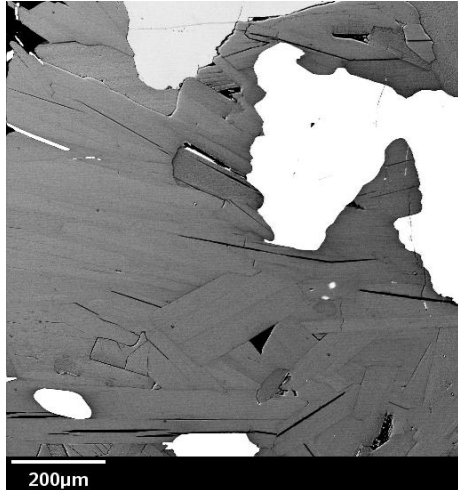
200µm

JG-11-072.



200µm

JG-11-072.



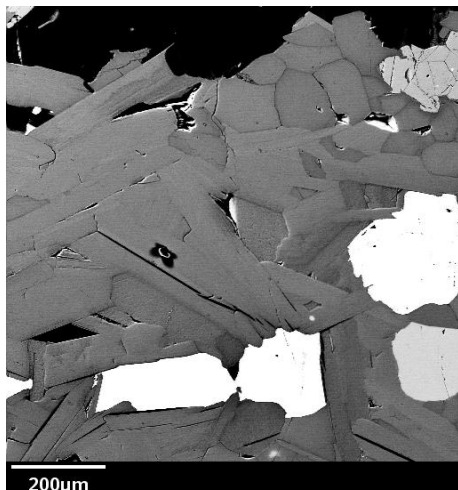
200µm

JG-11-072.



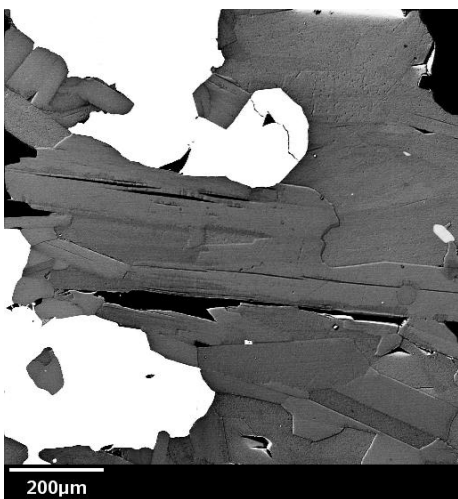
200µm

JG-11-072.



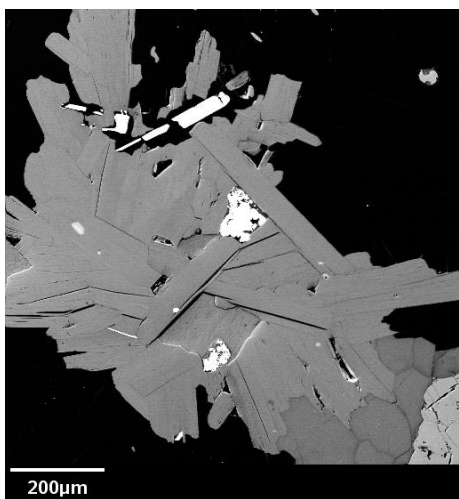
200µm

JG-11-072.



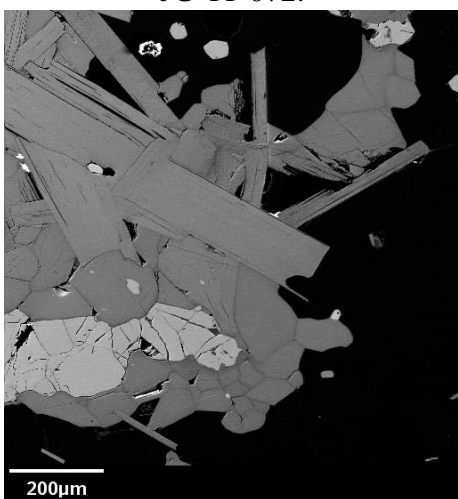
200µm

JG-11-072.



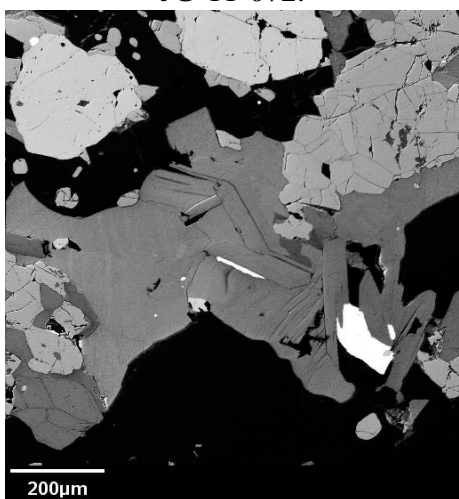
200µm

JG-11-072.



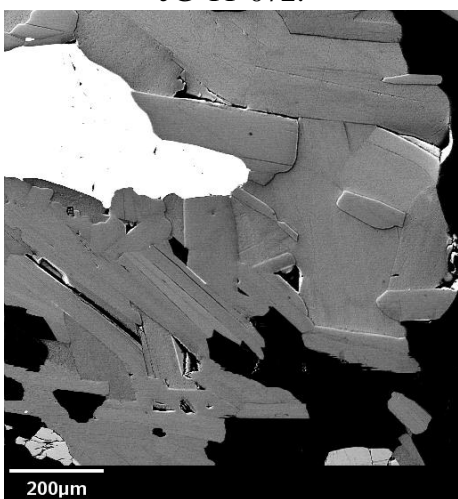
200µm

JG-11-072.



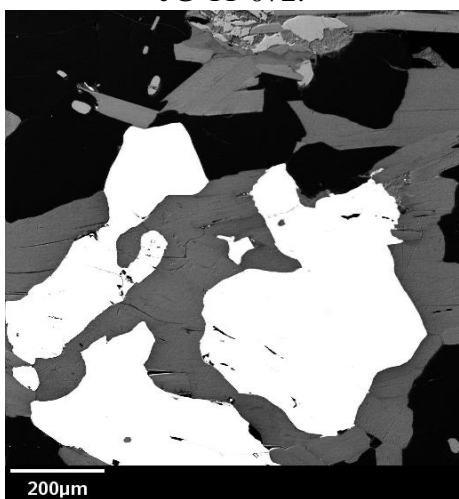
200µm

JG-11-072.



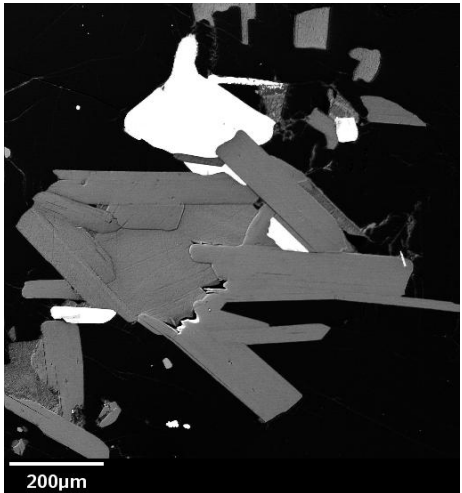
200µm

JG-11-072.

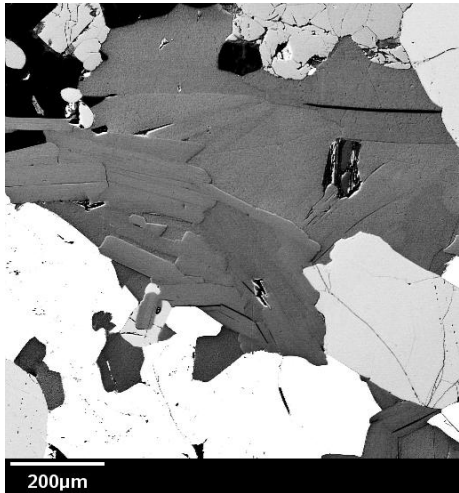


200µm

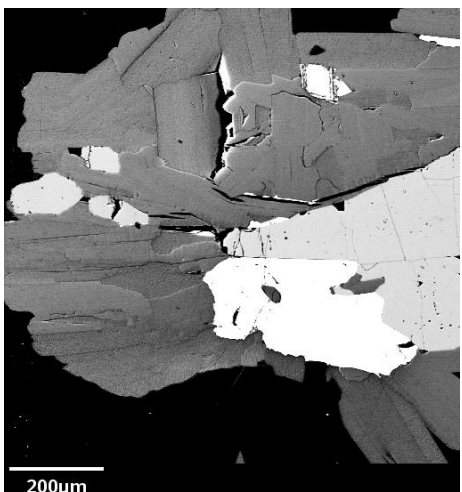
JG-11-072.



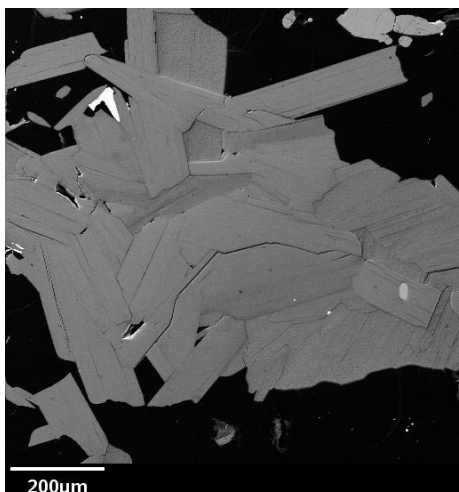
JG-11-072.



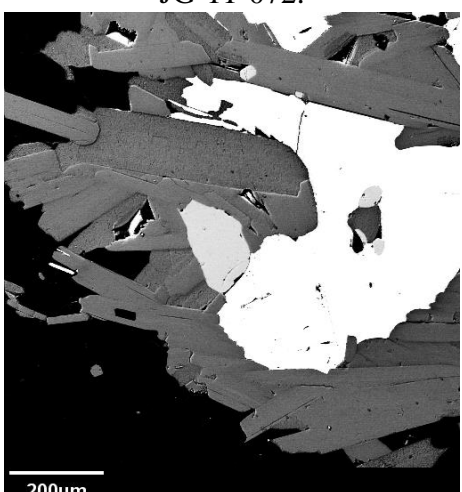
JG-11-072.



JG-11-072.



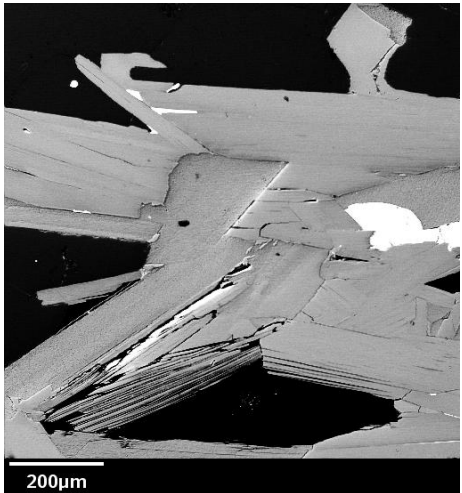
JG-11-072.



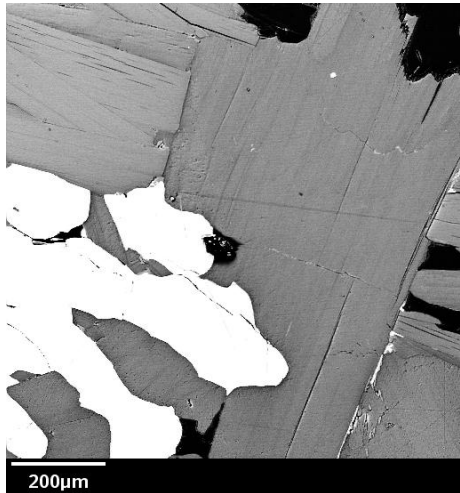
JG-11-072.



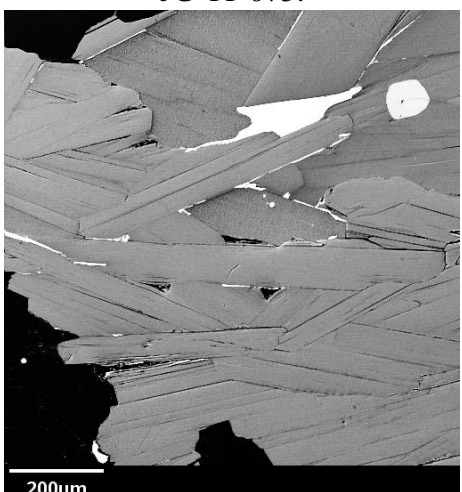
JG-11-075.



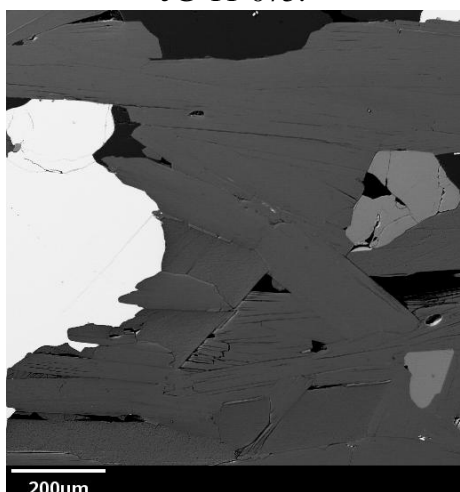
JG-11-075.



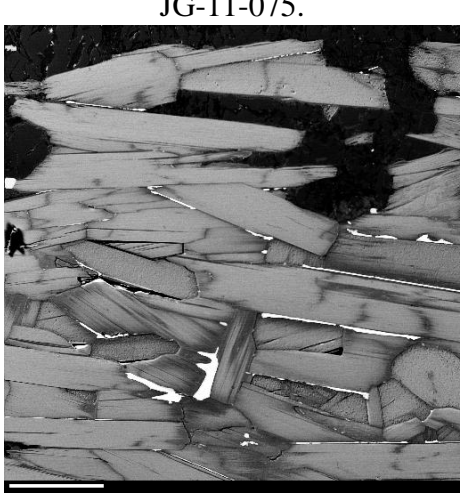
JG-11-075.



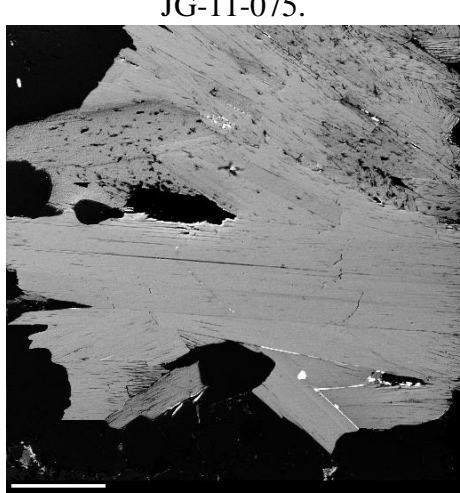
JG-11-075.



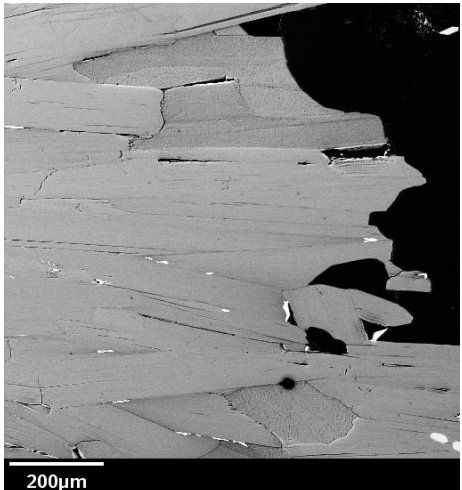
JG-11-075.



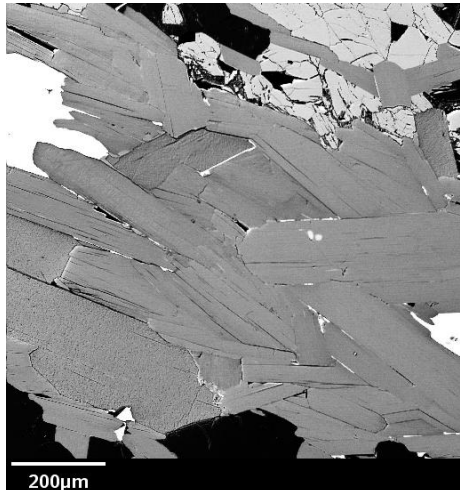
JG-11-075.



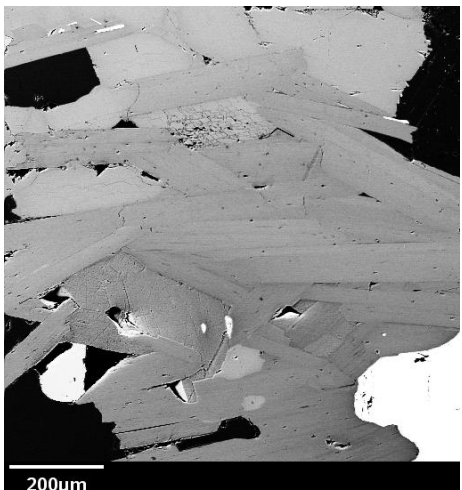
JG-11-075.



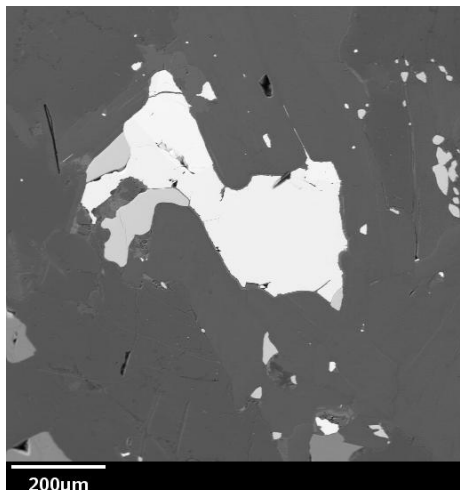
JG-11-075.



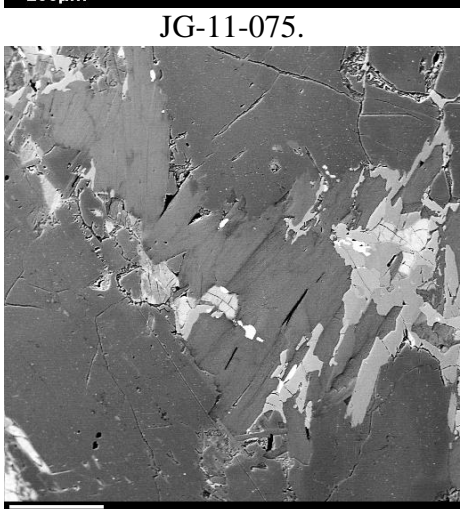
JG-11-075.



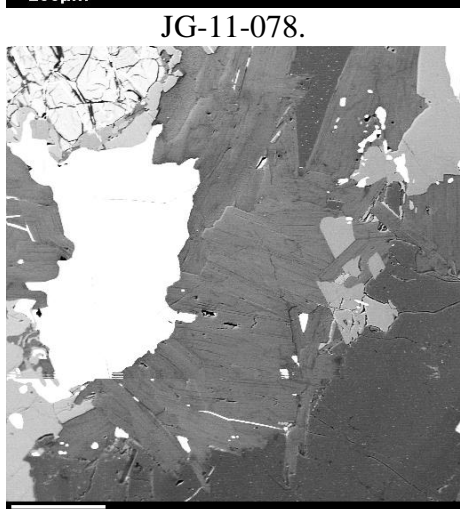
JG-11-075.



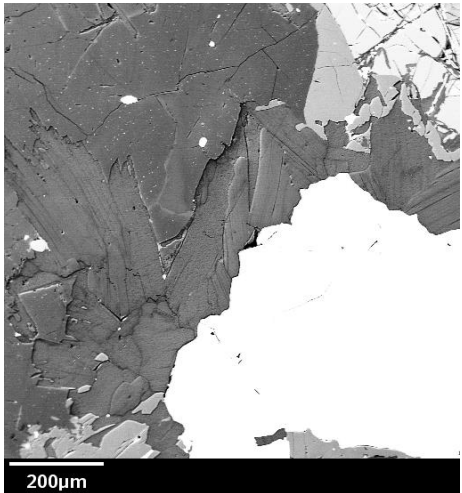
JG-11-078.



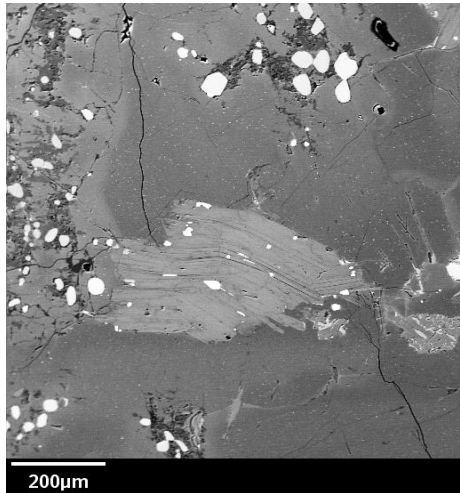
JG-11-078.



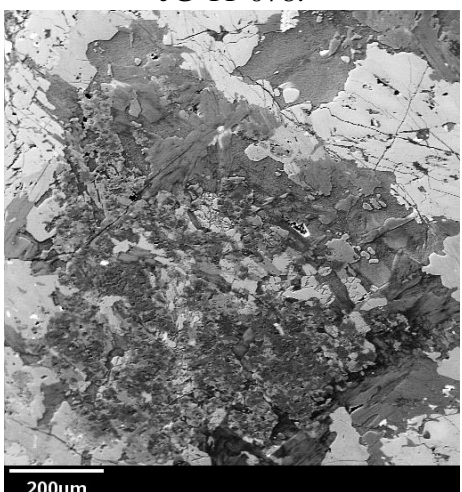
JG-11-078.



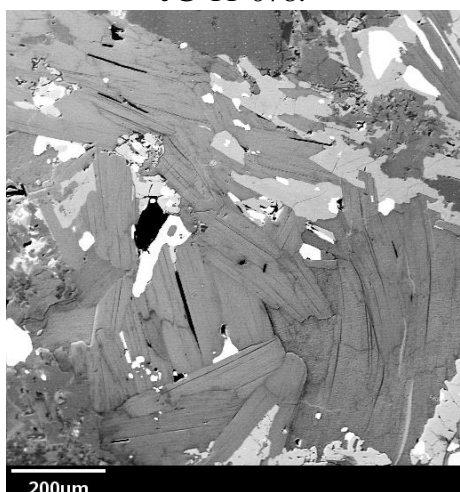
JG-11-078.



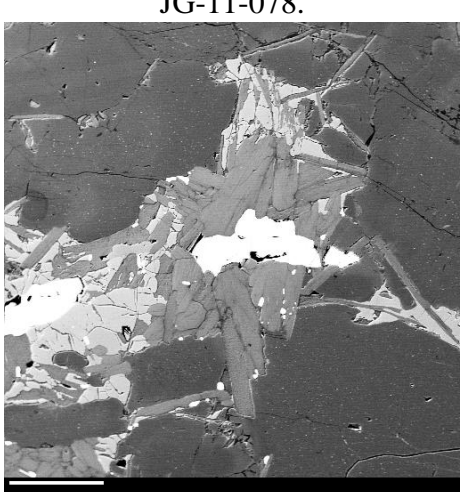
JG-11-078.



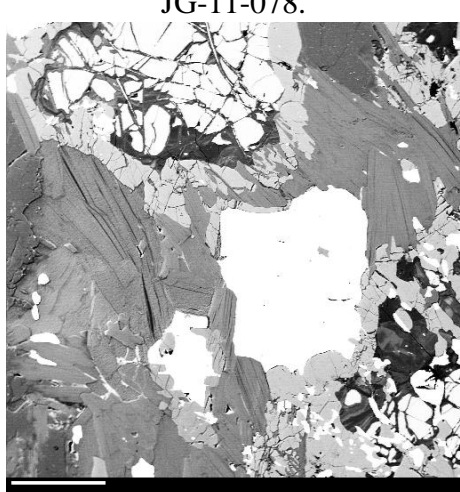
JG-11-078.



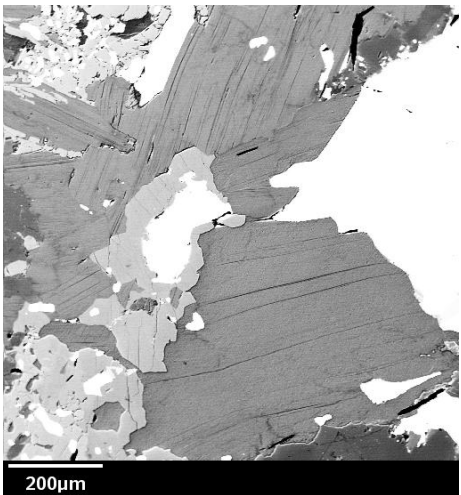
JG-11-078.



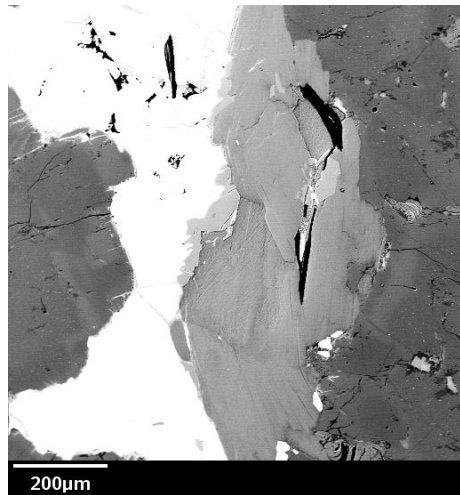
JG-11-078.



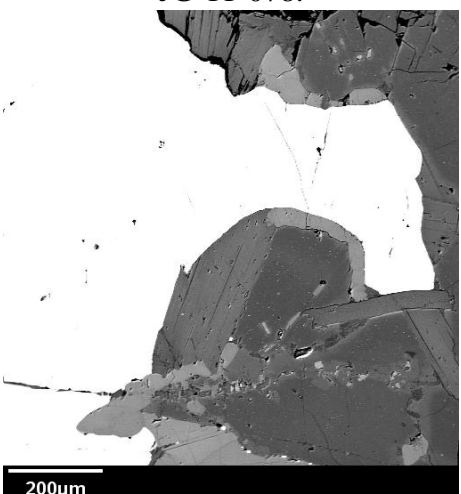
JG-11-078.



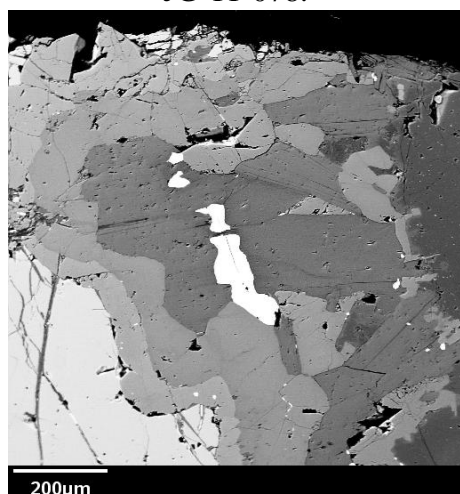
JG-11-078.



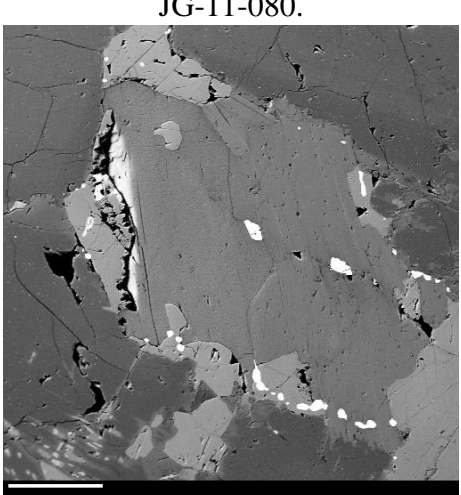
JG-11-078.



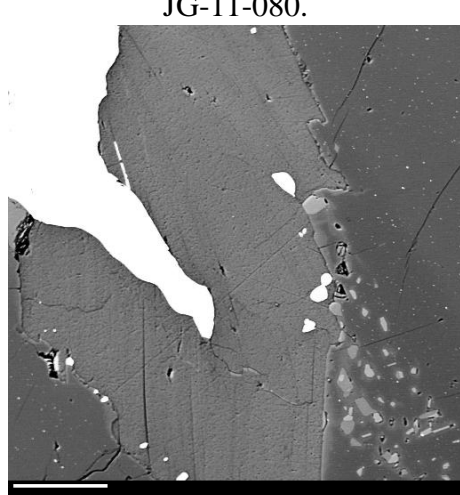
JG-11-080.



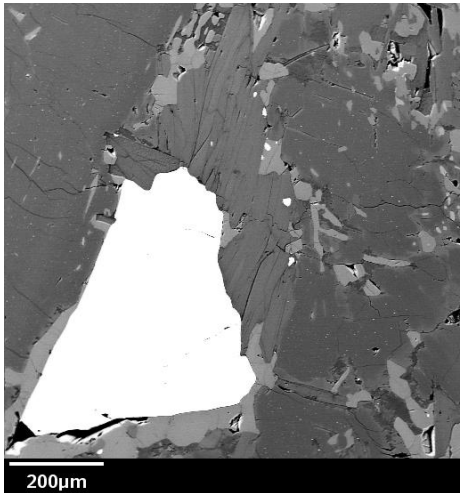
JG-11-080.



JG-11-080.

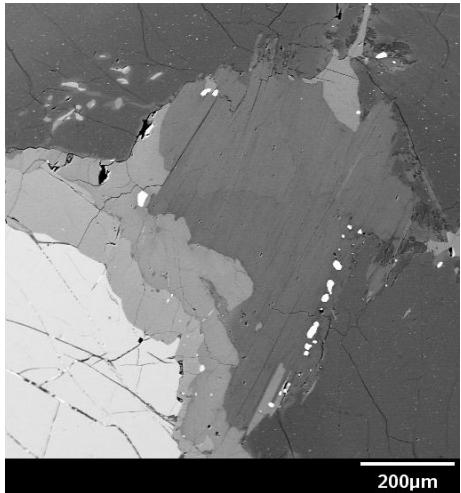


JG-11-080.



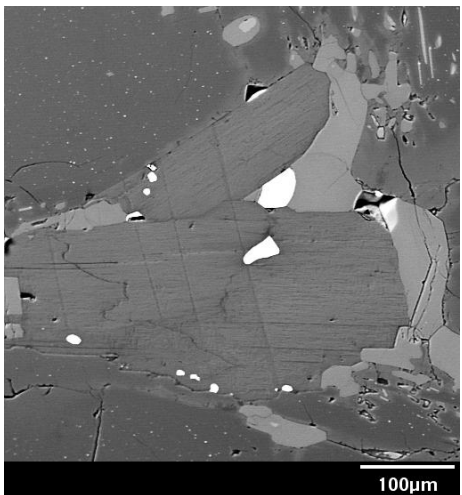
200μm

JG-11-080.



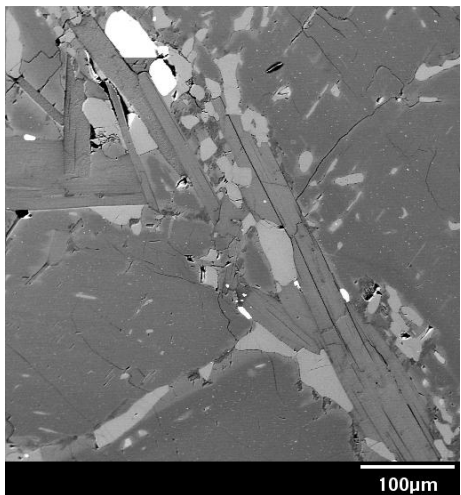
200μm

JG-11-080.



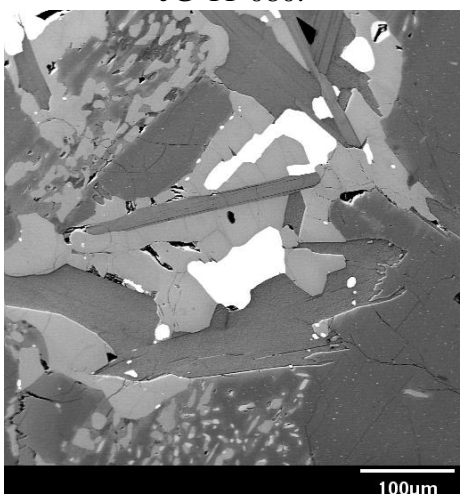
100μm

JG-11-080.



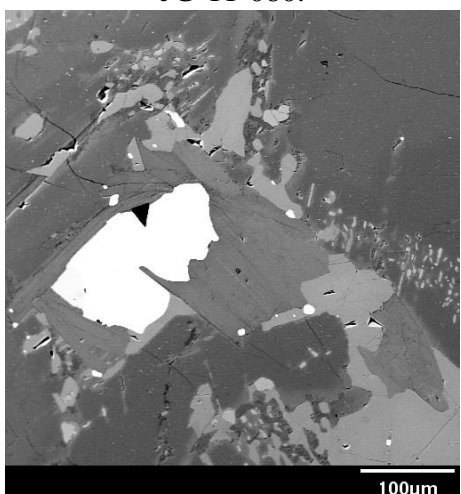
100μm

JG-11-080.



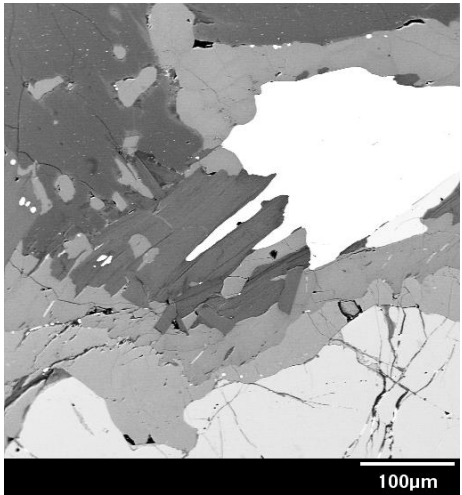
100μm

JG-11-080.

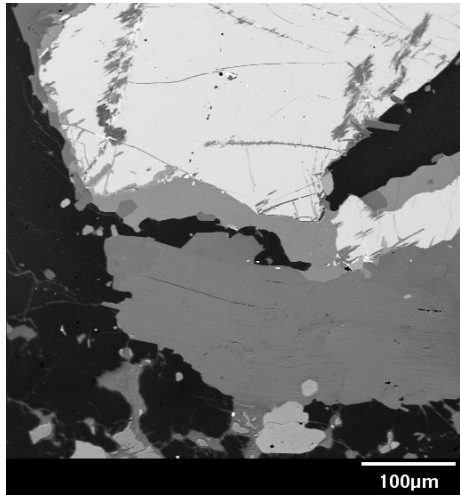


100μm

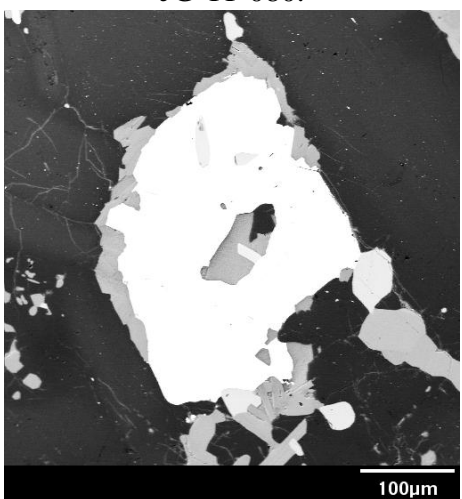
JG-11-080.



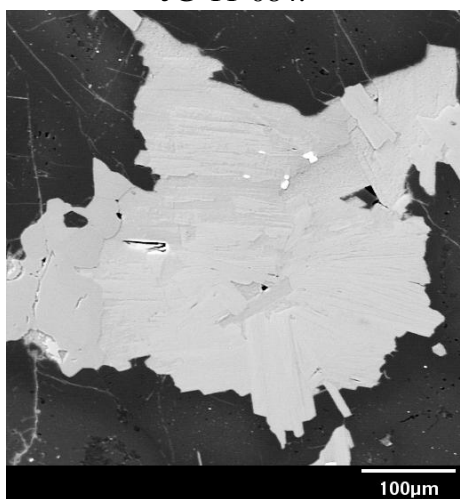
JG-11-080.



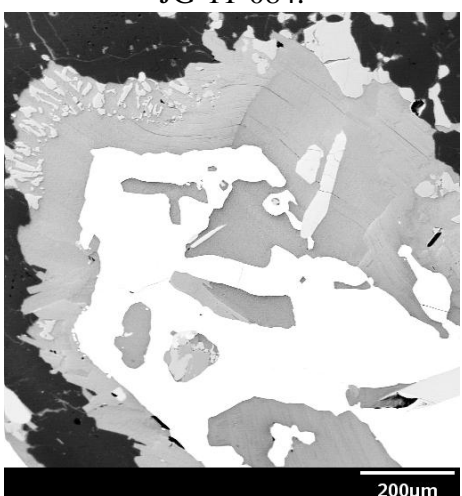
JG-11-084.



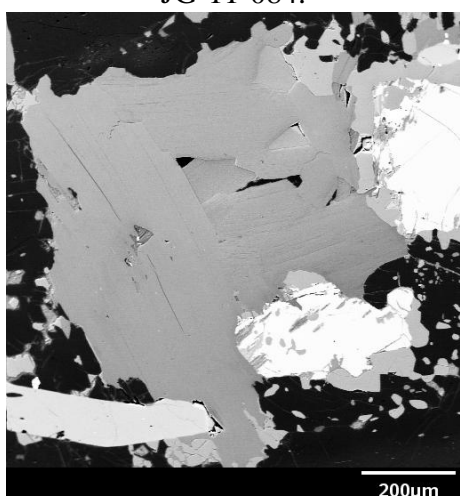
JG-11-084.



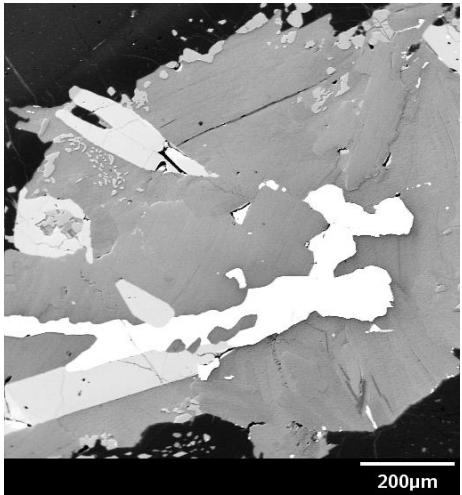
JG-11-084.



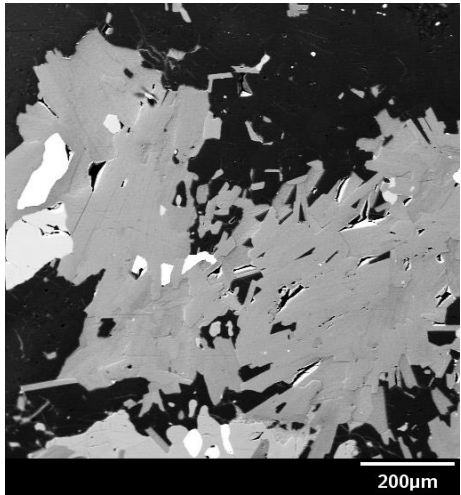
JG-11-084.



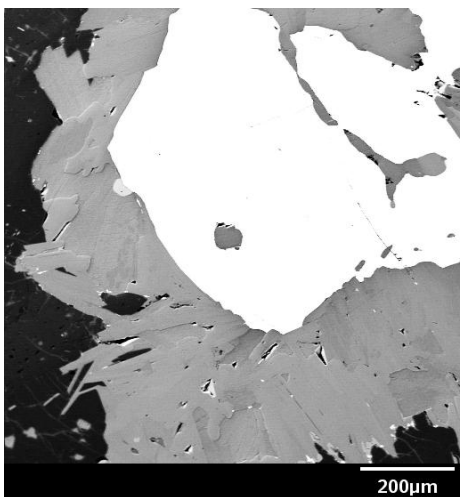
JG-11-084.



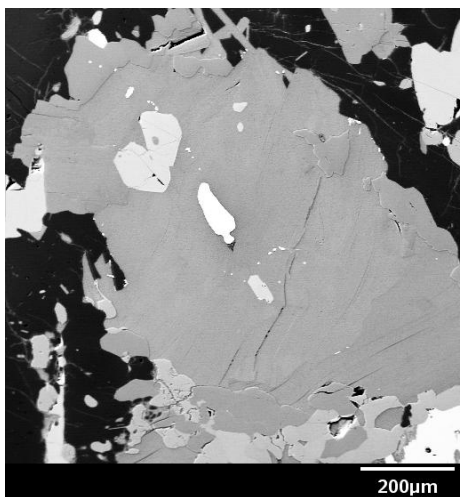
JG-11-084.



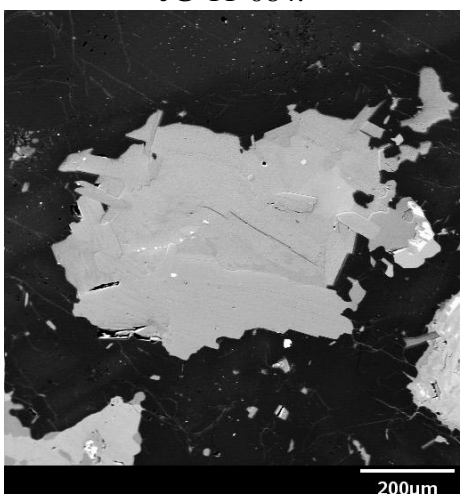
JG-11-084.



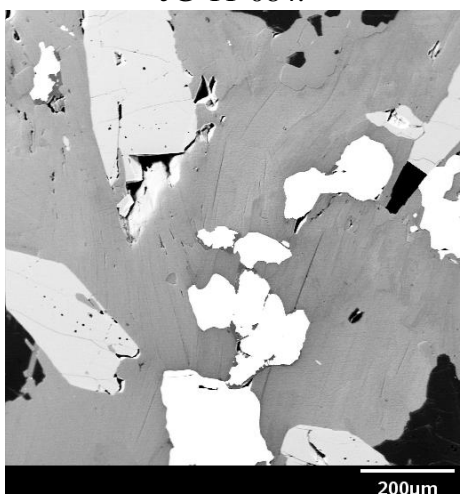
JG-11-084.



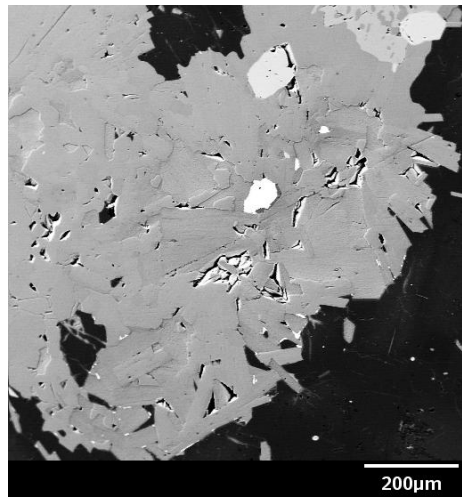
JG-11-084.



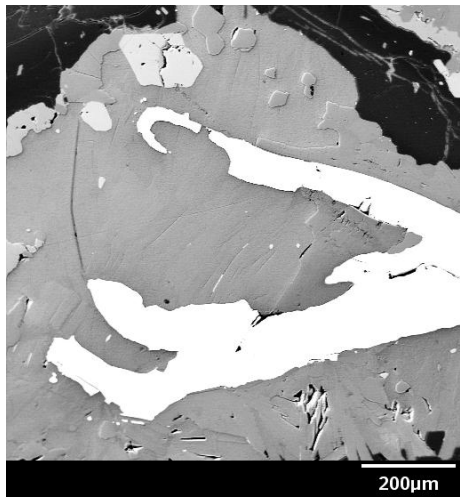
JG-11-084.



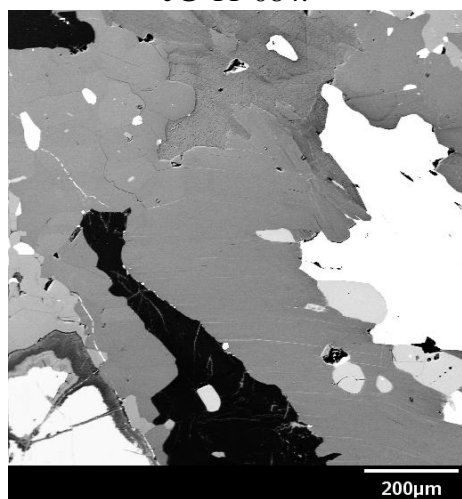
JG-11-084.



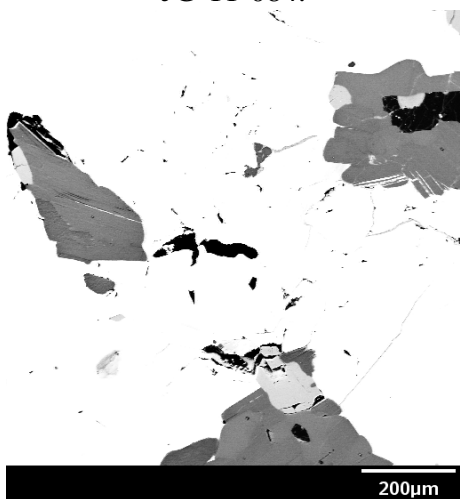
JG-11-084.



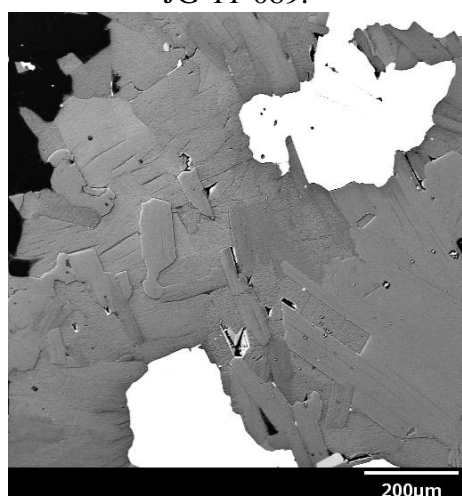
JG-11-084.



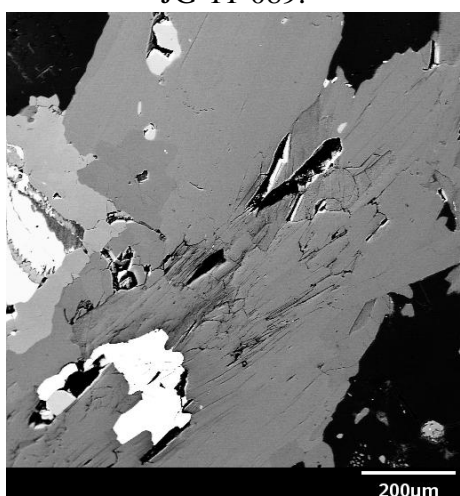
JG-11-089.



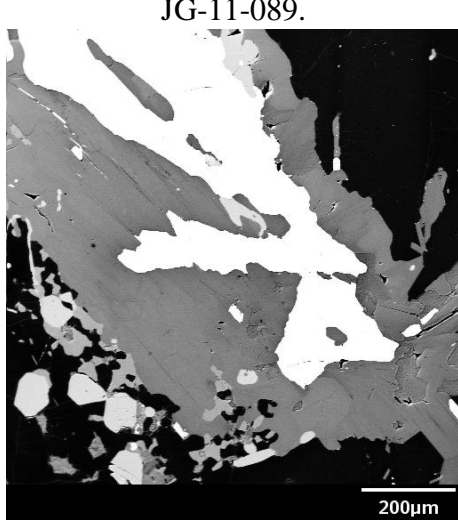
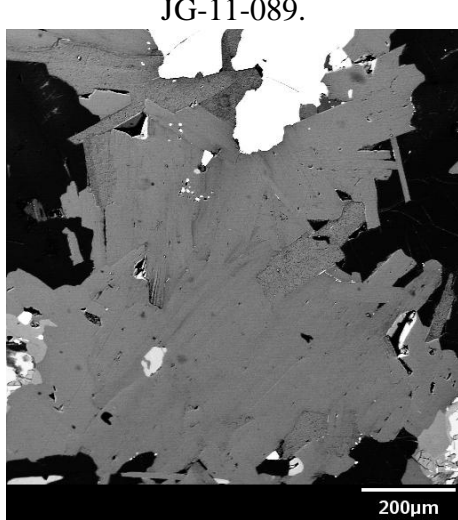
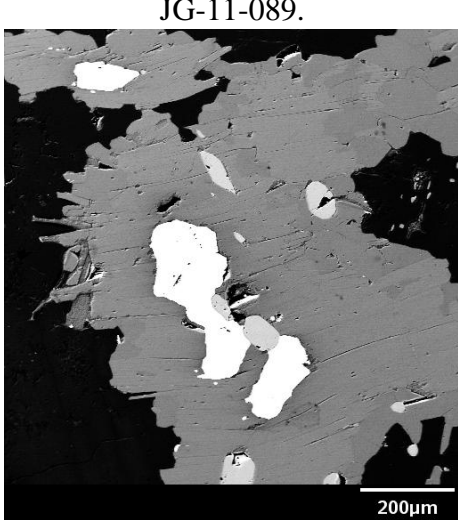
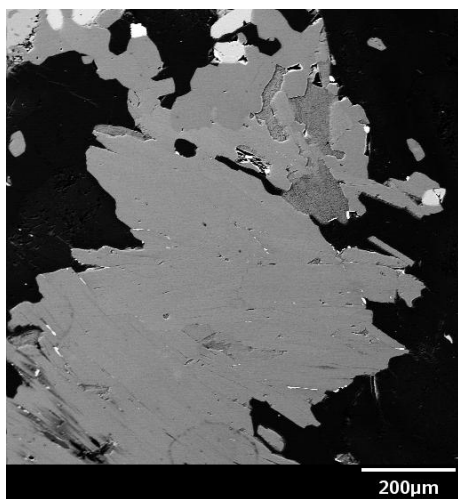
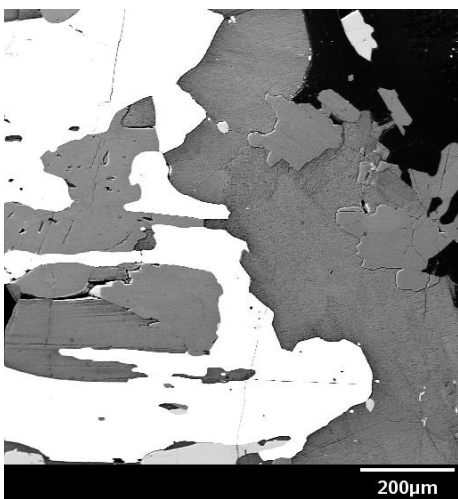
JG-11-089.

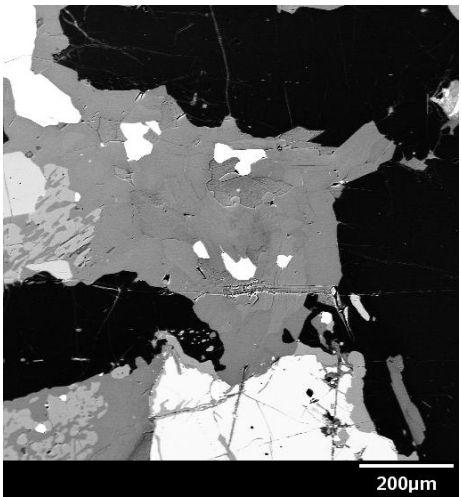


JG-11-089.

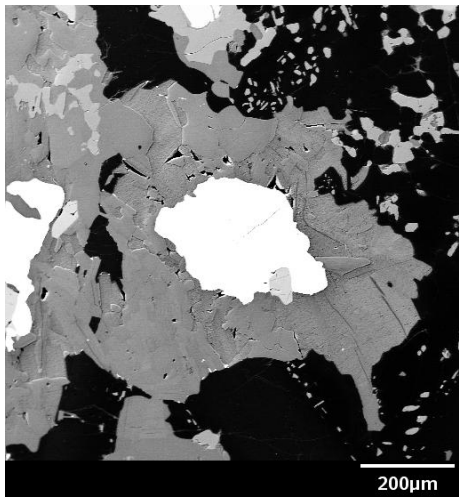


JG-11-089.

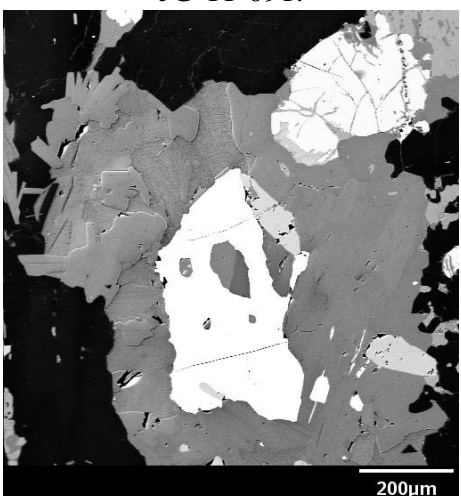




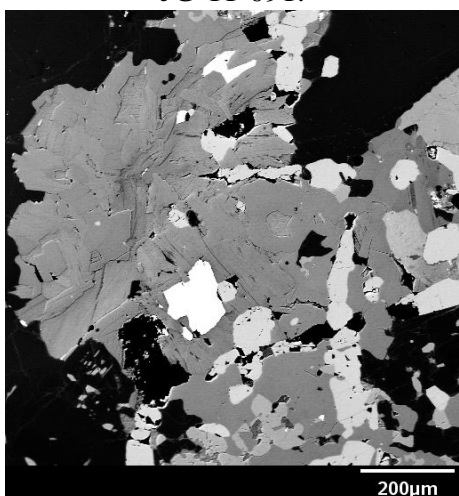
JG-11-091.



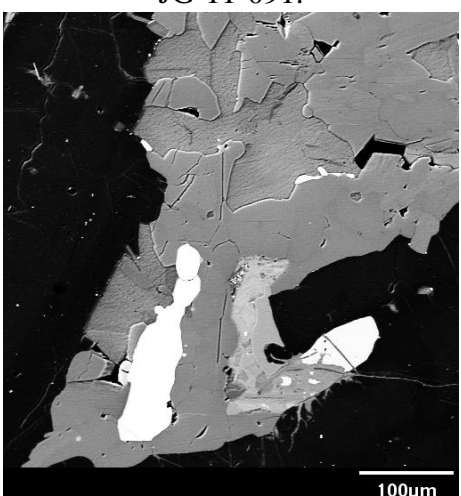
JG-11-091.



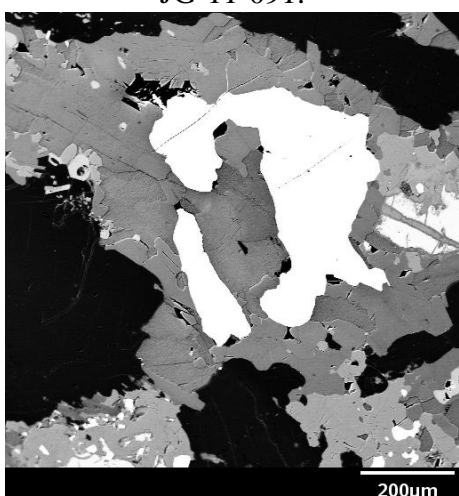
JG-11-091.



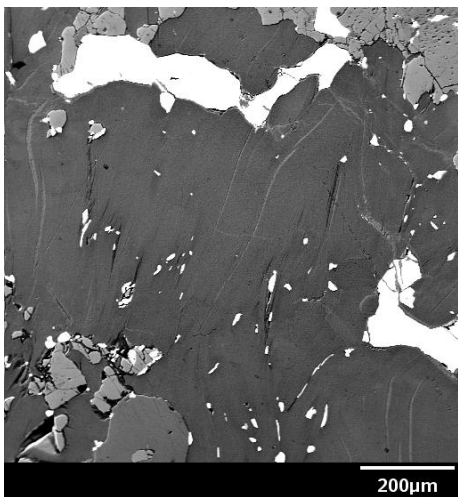
JG-11-091.



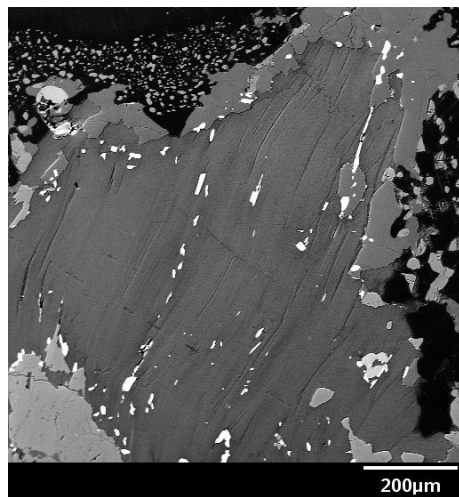
JG-11-091.



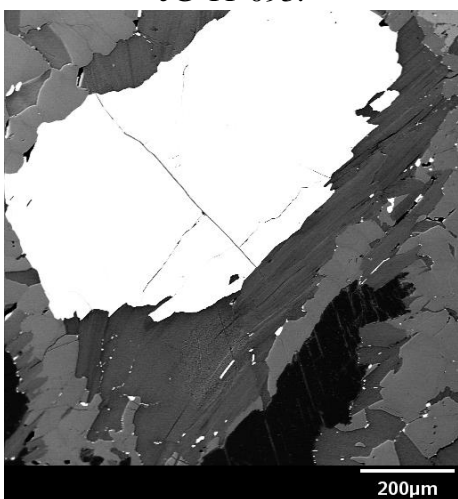
JG-11-091.



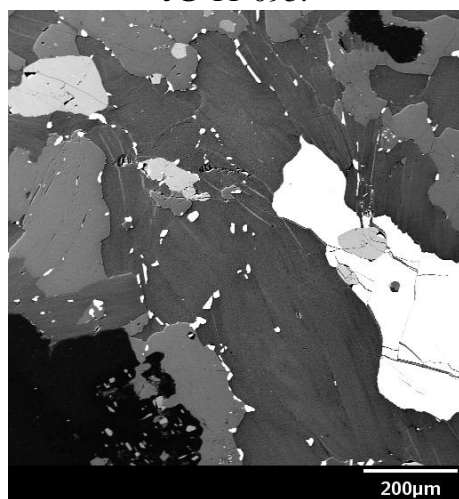
JG-11-093.



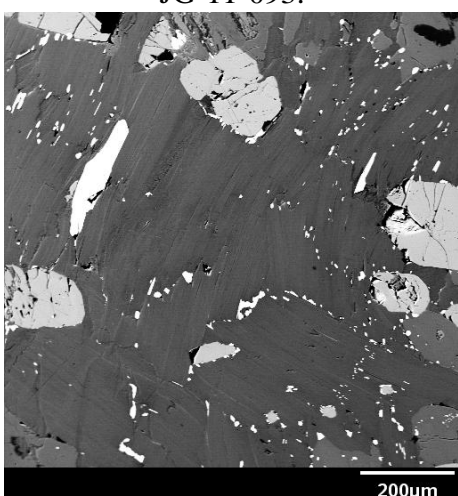
JG-11-093.



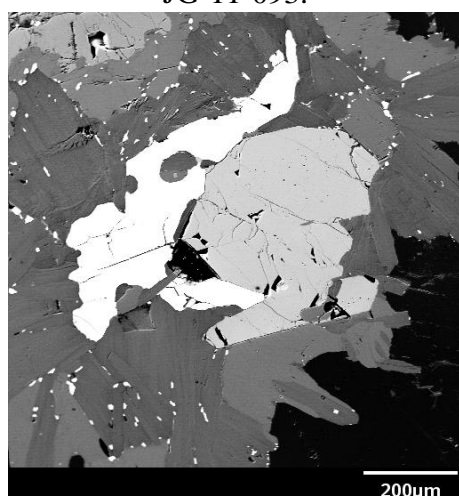
JG-11-093.



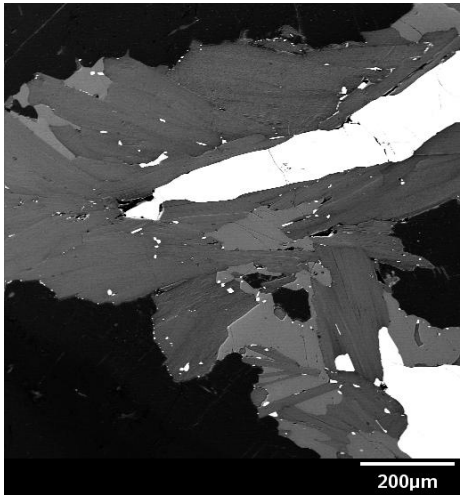
JG-11-093.



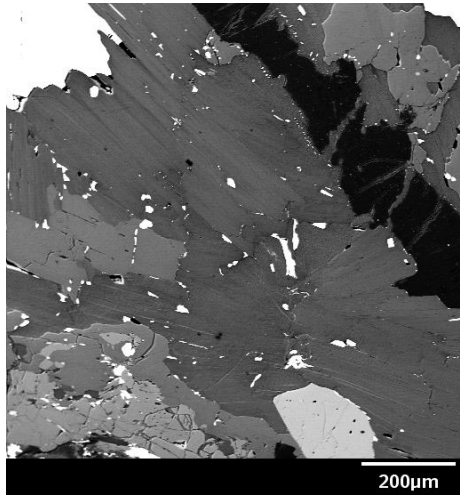
JG-11-093.



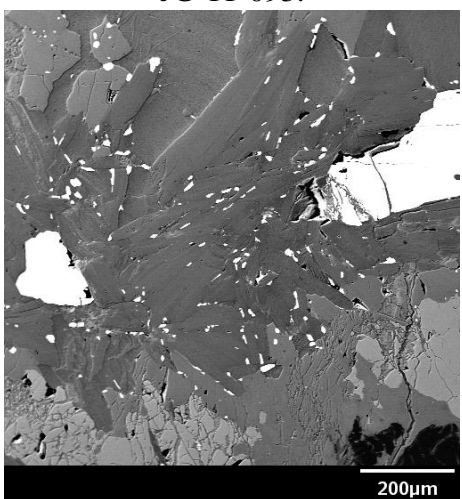
JG-11-093.



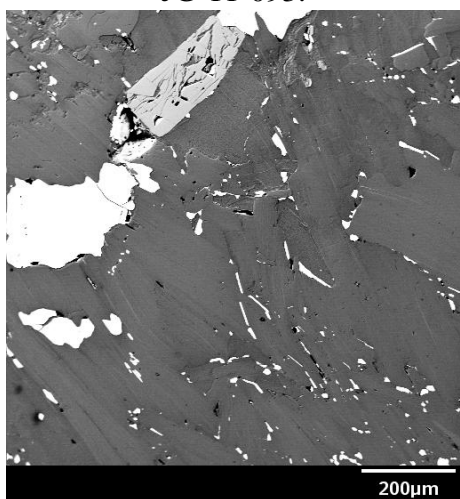
JG-11-093.



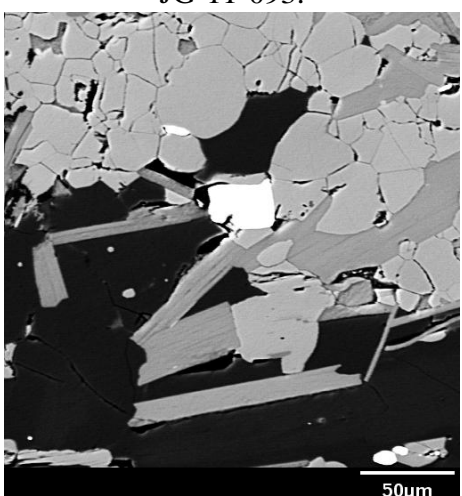
JG-11-093.



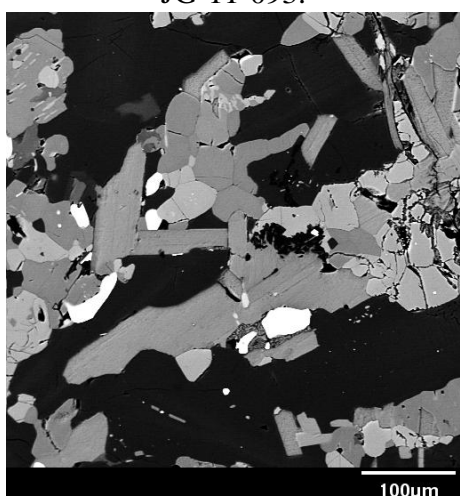
JG-11-093.



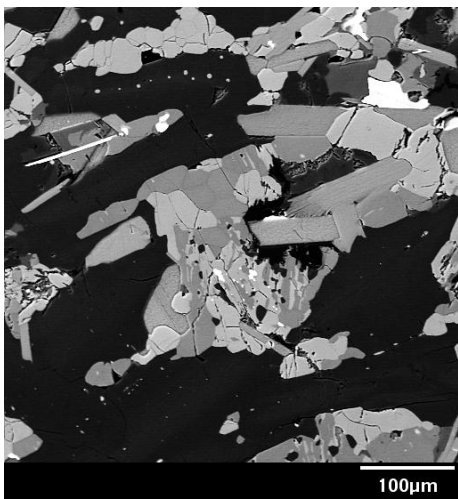
JG-11-093.



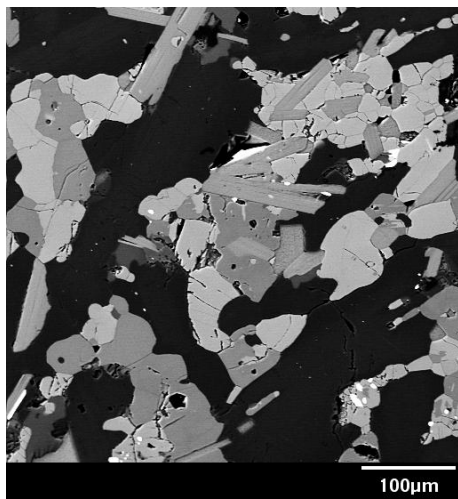
JG-11-100.



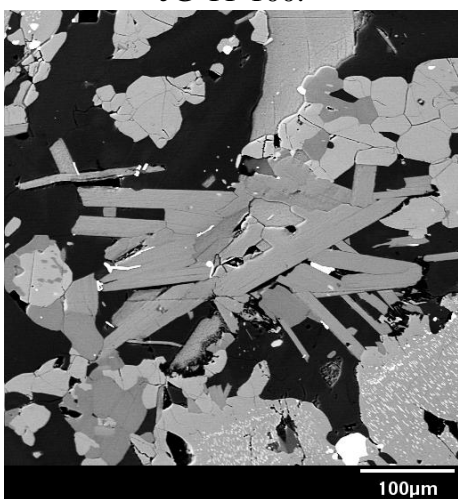
JG-11-100.



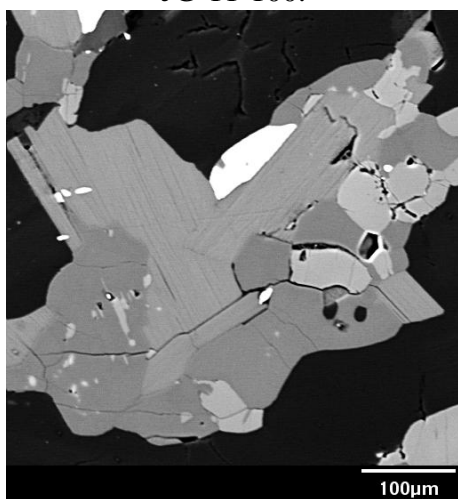
JG-11-100.



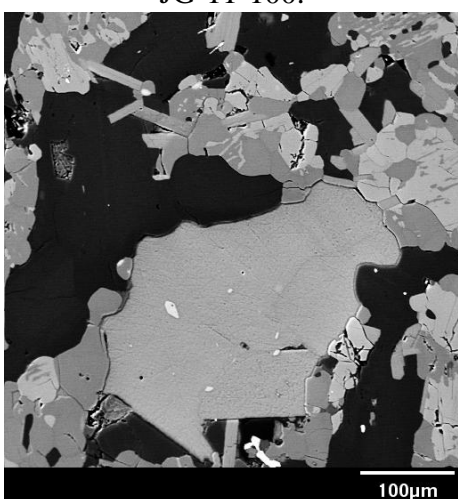
JG-11-100.



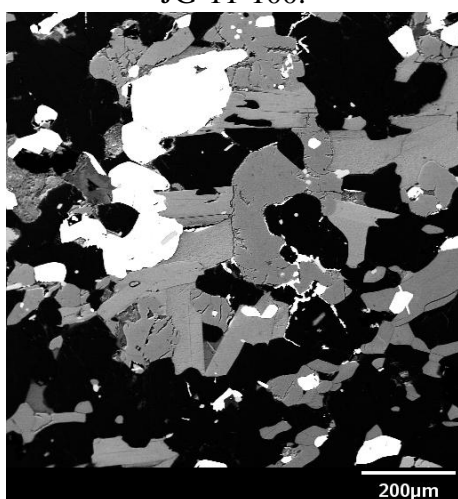
JG-11-100.



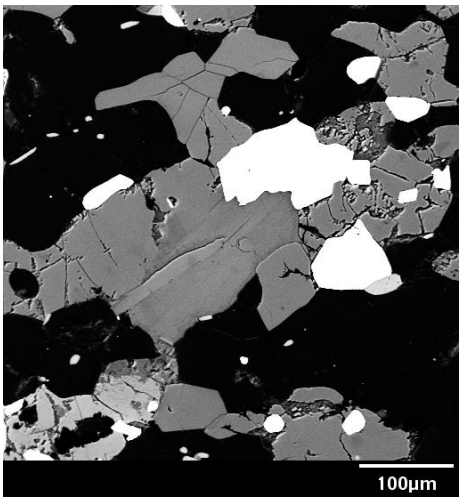
JG-11-100.



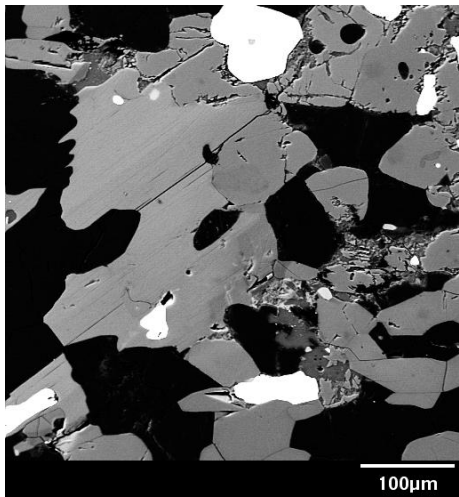
JG-11-100.



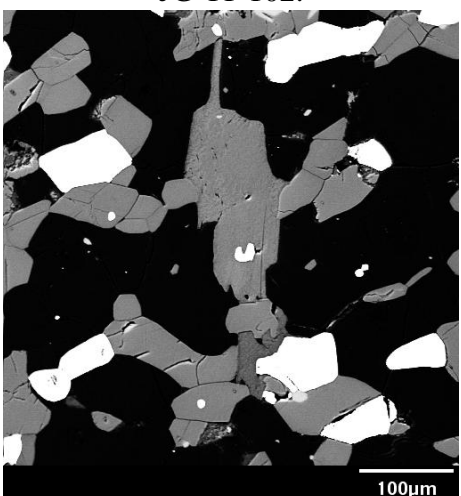
JG-11-102.



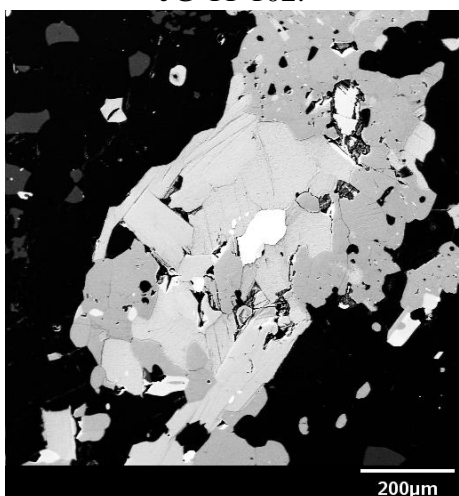
JG-11-102.



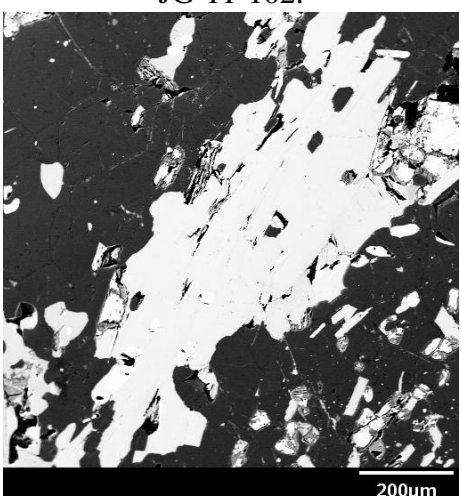
JG-11-102.



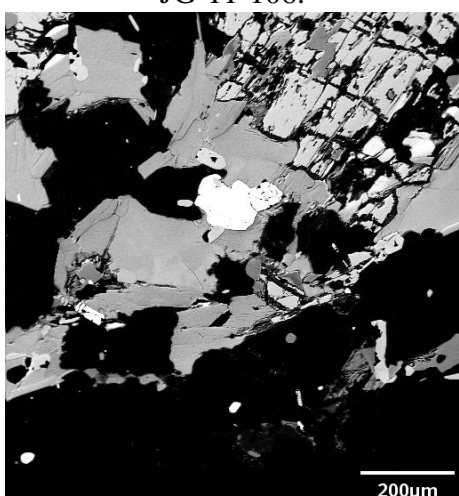
JG-11-102.



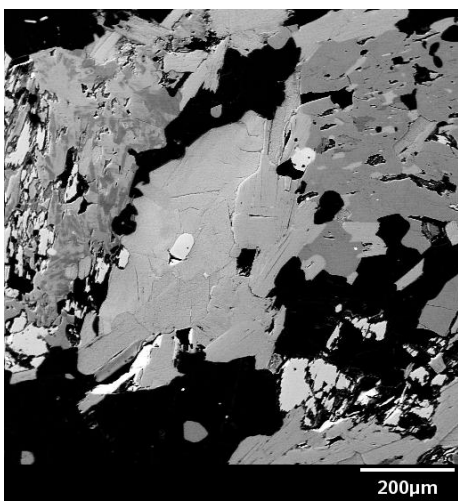
JG-11-106.



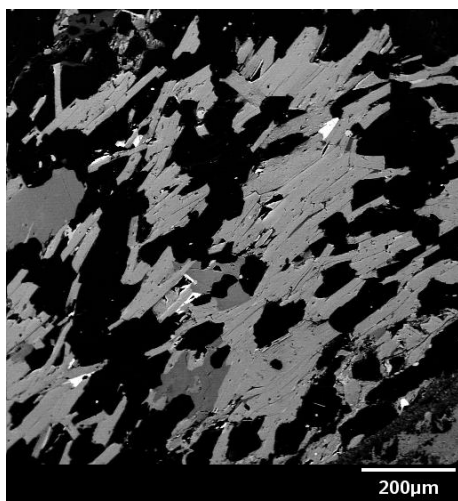
JG-11-106.



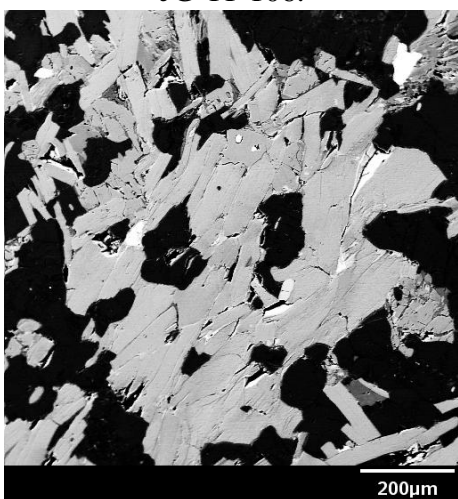
JG-11-106.



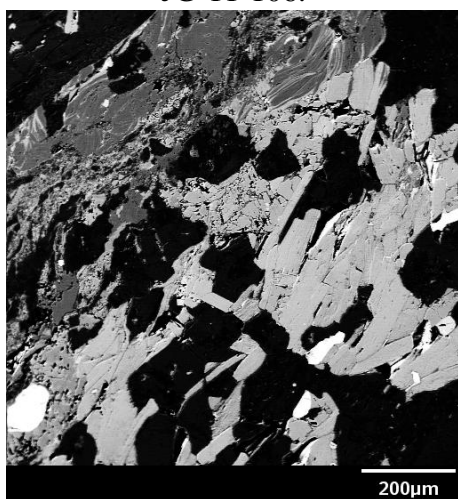
JG-11-106.



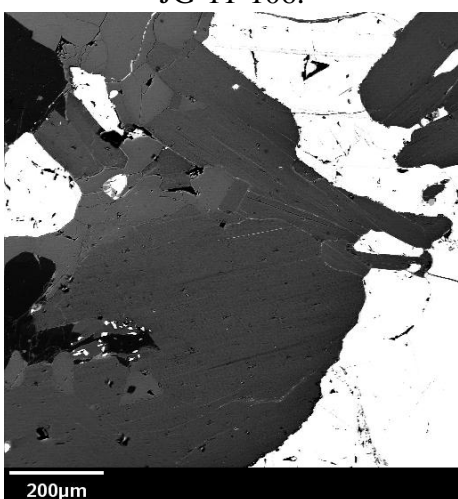
JG-11-106.



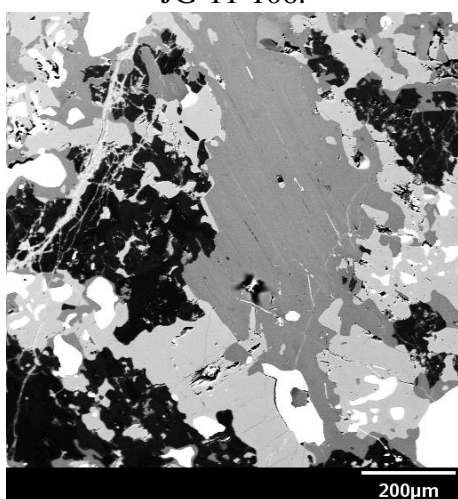
JG-11-106.



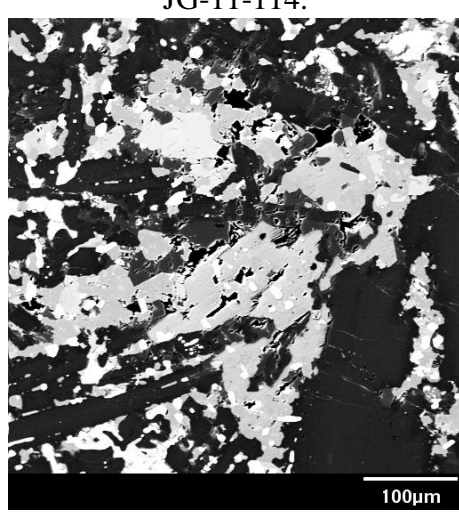
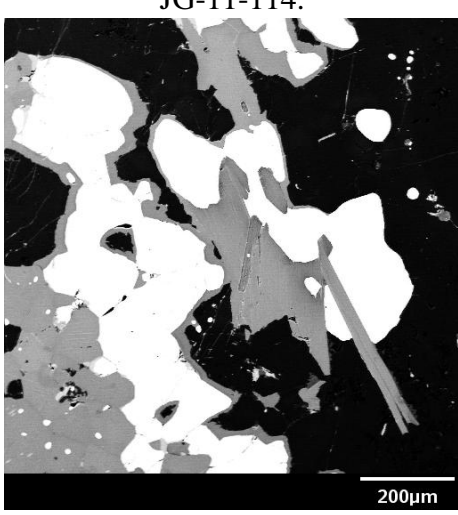
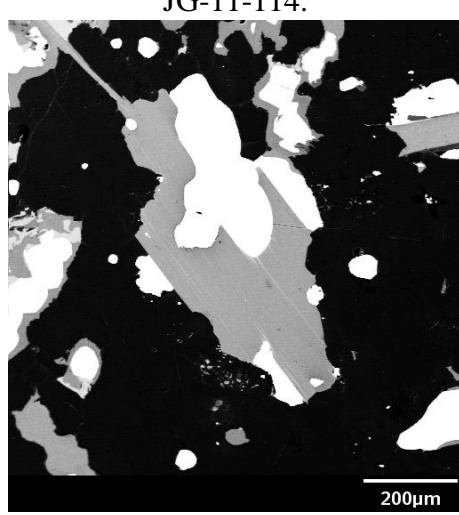
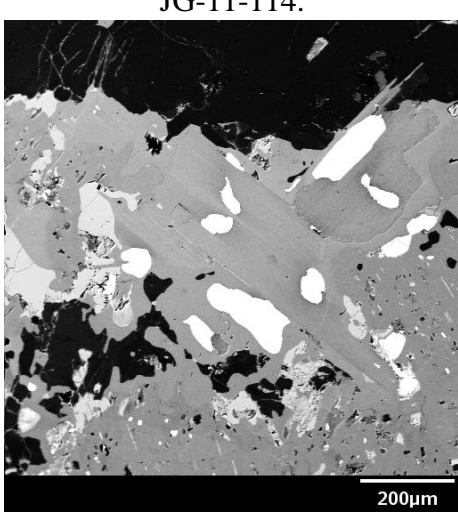
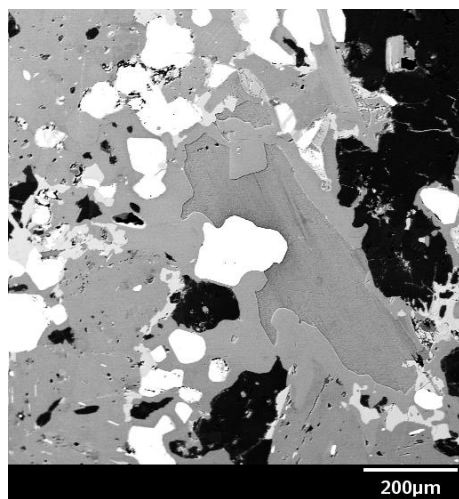
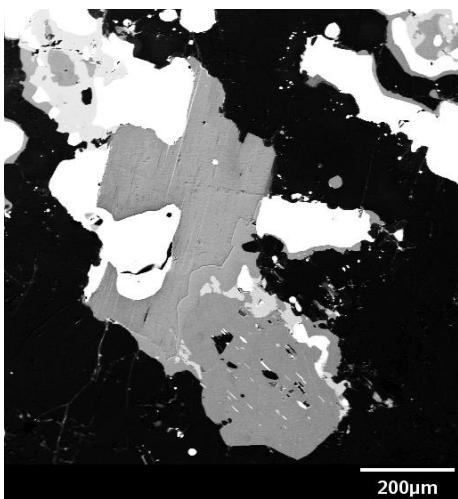
JG-11-106.

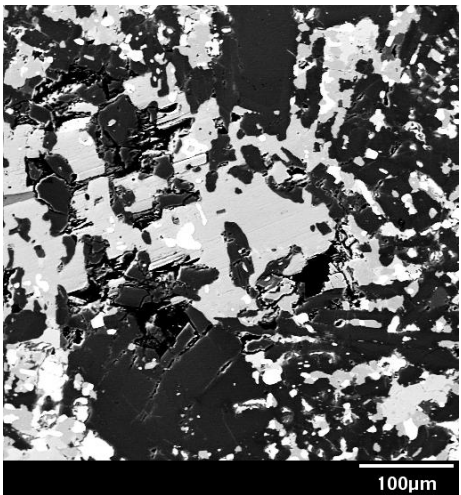


JG-11-106.

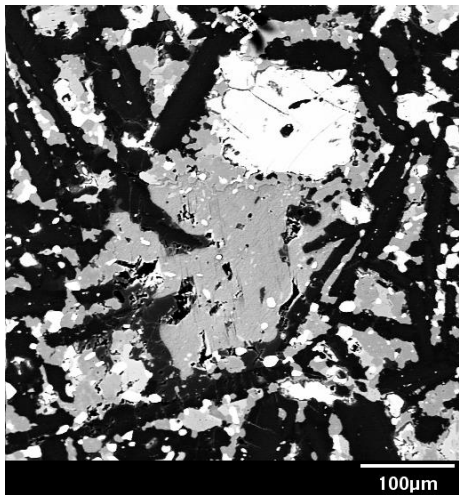


JG-11-114.

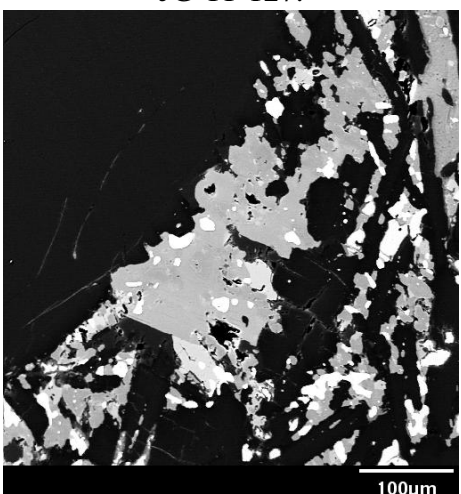




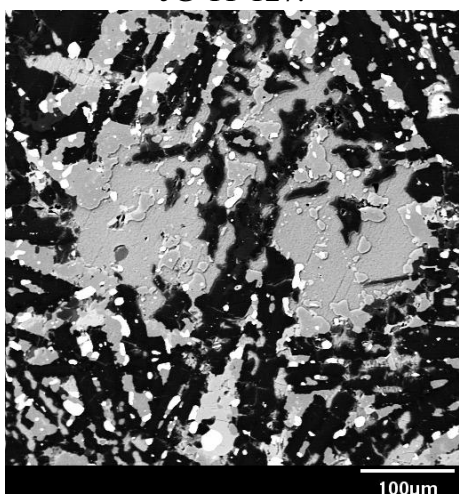
JG-11-127.



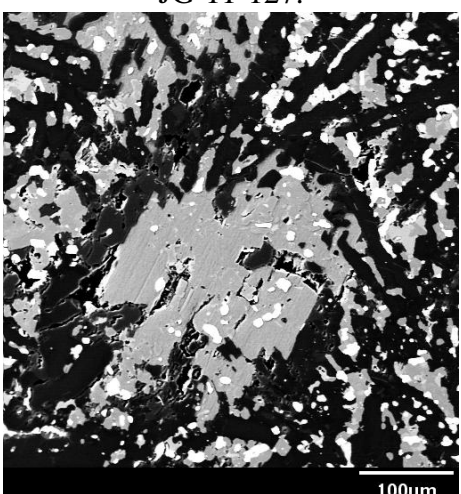
JG-11-127.



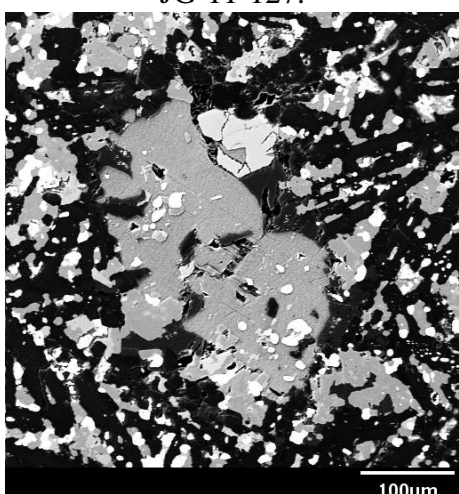
JG-11-127.



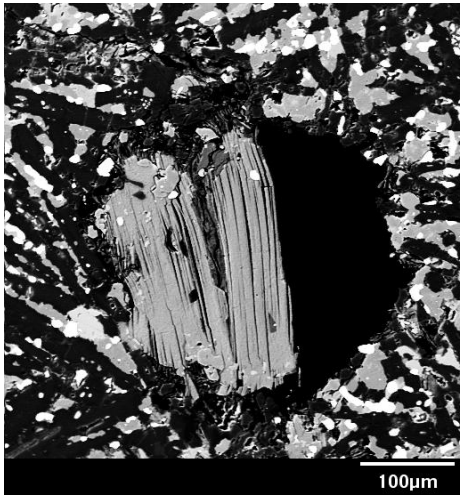
JG-11-127.



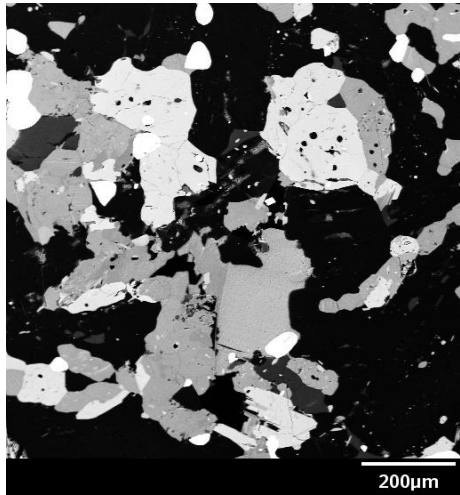
JG-11-127.



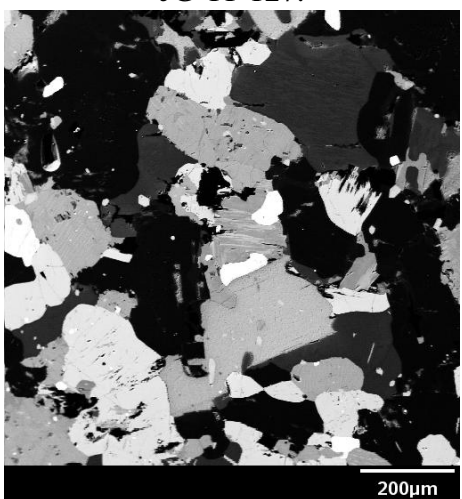
JG-11-127.



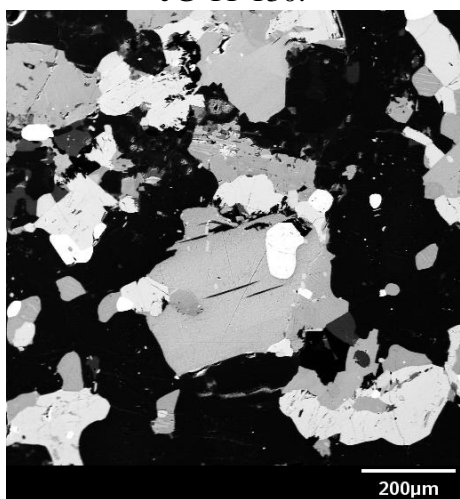
JG-11-127.



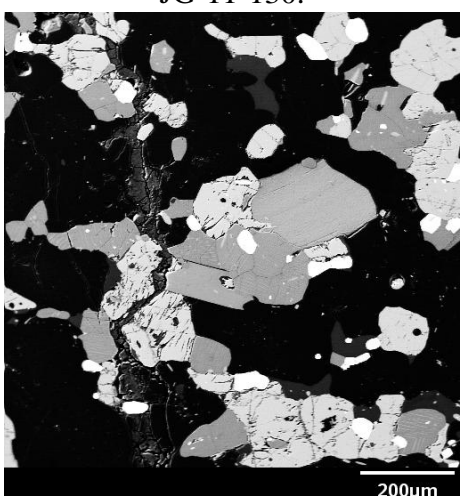
JG-11-130.



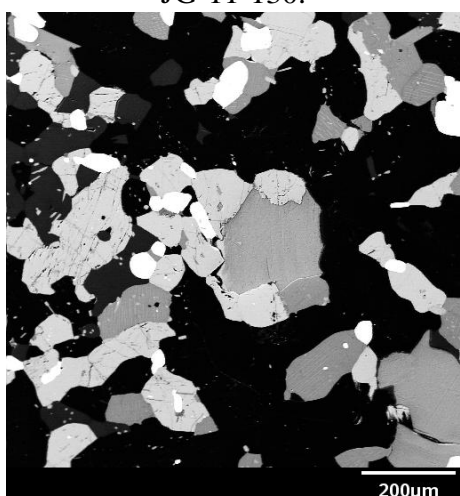
JG-11-130.



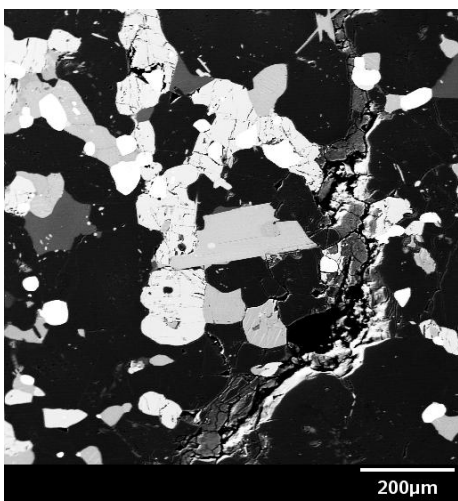
JG-11-130.



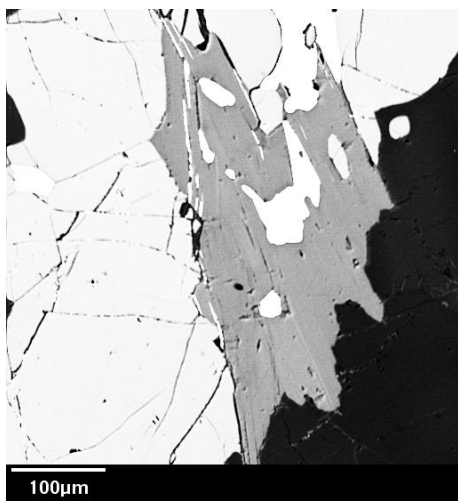
JG-11-130.



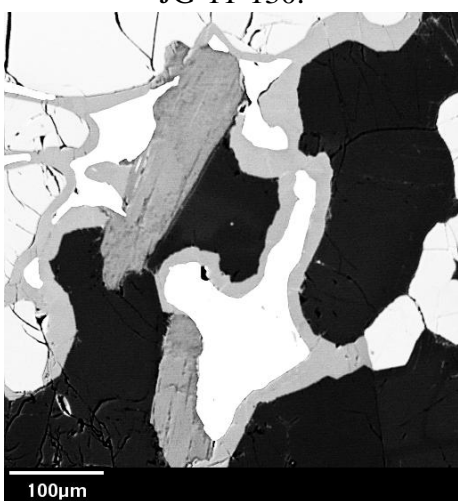
JG-11-130.



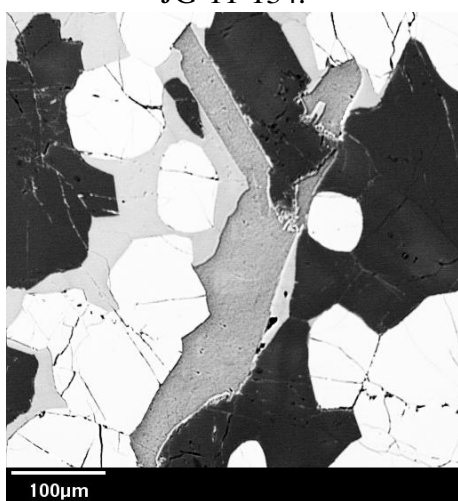
JG-11-130.



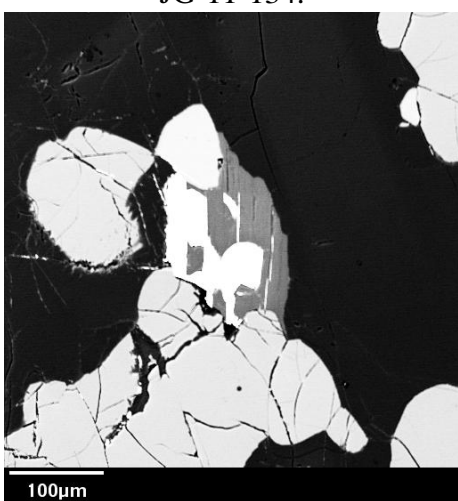
JG-11-134.



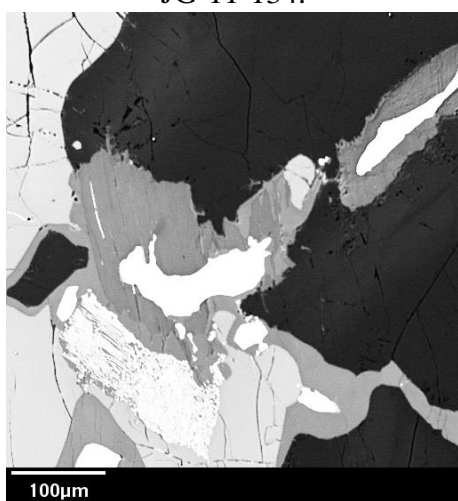
JG-11-134.



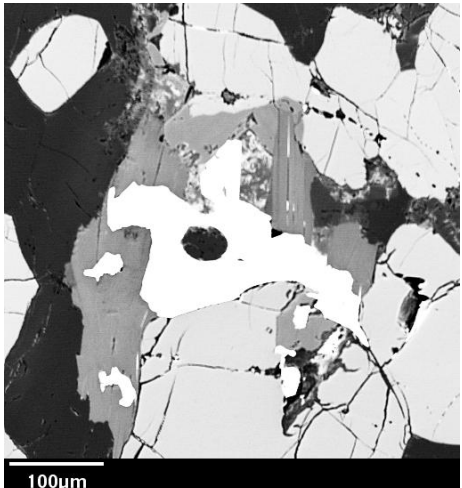
JG-11-134.



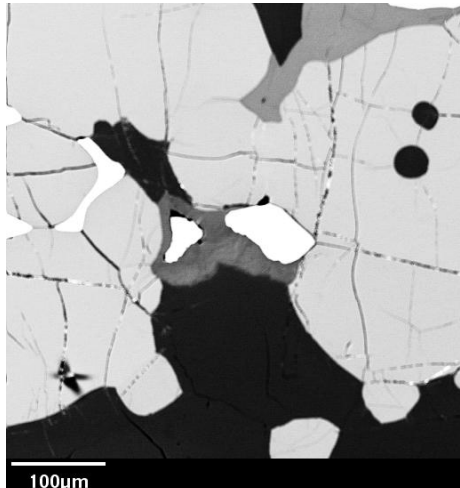
JG-11-134.



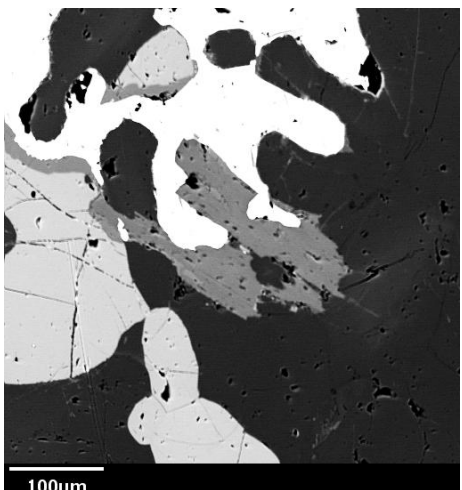
JG-11-134.



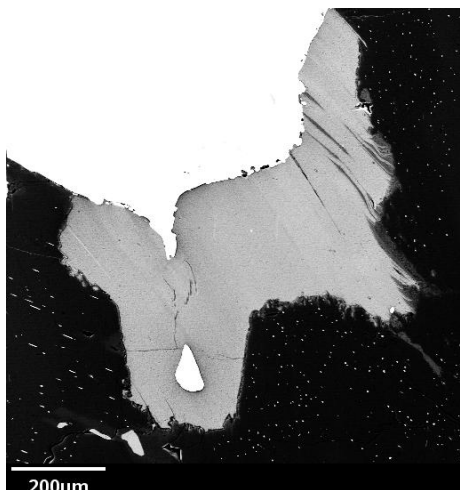
JG-11-134.



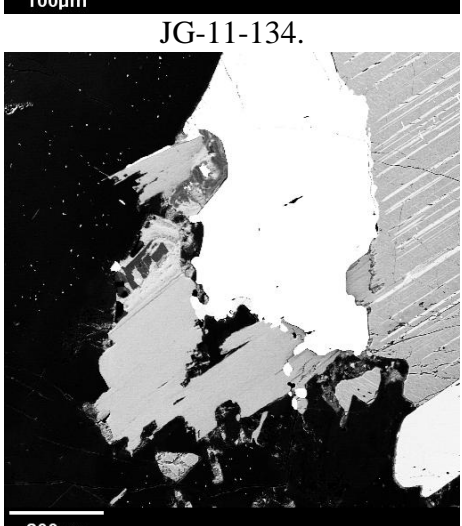
JG-11-134.



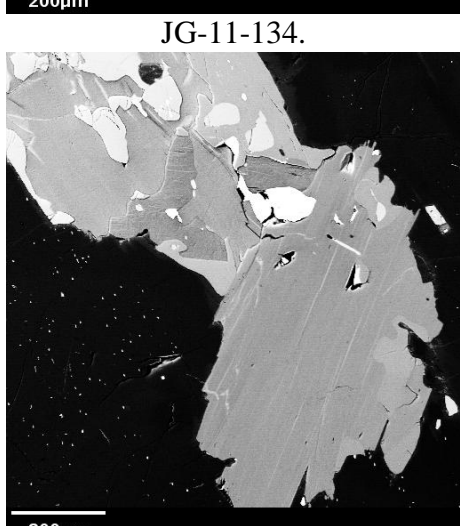
JG-11-134.



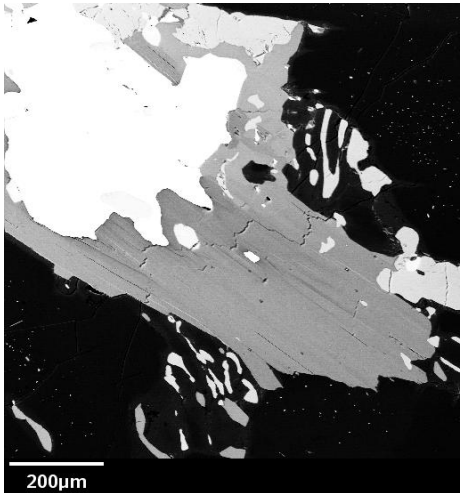
JG-11-134.



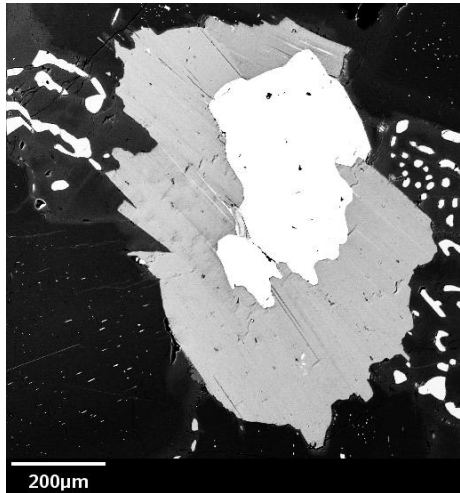
JG-11-137.



JG-11-137.



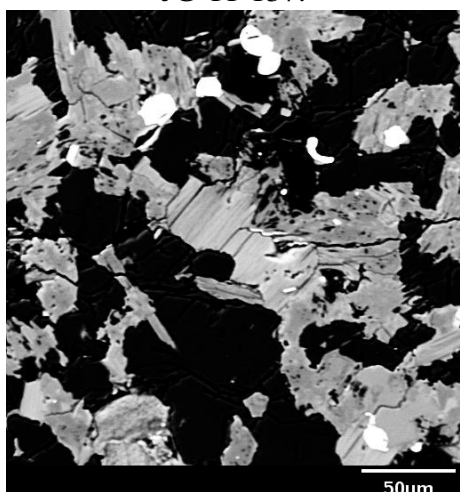
JG-11-137.



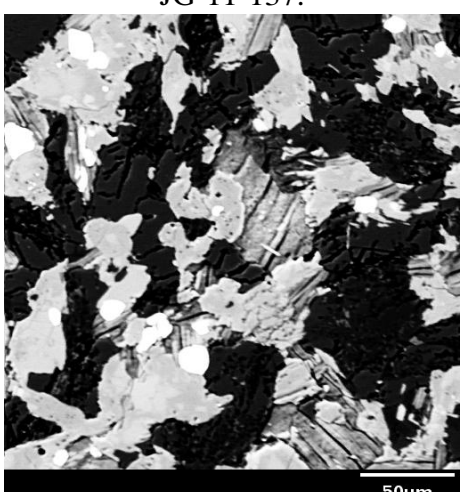
JG-11-137.



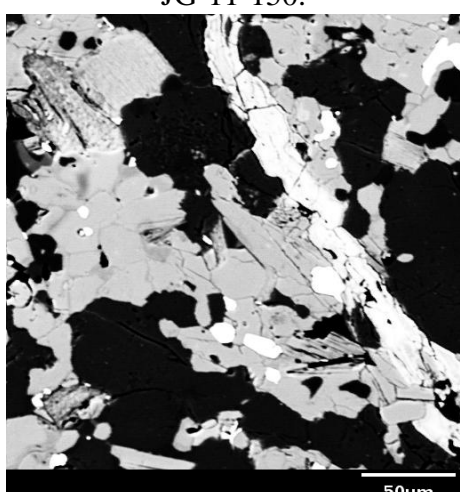
JG-11-137.



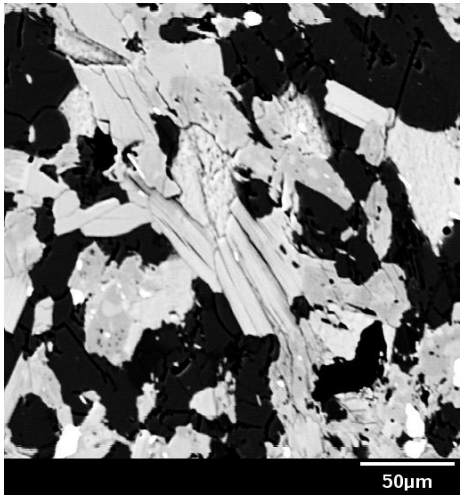
JG-11-150.



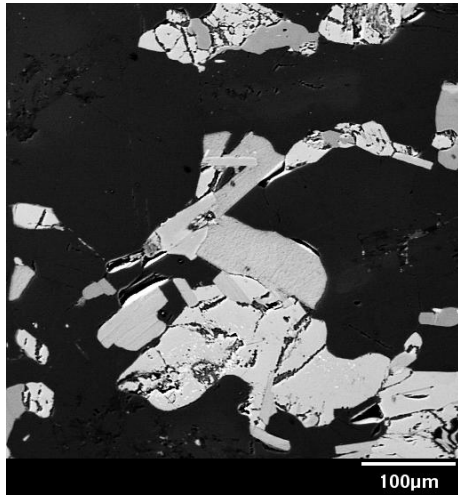
JG-11-150.



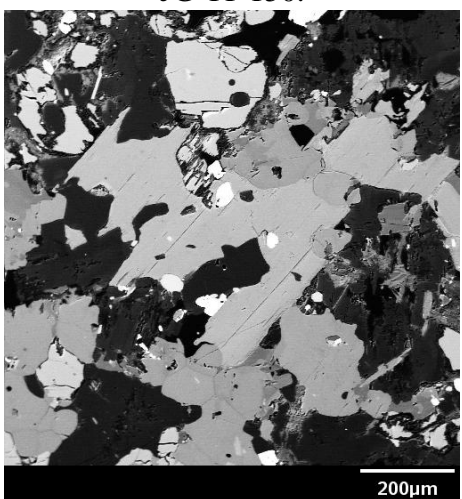
JG-11-150.



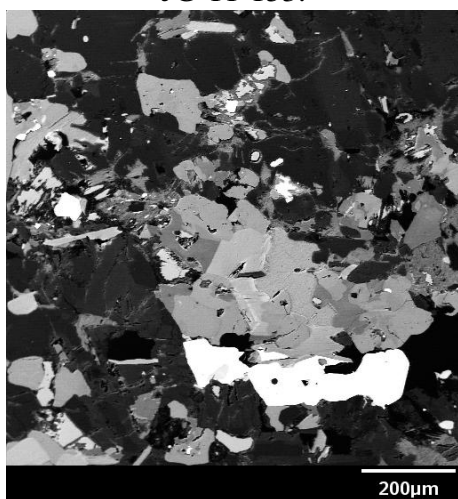
JG-11-150.



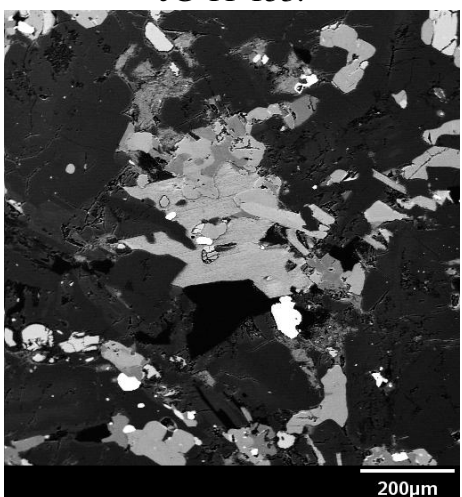
JG-11-153.



JG-11-153.



JG-11-153.



JG-11-153.

Appendix D

Whole rock lithogeochemical data.

Sample	SiO ₂ %	Al ₂ O ₃ %	Fe ₂ O ₃ %	CaO %	MgO %	Na ₂ O %	K ₂ O %
JG-11-001	45.4	18.85	10.05	8.71	9.26	3.12	0.42
JG-11-002	47	19.15	10.25	9.12	7.43	3.44	0.47
JG-11-003	45.9	19.7	8.9	9.23	9.63	2.98	0.31
JG-11-004	46	19.35	8.66	9.07	12.15	2.73	0.19
JG-11-005	48.2	14.75	15.7	7.02	6.19	3.59	0.5
JG-11-006	46.3	19.3	10.75	8.94	8.33	3.35	0.48
JG-11-007	55.8	18.15	5.78	6.44	2.72	5.17	2.99
JG-11-008	54.5	18.05	6.37	6.36	3.02	5.07	3.03
JG-11-009	53.9	17.95	6.4	5.92	3.18	5.64	2.41
JG-11-010	45.2	18.8	9.28	8.53	12.25	2.66	0.23
JG-11-011	49	21.1	8.59	8.46	5.77	3.86	0.49
JG-11-012	46.8	19.95	9.01	9.27	9.23	3.16	0.36
JG-11-013	72.5	12.05	4	1.54	0.25	3.27	4.21
JG-11-014	49.5	16.65	9.91	10.4	9.32	2.31	0.3
JG-11-015	45.8	17.55	11.55	8.47	12.75	2.73	0.28
JG-11-016	44.8	18.6	15.95	8.23	4.87	3.61	0.59
JG-11-017	26.8	9.87	43.6	4.42	4.15	2.17	0.44
JG-11-018	55.5	18.45	6.13	6.73	3.3	5.17	2.33
JG-11-019	44.8	16.9	12.15	7.9	12.3	2.78	0.28
JG-11-020	47.6	19.45	8.86	9.49	8.32	3.03	0.49
JG-11-021	47.7	18.55	10.8	8.38	10.65	2.99	0.72
JG-11-022	46.4	18.85	10.15	8.28	9.59	2.64	0.36
JG-11-023	45.5	17.65	11.25	8.37	10.2	3	0.39
JG-11-024	47.4	19.55	8.91	8.84	10.05	3.05	0.37
JG-11-025	57.4	19	5.9	6.42	2.88	5.09	2.27
JG-11-026	55.7	18	6.14	6.2	3.06	4.88	2.4
JG-11-027	45.5	15.95	14.95	7.8	5.9	3.37	0.94
JG-11-028	44.5	16.15	14.15	7.58	5.73	3.19	0.78
JG-11-029	39.7	18.95	22.9	5.85	4.8	2.24	0.81
JG-11-030	43.9	19.75	11.7	8.22	9.01	2.68	0.35
JG-11-031	49	22.4	7.22	10.2	6.41	2.96	0.52
JG-11-032	48.3	20.4	8.11	9.4	6.79	3.3	0.63
JG-11-033	48.8	21.1	8.19	9.41	8.87	2.84	0.46
JG-11-034	47.7	20.3	8.03	8.76	8.54	2.75	0.63
JG-11-035	47.6	18.55	10	9.16	10.4	2.5	0.31
JG-11-036	58.4	13.65	11.6	5.66	2.35	2.63	2.33
JG-11-037	41.2	16.7	13.4	9.8	7.17	2.44	0.6
JG-11-038	66.6	15.55	5.63	1.25	2.02	2.15	3.89
JG-11-039	73.8	12.65	4.68	1.17	1.72	1.9	2.78
JG-11-040	48.3	18.7	11.9	7	6.96	2.9	1.41
JG-11-041	52	18.7	8.37	8.18	6.3	3.1	1.49
JG-11-042	48.9	20.5	8.49	9.11	7.22	3.55	0.48
JG-11-043	48.7	19.5	9.59	9.34	7.52	3.43	0.63
JG-11-044	48.1	19.65	9.77	8.74	7.77	3.12	0.66
JG-11-045	47.1	16.75	12.45	8.33	9.12	2.54	0.7
JG-11-046	48.1	19	9.59	8.93	7.61	3.3	0.46
JG-11-047	45.5	15.4	12.75	7.58	12.9	2.49	0.3
JG-11-048	59.3	13.6	14.35	5.74	0.74	3.18	2.5
JG-11-049	55.4	11.7	20.1	6.83	1.14	2.33	1.29
JG-11-050	52.7	17.7	8.79	7.31	6.7	3.69	0.33
JG-11-051	51.4	17.85	9.36	7.74	4.77	4.48	0.16
JG-11-052	41.7	7.77	21.4	3.58	26.4	1.05	0.05
JG-11-053	41.1	7.88	22.7	4.28	21.7	1.44	0.19
JG-11-054	78.6	6.67	5.06	2.06	2.28	0.91	0.88

Sample	SiO ₂ %	Al ₂ O ₃ %	Fe ₂ O ₃ %	CaO %	MgO %	Na ₂ O %	K ₂ O %
JG-11-055	46.8	14.15	21.2	4.89	3.93	3.19	0.79
JG-11-056	71.2	12.6	6.74	2.33	2.16	1.98	0.52
JG-11-057	63.1	14.45	6.91	2.16	2.66	2.33	3.14
JG-11-058	53.8	18.95	7.76	7.52	6.25	2.82	1.73
JG-11-059	50	19	10.1	8.22	6.42	3.26	0.74
JG-11-060	47.8	15.65	13.1	7.34	10.95	2.73	0.42
JG-11-061	47.1	14.55	14.95	7.29	11.8	2.31	0.51
JG-11-062	40	6.67	21.6	4.7	21.9	0.89	0.25
JG-11-063	46.8	18.4	10.7	9.18	7.94	3.25	0.44
JG-11-064	59.7	13.15	12.4	5	0.52	3.03	2.75
JG-11-065	42.4	12.55	17.15	10.1	4.59	3.15	0.73
JG-11-066	43.7	8.06	22.6	10.55	5	1.64	1.43
JG-11-067	49.3	19.95	8.85	8.72	7.51	3.14	0.37
JG-11-068	49.1	19.9	9.56	8.21	7.44	3.13	0.46
JG-11-069	43.4	12.05	21.4	7.36	7.63	2.33	0.43
JG-11-070	48	15.15	12.55	9.82	3.12	3.75	0.78
JG-11-071	47.3	18.7	12.9	8.13	7.83	3.08	0.49
JG-11-072	45	16.7	13.95	8.3	5.33	3.69	0.99
JG-11-073	43.5	16.5	14.3	7.63	5.84	3.57	1.71
JG-11-074	43.8	16.7	14.9	7.74	5.11	3.77	1.12
JG-11-075	44.5	16.7	14.3	7.58	5.64	3.76	0.96
JG-11-076	42.8	15.9	17	7.42	4.62	3.72	1.19
JG-11-077	45.2	18.5	13	8.41	6.4	3.64	0.62
JG-11-078	43.7	19.9	12.25	7.48	8.94	2.2	0.58
JG-11-079	46.9	20.2	11.45	8.58	7.94	2	0.42
JG-11-080	49.4	22.1	6.06	9.66	6.27	3.02	0.48
JG-11-081	23.3	7.64	55.6	3.2	2.58	0.23	0.83
JG-11-082	38.5	17.3	22.9	6.08	5.57	1.79	0.28
JG-11-083	35.9	13.8	30.8	4.24	5.84	0.66	1.39
JG-11-084	45.7	16.95	13.6	7.61	5.54	3.8	1.33
JG-11-085	45.6	16.65	14.85	7.75	5.56	3.88	1.06
JG-11-086	41.4	16.45	18.45	6.63	5.94	3.67	1.59
JG-11-087	45.8	15.8	13.9	7.46	5.53	3.41	1.75
JG-11-088	46.1	19.6	14.45	7.51	4.23	3.55	0.7
JG-11-089	46.4	17	14.55	7.89	6.51	3.82	0.99
JG-11-090	46.9	15.65	14.05	7.36	5.62	3.42	1.19
JG-11-091	45.1	16.55	13.75	7.55	6	3.27	0.95
JG-11-092	56.8	17.3	5.91	5.38	2.93	4.75	3.27
JG-11-093	47.3	17.35	11.95	7.6	6.41	3.45	0.78
JG-11-094	46.9	16.9	11.15	7.41	5.9	3.75	0.64
JG-11-095	48.7	20.2	8.05	8.38	8.35	3.2	0.43
JG-11-096	43.6	17.95	15.7	7.59	7	2.96	0.51
JG-11-097	45.4	16.95	14	7.13	7.08	3.36	0.79
JG-11-098	46.7	16.9	12.3	7.34	5.9	3.48	0.87
JG-11-099	52.9	15.3	9.81	9.27	7.05	2.41	0.66
JG-11-100	51.6	15.45	9.7	10	7.76	2.58	0.65
JG-11-101	52.1	15.65	10.5	10.3	7.78	2.87	0.46
JG-11-102	47.8	14.1	16.5	7.81	5.09	3.77	0.59
JG-11-103	52.5	17.85	9.72	7.98	4.28	4.53	0.85
JG-11-104	49.9	14.8	13.35	9.42	7.24	2.33	0.49
JG-11-105	50.6	15.25	10	9.82	7.79	2.62	0.6
JG-11-106	53.6	16.9	9.02	5.47	4	4.55	2.29
JG-11-107	51.7	15.3	9.92	8.79	6.88	2.48	0.82
JG-11-108	35	13.2	26.1	5.25	5.08	2.47	0.71

Sample	SiO ₂ %	Al ₂ O ₃ %	Fe ₂ O ₃ %	CaO %	MgO %	Na ₂ O %	K ₂ O %
JG-11-109	45.3	16.15	14.05	6.74	5.39	3.13	1.59
JG-11-110	48	7.28	11.8	20.2	9.26	0.37	0.91
JG-11-111	47.9	7.74	17.35	9.61	10.35	0.69	1.25
JG-11-112	49.4	6.66	13.65	19.05	7.15	0.37	1.22
JG-11-113	42.8	11.45	18.45	9.42	8.82	1.12	1.28
JG-11-114	49.1	14.4	14.8	9.67	7.29	1.96	0.23
JG-11-115	45.3	14.2	22.5	4.97	3.58	3.79	0.49
JG-11-116	47.8	6.16	14.25	15.6	8.89	0.7	1.03
JG-11-117	47.1	13.7	15.5	10.3	6.53	1.07	0.68
JG-11-118	48.9	14	15.15	10.15	6.27	0.84	0.68
JG-11-119	56.7	15.8	9.08	7.34	6.18	1.25	1.67
JG-11-120	49.8	19.75	9.13	8.94	7.99	3	0.55
JG-11-121	48.6	18.65	9.94	8.76	9.17	2.89	0.35
JG-11-122	48.8	19.25	9.15	8.66	8.33	3.07	0.41
JG-11-123	47.8	18.9	9.55	8.66	9.39	2.86	0.47
JG-11-124	42.9	15.2	13.65	7.34	5.49	3.43	1.02
JG-11-125	44.6	16.35	12.3	9.31	7.54	2.5	0.15
JG-11-126	45	16.6	12.2	9.59	6.46	2.61	0.14
JG-11-127	48.4	14.55	16.5	7.95	5.14	3.67	0.94
JG-11-128	45.2	13.1	20.8	8.24	3.73	3.41	0.49
JG-11-129	49.6	15.25	9.53	10.85	5.4	3.65	0.47
JG-11-130	51.8	13.1	14.7	7.08	4.45	3.53	0.94
JG-11-131	51.3	18.85	8.44	10.6	5.2	3.62	0.57
JG-11-132	42.3	11.95	17.35	5.41	20.9	1.64	0.09
JG-11-133	40.9	7.49	21.5	3.35	25.1	0.94	0.04
JG-11-134	44	12.3	18.6	5.7	18.4	2.1	0.21
JG-11-135	47.6	18.9	14.1	8.11	6.83	3.76	0.32
JG-11-136	49.1	22.9	8.87	10.15	6.07	3.48	0.26
JG-11-137	49.9	24.6	5.06	11.3	2.6	3.7	0.37
JG-11-138	44.8	11.45	20	6.67	9.28	2.52	0.54
JG-11-139	41.6	8.43	23.9	3.71	22.3	1.46	0.12
JG-11-140	53.3	15.75	10.25	9.51	7.19	2.92	0.89
JG-11-141	50.4	17.3	11.4	6.84	4.55	3.77	0.58
JG-11-142	42	12.8	19.2	8.1	3.99	3.07	1.09
JG-11-143	43.4	17.75	17.35	3.87	5.22	2.46	1.61
JG-11-144	57.6	16.55	7.65	3.07	2.88	4.09	2.25
JG-11-145	52.4	17.35	8.46	5.71	4.1	5.11	2.21
JG-11-146	46.4	18.2	10.55	8.2	4.96	3.42	0.71
JG-11-147	60.8	7.79	17.8	1.6	3.3	0.36	0.41
JG-11-148	55.2	15.8	7.32	3.54	2.79	4.23	2.77
JG-11-149	57.5	17.85	6.12	4.49	3.48	5.55	2.44
JG-11-150	48.2	13.6	16.3	6.88	4.52	4.07	1.05
JG-11-151	54.9	18.7	6.66	7.79	3.93	5.29	1.74
JG-11-152	48.7	15.3	10	9.56	8.7	3.06	1.29
JG-11-153	51.2	16.15	9.78	9.23	7	3.04	0.89

Sample	Cr ₂ O ₃ %	TiO ₂ %	MnO %	P ₂ O ₅ %	SrO %	BaO %	C %	S %
JG-11-001	0.01	1.27	0.11	0.33	0.06	0.02	0.12	0.09
JG-11-002	0.01	1.61	0.12	0.27	0.06	0.03	0.04	0.07
JG-11-003	0.01	0.75	0.1	0.18	0.07	0.02	0.04	0.04
JG-11-004	0.01	0.5	0.09	0.15	0.07	0.01	0.04	0.03
JG-11-005	0.01	0.55	0.14	0.1	0.05	0.04	0.07	2.74
JG-11-006	0.01	1.4	0.11	0.33	0.07	0.03	0.05	0.3
JG-11-007	<0.01	0.76	0.09	0.45	0.17	0.2	0.07	0.01
JG-11-008	0.01	0.89	0.09	0.47	0.18	0.21	0.06	0.01
JG-11-009	0.01	0.79	0.1	0.5	0.16	0.18	0.05	0.01
JG-11-010	0.01	0.53	0.1	0.14	0.06	0.01	0.04	0.03
JG-11-011	0.01	0.49	0.08	0.14	0.07	0.02	0.04	1.01
JG-11-012	0.01	0.89	0.1	0.24	0.07	0.02	0.05	0.06
JG-11-013	<0.01	0.5	0.05	0.12	0.02	0.2	0.04	0.02
JG-11-014	0.02	0.39	0.15	0.08	0.05	0.02	0.04	0.03
JG-11-015	0.01	0.7	0.12	0.2	0.06	0.02	0.04	0.16
JG-11-016	0.01	2.43	0.11	0.51	0.07	0.03	0.04	2.95
JG-11-017	0.01	1.86	0.21	0.36	0.04	0.03	0.04	14.1
JG-11-018	0.01	0.74	0.08	0.58	0.17	0.16	0.08	0.01
JG-11-019	0.05	0.93	0.13	0.2	0.06	0.02	0.06	0.16
JG-11-020	0.01	1.2	0.1	0.26	0.07	0.02	0.05	0.05
JG-11-021	0.01	1.15	0.13	0.3	0.07	0.03	0.07	0.28
JG-11-022	0.02	0.94	0.1	0.25	0.06	0.02	0.08	0.51
JG-11-023	0.02	1.51	0.13	0.29	0.07	0.02	0.04	0.44
JG-11-024	0.01	0.92	0.1	0.22	0.07	0.02	0.05	0.13
JG-11-025	<0.01	0.8	0.09	0.41	0.14	0.13	0.04	0.01
JG-11-026	<0.01	0.79	0.09	0.5	0.13	0.15	0.04	0.01
JG-11-027	0.01	3.75	0.18	0.99	0.06	0.06	0.1	0.1
JG-11-028	0.01	3.6	0.18	0.91	0.06	0.05	0.04	0.09
JG-11-029	0.03	1.81	0.11	0.38	0.05	0.04	0.05	5.48
JG-11-030	0.05	1.07	0.1	0.25	0.06	0.02	0.06	1.22
JG-11-031	0.01	1.29	0.09	0.32	0.08	0.03	0.04	0.07
JG-11-032	0.01	1.46	0.1	0.36	0.07	0.03	0.04	0.06
JG-11-033	0.01	0.8	0.1	0.22	0.07	0.02	0.04	0.08
JG-11-034	0.01	1.04	0.1	0.24	0.07	0.03	0.04	0.03
JG-11-035	0.02	1.35	0.12	0.23	0.06	0.02	0.04	0.06
JG-11-036	<0.01	1.25	0.13	0.35	0.04	0.17	0.07	0.09
JG-11-037	0.02	3.18	0.16	0.72	0.04	0.03	0.04	1.55
JG-11-038	0.01	0.75	0.05	0.06	0.03	0.1	0.11	0.07
JG-11-039	0.01	0.51	0.05	0.08	0.03	0.1	0.06	0.05
JG-11-040	0.03	0.94	0.1	0.18	0.05	0.03	0.08	1.81
JG-11-041	0.01	0.86	0.11	0.26	0.06	0.07	0.03	<0.01
JG-11-042	0.01	1.16	0.11	0.26	0.07	0.03	0.03	0.05
JG-11-043	0.02	1.91	0.12	0.46	0.07	0.04	0.04	0.04
JG-11-044	0.01	1.6	0.12	0.36	0.07	0.03	0.02	0.01
JG-11-045	0.01	2.13	0.15	0.25	0.05	0.04	0.05	0.01
JG-11-046	0.01	1.22	0.11	0.34	0.05	0.03	0.05	0.06
JG-11-047	0.02	1.39	0.15	0.11	0.05	0.02	0.05	0.02
JG-11-048	<0.01	1.64	0.18	0.55	0.04	0.27	0.05	0.09
JG-11-049	<0.01	2.29	0.24	0.64	0.03	0.15	0.03	0.12
JG-11-050	0.04	0.36	0.11	0.04	0.06	0.02	0.06	0.85
JG-11-051	0.02	1.85	0.11	0.66	0.17	0.03	0.12	0.1
JG-11-052	<0.01	0.14	0.23	<0.01	0.02	0.01	0.01	0.01
JG-11-053	<0.01	0.84	0.25	0.13	0.02	0.01	0.03	0.04
JG-11-054	0.02	1.01	0.05	0.02	0.02	0.03	0.04	0.1

Sample	Cr ₂ O ₃ %	TiO ₂ %	MnO %	P ₂ O ₅ %	SrO %	BaO %	C %	S %
JG-11-055	0.02	3.65	0.17	0.64	0.04	0.06	0.03	0.04
JG-11-056	0.02	0.48	0.11	0.04	0.03	0.01	0.34	0.14
JG-11-057	0.02	0.7	0.07	0.06	0.03	0.11	1.41	1.06
JG-11-058	0.01	0.92	0.09	0.24	0.06	0.08	0.05	0.03
JG-11-059	0.01	1.71	0.12	0.33	0.06	0.03	0.05	0.05
JG-11-060	0.01	1.78	0.16	0.32	0.05	0.02	0.04	0.06
JG-11-061	0.03	1.97	0.17	0.43	0.05	0.02	0.04	0.09
JG-11-062	0.04	2.54	0.26	0.22	0.02	0.01	0.08	0.06
JG-11-063	0.01	2.19	0.14	0.26	0.06	0.03	0.04	0.06
JG-11-064	<0.01	1.29	0.15	0.43	0.04	0.28	0.08	0.07
JG-11-065	<0.01	4.14	0.22	2.8	0.05	0.05	0.05	0.19
JG-11-066	<0.01	4.86	0.29	2.98	0.03	0.12	0.03	0.24
JG-11-067	0.02	0.89	0.1	0.17	0.06	0.02	0.04	0.04
JG-11-068	0.06	0.98	0.11	0.26	0.06	0.03	0.08	0.08
JG-11-069	0.03	2.13	0.18	0.37	0.04	0.03	0.09	3.28
JG-11-070	<0.01	3.29	0.15	2.33	0.06	0.06	0.06	0.36
JG-11-071	0.06	1.93	0.16	0.43	0.06	0.03	0.06	0.04
JG-11-072	0.01	3.95	0.17	0.91	0.06	0.05	0.09	0.12
JG-11-073	0.01	4.21	0.19	0.91	0.06	0.06	0.06	0.07
JG-11-074	0.01	3.99	0.18	0.89	0.07	0.05	0.14	0.14
JG-11-075	0.01	4.13	0.18	0.81	0.06	0.05	0.05	0.21
JG-11-076	0.01	4.36	0.19	1.03	0.06	0.06	0.15	1.55
JG-11-077	0.01	2.38	0.14	0.54	0.08	0.04	0.15	1.02
JG-11-078	0.06	0.59	0.08	0.17	0.05	0.02	0.11	2.28
JG-11-079	0.01	0.95	0.09	0.34	0.06	0.02	0.06	1.62
JG-11-080	0.01	0.99	0.07	0.36	0.07	0.02	0.04	0.03
JG-11-081	0.19	0.4	0.15	<0.01	0.01	0.03	0.57	3.3
JG-11-082	0.03	0.82	0.15	0.19	0.05	0.01	0.12	4.87
JG-11-083	0.02	1.17	0.23	0.26	0.02	0.05	0.02	3.2
JG-11-084	0.01	3.76	0.18	0.89	0.07	0.06	0.03	0.09
JG-11-085	0.01	4.35	0.18	0.97	0.06	0.06	0.04	0.13
JG-11-086	0.02	2.36	0.13	0.42	0.07	0.06	0.03	3.06
JG-11-087	0.01	3.69	0.19	1.14	0.06	0.06	0.03	0.12
JG-11-088	0.02	1.38	0.09	0.33	0.08	0.04	0.06	2.91
JG-11-089	0.01	3.49	0.17	0.89	0.07	0.05	0.06	0.27
JG-11-090	0.01	3.6	0.17	1.06	0.07	0.05	0.02	0.04
JG-11-091	0.01	3.95	0.14	0.88	0.06	0.04	0.03	0.16
JG-11-092	0.01	0.84	0.07	0.51	0.12	0.14	0.02	0.01
JG-11-093	0.01	2.35	0.13	0.64	0.06	0.04	0.04	0.23
JG-11-094	0.01	2.77	0.12	0.68	0.06	0.04	0.15	0.2
JG-11-095	0.01	0.9	0.08	0.28	0.08	0.03	0.04	0.17
JG-11-096	0.01	1.26	0.09	0.34	0.07	0.03	0.06	3.32
JG-11-097	0.01	1.98	0.12	0.39	0.07	0.04	0.07	1.9
JG-11-098	0.01	3.06	0.14	0.68	0.07	0.04	0.06	0.46
JG-11-099	0.04	0.73	0.15	0.1	0.02	0.04	0.03	0.07
JG-11-100	0.05	0.59	0.15	0.15	0.02	0.03	0.04	0.09
JG-11-101	0.04	0.7	0.17	0.13	0.02	0.03	0.05	0.09
JG-11-102	<0.01	1.64	0.19	0.17	0.04	0.03	0.1	0.12
JG-11-103	0.01	1.22	0.16	0.35	0.06	0.04	0.07	0.06
JG-11-104	0.05	0.62	0.18	0.14	0.02	0.03	0.09	0.82
JG-11-105	0.07	0.7	0.15	0.16	0.03	0.02	0.04	0.09
JG-11-106	0.01	1.84	0.1	0.47	0.1	0.1	0.08	0.09
JG-11-107	0.03	0.85	0.14	0.15	0.03	0.05	0.05	0.09
JG-11-108	0.01	3.18	0.14	0.38	0.06	0.05	0.03	7.48

Sample	Cr ₂ O ₃ %	TiO ₂ %	MnO %	P ₂ O ₅ %	SrO %	BaO %	C %	S %
JG-11-109	0.01	3.54	0.13	0.89	0.06	0.07	0.05	0.11
JG-11-110	0.12	2.13	0.14	0.15	0.03	0.02	0.12	0.85
JG-11-111	0.11	2.02	0.22	0.27	0.03	0.04	0.06	0.48
JG-11-112	0.11	1.87	0.18	0.3	0.05	0.04	0.07	0.65
JG-11-113	0.06	4.14	0.25	0.63	0.04	0.05	0.07	0.11
JG-11-114	0.03	1.08	0.22	0.06	0.02	0.01	0.05	0.8
JG-11-115	0.03	0.54	0.2	0.16	0.02	0.02	0.06	6.04
JG-11-116	0.1	1.8	0.25	0.36	0.02	0.05	0.34	0.15
JG-11-117	0.02	1.8	0.21	0.25	0.02	0.02	0.1	0.47
JG-11-118	0.02	1.57	0.2	0.2	0.02	0.02	0.23	0.35
JG-11-119	0.03	0.81	0.14	0.23	0.03	0.06	0.04	0.02
JG-11-120	0.01	1.32	0.11	0.3	0.07	0.03	0.03	0.05
JG-11-121	0.02	1.37	0.12	0.31	0.06	0.02	0.05	0.06
JG-11-122	<0.01	1.16	0.11	0.38	0.06	0.03	0.03	0.05
JG-11-123	0.01	1.4	0.12	0.32	0.06	0.03	0.03	0.06
JG-11-124	0.01	3.88	0.16	1.06	0.05	0.05	0.04	0.16
JG-11-125	0.01	1.38	0.17	0.15	0.03	0.01	0.04	0.04
JG-11-126	0.01	1.44	0.16	0.16	0.03	0.01	0.04	0.11
JG-11-127	0.01	2.83	0.21	0.9	0.04	0.05	0.14	0.13
JG-11-128	<0.01	3.07	0.24	0.36	0.04	0.07	0.07	0.1
JG-11-129	0.01	4.58	0.12	0.22	0.05	0.03	0.02	0.2
JG-11-130	0.01	2.38	0.19	0.5	0.04	0.07	0.04	0.06
JG-11-131	0.01	0.9	0.11	0.3	0.08	0.04	0.06	0.3
JG-11-132	<0.01	0.14	0.19	0.03	0.03	0.01	0.01	0.01
JG-11-133	<0.01	0.08	0.23	0.05	0.02	<0.01	<0.01	<0.01
JG-11-134	0.01	0.62	0.21	0.09	0.03	0.01	0.01	0.02
JG-11-135	0.06	1.53	0.15	0.07	0.05	0.02	0.03	0.04
JG-11-136	<0.01	0.45	0.11	0.09	0.06	0.02	0.04	0.02
JG-11-137	<0.01	0.76	0.06	0.1	0.07	0.02	0.02	0.02
JG-11-138	<0.01	4.52	0.23	0.18	0.04	0.04	0.03	0.14
JG-11-139	<0.01	0.24	0.27	0.06	0.03	0.01	0.04	0.01
JG-11-140	0.04	0.81	0.15	0.11	0.03	0.04	0.05	0.12
JG-11-141	0.01	2.77	0.15	0.65	0.07	0.04	0.01	0.63
JG-11-142	<0.01	3.18	0.3	1.33	0.03	0.08	0.09	0.21
JG-11-143	0.02	1.86	0.12	0.44	0.06	0.1	0.29	0.85
JG-11-144	0.01	0.54	0.07	0.33	0.06	0.06	0.52	0.16
JG-11-145	0.01	1.72	0.11	0.57	0.09	0.09	0.06	0.05
JG-11-146	0.01	2.58	0.12	0.56	0.07	0.04	0.04	0.1
JG-11-147	0.01	1.34	0.07	0.34	<0.01	0.02	0.07	3.05
JG-11-148	0.01	0.67	0.07	0.35	0.11	0.15	0.07	0.07
JG-11-149	0.02	0.54	0.08	0.33	0.14	0.13	0.07	0.04
JG-11-150	0.01	2.11	0.18	0.42	0.06	0.08	0.04	0.23
JG-11-151	0.01	0.8	0.1	0.5	0.22	0.14	0.03	0.01
JG-11-152	0.05	1.32	0.16	0.23	0.09	0.03	0.03	0.01
JG-11-153	0.04	0.8	0.15	0.12	0.04	0.05	0.03	0.09

Sample	Ag ppm	Ba ppm	Ce ppm	Co ppm	Cr ppm	Cs ppm	Cu ppm	Dy ppm
JG-11-001	<1	215	23	77.3	70	0.03	12	2.37
JG-11-002	<1	243	18.5	71.1	90	0.05	26	2.09
JG-11-003	<1	180	12.3	82	70	0.04	20	1.34
JG-11-004	<1	123	9.6	89	70	0.01	5	0.93
JG-11-005	<1	337	11.9	96.1	100	0.07	607	1.15
JG-11-006	<1	236	23	99.2	80	0.05	401	2.49
JG-11-007	<1	1685	93.5	43.7	40	0.1	66	3.87
JG-11-008	<1	1795	93.8	52.5	40	0.21	49	3.07
JG-11-009	<1	1485	87.8	40.4	40	0.48	47	3.08
JG-11-010	<1	122	7.6	93.6	90	0.02	15	0.8
JG-11-011	<1	194.5	11.9	115	80	0.2	639	1.22
JG-11-012	<1	185	15	82.5	100	0.03	43	1.65
JG-11-013	<1	1570	128	106.5	<10	0.13	5	6.58
JG-11-014	<1	164	9.2	66.2	170	0.04	13	1.45
JG-11-015	<1	166.5	12.2	102.5	90	0.02	94	1.21
JG-11-016	1	270	31.9	198.5	80	0.07	2110	3.79
JG-11-017	1	224	22	817	80	0.07	5250	2.1
JG-11-018	<1	1390	92.1	43.5	50	0.11	37	3.05
JG-11-019	<1	157	13	108.5	390	0.02	98	1.44
JG-11-020	<1	206	35.4	70.6	110	0.08	38	3.66
JG-11-021	<1	256	23.8	96.6	80	0.39	267	2.27
JG-11-022	<1	212	15.7	92.9	150	0.13	324	1.57
JG-11-023	<1	223	19.3	109.5	170	0.02	294	2.03
JG-11-024	<1	200	15.7	95	80	0.16	109	1.51
JG-11-025	<1	1185	94.7	44.1	40	0.6	70	2.67
JG-11-026	<1	1475	88.3	44.3	40	0.26	43	2.56
JG-11-027	<1	528	66.3	66.6	70	0.11	151	6.03
JG-11-028	<1	475	66	63.3	70	0.18	106	5.87
JG-11-029	1	364	42	360	230	0.09	2090	3
JG-11-030	<1	229	18	174	400	0.02	527	1.66
JG-11-031	<1	269	24.4	56.5	70	0.09	23	2.37
JG-11-032	<1	263	33.3	63.4	90	0.09	15	3.19
JG-11-033	<1	207	16.6	79.1	70	0.07	22	1.53
JG-11-034	<1	314	18.8	66.9	70	0.04	7	1.86
JG-11-035	<1	223	20.2	81.8	130	0.02	12	2.17
JG-11-036	<1	1700	93.8	71.2	40	0.03	29	9.8
JG-11-037	1	242	51.1	182	120	0.12	2230	4.56
JG-11-038	<1	892	191.5	85.4	100	0.32	29	8.32
JG-11-039	<1	885	90.5	127	90	0.14	21	4.43
JG-11-040	<1	242	70.5	161	220	0.12	863	4.56
JG-11-041	<1	670	41	71.5	60	0.06	13	4.97
JG-11-042	<1	281	20.8	75.6	90	0.02	15	2.02
JG-11-043	<1	355	31	75.9	120	0.04	15	3.22
JG-11-044	<1	316	28	74.2	40	0.04	24	2.67
JG-11-045	<1	336	26	81.7	70	0.08	24	3.09
JG-11-046	<1	256	20.9	79.5	60	0.03	26	2.13
JG-11-047	<1	208	238	102.5	160	0.03	27	3.19
JG-11-048	<1	2430	116	73.3	<10	0.02	18	11.85
JG-11-049	<1	1375	127	63.9	<10	0.02	23	14.45
JG-11-050	<1	184.5	10.1	109.5	320	0.03	380	0.78
JG-11-051	<1	244	22.7	69	150	0.01	105	1.02
JG-11-052	<1	45.3	2.6	207	50	<0.01	7	0.31
JG-11-053	<1	125.5	14.5	188.5	50	0.03	24	2.13
JG-11-054	<1	250	38.4	155.5	170	0.14	85	1.07

Sample	Ag ppm	Ba ppm	Ce ppm	Co ppm	Cr ppm	Cs ppm	Cu ppm	Dy ppm
JG-11-055	<1	531	40.8	90.8	160	0.16	5	3.71
JG-11-056	<1	118.5	43.2	110	110	0.03	9	6.65
JG-11-057	<1	993	69.1	85.6	130	0.2	50	4.58
JG-11-058	<1	760	40.5	80.9	60	0.03	11	3.85
JG-11-059	<1	308	30.5	68.8	70	0.37	22	2.76
JG-11-060	<1	246	21.3	98.7	70	0.04	18	2.33
JG-11-061	<1	247	27.2	103.5	210	0.02	30	2.87
JG-11-062	<1	110	14.9	149	290	0.06	15	1.85
JG-11-063	<1	236	21.1	69.3	90	0.02	12	2.32
JG-11-064	<1	2480	121	63.5	<10	0.05	15	11.8
JG-11-065	<1	478	93.4	56.9	<10	0.06	50	10.05
JG-11-066	<1	1180	186.5	80.4	10	0.04	41	20.7
JG-11-067	<1	226	15.8	72.8	170	0.02	27	1.62
JG-11-068	<1	258	18.1	78.7	460	0.02	31	1.75
JG-11-069	<1	291	25.3	188.5	240	0.03	400	3.14
JG-11-070	<1	580	97.2	61.2	10	0.04	73	10.3
JG-11-071	<1	287	32.3	82.4	420	0.04	18	3.03
JG-11-072	<1	493	65	64.4	70	0.14	64	6.14
JG-11-073	<1	580	65.7	63.1	70	1.15	102	5.75
JG-11-074	<1	482	61.2	73.2	60	0.42	71	6
JG-11-075	<1	497	59.9	91.6	80	0.22	123	5.46
JG-11-076	<1	530	69.8	131	50	0.16	719	6.18
JG-11-077	<1	346	39.2	117	50	0.14	457	3.59
JG-11-078	1	178	27.6	188.5	490	0.23	1090	1.99
JG-11-079	<1	201	24.3	160.5	70	0.08	732	2.26
JG-11-080	<1	252	26.7	67.2	50	0.08	16	2.52
JG-11-081	2	249	6.2	787	1600	0.8	7350	0.39
JG-11-082	1	91.6	12.4	467	240	0.04	1975	1.02
JG-11-083	1	417	26.4	276	120	0.02	4180	1.84
JG-11-084	<1	560	66.3	68.9	60	0.33	71	6.03
JG-11-085	<1	512	70.3	68.2	80	0.14	38	6.6
JG-11-086	1	534	35.8	221	160	0.55	2170	3.08
JG-11-087	<1	634	86.2	66.2	60	0.84	155	6.89
JG-11-088	1	364	27.7	234	140	0.28	1860	2.51
JG-11-089	1	510	66	81.9	50	0.09	531	6.15
JG-11-090	1	492	58.9	57.4	60	0.13	187	4.94
JG-11-091	<1	393	51	64.4	70	0.12	40	4.9
JG-11-092	<1	1170	92.5	37.1	50	0.27	57	3.07
JG-11-093	<1	356	40.9	69.3	60	0.18	331	4.11
JG-11-094	<1	333	45.9	59.9	80	0.34	39	4.68
JG-11-095	1	233	16.1	82.5	40	0.06	927	1.39
JG-11-096	1	240	20	235	80	0.06	1665	1.92
JG-11-097	1	346	30.3	153	90	0.08	1405	2.91
JG-11-098	<1	416	47.4	81.5	60	0.09	230	4.71
JG-11-099	<1	327	33.2	56.2	340	0.11	82	3.97
JG-11-100	<1	287	23.5	64.1	440	0.08	73	3.96
JG-11-101	<1	291	25.6	66.2	350	0.06	33	4.05
JG-11-102	<1	238	22.7	73.5	20	0.09	84	4.8
JG-11-103	<1	326	55	61.2	60	0.02	251	5.43
JG-11-104	<1	260	25.6	115.5	440	0.09	470	3.95
JG-11-105	<1	203	28.6	72.7	550	0.08	75	4.49
JG-11-106	<1	941	71.3	54.2	70	0.37	145	2.65
JG-11-107	<1	409	34.4	67.9	270	0.11	20	4.31
JG-11-108	1	466	28.1	453	120	0.32	7030	2.26

Sample	Ag ppm	Ba ppm	Ce ppm	Co ppm	Cr ppm	Cs ppm	Cu ppm	Dy ppm
JG-11-109	<1	577	60.6	80	70	0.71	273	4.91
JG-11-110	<1	175.5	34.7	93.5	830	0.3	399	4.39
JG-11-111	<1	343	54.8	112	850	0.98	306	5.5
JG-11-112	<1	394	72.5	110	880	0.2	313	4.81
JG-11-113	<1	429	105	85.8	440	0.36	119	7.62
JG-11-114	<1	51.3	7.1	116.5	240	0.04	258	3.41
JG-11-115	<1	169	16.2	368	260	0.22	1390	1.98
JG-11-116	3	479	102	96.9	780	0.75	360	5.32
JG-11-117	<1	157	32.7	71.5	160	0.13	148	5.66
JG-11-118	<1	144.5	19.5	67.2	160	0.07	171	4.8
JG-11-119	<1	505	38.1	53.7	240	0.24	85	4.29
JG-11-120	<1	305	22.8	69.6	100	0.04	24	2.6
JG-11-121	<1	210	19.6	79.6	150	0.01	36	2.28
JG-11-122	<1	244	23	74.2	40	<0.01	58	2.47
JG-11-123	<1	241	24.4	79.6	100	0.02	51	2.64
JG-11-124	<1	500	69.8	61.6	70	0.14	59	6.85
JG-11-125	<1	81.1	12.6	62.6	80	0.08	60	4.59
JG-11-126	<1	68.3	12.3	61.3	70	0.09	59	4.68
JG-11-127	<1	430	80.5	77.3	50	0.2	40	8.43
JG-11-128	<1	611	80	85.2	30	0.01	40	9.17
JG-11-129	<1	251	28.2	107	70	0.03	164	3.06
JG-11-130	<1	657	81.3	69	60	0.14	19	7.26
JG-11-131	<1	354	53.8	60.2	100	0.07	126	3.25
JG-11-132	<1	60.8	2.5	165.5	40	<0.01	8	0.24
JG-11-133	<1	37.9	1.4	202	40	<0.01	5	0.12
JG-11-134	<1	118.5	10.1	149.5	40	0.02	21	1.41
JG-11-135	<1	166	6.8	105.5	420	0.01	53	1.01
JG-11-136	<1	135	9.5	81	20	0.02	12	1.13
JG-11-137	<1	169.5	14.8	51.7	20	0.04	13	1.58
JG-11-138	<1	336	29.1	111	20	0.06	39	2.98
JG-11-139	<1	79.3	4.3	195	40	0.01	7	0.45
JG-11-140	<1	386	33.9	60	290	0.11	69	3.99
JG-11-141	3	367	64.2	64	70	0.1	4400	4.6
JG-11-142	<1	680	126	49.9	20	0.38	51	14.15
JG-11-143	<1	890	17.3	175	150	0.14	2570	1.71
JG-11-144	<1	514	61.4	61.4	80	0.1	1215	1.91
JG-11-145	<1	847	69.1	44.2	50	0.33	122	3.65
JG-11-146	<1	377	36.5	55.9	40	0.06	118	3.6
JG-11-147	<1	151.5	40.3	154	50	0.01	5290	1.42
JG-11-148	<1	1405	73.7	47.3	110	0.2	450	2.33
JG-11-149	<1	1225	58.1	45.1	130	0.15	269	2.08
JG-11-150	2	712	75.8	71.3	40	0.08	1545	8.38
JG-11-151	<1	1295	70.1	48.2	60	0.1	50	2.68
JG-11-152	<1	257	32.8	65.7	360	1.11	43	3.54
JG-11-153	<1	483	31.5	53.1	270	0.12	42	4.05

Sample	Er ppm	Eu ppm	Ga ppm	Gd ppm	Hf ppm	Ho ppm	La ppm	Lu ppm
JG-11-001	1.2	1.26	14.8	2.79	1.8	0.44	10.1	0.15
JG-11-002	1.07	1.27	16.6	2.44	1.6	0.39	8.2	0.14
JG-11-003	0.68	0.94	13.8	1.56	1.1	0.24	5.5	0.08
JG-11-004	0.48	0.78	12.4	1.15	0.6	0.17	4.4	0.06
JG-11-005	0.66	0.86	16.7	1.23	1	0.23	6.6	0.1
JG-11-006	1.29	1.36	15.7	2.95	1.9	0.46	10	0.15
JG-11-007	1.81	1.96	23.8	5.5	6.1	0.69	48.2	0.22
JG-11-008	1.43	2.1	23.5	4.77	5.6	0.55	48.8	0.19
JG-11-009	1.39	1.93	21.9	4.8	4.7	0.54	43.8	0.18
JG-11-010	0.39	0.75	11.8	0.93	0.6	0.15	3.5	0.06
JG-11-011	0.63	1.05	17.1	1.31	0.8	0.23	5.8	0.08
JG-11-012	0.84	1.06	14.4	1.94	1.3	0.31	6.8	0.1
JG-11-013	3.7	2.16	17.8	7.6	12.3	1.3	69.7	0.55
JG-11-014	0.85	0.81	15.2	1.51	1.4	0.29	4.3	0.11
JG-11-015	0.62	0.94	13.8	1.47	0.9	0.23	5.5	0.08
JG-11-016	1.8	1.72	17.1	4.28	3.1	0.7	15.5	0.22
JG-11-017	1.04	1.07	11.1	2.51	2	0.38	9.5	0.12
JG-11-018	1.41	2.09	22.9	4.79	1.9	0.55	47.8	0.17
JG-11-019	0.74	0.92	13.1	1.73	1.1	0.28	6	0.1
JG-11-020	1.96	1.23	15.6	3.89	2.2	0.7	17.3	0.25
JG-11-021	1.18	1.21	15.3	2.52	1.9	0.45	10.3	0.16
JG-11-022	0.81	1.18	15.1	1.96	1.2	0.31	6.7	0.11
JG-11-023	1.01	1.23	14.5	2.46	1.7	0.39	8.1	0.13
JG-11-024	0.76	1.07	14.8	1.87	1.2	0.29	6.7	0.1
JG-11-025	1.29	2.12	25.4	4.45	6.5	0.49	48.8	0.17
JG-11-026	1.2	1.77	24.6	4.71	8.6	0.46	43.6	0.16
JG-11-027	2.82	2.94	20.5	7.7	5.4	1.1	27.1	0.33
JG-11-028	2.79	2.89	21.1	7.77	5.1	1.09	26.7	0.33
JG-11-029	1.52	1.58	26.5	3.96	3.4	0.59	19.1	0.19
JG-11-030	0.85	1.28	21	2.04	1.3	0.33	7.9	0.11
JG-11-031	1.22	1.52	16.6	2.84	1.9	0.47	10.7	0.16
JG-11-032	1.63	1.49	17.1	3.7	1.9	0.63	14.7	0.21
JG-11-033	0.77	1.09	14.9	1.82	1.3	0.3	7.2	0.1
JG-11-034	0.97	1.18	14.8	2.22	1.4	0.36	8	0.13
JG-11-035	1.08	1.36	15.1	2.58	1.6	0.42	8.3	0.14
JG-11-036	5.26	3.59	24.1	11.15	12.8	1.94	43.1	0.78
JG-11-037	2.17	2.33	22.9	5.88	4	0.85	21.6	0.26
JG-11-038	3.67	1.52	27.5	10.8	6.6	1.46	91.9	0.46
JG-11-039	2.57	1.53	16.2	4.76	6.5	0.91	47.4	0.38
JG-11-040	2.62	1.22	20.7	5.06	3.1	0.93	34.2	0.37
JG-11-041	2.8	1.78	18.2	5.22	3.2	1.01	18.1	0.41
JG-11-042	1.04	1.39	16.8	2.49	1.5	0.4	8.7	0.13
JG-11-043	1.64	1.71	17.5	3.94	3.2	0.62	13	0.22
JG-11-044	1.44	1.48	16.2	3.25	2.2	0.54	12	0.18
JG-11-045	1.65	1.43	16.1	3.55	2.1	0.62	10.8	0.23
JG-11-046	1.11	1.36	16.8	2.59	1.4	0.41	8.9	0.13
JG-11-047	1.46	2.81	14.9	5.06	1.7	0.59	145.5	0.18
JG-11-048	6.26	4.92	26.5	13.8	17.4	2.36	53.9	0.97
JG-11-049	7.83	4.42	24.6	17	19.5	2.95	55.3	1.17
JG-11-050	0.48	0.67	18	0.86	1.4	0.17	5.3	0.08
JG-11-051	0.39	1.39	23.7	1.95	1.2	0.17	10.7	0.04
JG-11-052	0.22	0.32	6.3	0.34	0.2	0.07	1.3	0.05
JG-11-053	1.29	0.9	10.1	2.2	1.7	0.46	6.2	0.19
JG-11-054	0.64	0.7	11.8	1.56	9.4	0.21	20.8	0.11

Sample	Er ppm	Eu ppm	Ga ppm	Gd ppm	Hf ppm	Ho ppm	La ppm	Lu ppm
JG-11-055	1.91	1.4	31.1	4.86	14.2	0.73	17.9	0.26
JG-11-056	5.27	0.95	15.5	5.37	10.6	1.58	24.2	0.96
JG-11-057	2.85	1.65	20	4.67	16.1	0.94	39.9	0.51
JG-11-058	2	1.76	17.7	4.67	5.8	0.73	18.9	0.28
JG-11-059	1.47	1.5	19.2	3.28	1.9	0.54	13.6	0.19
JG-11-060	1.22	1.3	16.5	2.7	2.2	0.44	9.3	0.16
JG-11-061	1.39	1.49	15.6	3.59	2	0.53	11.4	0.18
JG-11-062	0.97	0.7	8.2	2.03	1.5	0.36	6.3	0.13
JG-11-063	1.22	1.25	16.8	2.78	1.8	0.45	9.1	0.14
JG-11-064	6.51	4.65	26	13.7	20	2.35	55.8	0.98
JG-11-065	4.6	4.66	22.3	14.8	3.3	1.86	36.8	0.45
JG-11-066	10.25	4.76	19.7	26.6	7.8	3.93	75.9	1.21
JG-11-067	0.84	1.22	17.5	1.9	1.1	0.32	7	0.11
JG-11-068	0.89	1.28	18.1	2.11	1.5	0.34	7.9	0.11
JG-11-069	1.57	2.4	17.6	3.6	1.9	0.59	10.7	0.2
JG-11-070	4.61	4.78	26.8	14.4	2.7	1.89	38.5	0.45
JG-11-071	1.57	1.56	19.2	3.69	2.2	0.58	14.2	0.2
JG-11-072	3.04	2.83	22.1	7.87	5	1.15	27.2	0.36
JG-11-073	2.9	2.76	21.4	7.63	5	1.09	27.6	0.35
JG-11-074	2.92	2.7	22.4	7.7	5	1.14	25.6	0.33
JG-11-075	2.72	2.57	21.3	7.09	5	1.03	25	0.32
JG-11-076	2.94	2.81	22.6	7.99	5.1	1.14	29.5	0.35
JG-11-077	1.73	1.91	18.4	4.6	3.1	0.67	16.7	0.21
JG-11-078	1.11	1.18	22.9	2.35	1.5	0.4	13.4	0.15
JG-11-079	1.18	1.44	17.7	2.72	1.6	0.43	10.8	0.15
JG-11-080	1.32	1.47	17.2	3.02	1.7	0.48	11.6	0.15
JG-11-081	0.22	0.43	28.7	0.31	0.3	0.08	3.3	0.04
JG-11-082	0.56	1.06	16.4	1.26	1	0.19	6.1	0.07
JG-11-083	1	1.09	18.1	2.31	1.3	0.37	13.3	0.14
JG-11-084	2.92	2.81	22.1	7.68	5.2	1.12	28.2	0.36
JG-11-085	3.3	2.91	23.3	8.35	6	1.25	29.4	0.39
JG-11-086	1.51	1.63	16.4	3.81	2.4	0.57	15.1	0.18
JG-11-087	3.18	3.26	22.5	9.22	5.7	1.25	35.5	0.36
JG-11-088	1.28	1.39	19.6	3.02	2	0.49	12.5	0.16
JG-11-089	2.85	2.81	22.6	7.94	5.1	1.15	27.6	0.34
JG-11-090	2.28	2.37	19.4	6.73	3.6	0.87	25.6	0.26
JG-11-091	2.3	2.3	20.3	6.34	3.8	0.87	21.4	0.28
JG-11-092	1.43	1.87	22.4	4.74	9.3	0.54	46.5	0.19
JG-11-093	1.94	2.04	18.9	5.25	3.3	0.77	17.4	0.24
JG-11-094	2.23	2.18	19	5.75	3.6	0.86	19.3	0.28
JG-11-095	0.71	1.16	14.4	1.95	1.1	0.27	7.1	0.09
JG-11-096	0.88	1.29	14.2	2.44	1.4	0.34	8.9	0.11
JG-11-097	1.41	1.61	16.3	3.75	2.4	0.53	13.1	0.17
JG-11-098	2.33	2.26	19.7	5.9	3.7	0.88	20.3	0.28
JG-11-099	2.48	0.98	17.6	3.55	2.6	0.86	16.8	0.39
JG-11-100	2.5	0.84	16.8	3.12	1.9	0.83	11.5	0.39
JG-11-101	2.63	0.96	16.9	3.41	2.1	0.87	12.7	0.42
JG-11-102	2.52	1.43	24.7	4.67	2.2	0.92	9.4	0.33
JG-11-103	3.06	1.64	21.6	5.82	4	1.04	26.6	0.47
JG-11-104	2.71	0.86	17.5	3.28	1.9	0.85	13	0.42
JG-11-105	2.97	1	17.2	3.77	1.8	1	13.7	0.45
JG-11-106	1.29	1.63	19.4	3.93	5.7	0.48	35	0.18
JG-11-107	2.62	1.16	18.2	4.11	2.8	0.86	17.2	0.39
JG-11-108	0.99	1.31	14.1	2.84	2.1	0.42	13	0.14

Sample	Er ppm	Eu ppm	Ga ppm	Gd ppm	Hf ppm	Ho ppm	La ppm	Lu ppm
JG-11-109	2.31	2.47	18.9	6.43	3.9	0.89	26.5	0.28
JG-11-110	1.97	1.37	16.5	5.22	4.7	0.78	11.2	0.19
JG-11-111	2.48	1.52	17.4	6.41	5.7	0.98	22.3	0.29
JG-11-112	2.03	2.04	16.1	6.12	4.2	0.81	33.3	0.22
JG-11-113	3.51	2.76	26.7	9.85	7.2	1.36	46.7	0.4
JG-11-114	2.42	0.78	18.6	2.74	1.1	0.76	2.9	0.38
JG-11-115	1.34	0.97	18.8	1.71	1.3	0.42	8.6	0.22
JG-11-116	2.15	2.46	18.3	7.56	4.4	0.87	47.6	0.21
JG-11-117	2.88	1.06	21.9	6.3	1.7	1.04	10.1	0.37
JG-11-118	2.75	1.17	20.8	4.6	2.7	1	7.7	0.41
JG-11-119	2.76	1.04	18.3	4.05	2.8	0.9	18.4	0.43
JG-11-120	1.22	1.42	16.4	2.92	1.7	0.47	10	0.18
JG-11-121	1.17	1.2	15.6	2.73	1.7	0.43	8.5	0.16
JG-11-122	1.27	1.37	16.9	2.97	1.6	0.48	9.9	0.17
JG-11-123	1.39	1.42	16.8	3.15	1.7	0.5	10.7	0.17
JG-11-124	3.34	3.05	22.6	9.05	5.4	1.24	29.4	0.39
JG-11-125	2.34	1.27	17.7	3.52	2.2	0.96	5.5	0.35
JG-11-126	2.4	1.28	17.8	3.57	2.3	1	5.2	0.36
JG-11-127	4.65	2.77	22.2	8.89	7.3	1.65	36.3	0.67
JG-11-128	4.42	3.02	27.3	10.7	7.7	1.68	35.1	0.56
JG-11-129	1.49	1.71	18.3	3.61	2.2	0.56	12.2	0.18
JG-11-130	3.78	2.69	22.5	8.02	6.5	1.39	38.9	0.55
JG-11-131	1.71	1.52	22.5	4.35	1.2	0.61	25.5	0.22
JG-11-132	0.14	0.36	9.4	0.27	0.2	0.05	1.4	0.03
JG-11-133	0.1	0.25	6.3	0.15	<0.2	0.03	0.7	0.03
JG-11-134	0.85	0.68	12.4	1.55	1	0.28	4.6	0.12
JG-11-135	0.56	0.87	21.1	1.08	0.7	0.21	3.3	0.08
JG-11-136	0.7	0.84	17.7	1.35	0.8	0.25	4.4	0.09
JG-11-137	0.88	1.03	18.6	1.7	1	0.31	6.8	0.12
JG-11-138	1.8	1.22	15.6	3.48	2.5	0.61	13.3	0.24
JG-11-139	0.28	0.36	8	0.52	0.3	0.09	2.1	0.05
JG-11-140	2.58	0.94	17.8	3.88	2.6	0.85	16.9	0.39
JG-11-141	2.2	2.12	20.6	6.29	3.2	0.82	28.9	0.24
JG-11-142	8.11	3.99	26.6	15.8	11.5	2.81	55.8	1.16
JG-11-143	0.86	0.89	19.8	2.38	2.3	0.31	7.3	0.11
JG-11-144	0.94	0.99	18.8	3.13	2.2	0.36	32.4	0.13
JG-11-145	1.83	1.73	21.5	5.14	5	0.68	33.8	0.23
JG-11-146	1.65	1.82	18	4.75	2.9	0.64	15.6	0.19
JG-11-147	0.53	0.68	15.9	2.43	2.1	0.23	19.7	0.06
JG-11-148	1.28	1.29	20.8	3.74	5.2	0.44	38.2	0.17
JG-11-149	1.05	1.27	20.7	3.31	3.6	0.38	30	0.14
JG-11-150	4.71	2.01	21.5	9.38	4.1	1.6	34.4	0.64
JG-11-151	1.21	1.82	23.2	4.65	2	0.45	34.7	0.13
JG-11-152	1.68	1.06	17.7	4.31	1.6	0.63	13.8	0.22
JG-11-153	2.64	0.98	18.3	3.8	2.5	0.86	15.6	0.4

Sample	Mo ppm	Nb ppm	Nd ppm	Ni ppm	Pb ppm	Pr ppm	Rb ppm	Sm ppm
JG-11-001	<2	5	13.8	186	<5	3.07	4.3	3
JG-11-002	<2	3.9	11.6	109	<5	2.52	5.4	2.54
JG-11-003	<2	2.5	7.6	259	<5	1.69	2.8	1.64
JG-11-004	<2	1.7	5.7	334	<5	1.26	1.3	1.18
JG-11-005	10	1.7	6	168	<5	1.41	6.3	1.24
JG-11-006	<2	4.8	14.1	778	<5	3.1	5.3	3.11
JG-11-007	<2	10.6	45.5	34	18	11.5	57.5	7.88
JG-11-008	<2	9.3	45.1	34	17	11.45	65.2	7.56
JG-11-009	<2	9.3	42.4	32	15	10.65	58	7.28
JG-11-010	<2	1.6	4.6	363	<5	1.01	2	0.99
JG-11-011	<2	1.9	6.7	1140	7	1.51	8.8	1.34
JG-11-012	<2	3.1	9.3	296	<5	2.05	3.5	2.04
JG-11-013	3	15.9	57	<5	19	14.95	60.7	9.69
JG-11-014	<2	1	5.6	64	<5	1.21	3.4	1.4
JG-11-015	<2	2.4	7.3	492	<5	1.64	1.9	1.57
JG-11-016	3	7.5	20.5	3930	9	4.43	5.8	4.48
JG-11-017	4	5.6	13.5	>10000	34	3.03	4.9	2.81
JG-11-018	<2	8.8	43.9	39	15	11.2	46.2	7.42
JG-11-019	<2	2.6	8	500	<5	1.74	2	1.75
JG-11-020	<2	4	19.1	274	<5	4.44	8.1	4.18
JG-11-021	<2	4.2	13.3	742	<5	3.07	17.1	2.8
JG-11-022	<2	2.8	9.5	999	<5	2.11	5.1	2.06
JG-11-023	<2	3.8	11.7	966	<5	2.58	3.2	2.54
JG-11-024	<2	2.9	9.2	501	<5	2.08	5.2	1.93
JG-11-025	<2	10.8	41.8	30	17	11.15	57.8	6.58
JG-11-026	<2	8.7	41.5	39	16	10.45	62.1	6.83
JG-11-027	2	13	40.3	75	7	8.99	10.3	8.43
JG-11-028	2	12.8	39.7	194	5	8.89	9.3	8.36
JG-11-029	2	8.9	22	4170	23	5.2	20.9	4.48
JG-11-030	<2	3.4	10.3	1895	<5	2.34	3.6	2.09
JG-11-031	<2	4.1	14.2	106	<5	3.18	7.2	3.04
JG-11-032	<2	5	18.5	139	<5	4.25	9.7	3.83
JG-11-033	<2	2.7	9.4	186	<5	2.14	7.1	1.92
JG-11-034	<2	3.6	10.7	177	<5	2.45	11.1	2.27
JG-11-035	<2	3.7	12.4	235	<5	2.7	2.6	2.68
JG-11-036	3	17.5	56	52	12	12.6	37.4	11.85
JG-11-037	2	10	30.3	2600	18	6.81	14.7	6.29
JG-11-038	2	21.2	79.2	41	30	21.7	136	13.5
JG-11-039	<2	8.3	36.3	34	20	10.05	78.4	6
JG-11-040	<2	5.6	30.2	2290	16	7.9	35.4	5.46
JG-11-041	<2	4.2	24	112	8	5.42	25.1	5.39
JG-11-042	<2	4	12	117	<5	2.67	3.9	2.5
JG-11-043	<2	6.3	18.8	120	<5	4.2	7.1	4.04
JG-11-044	<2	5.4	16.1	127	<5	3.67	8.7	3.39
JG-11-045	<2	4.9	16.1	178	<5	3.52	12.8	3.59
JG-11-046	<2	3.5	12.3	155	<5	2.77	4.8	2.65
JG-11-047	<2	3.3	71.7	284	11	22.8	2.9	8.46
JG-11-048	3	30.9	68.4	<5	13	15.4	29.2	14.2
JG-11-049	4	29.3	79.7	5	8	17.55	14.6	17.15
JG-11-050	<2	1.1	4.5	897	5	1.14	3	0.85
JG-11-051	<2	9.2	13.5	103	<5	2.94	0.6	2.42
JG-11-052	<2	0.5	1.4	868	<5	0.33	0.5	0.3
JG-11-053	<2	3.4	8.5	591	<5	1.89	2.6	1.98
JG-11-054	<2	7.8	14.4	57	6	4.08	18.7	2.06

Sample	Mo ppm	Nb ppm	Nd ppm	Ni ppm	Pb ppm	Pr ppm	Rb ppm	Sm ppm
JG-11-055	<2	22.7	22.8	114	12	5.15	15.2	4.7
JG-11-056	<2	2.8	16.6	25	8	4.85	6	3.82
JG-11-057	7	9.7	24.4	55	17	6.95	104.5	4.11
JG-11-058	<2	6.2	22.9	147	8	5.24	26.2	4.64
JG-11-059	<2	5.1	17	104	5	3.94	26.4	3.58
JG-11-060	<2	4.6	13	182	<5	2.92	5.6	2.73
JG-11-061	<2	5	17	179	<5	3.71	4.9	3.63
JG-11-062	<2	4.8	9.3	453	<5	2.02	4.4	2.09
JG-11-063	<2	4.4	12.8	168	<5	2.86	4.2	2.74
JG-11-064	2	27.3	68.7	<5	14	15.5	38.6	14.25
JG-11-065	<2	9.9	66.4	5	<5	13.55	8.4	14.75
JG-11-066	2	17.9	125	9	7	26.5	21	26.8
JG-11-067	<2	2.5	9.3	153	<5	2.08	3.4	1.99
JG-11-068	<2	3	10.7	97	<5	2.44	4.9	2.24
JG-11-069	8	4.9	16.1	235	<5	3.51	5.4	3.69
JG-11-070	<2	9.2	68.6	6	<5	14	8	14.95
JG-11-071	<2	5.7	18.4	81	<5	4.24	5.3	3.89
JG-11-072	<2	13.4	40	55	6	8.8	13.5	8.42
JG-11-073	5	14.4	40.8	80	7	8.86	76.3	8.46
JG-11-074	2	13.9	37.6	112	6	8.41	29	8.06
JG-11-075	<2	13	36.5	181	15	8.05	14.9	7.51
JG-11-076	2	17	42.5	1260	23	9.53	14.8	8.95
JG-11-077	<2	8	23.4	971	12	5.29	7.9	4.98
JG-11-078	2	4.1	13.4	3790	22	3.35	21.5	2.52
JG-11-079	2	4.4	13.9	1955	7	3.15	8.8	2.89
JG-11-080	<2	4.3	15.3	137	<5	3.46	12.2	3.3
JG-11-081	10	1.5	2.3	3520	6	0.67	56.5	0.43
JG-11-082	3	2.2	6.9	6530	18	1.57	9.7	1.39
JG-11-083	2	4	13.1	2970	18	3.21	30.8	2.6
JG-11-084	2	13.9	40.5	63	13	9.05	23.2	8.34
JG-11-085	2	14.5	43	59	<5	9.59	13.4	8.91
JG-11-086	5	6.9	20.9	2780	14	4.72	49.1	4.26
JG-11-087	5	16.8	52.2	71	15	11.75	48.1	10.5
JG-11-088	2	5.1	16	4890	67	3.61	19.4	3.38
JG-11-089	<2	13	40.5	282	25	9	12.1	8.45
JG-11-090	<2	12.6	35.9	122	100	7.91	39.7	8.12
JG-11-091	<2	10.7	32.9	76	<5	7.24	24.3	7.55
JG-11-092	<2	13.5	43.1	37	20	11.2	91.1	7.45
JG-11-093	<2	8.5	25.8	191	19	5.73	13.3	5.9
JG-11-094	<2	10	29.6	93	8	6.44	12.9	6.69
JG-11-095	<2	2.9	10	447	77	2.22	7.2	2.26
JG-11-096	<2	3.8	12.4	3610	15	2.75	8.4	2.78
JG-11-097	<2	5.9	18.7	1805	20	4.22	11.9	4.25
JG-11-098	<2	9.6	30.5	475	8	6.72	12.7	7.1
JG-11-099	<2	4	16	51	7	3.96	17.2	3.61
JG-11-100	<2	3.4	12	78	5	2.97	18.3	3.06
JG-11-101	<2	3.2	13.1	67	<5	3.16	9.5	3.14
JG-11-102	<2	3.6	15.1	85	<5	3.29	7.7	4.24
JG-11-103	<2	12.5	29.1	22	8	7.04	9.1	6.74
JG-11-104	<2	3.1	12.6	820	54	3.1	12.5	3
JG-11-105	<2	3	14.1	120	8	3.41	14	3.41
JG-11-106	<2	9.7	33.3	199	18	8.62	66.5	5.68
JG-11-107	<2	4.2	17.3	35	5	4.25	23.4	3.99
JG-11-108	2	6	16.3	8720	50	3.67	15.7	3.74

Sample	Mo ppm	Nb ppm	Nd ppm	Ni ppm	Pb ppm	Pr ppm	Rb ppm	Sm ppm
JG-11-109	9	11.3	36.8	592	15	8.31	54.3	8
JG-11-110	<2	17.4	24.3	780	<5	5.34	40.5	6.2
JG-11-111	<2	24.6	31.7	900	5	7.46	70.6	7.6
JG-11-112	4	32.9	36.6	746	<5	9.04	51.9	7.74
JG-11-113	<2	42	56.2	382	9	13.75	42.7	12.55
JG-11-114	<2	1.6	5.9	788	10	1.1	5.8	2.14
JG-11-115	2	3.2	7.7	5080	42	1.89	7.6	1.7
JG-11-116	<2	38.7	49.6	816	426	12.55	39.8	10.15
JG-11-117	<2	7.8	25.9	127	<5	5.5	22.3	7.53
JG-11-118	<2	6.3	13.7	86	<5	2.85	24.1	4.25
JG-11-119	<2	4.9	18.6	29	8	4.64	77.7	4.28
JG-11-120	<2	4.3	14.4	192	<5	3.17	7.8	3.51
JG-11-121	<2	3.9	12.6	225	<5	2.81	3.4	3.13
JG-11-122	<2	3.8	14.7	206	<5	3.26	3.5	3.35
JG-11-123	<2	4.6	15.4	253	<5	3.4	5.3	3.63
JG-11-124	2	14	45.5	58	6	9.92	13.9	10.35
JG-11-125	<2	4.6	9.2	108	<5	2.07	3	2.92
JG-11-126	<2	4.7	9	105	<5	1.98	3.2	2.88
JG-11-127	2	16.9	39.4	56	<5	9.93	17.6	8.1
JG-11-128	<2	17.2	42.7	51	6	10	2	9.78
JG-11-129	<2	5.9	15.7	62	<5	3.6	4.2	3.36
JG-11-130	<2	12	40.2	48	7	9.97	14	7.95
JG-11-131	<2	4.8	27.2	68	8	6.56	6.3	5.08
JG-11-132	<2	0.4	1.4	641	<5	0.3	0.4	0.32
JG-11-133	<2	0.2	0.7	781	<5	0.17	0.2	0.17
JG-11-134	<2	2.1	6.1	512	<5	1.33	2.2	1.39
JG-11-135	<2	1.6	4.1	117	<5	0.88	2.6	0.96
JG-11-136	<2	1.8	5.6	112	<5	1.25	3.1	1.21
JG-11-137	<2	2.6	8.1	47	<5	1.85	5.9	1.75
JG-11-138	<2	10.5	16.1	206	<5	3.74	10.5	3.39
JG-11-139	<2	0.7	2.2	548	<5	0.54	1	0.47
JG-11-140	<2	4.2	16.6	45	5	4.1	22.8	3.44
JG-11-141	<2	12.5	34.9	735	18	8.07	9	7.02
JG-11-142	3	27.5	69.5	32	9	15.85	27.8	15.25
JG-11-143	<2	8.2	11.7	2600	14	2.43	48.6	2.6
JG-11-144	<2	5	27.5	462	12	7.02	71.4	4.51
JG-11-145	<2	10.1	34	58	22	8.27	69.7	6.1
JG-11-146	<2	7.5	23.2	79	5	5.02	9.1	5.1
JG-11-147	6	7.9	18.3	2180	<5	4.76	7	3.23
JG-11-148	<2	9.6	32.5	351	42	8.46	65.2	5.44
JG-11-149	<2	5.7	27.6	508	29	6.85	46.1	4.54
JG-11-150	<2	12.9	41.7	582	14	9.74	14.7	9.36
JG-11-151	<2	2.4	36.5	74	11	8.7	24.4	6.3
JG-11-152	<2	3.8	20	325	12	4.43	64.3	4.47
JG-11-153	<2	4	16.2	41	6	3.79	25.9	3.42

Sample	Sn ppm	Sr ppm	Ta ppm	Tb ppm	Th ppm	Tl ppm	Tm ppm	U ppm
JG-11-001	1	494	0.6	0.38	0.31	<0.5	0.16	0.07
JG-11-002	1	487	0.6	0.34	0.26	<0.5	0.14	0.05
JG-11-003	<1	516	0.6	0.22	0.14	<0.5	0.09	<0.05
JG-11-004	<1	532	0.4	0.15	0.11	<0.5	0.06	<0.05
JG-11-005	<1	436	0.3	0.18	0.25	<0.5	0.09	0.37
JG-11-006	1	545	0.7	0.41	0.28	<0.5	0.17	0.06
JG-11-007	1	1390	0.8	0.68	1.88	<0.5	0.24	0.49
JG-11-008	1	1400	0.9	0.58	1.22	<0.5	0.2	0.23
JG-11-009	1	1255	0.6	0.56	2.21	<0.5	0.19	0.45
JG-11-010	<1	493	0.6	0.14	0.08	<0.5	0.05	<0.05
JG-11-011	1	531	0.7	0.2	0.3	<0.5	0.09	0.07
JG-11-012	<1	534	0.6	0.27	0.2	<0.5	0.11	0.06
JG-11-013	1	148.5	2.2	1.08	4.92	<0.5	0.51	0.54
JG-11-014	<1	369	0.4	0.23	0.19	<0.5	0.11	0.16
JG-11-015	<1	486	0.5	0.21	0.16	<0.5	0.08	<0.05
JG-11-016	1	511	0.7	0.6	0.42	<0.5	0.24	0.09
JG-11-017	3	308	0.5	0.34	0.32	<0.5	0.12	0.08
JG-11-018	1	1365	0.6	0.56	0.74	<0.5	0.18	0.1
JG-11-019	<1	469	0.6	0.24	0.2	<0.5	0.1	0.36
JG-11-020	1	528	0.6	0.58	1.21	<0.5	0.25	0.09
JG-11-021	1	580	0.7	0.39	0.5	<0.5	0.17	0.09
JG-11-022	1	540	0.3	0.29	0.19	<0.5	0.12	<0.05
JG-11-023	1	557	0.6	0.36	0.25	<0.5	0.15	0.05
JG-11-024	<1	593	0.8	0.27	0.24	<0.5	0.11	0.05
JG-11-025	1	1375	0.8	0.54	1.71	<0.5	0.18	0.47
JG-11-026	1	1255	0.5	0.49	0.4	<0.5	0.17	0.24
JG-11-027	2	518	1.2	1.1	0.57	<0.5	0.4	0.15
JG-11-028	2	518	1.1	1.09	0.55	<0.5	0.39	0.15
JG-11-029	1	414	0.8	0.57	2.53	<0.5	0.22	0.27
JG-11-030	1	527	0.8	0.3	0.35	<0.5	0.12	0.06
JG-11-031	1	673	0.6	0.43	0.52	<0.5	0.18	0.09
JG-11-032	1	595	0.7	0.56	1.37	<0.5	0.24	0.17
JG-11-033	1	618	0.7	0.27	0.34	<0.5	0.11	0.05
JG-11-034	<1	592	0.5	0.33	0.46	<0.5	0.14	0.07
JG-11-035	<1	550	0.6	0.39	0.23	<0.5	0.15	0.05
JG-11-036	<1	366	1.5	1.69	0.64	<0.5	0.76	0.11
JG-11-037	3	363	0.8	0.85	0.84	<0.5	0.31	0.17
JG-11-038	1	213	2	1.57	23.5	0.6	0.51	1.09
JG-11-039	<1	230	1.9	0.75	15.2	<0.5	0.39	1.2
JG-11-040	1	425	0.8	0.79	5.18	<0.5	0.4	0.48
JG-11-041	1	527	0.8	0.85	0.81	<0.5	0.43	0.11
JG-11-042	<1	595	0.8	0.37	0.29	<0.5	0.15	0.05
JG-11-043	1	550	1	0.6	0.5	<0.5	0.23	0.09
JG-11-044	1	562	0.8	0.48	0.63	<0.5	0.21	0.1
JG-11-045	1	472	0.8	0.55	0.64	<0.5	0.25	0.1
JG-11-046	1	556	0.9	0.38	0.42	<0.5	0.15	0.06
JG-11-047	<1	660	0.6	0.64	1.65	<0.5	0.21	1.64
JG-11-048	<1	377	2.1	2.08	1.07	<0.5	0.94	0.15
JG-11-049	<1	338	1.7	2.54	0.96	<0.5	1.14	0.15
JG-11-050	<1	522	0.6	0.13	0.15	<0.5	0.07	<0.05
JG-11-051	<1	1400	1.1	0.23	<0.05	<0.5	0.05	<0.05
JG-11-052	<1	178.5	0.3	0.06	<0.05	<0.5	0.03	<0.05
JG-11-053	1	184	0.8	0.36	0.32	<0.5	0.19	0.07
JG-11-054	1	125	2.6	0.21	4.55	<0.5	0.09	0.42

Sample	Sn ppm	Sr ppm	Ta ppm	Tb ppm	Th ppm	Tl ppm	Tm ppm	U ppm
JG-11-055	4	373	1.7	0.69	0.9	<0.5	0.27	0.62
JG-11-056	<1	229	1.4	0.97	1.76	<0.5	0.87	0.49
JG-11-057	<1	234	1.2	0.76	2.85	0.5	0.44	0.81
JG-11-058	<1	502	0.9	0.66	0.41	<0.5	0.3	0.08
JG-11-059	2	517	0.6	0.49	0.96	<0.5	0.2	0.15
JG-11-060	1	456	0.6	0.39	0.37	<0.5	0.17	0.08
JG-11-061	1	419	0.6	0.51	0.4	<0.5	0.19	0.08
JG-11-062	1	181	0.4	0.3	0.37	<0.5	0.14	0.08
JG-11-063	1	499	0.4	0.41	0.38	<0.5	0.17	0.07
JG-11-064	1	345	1.7	2.01	1.88	<0.5	0.94	0.26
JG-11-065	1	408	0.7	1.88	0.94	<0.5	0.58	0.17
JG-11-066	1	272	1.3	3.71	1.73	<0.5	1.35	0.26
JG-11-067	<1	564	0.3	0.28	0.21	<0.5	0.12	<0.05
JG-11-068	1	560	0.4	0.3	0.24	<0.5	0.13	0.06
JG-11-069	1	380	0.4	0.51	0.48	<0.5	0.22	0.08
JG-11-070	1	531	0.8	1.92	0.98	<0.5	0.56	0.18
JG-11-071	1	502	0.7	0.53	0.94	<0.5	0.22	0.15
JG-11-072	2	513	1	1.11	0.76	<0.5	0.41	0.19
JG-11-073	2	518	0.9	1.1	0.48	<0.5	0.38	0.23
JG-11-074	2	527	1	1.07	0.64	<0.5	0.39	0.19
JG-11-075	2	506	1.1	0.98	0.95	<0.5	0.36	0.22
JG-11-076	3	478	1.2	1.14	0.9	<0.5	0.4	0.21
JG-11-077	1	636	0.5	0.65	0.46	<0.5	0.24	0.11
JG-11-078	2	493	0.4	0.35	2.09	<0.5	0.15	0.3
JG-11-079	1	587	0.6	0.4	0.84	<0.5	0.16	0.11
JG-11-080	1	668	0.7	0.44	0.69	<0.5	0.17	0.14
JG-11-081	1	141.5	<0.1	0.06	0.07	<0.5	0.04	<0.05
JG-11-082	1	410	0.1	0.19	0.55	<0.5	0.07	0.07
JG-11-083	2	167.5	0.2	0.32	1	<0.5	0.14	0.12
JG-11-084	2	533	1	1.06	0.93	<0.5	0.4	0.24
JG-11-085	2	498	1.1	1.17	0.99	<0.5	0.43	0.22
JG-11-086	3	570	0.4	0.53	0.45	<0.5	0.21	0.19
JG-11-087	2	547	1.1	1.26	0.66	<0.5	0.41	0.2
JG-11-088	5	746	0.3	0.42	0.42	<0.5	0.17	0.16
JG-11-089	2	556	1.1	1.08	0.79	<0.5	0.4	0.18
JG-11-090	2	594	0.9	0.91	0.88	<0.5	0.3	0.18
JG-11-091	1	495	0.9	0.87	0.48	<0.5	0.3	0.14
JG-11-092	2	1065	0.7	0.57	0.39	<0.5	0.2	0.25
JG-11-093	2	552	0.8	0.73	0.93	<0.5	0.27	0.26
JG-11-094	1	494	0.7	0.82	0.73	<0.5	0.3	0.17
JG-11-095	1	703	0.6	0.26	0.19	<0.5	0.09	<0.05
JG-11-096	1	637	0.5	0.35	0.24	<0.5	0.13	0.05
JG-11-097	2	625	0.7	0.52	0.39	<0.5	0.19	0.09
JG-11-098	1	587	1	0.83	0.65	<0.5	0.3	0.15
JG-11-099	1	194.5	0.6	0.59	2.73	<0.5	0.38	0.29
JG-11-100	<1	169.5	0.5	0.56	1.58	<0.5	0.39	0.23
JG-11-101	<1	172	0.5	0.6	1.25	<0.5	0.39	0.14
JG-11-102	2	315	0.4	0.76	0.39	<0.5	0.35	0.1
JG-11-103	2	496	1.1	0.87	0.84	<0.5	0.46	0.55
JG-11-104	3	164.5	0.4	0.58	1.27	<0.5	0.39	0.22
JG-11-105	2	198.5	0.5	0.65	1.25	<0.5	0.46	0.37
JG-11-106	1	827	0.7	0.52	1.05	<0.5	0.18	0.31
JG-11-107	<1	252	0.7	0.62	2.79	<0.5	0.38	0.3
JG-11-108	3	440	0.5	0.39	0.46	0.9	0.14	0.12

Sample	Sn ppm	Sr ppm	Ta ppm	Tb ppm	Th ppm	Tl ppm	Tm ppm	U ppm
JG-11-109	2	491	0.9	0.88	0.83	<0.5	0.3	0.2
JG-11-110	12	190.5	2.1	0.79	3.78	<0.5	0.24	1.34
JG-11-111	3	184	1.9	0.98	3.03	<0.5	0.34	1.11
JG-11-112	8	444	2.6	0.86	7.84	<0.5	0.26	3.74
JG-11-113	4	288	2.9	1.36	4.6	<0.5	0.46	1.59
JG-11-114	1	128.5	0.4	0.51	0.42	<0.5	0.35	0.18
JG-11-115	<1	180.5	0.5	0.29	0.87	<0.5	0.2	0.25
JG-11-116	6	164	2.7	1	10.35	<0.5	0.25	1.97
JG-11-117	1	131	0.6	0.99	1.18	<0.5	0.39	0.24
JG-11-118	<1	136.5	0.5	0.79	1.48	<0.5	0.41	0.32
JG-11-119	1	186.5	0.6	0.68	4.22	<0.5	0.39	1.82
JG-11-120	<1	560	0.5	0.46	0.39	<0.5	0.18	0.07
JG-11-121	<1	515	0.7	0.4	0.27	<0.5	0.16	0.06
JG-11-122	<1	571	0.6	0.45	0.31	<0.5	0.18	0.06
JG-11-123	<1	567	0.6	0.46	0.35	<0.5	0.19	0.07
JG-11-124	2	474	1.1	1.26	0.66	<0.5	0.44	0.17
JG-11-125	1	252	0.3	0.69	0.3	<0.5	0.36	0.07
JG-11-126	1	236	0.4	0.72	0.27	<0.5	0.37	0.07
JG-11-127	2	277	1.4	1.36	1.92	<0.5	0.67	0.36
JG-11-128	3	339	1.4	1.55	1.65	<0.5	0.6	0.23
JG-11-129	<1	440	2.1	0.52	0.42	<0.5	0.2	0.08
JG-11-130	2	379	1	1.19	1.81	<0.5	0.57	0.33
JG-11-131	1	715	0.6	0.55	0.53	<0.5	0.21	0.29
JG-11-132	<1	263	0.4	0.04	<0.05	<0.5	0.03	<0.05
JG-11-133	<1	165.5	0.3	0.03	<0.05	<0.5	0.02	<0.05
JG-11-134	<1	246	0.5	0.21	0.21	<0.5	0.13	0.05
JG-11-135	<1	352	1	0.16	0.08	<0.5	0.08	<0.05
JG-11-136	<1	502	0.8	0.19	0.17	<0.5	0.09	<0.05
JG-11-137	1	552	0.8	0.24	0.52	<0.5	0.13	0.07
JG-11-138	1	292	0.9	0.48	0.62	<0.5	0.25	0.12
JG-11-139	<1	195.5	0.3	0.07	0.08	<0.5	0.04	<0.05
JG-11-140	<1	209	0.6	0.58	2.65	<0.5	0.38	0.29
JG-11-141	1	558	1	0.77	0.62	<0.5	0.28	0.15
JG-11-142	4	230	1.7	2.33	3.51	<0.5	1.13	0.86
JG-11-143	4	495	0.5	0.29	0.75	0.5	0.11	0.22
JG-11-144	2	534	0.5	0.35	0.86	0.5	0.14	0.45
JG-11-145	1	769	0.8	0.64	2.53	<0.5	0.25	0.49
JG-11-146	2	674	0.7	0.59	0.42	<0.5	0.23	0.1
JG-11-147	2	40.5	1.3	0.28	5.03	<0.5	0.06	0.81
JG-11-148	3	1010	0.7	0.43	0.66	<0.5	0.18	0.72
JG-11-149	2	1135	0.5	0.38	0.43	<0.5	0.15	0.24
JG-11-150	5	448	1.1	1.29	1.64	<0.5	0.64	0.4
JG-11-151	1	1775	0.5	0.48	0.39	<0.5	0.15	0.16
JG-11-152	2	720	0.5	0.58	1.03	<0.5	0.23	0.36
JG-11-153	<1	280	0.4	0.58	1.79	<0.5	0.39	0.2

Sample	V ppm	W ppm	Y ppm	Yb ppm	Zn ppm	Zr ppm	As ppm	Bi ppm
JG-11-001	75	76	12	1.01	80	71	<0.1	<0.01
JG-11-002	102	84	10.4	0.89	82	55	<0.1	<0.01
JG-11-003	48	106	6.6	0.55	63	46	<0.1	<0.01
JG-11-004	32	94	4.7	0.37	55	25	<0.1	<0.01
JG-11-005	143	66	6.1	0.63	144	35	0.2	0.03
JG-11-006	78	97	12.7	1.06	85	71	0.2	0.02
JG-11-007	107	100	18.9	1.56	88	238	<0.1	0.01
JG-11-008	116	130	14.6	1.23	94	218	0.1	<0.01
JG-11-009	118	80	14.5	1.21	94	178	0.3	<0.01
JG-11-010	36	105	3.8	0.33	61	22	<0.1	<0.01
JG-11-011	46	154	6.3	0.57	62	28	<0.1	0.05
JG-11-012	60	99	8.2	0.7	67	50	<0.1	<0.01
JG-11-013	7	423	34.1	3.35	74	489	0.2	0.01
JG-11-014	157	75	7.6	0.75	74	50	<0.1	<0.01
JG-11-015	41	89	6.2	0.53	78	37	<0.1	0.01
JG-11-016	120	64	18.4	1.46	87	114	0.3	0.2
JG-11-017	105	65	10.2	0.88	246	81	1.3	0.26
JG-11-018	121	93	14.8	1.15	93	72	<0.1	<0.01
JG-11-019	57	99	7.2	0.65	84	42	<0.1	0.01
JG-11-020	75	76	18.6	1.67	80	80	<0.1	0.01
JG-11-021	62	88	12.5	1.04	92	85	<0.1	0.02
JG-11-022	56	45	8.3	0.67	76	47	<0.1	0.03
JG-11-023	83	89	10.8	0.88	90	69	<0.1	0.02
JG-11-024	54	119	7.9	0.65	72	50	<0.1	0.01
JG-11-025	111	102	13.6	1.08	96	283	0.9	0.02
JG-11-026	121	93	12.3	1.01	104	383	<0.1	<0.01
JG-11-027	162	66	29.8	2.28	155	223	<0.1	0.01
JG-11-028	163	42	30.1	2.2	150	214	<0.1	0.01
JG-11-029	158	79	16.3	1.33	306	139	1	0.23
JG-11-030	105	124	8.8	0.73	116	56	<0.1	0.05
JG-11-031	78	92	12.5	1.04	74	77	<0.1	<0.01
JG-11-032	87	84	16.9	1.4	80	75	<0.1	<0.01
JG-11-033	49	115	8.3	0.64	73	54	0.4	0.01
JG-11-034	53	76	10	0.86	73	59	<0.1	<0.01
JG-11-035	87	87	11.1	0.93	85	62	<0.1	<0.01
JG-11-036	52	224	51.6	4.7	180	577	<0.1	<0.01
JG-11-037	166	37	23.4	1.79	147	168	0.2	0.16
JG-11-038	112	322	42	3.07	187	228	0.1	0.02
JG-11-039	83	491	26.2	2.42	70	245	<0.1	<0.01
JG-11-040	76	107	25.6	2.36	100	111	2.6	0.11
JG-11-041	61	138	27.6	2.62	108	124	<0.1	<0.01
JG-11-042	71	122	10.8	0.86	73	65	<0.1	<0.01
JG-11-043	115	118	16.9	1.41	94	139	<0.1	<0.01
JG-11-044	84	97	14.6	1.23	93	93	<0.1	<0.01
JG-11-045	124	95	16.5	1.48	122	80	0.7	<0.01
JG-11-046	81	119	11.1	0.9	84	55	<0.1	<0.01
JG-11-047	95	93	17.3	1.24	108	70	<0.1	<0.01
JG-11-048	46	254	63.6	5.84	218	820	<0.1	<0.01
JG-11-049	70	194	77.1	7.19	290	912	<0.1	<0.01
JG-11-050	62	130	4.5	0.48	68	56	<0.1	0.02
JG-11-051	114	140	4.6	0.25	125	45	<0.1	<0.01
JG-11-052	20	80	1.9	0.24	126	8	<0.1	<0.01
JG-11-053	90	111	12.3	1.21	145	67	<0.1	<0.01
JG-11-054	131	642	5.8	0.66	47	370	<0.1	0.01

Sample	V ppm	W ppm	Y ppm	Yb ppm	Zn ppm	Zr ppm	As ppm	Bi ppm
JG-11-055	373	159	19.6	1.62	189	550	<0.1	0.01
JG-11-056	104	465	43.8	5.78	270	415	0.3	<0.01
JG-11-057	196	313	26.2	2.92	138	595	0.1	0.02
JG-11-058	48	185	19.7	1.69	85	231	<0.1	<0.01
JG-11-059	102	92	14.6	1.2	115	69	<0.1	0.01
JG-11-060	107	106	12.1	1.01	111	87	<0.1	<0.01
JG-11-061	124	91	14.9	1.06	122	77	<0.1	<0.01
JG-11-062	145	63	9.7	0.79	174	53	<0.1	<0.01
JG-11-063	124	75	12.1	0.99	91	67	<0.1	<0.01
JG-11-064	33	230	61	5.8	191	808	<0.1	<0.01
JG-11-065	379	33	51.7	2.95	161	121	<0.1	<0.01
JG-11-066	517	109	104	7.49	286	315	<0.1	<0.01
JG-11-067	58	79	8.5	0.68	73	41	<0.1	<0.01
JG-11-068	98	84	9	0.68	80	57	<0.1	<0.01
JG-11-069	347	60	15.9	1.26	135	70	1.6	0.01
JG-11-070	321	76	51.5	3	140	98	<0.1	<0.01
JG-11-071	129	100	16	1.28	118	84	<0.1	<0.01
JG-11-072	173	64	31.7	2.36	150	200	0.1	0.01
JG-11-073	162	43	29.3	2.19	164	195	<0.1	<0.01
JG-11-074	177	76	30.1	2.26	162	192	<0.1	<0.01
JG-11-075	162	92	27.9	2.04	157	194	0.1	0.02
JG-11-076	169	68	31.5	2.34	175	205	0.2	0.16
JG-11-077	96	51	18.2	1.32	112	125	<0.1	0.07
JG-11-078	107	84	11.6	0.88	137	55	5.8	0.25
JG-11-079	81	94	11.6	0.92	113	61	2.1	0.09
JG-11-080	68	105	13	0.98	63	64	<0.1	<0.01
JG-11-081	320	14	2.5	0.22	229	13	0.4	0.12
JG-11-082	83	22	5.7	0.44	148	36	0.5	0.11
JG-11-083	57	8	10	0.83	110	48	10.8	0.16
JG-11-084	153	73	30.7	2.32	152	210	0.3	0.01
JG-11-085	186	67	33.5	2.48	163	233	0.1	<0.01
JG-11-086	94	41	16.3	1.22	146	96	0.3	0.22
JG-11-087	162	60	33.8	2.36	187	234	0.2	0.02
JG-11-088	80	44	13.2	0.96	102	74	0.4	0.71
JG-11-089	153	85	30.6	2.18	146	201	0.2	0.14
JG-11-090	135	32	20.5	1.69	142	142	<0.1	0.37
JG-11-091	147	48	21.2	1.85	141	160	<0.1	<0.01
JG-11-092	92	76	13	1.28	87	414	<0.1	<0.01
JG-11-093	102	62	17.5	1.62	116	132	0.2	0.02
JG-11-094	131	23	20.2	1.83	125	142	0.2	0.01
JG-11-095	36	92	6.2	0.55	65	44	<0.1	0.65
JG-11-096	51	68	8	0.71	75	58	0.4	0.19
JG-11-097	81	79	12.4	1.12	101	95	0.1	0.12
JG-11-098	105	80	20.5	1.85	114	150	0.1	0.02
JG-11-099	188	66	20.8	2.41	85	95	<0.1	0.01
JG-11-100	192	79	20.4	2.42	81	69	<0.1	<0.01
JG-11-101	200	88	21.1	2.61	89	72	<0.1	<0.01
JG-11-102	218	68	21.8	2.13	155	68	<0.1	0.01
JG-11-103	207	124	26.2	2.9	116	156	<0.1	0.01
JG-11-104	203	81	21.5	2.63	122	68	<0.1	0.03
JG-11-105	217	92	23.7	2.86	96	61	<0.1	<0.01
JG-11-106	95	59	11.7	1.06	102	237	<0.1	0.02
JG-11-107	202	119	21.5	2.51	88	100	<0.1	<0.01
JG-11-108	119	42	9.5	0.9	148	88	1.4	0.39

Sample	V ppm	W ppm	Y ppm	Yb ppm	Zn ppm	Zr ppm	As ppm	Bi ppm
JG-11-109	135	36	20.9	1.79	146	160	<0.1	0.05
JG-11-110	221	73	17.7	1.38	118	175	0.5	0.02
JG-11-111	217	61	23.5	1.95	201	206	0.1	0.02
JG-11-112	231	75	18.8	1.5	156	157	0.1	0.02
JG-11-113	435	34	31.2	2.67	213	266	<0.1	0.02
JG-11-114	319	82	17.9	2.3	121	31	<0.1	0.02
JG-11-115	147	49	10.2	1.31	139	49	0.7	0.07
JG-11-116	188	43	20.9	1.43	167	167	0.1	6
JG-11-117	413	47	25.2	2.4	157	49	<0.1	0.02
JG-11-118	367	38	23.3	2.61	129	100	<0.1	0.01
JG-11-119	182	81	22.3	2.58	85	98	<0.1	0.01
JG-11-120	78	70	11.5	1.1	77	66	<0.1	<0.01
JG-11-121	84	94	10.2	0.99	81	63	<0.1	<0.01
JG-11-122	68	82	11	1.02	79	66	<0.1	<0.01
JG-11-123	80	75	11.6	1.11	86	70	<0.1	<0.01
JG-11-124	156	45	29.2	2.62	162	217	<0.1	0.01
JG-11-125	239	25	21.8	2.11	93	83	<0.1	<0.01
JG-11-126	234	26	22.6	2.21	93	83	<0.1	<0.01
JG-11-127	230	79	44.8	4.41	148	323	0.1	0.01
JG-11-128	383	75	43.8	3.78	201	277	0.2	<0.01
JG-11-129	361	258	14.7	1.26	97	70	<0.1	<0.01
JG-11-130	264	68	37.6	3.54	147	252	<0.1	<0.01
JG-11-131	189	81	15.7	1.38	84	36	<0.1	0.01
JG-11-132	19	84	1.4	0.2	100	7	<0.1	<0.01
JG-11-133	17	77	0.9	0.15	132	3	<0.1	<0.01
JG-11-134	61	80	7.3	0.84	135	41	<0.1	<0.01
JG-11-135	293	166	5.2	0.54	102	27	<0.1	<0.01
JG-11-136	39	132	6.3	0.62	109	38	<0.1	<0.01
JG-11-137	73	129	8	0.77	45	40	<0.1	0.01
JG-11-138	369	76	15.8	1.73	173	97	<0.1	<0.01
JG-11-139	32	73	2.6	0.33	151	12	<0.1	<0.01
JG-11-140	221	80	23.4	2.65	92	96	<0.1	0.01
JG-11-141	131	65	21.2	1.83	150	137	<0.1	0.78
JG-11-142	97	17	73.1	7.56	225	534	0.8	0.02
JG-11-143	99	18	8.5	0.77	233	96	0.6	0.15
JG-11-144	74	90	9.8	0.83	58	91	<0.1	0.07
JG-11-145	109	53	17.9	1.56	120	209	<0.1	0.02
JG-11-146	105	63	16.5	1.43	100	119	<0.1	0.02
JG-11-147	103	260	6.2	0.42	159	85	0.3	0.18
JG-11-148	88	85	12.1	1.2	83	219	0.3	0.06
JG-11-149	79	58	10.3	0.97	88	146	<0.1	0.11
JG-11-150	212	44	43.3	4.26	129	166	<0.1	0.11
JG-11-151	133	102	11.6	0.97	91	79	<0.1	0.01
JG-11-152	132	73	16.4	1.4	134	57	<0.1	0.02
JG-11-153	230	54	23.1	2.6	92	91	<0.1	<0.01

Sample	Hg ppm	Sb ppm	Se ppm	Te ppm	LOI %	Total %	Ag ppm	As ppm
JG-11-001	0.054	<0.05	0.3	0.01	1.1	98.7	<0.5	<5
JG-11-002	0.067	<0.05	0.3	0.01	0.3	99.3	<0.5	<5
JG-11-003	0.098	<0.05	0.2	0.01	3.49	101.5	<0.5	<5
JG-11-004	0.098	<0.05	<0.2	0.01	-0.1	98.9	<0.5	<5
JG-11-005	0.068	<0.05	3.3	0.19	1.99	98.8	<0.5	<5
JG-11-006	0.091	<0.05	0.8	0.04	0.5	99.9	<0.5	<5
JG-11-007	0.093	<0.05	0.4	0.01	1.29	100	<0.5	<5
JG-11-008	0.116	<0.05	0.4	0.01	0.7	99	<0.5	<5
JG-11-009	0.079	<0.05	0.4	0.01	1.1	98.2	<0.5	<5
JG-11-010	0.101	<0.05	0.2	0.02	0.6	98.4	<0.5	<5
JG-11-011	0.14	<0.05	2.1	0.1	1.1	99.2	<0.5	<5
JG-11-012	0.095	<0.05	0.3	0.02	0.5	99.6	<0.5	<5
JG-11-013	0.445	<0.05	0.8	<0.01	0.99	99.7	<0.5	<5
JG-11-014	0.069	<0.05	<0.2	0.01	-0.5	98.6	<0.5	<5
JG-11-015	0.098	<0.05	0.5	0.03	-0.6	99.6	<0.5	<5
JG-11-016	0.074	<0.05	6.6	0.4	1.79	101.5	0.5	<5
JG-11-017	0.086	<0.05	26.7	1.36	5.08	99	2	<5
JG-11-018	0.09	<0.05	0.4	0.01	0.6	100	<0.5	<5
JG-11-019	0.096	<0.05	0.5	0.02	-0.1	98.4	<0.5	<5
JG-11-020	0.073	<0.05	0.3	0.01	0.7	99.6	0.6	<5
JG-11-021	0.087	<0.05	0.8	0.06	-0.2	101.5	<0.5	<5
JG-11-022	0.039	<0.05	1.1	0.06	3.2	101	<0.5	<5
JG-11-023	0.093	<0.05	1.2	0.07	0.2	98.6	0.5	5
JG-11-024	0.121	<0.05	0.4	0.03	0.6	100	<0.5	<5
JG-11-025	0.098	<0.05	0.4	0.01	0.6	101	1.1	<5
JG-11-026	0.086	<0.05	0.4	0.01	1.3	99.3	0.9	<5
JG-11-027	0.053	<0.05	0.8	0.01	0.9	100.5	0.5	5
JG-11-028	0.032	<0.05	0.8	0.01	1.2	98.1	0.5	<5
JG-11-029	0.094	<0.05	9.9	0.54	2.59	100.5	1.1	<5
JG-11-030	0.111	<0.05	2.3	0.12	2.2	99.4	0.5	<5
JG-11-031	0.061	<0.05	0.4	<0.01	-0.3	100	0.5	<5
JG-11-032	0.066	<0.05	0.3	<0.01	0.1	99.1	<0.5	<5
JG-11-033	0.081	<0.05	0.3	0.02	0.3	101	0.5	<5
JG-11-034	0.062	<0.05	0.2	0.01	-0.1	98.1	0.5	<5
JG-11-035	0.068	<0.05	0.3	<0.01	-0.1	100	<0.5	<5
JG-11-036	0.173	<0.05	0.9	0.01	-0.2	98.4	<0.5	<5
JG-11-037	0.033	<0.05	3.7	0.4	3.99	99.5	2.1	<5
JG-11-038	0.216	<0.05	0.3	0.02	1.49	99.6	<0.5	<5
JG-11-039	0.334	<0.05	0.2	0.02	0.3	99.8	<0.5	<5
JG-11-040	0.087	<0.05	3.5	0.2	1.1	99.6	0.7	<5
JG-11-041	0.109	<0.05	0.4	0.01	0.4	99.9	<0.5	<5
JG-11-042	0.099	<0.05	0.3	<0.01	-0.5	99.4	<0.5	7
JG-11-043	0.1	<0.05	0.4	0.01	0.2	101.5	0.5	<5
JG-11-044	0.068	<0.05	0.4	0.01	0.1	100	<0.5	<5
JG-11-045	0.073	<0.05	0.4	<0.01	0.6	100	<0.5	<5
JG-11-046	0.098	<0.05	0.3	0.01	0	98.8	<0.5	<5
JG-11-047	0.082	<0.05	0.3	0.01	-0.5	98.2	<0.5	<5
JG-11-048	0.274	<0.05	1.2	0.01	-0.8	101.5	<0.5	<5
JG-11-049	0.273	<0.05	1.6	0.01	-1.29	101	<0.5	5
JG-11-050	0.116	<0.05	1.2	0.05	1.1	99	0.5	<5
JG-11-051	0.124	<0.05	0.3	0.01	0.9	99.5	1.2	<5
JG-11-052	0.082	<0.05	0.2	0.02	-1	101.5	<0.5	<5
JG-11-053	0.128	<0.05	0.3	0.02	-0.7	99.8	<0.5	<5
JG-11-054	0.473	<0.05	0.2	0.01	0.8	98.4	<0.5	<5

Sample	Hg ppm	Sb ppm	Se ppm	Te ppm	LOI %	Total %	Ag ppm	As ppm
JG-11-055	0.153	<0.05	0.5	0.01	-0.3	99.2	<0.5	<5
JG-11-056	0.282	<0.05	0.3	0.02	1.2	99.4	<0.5	<5
JG-11-057	0.259	<0.05	2.2	0.05	2.59	98.3	<0.5	<5
JG-11-058	0.142	<0.05	0.3	0.01	0	100	<0.5	<5
JG-11-059	0.068	<0.05	0.3	<0.01	0.2	100.2	<0.5	<5
JG-11-060	0.088	<0.05	0.3	0.01	-0.2	100.13	<0.5	<5
JG-11-061	0.086	<0.05	0.4	0.01	0	101	<0.5	<5
JG-11-062	0.074	<0.05	0.3	0.02	-0.1	99	<0.5	<5
JG-11-063	0.063	<0.05	0.3	<0.01	-0.5	98.9	<0.5	<5
JG-11-064	0.236	<0.05	1	0.02	-0.4	98.3	<0.5	<5
JG-11-065	0.041	<0.05	2	0.01	2.19	100	<0.5	<5
JG-11-066	0.111	<0.05	2.6	0.01	-0.3	101	<0.5	<5
JG-11-067	0.075	<0.05	0.3	0.01	2.5	101.5	<0.5	<5
JG-11-068	0.074	<0.05	0.4	0.01	0.3	99.6	<0.5	<5
JG-11-069	0.073	<0.05	4.3	0.08	1.4	98.8	<0.5	<5
JG-11-070	0.085	<0.05	1.9	0.01	0.3	99.36	<0.5	<5
JG-11-071	0.089	<0.05	0.6	0.01	-0.3	101	<0.5	<5
JG-11-072	0.058	<0.05	0.8	0.01	0.5	99.6	<0.5	<5
JG-11-073	0.04	<0.05	0.9	0.01	1.3	99.8	<0.5	<5
JG-11-074	0.068	<0.05	0.7	0.01	0	98.3	<0.5	<5
JG-11-075	0.089	<0.05	0.9	0.02	0.1	98.8	<0.5	<5
JG-11-076	0.068	<0.05	4.8	0.38	1.49	99.9	<0.5	<5
JG-11-077	0.049	<0.05	2.2	0.11	1.29	100.5	<0.5	5
JG-11-078	0.086	<0.05	5.2	0.48	2.59	98.61	<0.5	<5
JG-11-079	0.085	<0.05	3.5	0.14	0.6	99.56	<0.5	<5
JG-11-080	0.094	<0.05	0.4	0.01	-0.1	98.41	<0.5	<5
JG-11-081	0.029	<0.05	6.3	0.13	5.39	99.6	3.4	<5
JG-11-082	0.029	<0.05	8.6	0.18	4.79	98.46	1.2	<5
JG-11-083	0.021	<0.05	5.1	0.2	4.4	98.78	2.7	8
JG-11-084	0.066	<0.05	0.8	0.01	0.7	100	<0.5	<5
JG-11-085	0.069	<0.05	1.1	0.01	0.3	101.5	<0.5	<5
JG-11-086	0.045	<0.05	5.8	0.45	1.7	98.9	1.2	<5
JG-11-087	0.05	<0.05	0.9	0.01	0.3	99.1	<0.5	<5
JG-11-088	0.038	<0.05	6.7	0.59	2.18	100.26	1.6	<5
JG-11-089	0.08	<0.05	1.6	0.13	0.2	102	<0.5	<5
JG-11-090	0.029	<0.05	0.9	0.1	2.18	101.5	<0.5	<5
JG-11-091	0.042	<0.05	0.8	0.02	1.79	100	<0.5	<5
JG-11-092	0.067	<0.05	0.6	0.01	0.7	98.7	<0.5	<5
JG-11-093	0.055	<0.05	0.7	0.04	1.29	99.4	<0.5	<5
JG-11-094	0.024	<0.05	0.9	0.01	3.1	99.4	<0.5	<5
JG-11-095	0.081	<0.05	0.8	0.26	0.9	99.6	1.6	<5
JG-11-096	0.067	<0.05	8.2	0.45	2.4	99.5	0.6	<5
JG-11-097	0.066	<0.05	4.2	0.25	1.39	98.7	0.5	<5
JG-11-098	0.074	<0.05	1.5	0.03	0.6	98.1	<0.5	<5
JG-11-099	0.054	<0.05	0.5	0.01	1.29	99.8	<0.5	<5
JG-11-100	0.068	<0.05	0.4	0.01	0.89	99.6	<0.5	<5
JG-11-101	0.079	<0.05	0.3	<0.01	0.6	101.5	<0.5	<5
JG-11-102	0.069	<0.05	0.5	0.01	0.6	98.3	<0.5	<5
JG-11-103	0.142	<0.05	0.5	0.02	1.5	101.05	<0.5	<5
JG-11-104	0.071	<0.05	1.6	0.12	0.5	99.07	<0.5	<5
JG-11-105	0.083	<0.05	0.3	<0.01	0.3	98.11	<0.5	<5
JG-11-106	0.053	<0.05	0.7	0.02	1.18	99.63	<0.5	<5
JG-11-107	0.1	<0.05	0.3	<0.01	NSS	NSS	<0.5	<5
JG-11-108	0.051	<0.05	11.6	0.96	5.58	97.2	1.8	<5

Sample	Hg ppm	Sb ppm	Se ppm	Te ppm	LOI %	Total %	Ag ppm	As ppm
JG-11-109	0.041	<0.05	0.9	0.04	2.19	99.24	<0.5	<5
JG-11-110	0.084	<0.05	0.9	0.07	1.1	101.5	<0.5	<5
JG-11-111	0.059	<0.05	0.9	0.04	0.7	98.28	<0.5	<5
JG-11-112	0.073	<0.05	0.9	0.05	0.8	100.85	<0.5	<5
JG-11-113	0.035	<0.05	0.5	0.02	1.18	99.69	<0.5	<5
JG-11-114	0.083	<0.05	1.6	0.1	0.69	99.56	<0.5	<5
JG-11-115	0.076	<0.05	10.7	0.79	2.39	98.2	0.5	<5
JG-11-116	0.049	<0.05	1.8	6.94	1.29	98.3	2.5	<5
JG-11-117	0.038	<0.05	0.9	0.03	1	98.2	<0.5	7
JG-11-118	0.034	<0.05	0.9	0.03	2.68	100.7	<0.5	<5
JG-11-119	0.072	<0.05	0.3	<0.01	1.38	100.7	<0.5	<5
JG-11-120	0.059	<0.05	0.2	<0.01	-0.2	100.8	<0.5	<5
JG-11-121	0.111	<0.05	0.3	0.01	-0.6	99.66	<0.5	<5
JG-11-122	0.089	<0.05	0.3	0.01	-0.2	99.21	<0.5	<5
JG-11-123	0.066	<0.05	0.3	0.01	0	99.6	<0.5	<5
JG-11-124	0.046	<0.05	0.5	0.01	0.9	95.1	<0.5	<5
JG-11-125	0.016	<0.05	0.5	0.01	4.4	98.9	<0.5	<5
JG-11-126	0.021	<0.05	0.7	0.01	4	98.4	<0.5	<5
JG-11-127	0.077	<0.05	0.7	0.01	0.4	101.5	<0.5	5
JG-11-128	0.069	<0.05	0.6	0.01	-0.5	98.3	<0.5	<5
JG-11-129	0.253	<0.05	0.4	<0.01	0.2	100	<0.5	<5
JG-11-130	0.063	<0.05	0.5	<0.01	0.1	98.9	<0.5	<5
JG-11-131	0.074	<0.05	0.3	0.02	0.7	100.5	<0.5	<5
JG-11-132	0.089	<0.05	<0.2	0.03	-0.7	99.3	<0.5	<5
JG-11-133	0.08	<0.05	0.2	0.03	-1.09	98.6	<0.5	<5
JG-11-134	0.086	<0.05	0.2	0.02	-1.2	101	<0.5	<5
JG-11-135	0.184	<0.05	0.2	0.01	-0.9	100.5	<0.5	<5
JG-11-136	0.14	<0.05	<0.2	0.01	-0.2	101.5	<0.5	<5
JG-11-137	0.134	<0.05	0.3	0.01	0.2	98.7	<0.5	<5
JG-11-138	0.074	<0.05	0.4	0.02	-0.4	99.9	<0.5	<5
JG-11-139	0.077	<0.05	0.2	0.04	-1.39	100.5	<0.5	<5
JG-11-140	0.069	<0.05	0.5	0.01	0.7	101.5	<0.5	<5
JG-11-141	0.082	<0.05	2.8	0.51	-0.2	98.3	5.1	<5
JG-11-142	0.019	<0.05	2.2	0.04	3.61	98.8	<0.5	<5
JG-11-143	0.022	<0.05	1.8	0.2	4.38	98.6	0.6	<5
JG-11-144	0.092	<0.05	0.8	0.07	4.37	99.5	0.5	<5
JG-11-145	0.045	<0.05	0.7	0.02	0.3	98.2	<0.5	<5
JG-11-146	0.055	<0.05	0.6	0.02	-0.8	95	<0.5	<5
JG-11-147	0.298	<0.05	6.6	0.12	4.79	98.6	1.8	<5
JG-11-148	0.095	<0.05	0.6	0.05	1	94	<0.5	<5
JG-11-149	0.058	<0.05	0.6	0.11	1.59	100.5	0.8	<5
JG-11-150	0.05	<0.05	1.9	0.14	1.4	98.9	2.7	<5
JG-11-151	0.088	<0.05	0.4	0.01	0.4	101	<0.5	<5
JG-11-152	0.069	<0.05	0.4	0.02	1.19	99.7	<0.5	<5
JG-11-153	0.046	<0.05	0.5	0.01	0.9	99.4	<0.5	<5

Sample	Cd ppm	Co ppm	Cu ppm	Mo ppm	Ni ppm	Pb ppm	Zn ppm
JG-11-001	<0.5	64	15	<1	167	<2	73
JG-11-002	<0.5	57	33	<1	94	<2	71
JG-11-003	<0.5	67	24	<1	225	<2	58
JG-11-004	<0.5	75	7	<1	301	<2	54
JG-11-005	<0.5	79	760	8	147	3	151
JG-11-006	<0.5	81	416	<1	719	<2	74
JG-11-007	<0.5	35	69	<1	28	14	85
JG-11-008	<0.5	43	50	<1	27	13	87
JG-11-009	<0.5	34	52	<1	27	12	94
JG-11-010	<0.5	80	17	<1	331	<2	60
JG-11-011	<0.5	99	712	<1	1090	4	60
JG-11-012	<0.5	65	42	<1	255	<2	60
JG-11-013	<0.5	100	6	2	2	17	79
JG-11-014	<0.5	56	11	<1	52	4	75
JG-11-015	<0.5	83	97	<1	434	<2	72
JG-11-016	<0.5	173	2480	<1	3870	6	67
JG-11-017	1.5	655	6750	<1	9870	22	189
JG-11-018	<0.5	35	38	<1	35	11	91
JG-11-019	<0.5	88	106	1	445	7	84
JG-11-020	<0.5	59	41	1	245	5	69
JG-11-021	<0.5	79	255	<1	648	4	81
JG-11-022	<0.5	76	337	<1	949	5	67
JG-11-023	<0.5	91	312	1	884	2	78
JG-11-024	<0.5	79	112	<1	442	4	64
JG-11-025	<0.5	36	69	1	23	12	91
JG-11-026	<0.5	38	44	<1	33	13	96
JG-11-027	<0.5	56	170	1	66	11	129
JG-11-028	<0.5	53	125	1	173	8	126
JG-11-029	0.8	305	2270	1	3880	27	204
JG-11-030	<0.5	138	532	1	1695	5	82
JG-11-031	<0.5	48	27	<1	93	2	63
JG-11-032	<0.5	54	16	1	123	2	72
JG-11-033	<0.5	66	24	<1	165	<2	67
JG-11-034	<0.5	56	9	<1	160	2	64
JG-11-035	<0.5	70	15	1	210	4	75
JG-11-036	<0.5	58	31	2	43	10	167
JG-11-037	0.5	144	3460	<1	2310	16	110
JG-11-038	<0.5	63	23	4	30	23	140
JG-11-039	<0.5	112	20	1	31	16	63
JG-11-040	<0.5	134	920	1	2160	15	78
JG-11-041	<0.5	58	13	1	95	6	99
JG-11-042	<0.5	64	16	<1	109	<2	65
JG-11-043	<0.5	62	18	1	104	2	72
JG-11-044	<0.5	62	22	1	103	3	81
JG-11-045	<0.5	67	29	1	151	5	101
JG-11-046	<0.5	65	27	<1	131	<2	68
JG-11-047	<0.5	80	28	<1	234	3	85
JG-11-048	<0.5	58	20	2	<1	10	206
JG-11-049	<0.5	57	27	3	1	12	290
JG-11-050	<0.5	93	400	1	832	5	66
JG-11-051	<0.5	59	109	<1	93	2	112
JG-11-052	<0.5	172	6	<1	736	6	124
JG-11-053	<0.5	156	26	1	523	10	143
JG-11-054	<0.5	130	85	1	50	3	36

Sample	Cd ppm	Co ppm	Cu ppm	Mo ppm	Ni ppm	Pb ppm	Zn ppm
JG-11-055	<0.5	72	12	<1	94	11	150
JG-11-056	<0.5	103	10	1	22	4	195
JG-11-057	0.6	71	46	5	43	16	131
JG-11-058	<0.5	66	9	<1	121	5	77
JG-11-059	<0.5	53	16	<1	77	2	93
JG-11-060	<0.5	78	15	<1	143	3	92
JG-11-061	<0.5	81	29	<1	136	<2	101
JG-11-062	<0.5	124	16	<1	376	<2	152
JG-11-063	<0.5	59	14	<1	144	2	75
JG-11-064	<0.5	57	14	2	<1	11	182
JG-11-065	<0.5	44	48	<1	<1	<2	125
JG-11-066	<0.5	60	41	<1	<1	4	231
JG-11-067	<0.5	58	24	<1	116	2	61
JG-11-068	<0.5	65	25	<1	77	3	66
JG-11-069	<0.5	160	463	5	195	<2	113
JG-11-070	<0.5	47	66	<1	<1	3	103
JG-11-071	<0.5	67	16	<1	61	3	100
JG-11-072	<0.5	53	64	<1	41	5	116
JG-11-073	<0.5	50	93	2	64	4	130
JG-11-074	<0.5	61	74	1	95	4	129
JG-11-075	<0.5	76	130	<1	154	8	126
JG-11-076	<0.5	108	758	1	1075	17	142
JG-11-077	<0.5	95	471	<1	813	10	92
JG-11-078	<0.5	151	1075	<1	3130	19	105
JG-11-079	<0.5	126	730	1	1600	5	91
JG-11-080	<0.5	55	15	<1	110	<2	48
JG-11-081	5.5	670	8240	4	3090	7	203
JG-11-082	0.8	399	2820	1	5840	16	131
JG-11-083	2.2	233	7360	<1	2560	16	91
JG-11-084	<0.5	54	87	1	52	7	120
JG-11-085	<0.5	50	33	<1	41	<2	116
JG-11-086	<0.5	177	3450	3	2720	10	124
JG-11-087	<0.5	53	156	2	54	11	153
JG-11-088	0.6	183	2550	<1	4570	51	81
JG-11-089	<0.5	66	524	<1	230	20	114
JG-11-090	<0.5	48	175	<1	101	81	118
JG-11-091	<0.5	54	45	<1	63	2	121
JG-11-092	<0.5	34	58	<1	30	15	86
JG-11-093	<0.5	59	336	<1	168	14	103
JG-11-094	<0.5	49	40	<1	74	3	102
JG-11-095	0.7	75	1085	<1	405	70	65
JG-11-096	<0.5	209	2160	<1	3470	12	65
JG-11-097	<0.5	135	1605	<1	1650	17	91
JG-11-098	<0.5	68	233	<1	423	7	96
JG-11-099	<0.5	49	65	<1	40	6	82
JG-11-100	<0.5	59	73	<1	65	4	84
JG-11-101	<0.5	61	34	<1	58	2	94
JG-11-102	<0.5	66	90	<1	73	2	160
JG-11-103	<0.5	57	261	<1	15	6	118
JG-11-104	<0.5	99	489	<1	726	47	121
JG-11-105	<0.5	61	73	<1	98	8	95
JG-11-106	<0.5	48	142	<1	179	14	90
JG-11-107	<0.5	59	18	<1	26	4	86
JG-11-108	2.2	415	9690	<1	8410	45	120

Sample	Cd ppm	Co ppm	Cu ppm	Mo ppm	Ni ppm	Pb ppm	Zn ppm
JG-11-109	<0.5	69	292	6	528	8	123
JG-11-110	<0.5	79	416	<1	679	<2	105
JG-11-111	<0.5	96	319	<1	797	2	199
JG-11-112	<0.5	89	313	2	630	<2	139
JG-11-113	<0.5	67	126	<1	318	4	183
JG-11-114	<0.5	97	257	<1	670	7	114
JG-11-115	0.6	354	2040	<1	4840	37	144
JG-11-116	<0.5	81	389	<1	710	384	159
JG-11-117	<0.5	61	158	<1	112	<2	157
JG-11-118	<0.5	58	180	<1	72	<2	124
JG-11-119	<0.5	46	86	<1	23	6	83
JG-11-120	<0.5	58	22	<1	158	<2	63
JG-11-121	<0.5	66	34	<1	187	<2	68
JG-11-122	<0.5	59	53	<1	167	<2	67
JG-11-123	<0.5	63	47	<1	203	<2	69
JG-11-124	<0.5	47	58	<1	41	5	124
JG-11-125	<0.5	53	57	<1	90	<2	85
JG-11-126	<0.5	55	59	<1	94	<2	87
JG-11-127	<0.5	60	48	1	45	2	136
JG-11-128	<0.5	65	47	<1	38	2	193
JG-11-129	<0.5	89	195	<1	55	<2	56
JG-11-130	<0.5	53	23	<1	39	6	146
JG-11-131	<0.5	54	137	<1	58	5	81
JG-11-132	<0.5	147	6	<1	613	<2	100
JG-11-133	<0.5	176	4	<1	713	<2	133
JG-11-134	<0.5	133	23	<1	472	3	123
JG-11-135	<0.5	97	57	<1	105	<2	96
JG-11-136	<0.5	71	11	<1	98	<2	55
JG-11-137	<0.5	48	14	<1	45	<2	42
JG-11-138	<0.5	102	46	<1	187	<2	149
JG-11-139	<0.5	176	6	<1	511	<2	156
JG-11-140	<0.5	56	79	<1	41	<2	93
JG-11-141	1.7	66	5390	<1	755	14	127
JG-11-142	<0.5	48	60	1	27	6	215
JG-11-143	0.5	161	3430	<1	2550	9	235
JG-11-144	<0.5	56	1305	<1	433	23	68
JG-11-145	<0.5	41	134	<1	50	19	89
JG-11-146	<0.5	52	131	<1	71	3	85
JG-11-147	0.8	146	6970	4	2230	3	143
JG-11-148	<0.5	44	499	<1	345	36	83
JG-11-149	<0.5	42	296	<1	508	24	84
JG-11-150	0.8	70	1715	<1	559	10	121
JG-11-151	<0.5	43	52	<1	65	7	84
JG-11-152	<0.5	57	44	<1	297	7	127
JG-11-153	<0.5	47	44	<1	32	11	92

Appendix E

Range, mean and median composition of biotite samples as determined by electron microprobe analysis.

Sample	JG-11-001			JG-11-003		
	Range	Mean	Median	Range	Mean	Median
SiO ₂	0.95	37.45	37.45	0.58	37.66	37.69
Al ₂ O ₃	0.54	15.46	15.43	0.33	15.90	15.93
TiO ₂	0.84	5.00	5.09	0.94	4.21	4.29
V ₂ O ₃	0.06	0.02	0.02	0.03	0.02	0.02
Cr ₂ O ₃	0.33	0.12	0.05	0.06	0.06	0.05
FeO	3.53	9.12	8.92	1.23	9.21	9.50
MnO	0.05	0.04	0.04	0.02	0.02	0.02
MgO	2.37	17.98	17.96	1.32	18.00	17.88
NiO	0.03	0.07	0.07	0.02	0.07	0.07
K ₂ O	0.53	9.23	9.22	0.42	8.71	8.72
Na ₂ O	0.32	0.53	0.55	0.33	0.82	0.81
CaO	0.07	0.01	0.01	0.04	0.01	0.00
BaO	0.31	0.38	0.38	0.16	0.37	0.39
F	0.21	0.18	0.17	0.11	0.12	0.12
Cl	0.04	0.01	0.01	0.04	0.03	0.02
TOTAL	1.71	95.60	95.64	0.88	95.20	95.21
O≠F,Cl	0.09	0.08	0.07	0.05	0.06	0.06
Σ -X	1.72	95.52	95.56	0.92	95.14	95.14

Number of ions on the basis of 12 (O, OH, F) or 22 positive charges

Si	0.07	5.46	5.46	0.06	5.49	5.49
Al	0.07	2.65	2.66	0.06	2.73	2.73
Ti	0.09	0.55	0.56	0.10	0.46	0.47
V	0.01	0.00	0.00	0.00	0.00	0.00
Cr	0.04	0.01	0.01	0.01	0.01	0.01
Fe	0.45	1.11	1.08	0.15	1.12	1.16
Mn	0.01	0.00	0.00	0.00	0.00	0.00
Mg	0.43	3.91	3.90	0.30	3.91	3.89
Ni	0.00	0.01	0.01	0.00	0.01	0.01
K	0.11	1.71	1.72	0.08	1.62	1.62
Na	0.09	0.15	0.16	0.09	0.23	0.23
Ca	0.01	0.00	0.00	0.01	0.00	0.00
Ba	0.02	0.02	0.02	0.01	0.02	0.02
Σ cations	0.08	15.57	15.57	0.07	15.58	15.59
F	0.10	0.08	0.08	0.05	0.05	0.06
Cl	0.01	0.00	0.00	0.01	0.01	0.01
Fe/FeMnMg	0.09	0.22	0.22	0.03	0.22	0.23
Al(IV)	0.07	2.54	2.54	0.06	2.51	2.51
Al(VI)	0.08	0.11	0.11	0.06	0.22	0.22
K/KNaBa	0.04	0.91	0.91	0.04	0.87	0.87

Sample	JG-11-006			JG-11-012		
	Range	Mean	Median	Range	Mean	Median
SiO ₂	0.92	36.50	36.40	0.76	37.73	37.72
Al ₂ O ₃	0.68	15.20	15.16	0.69	15.10	15.09
TiO ₂	0.89	5.14	5.18	1.34	4.77	4.90
V ₂ O ₃	0.05	0.02	0.01	0.11	0.02	0.00
Cr ₂ O ₃	0.09	0.01	0.00	0.25	0.07	0.05
FeO	2.55	12.54	12.46	3.17	9.57	10.03
MnO	0.04	0.04	0.04	0.05	0.04	0.05
MgO	1.96	15.32	15.12	2.56	17.53	17.26
NiO	0.08	0.17	0.18	0.04	0.10	0.09
K ₂ O	0.48	9.28	9.29	0.57	9.16	9.20
Na ₂ O	0.22	0.42	0.41	0.21	0.39	0.37
CaO	0.04	0.02	0.02	0.07	0.01	0.00
BaO	0.33	0.52	0.53	0.15	0.18	0.19
F	0.15	0.21	0.23	0.14	0.40	0.42
Cl	0.03	0.02	0.02	0.03	0.04	0.03
TOTAL	2.77	95.40	95.50	0.94	95.13	95.05
O≠F,Cl	0.06	0.09	0.10	0.05	0.17	0.18
Σ -X	2.76	95.31	95.44	0.91	94.95	94.87

Number of ions on the basis of 12 (O, OH, F) or 22 positive charges

Si	0.06	5.44	5.43	0.04	5.53	5.54
Al	0.06	2.67	2.67	0.08	2.61	2.62
Ti	0.10	0.58	0.58	0.16	0.53	0.54
V	0.01	0.00	0.00	0.01	0.00	0.00
Cr	0.01	0.00	0.00	0.03	0.01	0.01
Fe	0.33	1.56	1.57	0.40	1.17	1.23
Mn	0.00	0.00	0.00	0.01	0.01	0.01
Mg	0.39	3.40	3.36	0.50	3.83	3.79
Ni	0.01	0.02	0.02	0.00	0.01	0.01
K	0.09	1.76	1.77	0.11	1.71	1.73
Na	0.06	0.12	0.12	0.06	0.11	0.10
Ca	0.01	0.00	0.00	0.01	0.00	0.00
Ba	0.02	0.03	0.03	0.01	0.01	0.01
Σ cations	0.07	15.56	15.56	0.12	15.53	15.52
F	0.07	0.10	0.11	0.06	0.18	0.19
Cl	0.01	0.01	0.01	0.01	0.01	0.01
Fe/FeMnMg	0.07	0.31	0.32	0.08	0.23	0.24
Al(IV)	0.06	2.56	2.57	0.04	2.47	2.46
Al(VI)	0.08	0.11	0.10	0.11	0.14	0.16
K/KNaBa	0.03	0.92	0.92	0.04	0.93	0.93

Sample	JG-11-016			JG-11-017		
	Range	Mean	Median	Range	Mean	Median
SiO ₂	1.33	36.93	36.86	1.64	37.28	37.30
Al ₂ O ₃	1.34	16.07	15.88	0.74	15.53	15.61
TiO ₂	1.78	3.83	4.02	0.91	4.12	4.05
V ₂ O ₃	0.03	0.00	0.00	0.00	0.00	0.00
Cr ₂ O ₃	0.06	0.02	0.02	0.02	0.01	0.01
FeO	3.58	11.98	11.83	1.97	12.35	12.59
MnO	0.05	0.03	0.03	0.04	0.07	0.08
MgO	2.83	16.35	16.31	1.99	16.35	16.46
NiO	0.08	0.11	0.11	0.07	0.07	0.06
K ₂ O	0.39	8.71	8.73	1.04	8.76	8.78
Na ₂ O	0.29	0.88	0.88	0.22	0.84	0.83
CaO	0.03	0.01	0.00	0.03	0.01	0.00
BaO	0.41	0.40	0.37	0.14	0.50	0.51
F	0.15	0.12	0.11	0.13	0.18	0.18
Cl	0.02	0.01	0.01	0.03	0.01	0.01
TOTAL	1.24	95.44	95.33	2.97	96.08	96.12
O≠F,Cl	0.06	0.05	0.05	0.05	0.08	0.07
Σ -X	1.26	95.39	95.30	2.96	96.00	96.01

Number of ions on the basis of 12 (O, OH, F) or 22 positive charges

Si	0.09	5.45	5.44	0.08	5.48	5.49
Al	0.17	2.79	2.77	0.08	2.69	2.68
Ti	0.20	0.42	0.45	0.10	0.46	0.45
V	0.00	0.00	0.00	0.00	0.00	0.00
Cr	0.01	0.00	0.00	0.00	0.00	0.00
Fe	0.46	1.48	1.46	0.26	1.52	1.55
Mn	0.01	0.00	0.00	0.00	0.01	0.01
Mg	0.56	3.59	3.59	0.39	3.58	3.62
Ni	0.01	0.01	0.01	0.01	0.01	0.01
K	0.09	1.64	1.65	0.17	1.64	1.65
Na	0.08	0.25	0.25	0.06	0.24	0.24
Ca	0.01	0.00	0.00	0.00	0.00	0.00
Ba	0.02	0.02	0.02	0.01	0.03	0.03
Σ cations	0.08	15.65	15.65	0.08	15.63	15.63
F	0.07	0.05	0.05	0.06	0.08	0.08
Cl	0.01	0.00	0.00	0.01	0.00	0.00
Fe/FeMnMg	0.09	0.29	0.29	0.06	0.30	0.30
Al(IV)	0.09	2.55	2.56	0.08	2.52	2.51
Al(VI)	0.21	0.24	0.22	0.13	0.17	0.18
K/KNaBa	0.03	0.86	0.86	0.03	0.86	0.86

Sample	JG-11-021			JG-11-024		
	Range	Mean	Median	Range	Mean	Median
SiO ₂	1.08	37.50	37.51	0.91	37.76	37.76
Al ₂ O ₃	0.66	15.81	15.77	1.32	16.10	16.00
TiO ₂	1.65	3.28	3.39	2.52	3.96	4.03
V ₂ O ₃	0.02	0.00	0.00	0.06	0.03	0.03
Cr ₂ O ₃	0.19	0.05	0.03	0.16	0.04	0.01
FeO	1.76	12.19	12.30	3.08	9.28	9.63
MnO	0.06	0.04	0.05	0.05	0.03	0.03
MgO	1.23	16.54	16.61	2.76	18.24	18.12
NiO	0.05	0.15	0.15	0.03	0.10	0.10
K ₂ O	0.37	8.53	8.54	0.57	8.63	8.65
Na ₂ O	0.30	1.00	1.01	0.39	0.97	0.98
CaO	0.06	0.00	0.00	0.04	0.01	0.01
BaO	0.12	0.18	0.19	0.24	0.40	0.41
F	0.13	0.12	0.13	0.18	0.22	0.22
Cl	0.05	0.12	0.12	0.03	0.02	0.02
TOTAL	2.37	95.53	95.54	1.41	95.78	95.85
O≠F,Cl	0.06	0.08	0.08	0.07	0.10	0.10
Σ -X	2.37	95.45	95.46	1.46	95.69	95.78

Number of ions on the basis of 12 (O, OH, F) or 22 positive charges

Si	0.09	5.52	5.52	0.09	5.48	5.48
Al	0.10	2.74	2.75	0.19	2.75	2.74
Ti	0.18	0.36	0.38	0.28	0.43	0.44
V	0.00	0.00	0.00	0.01	0.00	0.00
Cr	0.02	0.01	0.00	0.02	0.00	0.00
Fe	0.21	1.50	1.50	0.39	1.13	1.17
Mn	0.01	0.01	0.01	0.01	0.00	0.00
Mg	0.29	3.63	3.65	0.56	3.94	3.91
Ni	0.01	0.02	0.02	0.00	0.01	0.01
K	0.08	1.60	1.60	0.10	1.60	1.60
Na	0.08	0.28	0.29	0.11	0.27	0.28
Ca	0.01	0.00	0.00	0.01	0.00	0.00
Ba	0.01	0.01	0.01	0.01	0.02	0.02
Σ cations	0.14	15.68	15.67	0.14	15.62	15.62
F	0.06	0.06	0.06	0.08	0.10	0.10
Cl	0.01	0.03	0.03	0.01	0.00	0.00
Fe/FeMnMg	0.04	0.29	0.29	0.08	0.22	0.23
Al(IV)	0.09	2.48	2.48	0.09	2.52	2.52
Al(VI)	0.14	0.26	0.25	0.24	0.23	0.22
K/KNaBa	0.04	0.84	0.84	0.05	0.84	0.84

Sample	JG-11-032			JG-11-033B		
	Range	Mean	Median	Range	Mean	Median
SiO ₂	1.90	39.24	39.30	1.02	39.70	39.77
Al ₂ O ₃	0.96	15.00	14.97	1.28	15.30	15.52
TiO ₂	0.90	2.32	2.36	1.47	2.32	2.31
V ₂ O ₃	0.11	0.04	0.03	0.06	0.03	0.03
Cr ₂ O ₃	0.12	0.05	0.05	0.28	0.14	0.19
FeO	4.57	9.88	9.69	3.39	7.49	7.23
MnO	0.04	0.04	0.05	0.02	0.01	0.01
MgO	3.56	18.76	18.82	2.86	20.46	20.39
NiO	0.04	0.05	0.05	0.03	0.05	0.05
K ₂ O	0.46	8.35	8.30	0.87	8.26	8.19
Na ₂ O	0.40	1.06	1.04	0.66	1.09	1.15
CaO	0.05	0.01	0.01	0.03	0.01	0.00
BaO	0.20	0.32	0.31	0.31	0.44	0.44
F	0.49	1.55	1.59	0.12	1.27	1.26
Cl	0.09	0.12	0.12	0.09	0.11	0.12
TOTAL	2.00	96.80	96.89	1.22	96.66	96.64
O≠F,Cl	0.19	0.68	0.69	0.05	0.56	0.56
Σ -X	1.95	96.12	96.18	1.20	96.10	96.05

Number of ions on the basis of 12 (O, OH, F) or 22 positive charges

Si	0.09	5.70	5.70	0.07	5.69	5.69
Al	0.14	2.57	2.56	0.16	2.58	2.60
Ti	0.10	0.25	0.26	0.17	0.25	0.25
V	0.01	0.00	0.00	0.01	0.00	0.00
Cr	0.01	0.01	0.01	0.03	0.02	0.02
Fe	0.59	1.20	1.18	0.42	0.90	0.87
Mn	0.01	0.01	0.01	0.00	0.00	0.00
Mg	0.65	4.06	4.09	0.54	4.37	4.35
Ni	0.00	0.01	0.01	0.00	0.01	0.01
K	0.14	1.55	1.54	0.19	1.51	1.49
Na	0.10	0.30	0.29	0.18	0.30	0.32
Ca	0.01	0.00	0.00	0.01	0.00	0.00
Ba	0.01	0.02	0.02	0.02	0.02	0.02
Σ cations	0.13	15.66	15.66	0.15	15.64	15.64
F	0.20	0.71	0.73	0.06	0.57	0.57
Cl	0.02	0.03	0.03	0.02	0.03	0.03
Fe/FeMnMg	0.11	0.23	0.22	0.08	0.17	0.17
Al(IV)	0.09	2.30	2.30	0.07	2.31	2.31
Al(VI)	0.08	0.27	0.28	0.13	0.28	0.29
K/KNaBa	0.05	0.83	0.83	0.09	0.82	0.81

Sample	JG-11-037			JG-11-035		
	Range	Mean	Median	Range	Mean	Median
SiO ₂	3.09	36.24	36.45	1.60	39.01	39.08
Al ₂ O ₃	3.43	15.87	15.39	0.98	14.70	14.73
TiO ₂	2.08	2.91	3.07	0.99	3.78	3.93
V ₂ O ₃	0.00	0.00	0.00	0.08	0.03	0.02
Cr ₂ O ₃	0.06	0.02	0.02	0.11	0.07	0.06
FeO	7.24	15.48	15.28	3.49	7.72	7.52
MnO	0.07	0.07	0.07	0.04	0.02	0.02
MgO	3.25	15.23	15.16	2.97	19.88	19.86
NiO	0.07	0.07	0.08	0.03	0.05	0.05
K ₂ O	2.93	8.21	8.37	0.57	9.55	9.48
Na ₂ O	1.19	0.32	0.19	0.24	0.33	0.30
CaO	0.14	0.03	0.02	0.04	0.01	0.00
BaO	0.32	0.35	0.36	0.82	0.51	0.50
F	0.12	0.15	0.15	0.36	1.02	1.04
Cl	0.04	0.02	0.02	0.03	0.03	0.02
TOTAL	3.25	94.99	95.04	1.79	96.71	96.64
O≠F,Cl	0.05	0.07	0.07	0.15	0.43	0.44
Σ -X	3.25	94.92	94.97	1.69	96.28	96.21

Number of ions on the basis of 12 (O, OH, F) or 22 positive charges

Si	0.36	5.44	5.48	0.05	5.62	5.63
Al	0.63	2.81	2.72	0.08	2.50	2.50
Ti	0.23	0.33	0.35	0.12	0.41	0.43
V	0.00	0.00	0.00	0.01	0.00	0.00
Cr	0.01	0.00	0.00	0.01	0.01	0.01
Fe	1.02	1.95	1.92	0.45	0.93	0.91
Mn	0.01	0.01	0.01	0.00	0.00	0.00
Mg	0.66	3.41	3.41	0.49	4.27	4.29
Ni	0.01	0.01	0.01	0.00	0.01	0.01
K	0.54	1.57	1.60	0.11	1.76	1.75
Na	0.34	0.09	0.06	0.07	0.09	0.08
Ca	0.02	0.01	0.00	0.01	0.00	0.00
Ba	0.02	0.02	0.02	0.05	0.03	0.03
Σ cations	0.17	15.63	15.62	0.10	15.61	15.60
F	0.06	0.07	0.07	0.15	0.46	0.47
Cl	0.01	0.01	0.00	0.01	0.01	0.01
Fe/FeMnMg	0.15	0.36	0.37	0.09	0.18	0.17
Al(IV)	0.36	2.56	2.52	0.05	2.38	2.37
Al(VI)	0.40	0.25	0.20	0.11	0.12	0.12
K/KNaBa	0.18	0.93	0.95	0.05	0.94	0.93

Sample	JG-11-059			JG-11-061		
	Range	Mean	Median	Range	Mean	Median
SiO ₂	2.37	38.43	38.48	1.67	38.50	38.43
Al ₂ O ₃	1.28	14.51	14.57	0.82	14.33	14.30
TiO ₂	2.16	1.52	1.92	2.37	4.65	4.53
V ₂ O ₃	0.09	0.04	0.03	0.15	0.09	0.08
Cr ₂ O ₃	0.08	0.04	0.04	0.23	0.11	0.06
FeO	6.59	13.11	13.20	4.18	9.55	9.62
MnO	0.05	0.03	0.03	0.06	0.04	0.04
MgO	4.89	17.32	17.53	4.20	18.08	18.25
NiO	0.03	0.03	0.03	0.03	0.04	0.04
K ₂ O	1.31	8.80	8.92	0.61	9.60	9.65
Na ₂ O	0.76	0.71	0.59	0.22	0.24	0.23
CaO	0.06	0.03	0.02	0.10	0.02	0.00
BaO	0.44	0.28	0.35	0.79	0.30	0.16
F	0.71	1.91	1.96	0.69	1.17	1.13
Cl	0.48	0.25	0.32	0.19	0.02	0.01
TOTAL	2.69	97.01	96.80	1.80	96.75	96.83
O≠F,Cl	0.28	0.86	0.86	0.29	0.50	0.48
Σ -X	2.74	96.15	95.96	1.86	96.25	96.30

Number of ions on the basis of 12 (O, OH, F) or 22 positive charges

Si	0.12	5.71	5.71	0.08	5.61	5.61
Al	0.19	2.54	2.54	0.14	2.46	2.46
Ti	0.24	0.17	0.21	0.27	0.51	0.49
V	0.01	0.00	0.00	0.02	0.01	0.01
Cr	0.01	0.00	0.01	0.03	0.01	0.01
Fe	0.88	1.63	1.66	0.53	1.16	1.18
Mn	0.01	0.00	0.00	0.01	0.00	0.00
Mg	0.93	3.83	3.88	0.82	3.92	3.95
Ni	0.00	0.00	0.00	0.00	0.00	0.00
K	0.30	1.67	1.71	0.12	1.78	1.79
Na	0.21	0.20	0.17	0.06	0.07	0.07
Ca	0.01	0.00	0.00	0.02	0.00	0.00
Ba	0.03	0.02	0.02	0.05	0.02	0.01
Σ cations	0.21	15.77	15.75	0.21	15.55	15.54
F	0.32	0.90	0.91	0.30	0.54	0.52
Cl	0.12	0.06	0.08	0.05	0.01	0.00
Fe/FeMnMg	0.17	0.30	0.30	0.12	0.23	0.23
Al(IV)	0.12	2.29	2.29	0.08	2.39	2.39
Al(VI)	0.21	0.25	0.24	0.13	0.07	0.07
K/KNaBa	0.12	0.88	0.90	0.05	0.95	0.96

Sample	JG-11-068			JG-11-069		
	Range	Mean	Median	Range	Mean	Median
SiO ₂	2.06	39.59	39.68	2.57	38.56	38.80
Al ₂ O ₃	0.74	13.78	13.79	0.85	14.01	13.95
TiO ₂	2.01	3.66	3.61	1.89	3.22	3.21
V ₂ O ₃	0.17	0.06	0.06	0.12	0.04	0.00
Cr ₂ O ₃	0.52	0.44	0.44	0.23	0.14	0.14
FeO	5.51	6.36	6.16	7.14	11.95	11.39
MnO	0.05	0.03	0.03	0.05	0.05	0.05
MgO	5.20	20.87	20.95	5.99	17.13	17.57
NiO	0.06	0.02	0.02	0.01	0.00	0.00
K ₂ O	1.46	9.76	9.63	0.66	9.73	9.75
Na ₂ O	0.43	0.32	0.32	0.37	0.23	0.26
CaO	0.04	0.02	0.01	0.14	0.02	0.02
BaO	0.86	0.39	0.31	0.65	0.52	0.47
F	1.21	2.92	2.91	0.85	1.76	1.81
Cl	0.03	0.03	0.02	0.08	0.03	0.03
TOTAL	3.13	98.25	98.30	1.09	97.39	97.36
O≠F,Cl	0.51	1.24	1.23	0.35	0.75	0.77
Σ -X	3.12	97.02	97.10	1.12	96.65	96.62

Number of ions on the basis of 12 (O, OH, F) or 22 positive charges

Si	0.15	5.70	5.69	0.17	5.69	5.70
Al	0.08	2.34	2.34	0.08	2.43	2.43
Ti	0.23	0.40	0.39	0.22	0.36	0.35
V	0.02	0.01	0.01	0.01	0.00	0.00
Cr	0.06	0.05	0.05	0.03	0.02	0.02
Fe	0.69	0.77	0.74	0.94	1.48	1.40
Mn	0.01	0.00	0.00	0.01	0.01	0.01
Mg	1.00	4.48	4.51	1.18	3.76	3.85
Ni	0.01	0.00	0.00	0.00	0.00	0.00
K	0.24	1.79	1.78	0.15	1.83	1.83
Na	0.12	0.09	0.09	0.10	0.07	0.07
Ca	0.01	0.00	0.00	0.02	0.00	0.00
Ba	0.05	0.02	0.02	0.04	0.03	0.03
Σ cations	0.26	15.63	15.62	0.14	15.65	15.65
F	0.53	1.33	1.33	0.37	0.82	0.85
Cl	0.01	0.01	0.01	0.02	0.01	0.01
Fe/FeMnMg	0.14	0.15	0.14	0.19	0.28	0.27
Al(IV)	0.15	2.30	2.31	0.17	2.31	2.30
Al(VI)	0.13	0.04	0.03	0.18	0.12	0.11
K/KNaBa	0.07	0.94	0.94	0.05	0.95	0.95

Sample	JG-11-072			JG-11-075		
	Range	Mean	Median	Range	Mean	Median
SiO ₂	1.42	36.93	36.91	1.65	36.93	36.93
Al ₂ O ₃	1.84	14.99	14.92	2.34	15.78	14.96
TiO ₂	1.82	3.87	3.92	1.11	3.35	3.80
V ₂ O ₃	0.01	0.00	0.00	0.00	0.00	0.00
Cr ₂ O ₃	0.03	0.02	0.02	0.05	0.02	0.02
FeO	3.41	17.27	17.40	2.63	15.64	17.36
MnO	0.06	0.06	0.06	0.07	0.04	0.06
MgO	3.26	13.20	13.06	1.03	14.15	13.22
NiO	0.03	0.02	0.03	0.04	0.04	0.03
K ₂ O	0.56	9.36	9.40	0.68	8.54	9.40
Na ₂ O	0.08	0.32	0.32	0.18	0.83	0.32
CaO	0.06	0.01	0.00	0.03	0.01	0.00
BaO	0.20	0.51	0.50	0.26	0.48	0.49
F	0.15	0.24	0.23	0.11	0.19	0.23
Cl	0.04	0.03	0.03	0.05	0.07	0.03
TOTAL	2.36	96.83	96.93	1.77	96.07	96.93
O≠F,Cl	0.06	0.11	0.10	0.06	0.10	0.10
Σ -X	2.37	96.72	96.82	1.78	95.97	96.82

Number of ions on the basis of 12 (O, OH, F) or 22 positive charges

Si	0.08	5.53	5.53	0.18	5.51	5.53
Al	0.24	2.65	2.64	0.37	2.77	2.64
Ti	0.21	0.44	0.44	0.12	0.38	0.43
V	0.00	0.00	0.00	0.00	0.00	0.00
Cr	0.00	0.00	0.00	0.01	0.00	0.00
Fe	0.46	2.16	2.19	0.36	1.95	2.19
Mn	0.01	0.01	0.01	0.01	0.00	0.01
Mg	0.66	2.95	2.92	0.23	3.15	2.94
Ni	0.00	0.00	0.00	0.00	0.00	0.00
K	0.08	1.79	1.79	0.11	1.63	1.78
Na	0.02	0.09	0.09	0.05	0.24	0.09
Ca	0.01	0.00	0.00	0.00	0.00	0.00
Ba	0.01	0.03	0.03	0.01	0.03	0.03
Σ cations	0.13	15.62	15.62	0.09	15.63	15.62
F	0.07	0.11	0.11	0.05	0.09	0.11
Cl	0.01	0.01	0.01	0.01	0.02	0.01
Fe/FeMnMg	0.10	0.42	0.43	0.06	0.38	0.43
Al(IV)	0.08	2.47	2.47	0.18	2.49	2.47
Al(VI)	0.22	0.18	0.17	0.26	0.28	0.17
K/KNaBa	0.01	0.94	0.94	0.03	0.86	0.94

Sample	JG-11-134			JG-11-137		
	Range	Mean	Median	Range	Mean	Median
SiO ₂	1.33	38.25	38.30	0.64	37.14	37.11
Al ₂ O ₃	1.18	14.74	14.75	1.05	15.28	15.43
TiO ₂	3.27	5.41	5.87	0.72	3.09	3.02
V ₂ O ₃	0.05	0.02	0.02	0.04	0.01	0.00
Cr ₂ O ₃	0.11	0.05	0.05	0.03	0.03	0.02
FeO	1.78	9.58	9.46	1.84	15.08	14.95
MnO	0.03	0.04	0.04	0.06	0.05	0.05
MgO	2.37	17.76	17.67	0.86	14.83	14.83
NiO	0.03	0.06	0.06	0.02	0.06	0.06
K ₂ O	0.76	10.29	10.41	0.74	9.58	9.68
Na ₂ O	0.07	0.03	0.02	0.17	0.13	0.12
CaO	0.13	0.02	0.00	0.08	0.03	0.03
BaO	0.29	0.22	0.21	0.09	0.25	0.26
F	0.16	0.59	0.59	0.22	0.71	0.71
Cl	0.04	0.04	0.04	0.04	0.07	0.07
TOTAL	1.95	97.11	97.21	0.85	96.34	96.34
O≠F,Cl	0.07	0.26	0.26	0.09	0.32	0.31
Σ -X	1.98	96.85	96.95	0.92	96.02	96.03

Number of ions on the basis of 12 (O, OH, F) or 22 positive charges

Si	0.16	5.53	5.53	0.07	5.55	5.56
Al	0.22	2.51	2.51	0.20	2.69	2.71
Ti	0.35	0.59	0.64	0.08	0.35	0.34
V	0.01	0.00	0.00	0.01	0.00	0.00
Cr	0.01	0.01	0.01	0.00	0.00	0.00
Fe	0.23	1.16	1.15	0.24	1.89	1.87
Mn	0.00	0.00	0.00	0.01	0.01	0.01
Mg	0.52	3.83	3.81	0.17	3.31	3.31
Ni	0.00	0.01	0.01	0.00	0.01	0.01
K	0.12	1.90	1.91	0.13	1.83	1.85
Na	0.02	0.01	0.01	0.05	0.04	0.03
Ca	0.02	0.00	0.00	0.01	0.01	0.00
Ba	0.02	0.01	0.01	0.01	0.01	0.02
Σ cations	0.27	15.56	15.55	0.08	15.67	15.68
F	0.07	0.27	0.27	0.10	0.34	0.34
Cl	0.01	0.01	0.01	0.01	0.02	0.02
Fe/FeMnMg	0.05	0.23	0.23	0.04	0.36	0.36
Al(IV)	0.16	2.47	2.47	0.07	2.45	2.44
Al(VI)	0.20	0.05	0.04	0.15	0.24	0.25
K/KNaBa	0.02	0.99	0.99	0.02	0.97	0.97

Sample	JG-11-040			JG-11-042		
	Range	Mean	Median	Range	Mean	Median
SiO ₂	1.16	39.12	39.11	1.28	39.40	39.33
Al ₂ O ₃	1.12	14.12	14.02	0.58	14.24	14.25
TiO ₂	1.28	3.48	3.52	1.61	4.41	4.45
V ₂ O ₃	0.16	0.05	0.00	0.06	0.04	0.05
Cr ₂ O ₃	0.25	0.16	0.15	0.09	0.04	0.05
FeO	2.72	11.16	10.93	2.52	8.16	8.27
MnO	0.05	0.03	0.03	0.04	0.03	0.03
MgO	1.33	17.66	17.61	2.91	19.30	19.20
NiO	0.04	0.09	0.09	0.03	0.03	0.04
K ₂ O	0.96	9.40	9.45	0.69	9.87	9.88
Na ₂ O	0.25	0.40	0.40	0.17	0.16	0.18
CaO	0.03	0.00	0.00	0.02	0.01	0.00
BaO	0.21	0.20	0.18	0.30	0.35	0.38
F	0.33	1.30	1.29	0.66	1.59	1.57
Cl	0.08	0.10	0.10	0.02	0.01	0.01
TOTAL	1.12	97.26	97.27	2.35	97.65	97.74
O≠F,Cl	0.15	0.57	0.57	0.28	0.67	0.66
Σ -X	1.02	96.69	96.67	2.28	96.98	97.02

Number of ions on the basis of 12 (O, OH, F) or 22 positive charges

Si	0.08	5.70	5.71	0.07	5.67	5.67
Al	0.19	2.43	2.41	0.08	2.41	2.42
Ti	0.14	0.38	0.39	0.18	0.48	0.48
V	0.02	0.01	0.00	0.01	0.00	0.01
Cr	0.03	0.02	0.02	0.01	0.00	0.01
Fe	0.35	1.36	1.33	0.32	0.98	1.00
Mn	0.01	0.00	0.00	0.00	0.00	0.00
Mg	0.28	3.84	3.83	0.56	4.14	4.12
Ni	0.00	0.01	0.01	0.00	0.00	0.00
K	0.16	1.75	1.76	0.12	1.81	1.80
Na	0.07	0.11	0.11	0.05	0.04	0.05
Ca	0.00	0.00	0.00	0.00	0.00	0.00
Ba	0.01	0.01	0.01	0.02	0.02	0.02
Σ cations	0.12	15.61	15.59	0.10	15.55	15.55
F	0.15	0.60	0.60	0.29	0.72	0.71
Cl	0.02	0.02	0.03	0.01	0.00	0.00
Fe/FeMnMg	0.06	0.26	0.26	0.07	0.19	0.19
Al(IV)	0.08	2.30	2.29	0.07	2.33	2.33
Al(VI)	0.17	0.13	0.12	0.14	0.08	0.08
K/KNaBa	0.03	0.93	0.93	0.02	0.97	0.97

Sample	JG-11-044			JG-11-047		
	Range	Mean	Median	Range	Mean	Median
SiO ₂	1.18	39.22	39.41	1.87	38.52	38.57
Al ₂ O ₃	0.71	13.78	13.70	0.83	14.82	14.78
TiO ₂	1.80	4.12	4.13	1.48	4.90	4.96
V ₂ O ₃	0.01	0.00	0.00	0.05	0.02	0.02
Cr ₂ O ₃	0.08	0.04	0.03	0.15	0.13	0.13
FeO	2.55	8.73	8.23	1.77	7.80	7.90
MnO	0.03	0.01	0.00	0.04	0.04	0.04
MgO	3.17	19.12	19.15	2.53	18.88	18.71
NiO	0.03	0.04	0.04	0.02	0.05	0.05
K ₂ O	0.46	9.82	9.85	0.32	9.82	9.80
Na ₂ O	0.18	0.24	0.25	0.23	0.35	0.34
CaO	0.01	0.00	0.00	0.02	0.00	0.00
BaO	0.45	0.47	0.46	0.44	0.36	0.32
F	0.70	1.71	1.73	0.25	0.80	0.79
Cl	0.09	0.05	0.05	0.03	0.01	0.02
TOTAL	1.87	97.34	97.52	2.13	96.49	96.83
O≠F,Cl	0.29	0.73	0.75	0.10	0.34	0.34
Σ -X	1.65	96.61	96.78	2.11	96.15	96.47

Number of ions on the basis of 12 (O, OH, F) or 22 positive charges

Si	0.08	5.69	5.69	0.07	5.57	5.56
Al	0.08	2.36	2.35	0.07	2.52	2.52
Ti	0.20	0.45	0.45	0.18	0.53	0.54
V	0.00	0.00	0.00	0.01	0.00	0.00
Cr	0.01	0.00	0.00	0.02	0.01	0.02
Fe	0.33	1.06	1.00	0.25	0.94	0.95
Mn	0.00	0.00	0.00	0.00	0.00	0.00
Mg	0.59	4.14	4.17	0.42	4.06	4.05
Ni	0.00	0.01	0.01	0.00	0.01	0.01
K	0.08	1.82	1.82	0.09	1.81	1.81
Na	0.05	0.07	0.07	0.06	0.10	0.10
Ca	0.00	0.00	0.00	0.00	0.00	0.00
Ba	0.03	0.03	0.03	0.03	0.02	0.02
Σ cations	0.12	15.59	15.59	0.11	15.57	15.57
F	0.30	0.79	0.79	0.10	0.36	0.36
Cl	0.02	0.01	0.01	0.01	0.00	0.00
Fe/FeMnMg	0.07	0.20	0.19	0.06	0.19	0.19
Al(IV)	0.08	2.31	2.31	0.07	2.43	2.44
Al(VI)	0.12	0.05	0.05	0.12	0.09	0.09
K/KNaBa	0.02	0.95	0.95	0.03	0.94	0.94

Sample	JG-11-078			JG-11-080		
	Range	Mean	Median	Range	Mean	Median
SiO ₂	0.96	39.56	39.60	0.94	39.87	39.81
Al ₂ O ₃	0.65	16.30	16.33	1.04	16.56	16.44
TiO ₂	1.92	1.96	2.04	0.52	1.74	1.71
V ₂ O ₃	0.05	0.01	0.00	0.09	0.02	0.00
Cr ₂ O ₃	0.28	0.18	0.19	0.15	0.07	0.06
FeO	1.78	6.58	6.62	1.73	5.97	6.06
MnO	0.04	0.02	0.02	0.04	0.03	0.03
MgO	2.11	21.26	21.06	2.16	21.66	21.49
NiO	0.03	0.07	0.07	0.04	0.05	0.05
K ₂ O	0.70	7.23	7.23	1.32	7.07	7.13
Na ₂ O	0.51	1.75	1.70	0.95	1.67	1.59
CaO	0.08	0.02	0.00	0.10	0.02	0.01
BaO	0.40	0.26	0.28	0.46	0.41	0.39
F	0.14	0.79	0.78	0.21	0.98	0.97
Cl	0.09	0.09	0.09	0.04	0.02	0.02
TOTAL	1.00	96.06	96.11	1.45	96.14	96.20
O≠F,Cl	0.07	0.35	0.35	0.08	0.42	0.41
Σ -X	0.98	95.71	95.77	1.45	95.72	95.76

Number of ions on the basis of 12 (O, OH, F) or 22 positive charges

Si	0.09	5.62	5.64	0.09	5.64	5.65
Al	0.12	2.73	2.73	0.11	2.76	2.75
Ti	0.21	0.21	0.22	0.06	0.19	0.18
V	0.01	0.00	0.00	0.01	0.00	0.00
Cr	0.03	0.02	0.02	0.02	0.01	0.01
Fe	0.22	0.78	0.79	0.21	0.71	0.72
Mn	0.00	0.00	0.00	0.00	0.00	0.00
Mg	0.42	4.50	4.47	0.42	4.57	4.53
Ni	0.00	0.01	0.01	0.00	0.01	0.01
K	0.13	1.31	1.31	0.25	1.28	1.28
Na	0.14	0.48	0.47	0.25	0.46	0.44
Ca	0.01	0.00	0.00	0.01	0.00	0.00
Ba	0.02	0.01	0.02	0.03	0.02	0.02
Σ cations	0.15	15.67	15.66	0.08	15.63	15.63
F	0.06	0.35	0.35	0.09	0.44	0.43
Cl	0.02	0.02	0.02	0.01	0.00	0.00
Fe/FeMnMg	0.04	0.15	0.15	0.04	0.13	0.14
Al(IV)	0.09	2.38	2.36	0.09	2.36	2.35
Al(VI)	0.12	0.35	0.35	0.13	0.41	0.40
K/KNaBa	0.07	0.73	0.73	0.14	0.73	0.74

Sample	JG-11-084			JG-11-089		
	Range	Mean	Median	Range	Mean	Median
SiO ₂	1.53	37.03	37.11	0.84	36.94	36.99
Al ₂ O ₃	0.89	14.24	14.23	0.59	15.01	15.00
TiO ₂	1.91	4.98	5.10	0.61	4.35	4.40
V ₂ O ₃	0.00	0.00	0.00	0.07	0.05	0.05
Cr ₂ O ₃	0.08	0.04	0.04	0.10	0.06	0.06
FeO	5.02	15.89	15.92	2.51	15.31	15.37
MnO	0.04	0.05	0.06	0.05	0.03	0.03
MgO	4.08	13.80	13.72	1.69	14.34	14.12
NiO	0.02	0.03	0.03	0.07	0.07	0.07
K ₂ O	1.50	8.84	8.87	0.27	8.81	8.83
Na ₂ O	0.34	0.36	0.38	0.17	0.66	0.67
CaO	0.03	0.01	0.00	0.04	0.00	0.00
BaO	0.31	0.43	0.40	0.25	0.40	0.40
F	0.15	0.20	0.19	0.11	0.18	0.18
Cl	0.05	0.02	0.02	0.03	0.03	0.03
TOTAL	1.69	95.92	95.90	1.80	96.24	96.08
O≠F,Cl	0.06	0.09	0.08	0.05	0.08	0.08
Σ -X	1.72	95.84	95.84	1.80	96.16	95.99

Number of ions on the basis of 12 (O, OH, F) or 22 positive charges

Si	0.09	5.55	5.55	0.07	5.50	5.50
Al	0.16	2.51	2.51	0.07	2.63	2.63
Ti	0.22	0.56	0.58	0.07	0.49	0.49
V	0.00	0.00	0.00	0.01	0.01	0.01
Cr	0.01	0.00	0.01	0.01	0.01	0.01
Fe	0.66	1.99	1.99	0.34	1.91	1.91
Mn	0.01	0.01	0.01	0.01	0.00	0.00
Mg	0.84	3.08	3.08	0.33	3.18	3.13
Ni	0.00	0.00	0.00	0.01	0.01	0.01
K	0.26	1.69	1.69	0.05	1.67	1.67
Na	0.09	0.10	0.11	0.05	0.19	0.19
Ca	0.01	0.00	0.00	0.01	0.00	0.00
Ba	0.02	0.03	0.02	0.01	0.02	0.02
Σ cations	0.13	15.50	15.49	0.07	15.60	15.59
F	0.07	0.10	0.09	0.05	0.08	0.08
Cl	0.01	0.00	0.00	0.01	0.01	0.01
Fe/FeMnMg	0.14	0.39	0.39	0.06	0.37	0.38
Al(IV)	0.09	2.45	2.45	0.07	2.50	2.50
Al(VI)	0.17	0.06	0.05	0.09	0.13	0.14
K/KNaBa	0.04	0.93	0.93	0.02	0.89	0.88

Sample	JG-11-091			JG-11-127		
	Range	Mean	Median	Range	Mean	Median
SiO ₂	1.35	36.79	36.78	0.91	37.47	37.52
Al ₂ O ₃	1.37	14.78	14.91	0.42	12.51	12.46
TiO ₂	1.38	4.65	4.67	0.62	5.73	5.73
V ₂ O ₃	0.11	0.09	0.09	0.06	0.07	0.06
Cr ₂ O ₃	0.07	0.04	0.03	0.02	0.01	0.01
FeO	2.98	15.48	15.40	1.78	20.27	20.33
MnO	0.05	0.05	0.05	0.03	0.07	0.07
MgO	2.14	14.40	14.23	1.02	11.09	11.11
NiO	0.02	0.03	0.03	0.02	0.02	0.02
K ₂ O	0.90	9.25	9.36	0.60	9.03	9.06
Na ₂ O	0.14	0.40	0.43	0.19	0.37	0.38
CaO	0.20	0.03	0.01	0.11	0.08	0.07
BaO	0.27	0.41	0.39	0.09	0.25	0.25
F	0.19	0.24	0.24	0.27	0.75	0.76
Cl	0.02	0.02	0.03	0.05	0.10	0.10
TOTAL	1.82	96.67	96.83	1.37	97.81	97.86
O≠F,Cl	0.08	0.11	0.11	0.11	0.34	0.34
Σ -X	1.80	96.56	96.71	1.30	97.47	97.51

Number of ions on the basis of 12 (O, OH, F) or 22 positive charges

Si	0.06	5.47	5.48	0.10	5.66	5.67
Al	0.21	2.59	2.60	0.09	2.23	2.22
Ti	0.16	0.52	0.52	0.08	0.65	0.65
V	0.01	0.01	0.01	0.01	0.01	0.01
Cr	0.01	0.01	0.00	0.00	0.00	0.00
Fe	0.37	1.93	1.92	0.23	2.56	2.56
Mn	0.01	0.01	0.01	0.00	0.01	0.01
Mg	0.45	3.20	3.16	0.23	2.50	2.50
Ni	0.00	0.00	0.00	0.00	0.00	0.00
K	0.16	1.76	1.77	0.11	1.74	1.74
Na	0.04	0.12	0.12	0.06	0.11	0.11
Ca	0.03	0.01	0.00	0.02	0.01	0.01
Ba	0.02	0.02	0.02	0.01	0.01	0.01
Σ cations	0.15	15.61	15.60	0.08	15.48	15.48
F	0.09	0.11	0.11	0.13	0.36	0.36
Cl	0.01	0.01	0.01	0.01	0.03	0.02
Fe/FeMnMg	0.06	0.38	0.38	0.04	0.51	0.51
Al(IV)	0.06	2.53	2.52	0.10	2.34	2.33
Al(VI)	0.19	0.07	0.09	0.04	-0.11	-0.12
K/KNaBa	0.02	0.93	0.92	0.03	0.93	0.93

Sample	JG-11-093			JG-11-100		
	Range	Mean	Median	Range	Mean	Median
SiO ₂	0.89	37.63	37.57	0.71	37.39	37.46
Al ₂ O ₃	0.91	16.08	16.17	0.31	13.71	13.75
TiO ₂	1.02	2.79	2.80	0.50	5.49	5.61
V ₂ O ₃	0.10	0.06	0.07	0.04	0.17	0.17
Cr ₂ O ₃	0.09	0.05	0.06	0.04	0.19	0.19
FeO	2.89	14.07	13.97	0.76	14.71	14.60
MnO	0.06	0.04	0.04	0.05	0.05	0.06
MgO	1.91	15.71	15.76	0.83	14.24	14.24
NiO	0.03	0.02	0.02	0.03	0.03	0.03
K ₂ O	0.77	8.07	8.04	0.34	9.77	9.81
Na ₂ O	0.51	0.93	0.97	0.04	0.02	0.02
CaO	0.03	0.01	0.00	0.19	0.03	0.01
BaO	0.21	0.15	0.15	0.17	0.46	0.48
F	0.11	0.16	0.16	0.14	0.69	0.68
Cl	0.06	0.02	0.01	0.05	0.03	0.04
TOTAL	1.76	95.78	95.86	1.35	96.98	97.19
O≠F,Cl	0.05	0.07	0.07	0.05	0.30	0.30
Σ -X	1.79	95.71	95.78	1.36	96.68	96.90

Number of ions on the basis of 12 (O, OH, F) or 22 positive charges

Si	0.11	5.54	5.54	0.10	5.57	5.57
Al	0.12	2.79	2.81	0.05	2.41	2.41
Ti	0.12	0.31	0.31	0.06	0.61	0.63
V	0.01	0.01	0.01	0.01	0.02	0.02
Cr	0.01	0.01	0.01	0.00	0.02	0.02
Fe	0.35	1.73	1.71	0.10	1.83	1.82
Mn	0.01	0.01	0.00	0.01	0.01	0.01
Mg	0.36	3.45	3.45	0.16	3.16	3.16
Ni	0.00	0.00	0.00	0.00	0.00	0.00
K	0.16	1.52	1.51	0.05	1.85	1.86
Na	0.15	0.26	0.28	0.01	0.00	0.01
Ca	0.00	0.00	0.00	0.03	0.01	0.00
Ba	0.01	0.01	0.01	0.01	0.03	0.03
Σ cations	0.09	15.63	15.64	0.10	15.50	15.51
F	0.05	0.07	0.07	0.06	0.32	0.32
Cl	0.02	0.00	0.00	0.01	0.01	0.01
Fe/FeMnMg	0.06	0.33	0.33	0.01	0.37	0.37
Al(IV)	0.11	2.46	2.46	0.10	2.43	2.43
Al(VI)	0.09	0.33	0.34	0.06	-0.03	-0.03
K/KNaBa	0.08	0.85	0.84	0.01	0.98	0.98

Sample	JG-11-102			JG-11-106		
	Range	Mean	Median	Range	Mean	Median
SiO ₂	1.06	38.02	37.92	1.80	36.45	36.53
Al ₂ O ₃	0.24	12.93	12.94	0.82	13.38	13.39
TiO ₂	0.63	4.68	4.63	0.38	4.62	4.58
V ₂ O ₃	0.05	0.03	0.03	0.01	0.00	0.00
Cr ₂ O ₃	0.00	0.00	0.00	0.09	0.04	0.04
FeO	1.75	15.26	15.32	3.21	20.73	20.30
MnO	0.03	0.10	0.10	0.07	0.11	0.12
MgO	1.67	14.64	14.50	1.61	10.74	11.03
NiO	0.01	0.03	0.03	0.10	0.07	0.04
K ₂ O	0.25	9.88	9.89	1.90	9.06	9.22
Na ₂ O	0.10	0.06	0.05	0.14	0.06	0.06
CaO	0.06	0.04	0.03	0.16	0.03	0.00
BaO	0.38	0.33	0.41	0.29	0.26	0.21
F	0.13	1.68	1.67	0.25	0.40	0.39
Cl	0.06	0.09	0.09	0.27	0.20	0.16
TOTAL	1.37	97.76	97.96	1.97	96.15	95.93
O≠F,Cl	0.06	0.73	0.72	0.09	0.21	0.22
Σ -X	1.36	97.03	97.22	1.94	95.94	95.73

Number of ions on the basis of 12 (O, OH, F) or 22 positive charges

Si	0.07	5.68	5.68	0.19	5.61	5.59
Al	0.04	2.28	2.27	0.13	2.43	2.44
Ti	0.08	0.53	0.52	0.04	0.53	0.53
V	0.01	0.00	0.00	0.00	0.00	0.00
Cr	0.00	0.00	0.00	0.01	0.01	0.01
Fe	0.25	1.91	1.92	0.47	2.67	2.63
Mn	0.00	0.01	0.01	0.01	0.01	0.02
Mg	0.32	3.26	3.24	0.34	2.46	2.52
Ni	0.00	0.00	0.00	0.01	0.01	0.01
K	0.05	1.88	1.88	0.35	1.78	1.81
Na	0.03	0.02	0.02	0.04	0.02	0.02
Ca	0.01	0.01	0.01	0.03	0.01	0.00
Ba	0.02	0.02	0.02	0.02	0.02	0.01
Σ cations	0.04	15.58	15.58	0.09	15.52	15.53
F	0.04	0.79	0.79	0.11	0.19	0.19
Cl	0.01	0.02	0.02	0.07	0.05	0.04
Fe/FeMnMg	0.05	0.37	0.37	0.06	0.52	0.51
Al(IV)	0.07	2.32	2.32	0.19	2.39	2.41
Al(VI)	0.06	-0.04	-0.03	0.12	0.03	0.04
K/KNaBa	0.02	0.98	0.98	0.01	0.98	0.98

Sample	JG-11-114			JG-11-130		
	Range	Mean	Median	Range	Mean	Median
SiO ₂	1.10	36.85	36.96	0.94	36.78	36.84
Al ₂ O ₃	0.66	14.82	14.83	0.39	12.58	12.59
TiO ₂	1.08	4.00	4.12	0.34	4.68	4.66
V ₂ O ₃	0.29	0.14	0.13	0.07	0.13	0.14
Cr ₂ O ₃	0.11	0.13	0.10	0.02	0.02	0.02
FeO	2.21	17.72	17.93	2.51	22.43	22.51
MnO	0.10	0.07	0.06	0.06	0.05	0.05
MgO	1.73	12.81	12.53	1.50	9.60	9.61
NiO	0.03	0.09	0.08	0.02	0.02	0.02
K ₂ O	0.52	9.14	9.18	0.29	9.23	9.20
Na ₂ O	0.33	0.32	0.29	0.04	0.01	0.00
CaO	0.05	0.02	0.01	0.01	0.00	0.00
BaO	0.13	0.12	0.12	0.32	0.48	0.53
F	0.11	0.22	0.19	0.33	0.84	0.84
Cl	0.02	0.02	0.01	0.08	0.44	0.45
TOTAL	0.76	96.47	96.41	1.04	97.28	97.29
O≠F,Cl	0.05	0.09	0.08	0.16	0.45	0.45
Σ -X	0.76	96.37	96.31	1.02	96.82	96.89

Number of ions on the basis of 12 (O, OH, F) or 22 positive charges

Si	0.08	5.53	5.54	0.03	5.69	5.69
Al	0.09	2.62	2.63	0.03	2.29	2.29
Ti	0.13	0.45	0.47	0.04	0.54	0.54
V	0.03	0.02	0.02	0.01	0.02	0.02
Cr	0.01	0.02	0.01	0.00	0.00	0.00
Fe	0.30	2.23	2.25	0.38	2.90	2.92
Mn	0.01	0.01	0.01	0.01	0.01	0.01
Mg	0.36	2.87	2.81	0.30	2.21	2.21
Ni	0.00	0.01	0.01	0.00	0.00	0.00
K	0.11	1.75	1.76	0.06	1.82	1.81
Na	0.09	0.09	0.08	0.01	0.00	0.00
Ca	0.01	0.00	0.00	0.00	0.00	0.00
Ba	0.01	0.01	0.01	0.02	0.03	0.03
Σ cations	0.07	15.60	15.61	0.08	15.49	15.49
F	0.05	0.10	0.09	0.16	0.41	0.41
Cl	0.00	0.00	0.00	0.02	0.12	0.12
Fe/FeMnMg	0.06	0.44	0.44	0.06	0.57	0.57
Al(IV)	0.08	2.47	2.46	0.03	2.31	2.31
Al(VI)	0.10	0.16	0.14	0.06	-0.02	-0.02
K/KNaBa	0.05	0.95	0.95	0.01	0.98	0.98

Sample	JG-11-150			JG-11-153		
	Range	Mean	Median	Range	Mean	Median
SiO ₂	0.80	35.36	35.56	0.53	37.14	37.19
Al ₂ O ₃	0.45	13.86	13.80	0.43	13.65	13.65
TiO ₂	0.83	3.13	3.07	0.47	5.02	4.93
V ₂ O ₃	0.04	0.04	0.05	0.11	0.10	0.09
Cr ₂ O ₃	0.01	0.02	0.02	0.18	0.13	0.12
FeO	0.81	25.27	25.07	0.42	16.75	16.76
MnO	0.01	0.07	0.07	0.04	0.04	0.04
MgO	0.43	6.93	7.03	0.56	13.12	13.12
NiO	0.12	0.10	0.07	0.02	0.01	0.02
K ₂ O	1.98	7.62	7.92	0.11	9.50	9.50
Na ₂ O	0.07	0.13	0.15	0.08	0.10	0.10
CaO	0.02	0.12	0.12	0.01	0.00	0.00
BaO	0.15	0.45	0.45	0.53	0.41	0.37
F	0.07	0.21	0.22	0.11	0.24	0.23
Cl	0.16	0.20	0.22	0.04	0.08	0.08
TOTAL	3.09	93.52	93.89	1.24	96.30	96.50
O≠F,Cl	0.06	0.13	0.14	0.04	0.12	0.11
Σ -X	3.03	93.39	93.74	1.23	96.18	96.38

Number of ions on the basis of 12 (O, OH, F) or 22 positive charges

Si	0.04	5.68	5.68	0.07	5.59	5.60
Al	0.10	2.63	2.65	0.06	2.42	2.41
Ti	0.10	0.38	0.38	0.05	0.57	0.56
V	0.01	0.01	0.01	0.01	0.01	0.01
Cr	0.00	0.00	0.00	0.02	0.02	0.01
Fe	0.19	3.40	3.35	0.05	2.11	2.11
Mn	0.00	0.01	0.01	0.01	0.01	0.01
Mg	0.06	1.66	1.68	0.11	2.94	2.95
Ni	0.01	0.01	0.01	0.00	0.00	0.00
K	0.37	1.56	1.62	0.01	1.82	1.82
Na	0.02	0.04	0.05	0.02	0.03	0.03
Ca	0.00	0.02	0.02	0.00	0.00	0.00
Ba	0.01	0.03	0.03	0.03	0.02	0.02
Σ cations	0.18	15.40	15.44	0.06	15.52	15.53
F	0.03	0.11	0.11	0.05	0.11	0.11
Cl	0.04	0.05	0.06	0.01	0.02	0.02
Fe/FeMnMg	0.02	0.67	0.67	0.01	0.42	0.42
Al(IV)	0.04	2.32	2.32	0.07	2.41	2.40
Al(VI)	0.14	0.31	0.33	0.01	0.01	0.01
K/KNaBa	0.02	0.96	0.95	0.02	0.97	0.97